Title
Advancing Sustainability Assessment of Renewable Energy System Production

Author
He, Haoyang

Publication Date
2020

Peer reviewed|Thesis/dissertation

UNIVERSITY OF CALIFORNIA,
IRVINE

Advancing Sustainability Assessment of Renewable Energy System Production

DISSERTATION

submitted in partial satisfaction of the requirements
for the degree of

DOCTOR OF PHILOSOPHY

in Materials Science and Engineering

by

Haoyang He

Dissertation Committee:
Professor Julie M. Schoenung, Chair
Associate Professor Daniel Mumm
Professor Scottt Samuelsen

2020

DEDICATION

To

People who support me along the way of my life

in recognition of their worth

TABLE OF CONTENTS

LIST OF FIGURES

LIST OF TABLES

ACKNOWLEDGEMENTS

I would like to express the deepest appreciation to my advisor and committee chair, Professor Julie M. Schoenung, who has offered me this opportunity to explore the research field of sustainability and supported my research during my whole Ph.D. study. I have benefited greatly from her rigorous academic attitude, continuous encouragement, and constructive advices. Without her patient guidance and persistent help, this dissertation would not have been possible.

I would also like to thank my committee members, Professor Scott Samuelsen and Professor Daniel Mumm, for their active participation of my dissertation with the helpful discussion and comments. Professor Scott Samuelsen, special thanks to all the resources provided from APEP.

In addition, I sincerely thank Professor Oladele A. Ogunseitan and Dr. Brian Tarroja for their mentoring along with this work and research. Their ideas and suggestions largely helped me to tackle with the difficulties running into my research life. Their professional expertise and effective project management have successfully led to the achievements of several critical reports and publications.

Further, I thank all the group members, lab mates, co-workers and co-authors, for their tremendous supports and assistances through the time of my Ph.D. life. Specially, Yadira Gutierrez and Professor Thomas M. Young, Professor Timothy F. Malloy, Professor Elsa A. Olivetti, Dr. Carl Lam, Professor Oladele A. Ogunseitan, Dr. Brian Tarroja and Professor Scott Samuelsen, thank you all for the support and help on several publications important to me with your professional knowledge and wise suggestions. In addition, Shan Tian and Chris Glaubensklee, your hard work and excellent contributions play an important role on supporting and improving my research.

Lastly, financial support was provided by the University of California, Irvine, PhD Bridge Fellowship program and California Energy Commission under agreement #: EPC-16-039. I'm grateful to the funding provided by them which allows me to conduct research and complete my degree.

VITA

Haoyang He

2015 B.A. in Functional Material, Huazhong University of Science and Technology

2017 M.S. in Materials Science and Engineering, University of California, Irvine

2020 Ph.D. in Materials Science and Engineering, University of California, Irvine

FIELD OF STUDY

Materials Science and Engineering, Sustainability

PUBLICATIONS

H. He, Y. Gutierrez, T.M. Young, J.M. Schoenung. The role of data source selection in chemical hazard assessment: A case on organic photovoltaics. J. Hazard. Mater. 365(2019)227-236

H. He, T.F. Malloy, J.M. Schoenung. Multicriteria decision analysis characterization on chemical hazard assessment data sources. Integr. Environ. Assess. Manag. 15(2019)895-908

H. He, S. Tian, B. Tarroja. O.A. Ogunseitan, S. Samuelsen, J.M. Scheonung. Flow battery production: Materials selection and environmental impact. J. Clean. Prod. 269(2020)121740

H. He, S. Tian, B. Tarroja, O.A. Ogunseitan, S. Samuelsen, J.M. Scheonung. A comparative assessment on potential toxicity hazard and health impacts of flow batteries and lithium-ion batteries production. To be submitted

B. Tarroja, **H. He**, S. Tian, O.A. Ogunseitan, J.M. Schoenung. A comparative, comprehensive life cycle assessment of the environmental and human health impacts of flow battery energy storage production and use. California Energy Commission. 2020

M.L.A. Ochoa, **H. He**, J.M. Scheonung. E. Helminen, T. Okrasinski, B. Schaeffer, B. Smith, J. Davignon, L. Marcanti, E.A. Olivetti. Design parameters and environmental impact of printed wiring board manufacture. J. Clean. Prod. 238(2019)117807

S. Tian, **H. He**, A. Kendall. S.J. Davis, O.A. Ogunseitan, J.M. Scheonung, S. Samuelsen, B. Environmental trade-offs of flow battery energy storage in California. Submitted for review

C.W. Lam, **H. He**, J.M. Schoenung. Hazardous materials Characterization and Assessment. R.A. Mayers, ed. Encyclopedia of Sustainability and Science and Technology. Springer, New York, 2018

ABSTRACT OF THE DISSERTATION

Advancing Sustainability Assessment of Renewable Energy System Production

by

Haoyang He

Doctor of Philosophy in Materials Science and Engineering

University of California, Irvine, 2020

Professor Julie M. Schoenung, Chair

The promotion of renewable energy in electric energy grids is motivated by the adverse effects from the use and production of conventional energy sources. To accommodate large amounts of renewable penetration, the deployment of energy storage systems is required to manage variable renewable resources such as wind and solar. In recent years, utility-based energy systems have been undergoing a significant transformation to increasingly integrate energy storage systems. However, these devices are diverse in terms of not only their use-phase performance, but also the design parameters and processing materials used for their production and waste generated throughout their life cycle. Thus, sustainability assessment toward those various energy storage systems is urgently needed. In contrast, advancing customized sustainability assessment to cover the rarely addressed sustainability issues on emerging energy storage systems is also important.

In this dissertation, we have conducted comprehensive sustainability assessment on several energy storage systems from the perspectives of environmental and human health

impact, chemical hazard, economic feasibility, and decision making. More specifically, a comprehensive investigation of the potential environmental and human health impact, chemical hazards, and economic feasibility associated with the production of three flow batteries: vanadium redox, zinc bromide, and all-iron flow batteries; is performed through life cycle impact assessment, chemical hazard assessment and techno-economic analysis. Further, the toxicity and hazard of processing chemicals used for the manufacturing of low band gap polymers in organic photovoltaics were assessed through a chemical hazard assessment approach. In addition, a multi-criteria decision analysis is applied to select different chemical toxicity data sources in order to promote a more comprehensive chemical hazard assessment.

Overall, this dissertation aims to provide insight into developing a strategy for comprehensive evaluation of the production and deployment of sustainable energy systems, with a focus on the effects of the product design and materials selection choices on the environmental footprint, hazard potential and economic feasibility of these novel energy devices. This strategy is designed to guide the selection of energy technologies in order to help utilities and regional governments to support their renewable energy penetration goals while minimizing environmental externalities.

Chapter 1: Introduction

The fast development of technology and economy has provided human society with abundant material life. However, there are also related adverse effects on environment such as pollution, global warming issues, toxic chemicals release and waste emissions that will offset or even exceed the benefits acquired. Sustainability, which was first proposed in 1987 and defined as "*Development that meets the need of the present without compromising the ability of future generation to meet their own needs*" [1], has been increasingly recognized, accepted and applied in many societies. In recent years, the research on sustainability has been expanded to a broad range of activities not only considering the environmental impact but also the economic development and social equity, as illustrated in **Figure 1.1** [2].

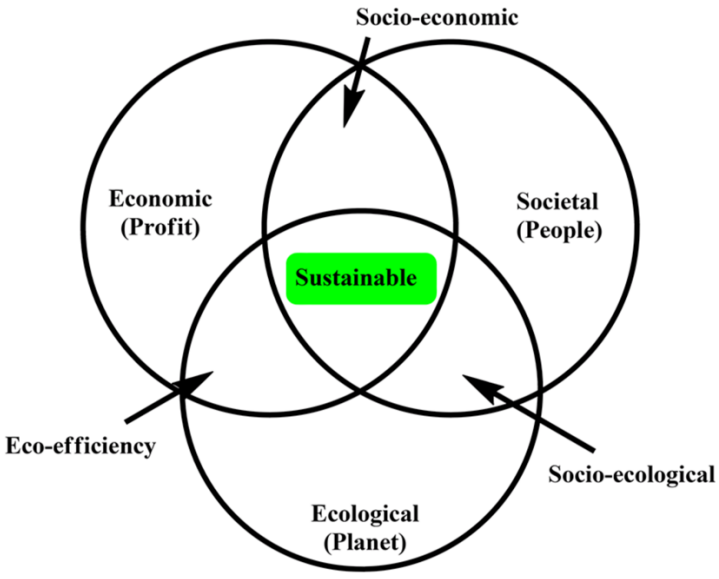

Figure 1.1. Sustainability metrics Venn Diagram [2].

With extensive issues included in sustainable development, several methods and tools such as life cycle assessment (LCA), alternatives assessment (AA) and chemical hazard assessment (CHA) have been created to address various aspects of environmental impact,

human health impact, material and resource intensity, toxicity, functional performance and economic feasibility. Life cycle assessment is designed to assess the environmental impact associated with the life cycle stages of products and systems [3,4,5]. Moreover, with the development of the LCA methodology, it has been gradually applied in the social ecology and economic fields with different methodologies developed such as the social life cycle assessment (SCLA) [6] and economic input-output life cycle assessment (EIO-LCA) [7]. Alternatives assessment, which is designed to promote adoption of safer alternatives in terms of hazard, economic cost, functional performance, and environment impact, is increasingly relevant to green chemistry and sustainable development through its application to chemical management and avoidance of regrettable substitutions [8, 9, 10]. The core part of AA is to identify and evaluate chemicals of concern, within which the methodological approach used to investigate the hazard potential of a chemical on human health or adverse environmental effects is defined as chemical hazard assessment (CHA) [11, 12]. There are a small set of CHA tools and decision frameworks now available [13 - 16]. In order to analyze and interpret the various results generated by different sustainable assessment tools for decision making, multi-criteria decision analysis (MCDA) is an appropriate tool, as it can evaluate alternatives with multiple conflicting criteria by providing an aggregated performance index [17]. MCDA is now widely used to perform robust aggregation of environmental impact assessment values such as in LCA and AA [18-25]. These case studies demonstrate that there is a synergistic effect between the sustainable assessment tools and decision analysis, which provides a solid base for their combined use on the improvement of the decision-making process.

As sustainable development has been applied to various research fields, of particular interest is the issue of sustainable energy. With the increasing recognition that the world's increasing prosperity and economic growth cannot be sustained without clean, affordable and reliable energy [26], the adverse environmental impacts from the production and usage of conventional energy resources demands that electric grids must achieve high renewable energy adoptions to reduce these impacts. California has established goals to meet, by the year 2050, 100% of the electricity demand with carbon-free energy resources and an 80% decrease in economy-wide greenhouse gas (GHG) emissions compared to 1990 levels [27, 28]. Meeting these goals will require the deployment of energy storage systems to manage variable renewable resources such as wind and solar. Several renewable energy storage systems, especially battery technologies, exhibit promising potential to fulfill the needs for a large penetration of renewable energy. Compared to other battery types such as lithium-ion (Li-ion), lead acid and sodium batteries, flow batteries have the advantage of scalability to high capacities, the separation of energy and power modules, long cycle life, and fast response times [29-31]. While significant research has focused on improving flow battery performance and efficiency, few studies have explored their potential environmental impacts. With the application of sustainable assessment tools, we seek to explore the environmental impacts, human health impacts, toxicity, waste management strategy and tech-economic feasibility associated with the raw materials extraction, product manufacturing, product assembly and end-of-life management of flow battery technologies. With the combined use of decision analysis, we seek to evaluate and compare flow batteries of different chemistry combinations and flow batteries with other energy storage devices such as the Li-ion batteries and to understand the trade-offs between each aspect assessed.

The use of sustainable assessment tools and decision analysis provides insight into the effects of product design and material selection choices on the potential environmental footprint of these novel energy storage devices. In return, the results illustrated by the case studies will highlight the strengths and weaknesses of each method, which will further help with the methodology improvement. More specifically, given the uncertainties associated with data sources due to data gaps and variations that are commonly encountered when performing sustainability assessment, it is urgent to identify high quality data sources in order to improve the robustness of assessment results. Through a case study on low band gap polymers used in organic photovoltaic energy systems, we evaluated how different toxicity data sources influence the CHA results. Further, decision analysis was applied to aid the selection of proper data sources for CHA from the perspective of data reliability, adequacy, transparency, volume and ease of use.

Chapter 2: Background

2.1 Alternatives Assessment and Chemical Hazard Assessment

The development of AA is motivated by several governmental organizations and research institutes to promote less hazardous chemicals use and avoid regrettable substitutions. For example, over 10,000 new chemicals have been registered each year since 2009 under the Registration, Evaluation, Authorization and Restriction of Chemicals (REACH) regulation [32]. With the growing number of new chemicals, it is urgent for government agencies and research institutions to improve chemical management. Recent legislative initiatives push for industry to utilize safer chemicals in their products and processes. For example, the Toxic Substances Control Act (TSCA) [33], a regulation recently revised by the U.S. Environmental Protection Agency (EPA), requires reporting, record-keeping, testing and restrictions relating to chemical substances and/or mixtures. The Safer Consumer Products Law (CA-SCP), which seeks to reduce toxic chemicals in products sold in the State of California, requires a comprehensive assessment of designated chemicals of concern and their alternatives [34]. In order to conduct a comprehensive AA, several aspects need to be addressed such as the chemical toxicity, functional performance, economic feasibility and environmental impact (**Figure 2.1**).

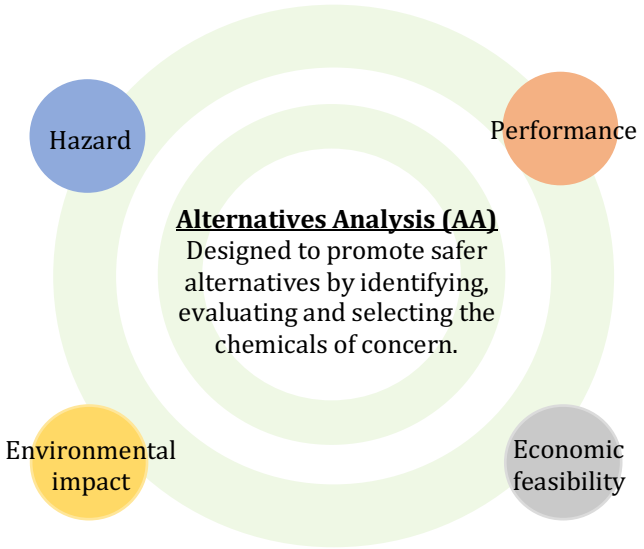

Figure 2.1. General components considered in alternative assessment (AA).

CHA is one core part of AA. Among several CHA tools and decision frameworks, the GreenScreen® for Safer Chemicals (GreenScreen®) is widely applied nowadays in sustainability standards, by industry associations and organizations, for corporate chemicals management, and by non-profit organizations and government [13]. GreenScreen® is a publicly available, transparent, attribute-driven CHA framework for identifying chemicals of high concern or toxicity [13]. The hazard traits of interest include: Carcinogenicity (C), Mutagenicity & Genotoxicity (M), Reproductive Toxicity (R), Developmental Toxicity (D), Endocrine Activity (E), Acute Mammalian Toxicity (AT), Systematic Toxicity & Organ Effects (ST-single), Neurotoxicity (N-single), Skin Irritation (IrS), Eye Irritation (IrE), Systematic Toxicity & Organ Effects-Repeated Exposure sub-endpoint (ST-repeated), Neurotoxicity-Repeated Exposure sub-endpoint (N-repeated), Skin Sensitization (SnS), Respiratory Sensitization (SnR), Acute Aquatic Toxicity (AA), Chronic Aquatic Toxicity (CA), Persistence (P), Bioaccumulation (B), Reactivity (Rx) and Flammability (F). These traits are categorized

into the five groups, shown in **Table 2.1**, of Human Health Group I, Human Health Group II, Human Health Group II*, Environmental Toxicity & Fate, and Physical Hazards. For each hazard trait, various data sources are used to derive hazard trait classification levels (Low (L), Moderate (M), High (H) or Very High (vH)), which are then used in conjunction with the GreenScreen® decision logic to generate an overall benchmark score for the chemical.

Table 2.1 The hazard traits evaluated in GreenScreen® for Safer Chemicals [13]

Human Health Group I	Human Health Group II	Human Health Group II*	Environmental Toxicity& Fate	Physical Hazards
Carcinogenicity (C)	Acute Mammalian Toxicity (AT)	Systematic Toxicity & Organ Effects* Repeated Exposure sub-endpoint (ST-repeated)	Acute Aquatic Toxicity (AA)	Reactivity (Rx)
Mutagenicity & Genotoxicity (M)	Systematic Toxicity & Organ Effects (ST-single)	Neurotoxicity- Repeated Exposure sub-endpoint (N-repeated)	Chronic Aquatic Toxicity (CA)	Flammability (F)
Reproductive Toxicity (R)	Neurotoxicity (N-single)	Skin Sensitization (SnS)	Persistence (P)	
Developmental Toxicity including Neurodevelopmental Toxicity (D)	Skin Irritation (IrS)	Respiratory Sensitization (SnR)	Bioaccumulation (B)	
Endocrine Activity (E)	Eye Irritation (IrE)			

Five benchmark (BM) scores are possible: Chemical of High Concern (BM-1), Use but Search for Safer Alternatives (BM-2), Use but Still Opportunity for Improvement (BM-3), Safer Chemical (BM-4), and Unspecified due to Insufficient Data (BM-U). The GreenScreen® decision logic used to assign these benchmark scores is a non-compensatory approach to prioritizing the hazard traits and their classifications. We include the details of this decision logic here, so that the results presented below are easier to understand, especially in terms of the relationship between hazard triggers and benchmark scores.

A chemical is assigned a BM-1 score if *any* of the following are true:

a. High P *and* High B, *and* {[Very High T, where T is Ecotoxicity (i.e., AA or CA) *or* any Group II Human (AT, ST-single, N-single, IrS or IrE)] *or* [High T, where T is Group I *or* II* Human]}

b. Very High P *and* Very High B

c. Very High P *and* {[Very High T (Ecotoxicity *or* Group II Human)] *or* [High T (Group I *or* II* Human)]}

d. Very High B *and* {[Very High T (Ecotoxity *or* Group II Human)] *or* [High T (Group I *or* II* Human)]}

e. High T (Group I Human)

If any of the BM-1 criteria are true, the CHA is complete for this chemical. If not, the process moves on to assess the BM-2 criteria, which are:

a. Moderate P *and* Moderate B *and* Moderate T (Ecotoxicity or Group I, II *or* II* Human)

b. High P *and* High B

c. High P *and* Moderate T (Ecotoxicity or Group I, II *or* II* Human)

d. High B *and* Moderate T (Ecotoxicity or Group I, II *or* II* Human)

e. Moderate T (Group I Human)

f. Very High T (Ecotoxicity *or* Group II Human) *or* High T (Group II* Human)

g. High Flammability *or* High Reactivity

If any of the BM-2 criteria are true, the CHA is complete for this chemical. If not, the process moves on to assess the BM-3 criteria, which are:

a. Moderate P *or* Moderate B
b. Moderate Ecotoxicity
c. Moderate T (Group II *or* II* Human)
d. Moderate Flammability, *or* Moderate Reactivity

If any of the BM-3 criteria are true, the CHA is complete for this chemical. If not, the process moves on to assess the BM-4 criteria, which are:

a. Low P *and* Low B *and* Low T (Ecotoxicity, Group I, Group II, *and* Group II* Human) *and* Low Physical Hazards (Flammability and Reactivity)

2.2 Life Cycle Assessment

With the wide application of LCA, there are several environmental impact categories considered in the LCA frameworks. Based on different pathways towards environmental endpoints, there are also several midpoint indicators including the cumulative energy demand (CED), abiotic resource depletion (ADP), water use and land use, global warming potential (GWP), ozone depletion potential (ODP), ionizing radiation, particulate matter (PM), photochemical ozone formation, acidification potential (AP), eutrophication potential (EP), ecotoxicity (E) and human toxicity potential (HTP) [35-39]. To fully investigate the cause-effect chain of the contributed inventory to certain impact categories usually requires extensive research on the impact pathways, affected area of protection and spatial and temporal variability. Several research institutes and organizations have developed different

modeling approaches to calculate the related environmental burden, such as the ReCiPe [35], CML [36], IMPACT 2002+ [37], TRACI [38] and ICLD [39].

To conduct a life cycle assessment, there are four basic steps (**Figure 2.1**): 1. Goal and scope definition; 2. Life cycle inventory; 3. Impact assessment and 4. Interpretation. The goal and scope definition is the description of the product system in terms of the system boundary and functional unit [32]. The life cycle inventory (LCI) lays an essential foundation of the whole LCA project. LCI is a method used to estimate the consumption of material, energy and resources and the quantities of waste flows and emissions caused by or attributable to a product's life cycle [40]. It involves the collection of data that depend on related LCI data sources and the modeling of the product system within a designated system boundary.

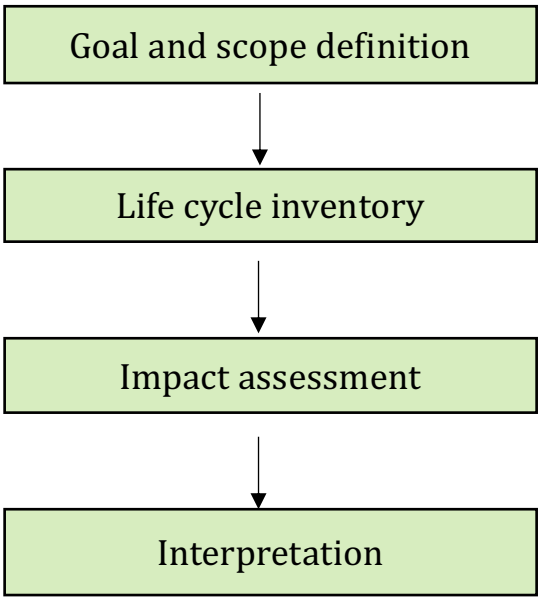

Figure 2.2. The four components of the life cycle assessment.

Life cycle impact assessment (LCIA) refers to the evaluation, characterization, and calculation of the potential impacts associated the constructed life cycle inventories within the range of the selected system boundary, which may include the raw materials extraction, transportation, production manufacturing and assembly, use phase and end of life. According to ISO 14042 [41], there are three mandatory elements required to perform a LCIA:

1. Selection of impact categories, categories indicators and characterization models;
2. Assignment of the inventory data to the chosen impact categories, and
3. Calculation of impact category indicators using characterization factors.

Other important elements are specified but are not designated as mandatory. These include normalization, grouping and weighting [42]. Based on the goal and scope of the study, there is a wide range of impact categories available for use. These indicators are related with the resource use, human health consequences, and ecological consequences that are also used as endpoint indicators. The impact results are usually represented as an aggregated score based on the characterization factor (CF) which can be seen as an integrated model output. The calculation of CF usually will relate or translate the elementary flow into its impact on the chosen indicator for the impact category [42]. A generic framework can be expressed as [43]:

$$CF = FF \cdot XF \cdot EF \quad (1)$$

where the characterization factor (CF) is the product of a fate factor (FF), an exposure factor (XF) and an effect factor (EF). The application of the characterization factor to the impact score (IS) is straightforward [43]:

$$IS = Q \cdot CF \tag{2}$$

where Q is the quantity of the elementary flow and the total impact score is the aggregation of the impact score of each elementary flow.

In this work, several life cycle impact assessment methodologies were applied to evaluate various impact categories associated with environment, human health and resource. For example, USETox®, an environmental model for characterization of human toxicological and ecotoxicological impacts endorsed by UNEP-SETAC Life Cycle Initiative [44-46], was used to calculate the potential ecotoxicity and human health cancer and non-cancer effects.

2.3 Techno-Economic Analysis

The techno-economic analysis (TEA) has been widely applied to assess the economic feasibility of emerging materials, products and technologies [47-50]. The principle of TEA is to evaluate the cost-benefit comparison for selected specific projects using different approaches. Not only for evaluating the economic feasibility of emerging products, other functional uses of TEA also include: investigating cash flows over a product lifetime; evaluating the likelihood of different technology scales and applications; and to compare the economic quality of different technology applications providing the same service [51]. Based on the purpose and object of the research project, cost models can be applied in different

levels to meet with the basic requirement and highlight the most important part [52]. For example, if the project is aimed to explore the economic feasibility of a new product, then the associated raw materials and processing cost would be the major priority in order to understand what component would be the major driver of cost which is critical for further optimization. On the other hand, if the project is to evaluate the cash flow and the payback period for a market product by the investors, then the capital investment and fixed cost such as equipment, maintenance and labor cost would be highly important for a real plant operation, also counting the discount ratio and inflation over the production periods.

In order to perform a TEA, the first step is to identify the manufacturing process associated with the production. The cost inputs associated with the TEA model are ofte categorized as materials cost, utility cost, labor cost and fixed cost. The materials cost focuses on the cost of raw materials used for the manufacturing, and the utility cost is designed to estimate cost of the utilities used during the manufacturing processes and the types considered usually include electricity, water and fuel use. If considering a real plant operation, the labor cost and fixed cost are also important inputs for the cost model. For example, the building and space construction, the purchase and installation of major equipment and the future operation and maintenance cost would be important items to be considered from an investment perspective.

2.4 Multi-Criteria Decision Analysis

In recent years, there are many MCDA tools and methodologies developed such as the multi-attribute value theory (MAVT), multi-attribute utility theory (MAUT), analytical hierarchy process (AHP), the technique for order of preference by similarity to ideal solution

(TOPSIS) and preference ranking organization method for enrichment evaluation (PROMETHEE) [53]. With the combined use of probabilistic theory, several extensive MCDA methods such as Fuzz MAUT, and stochastic multicriteria acceptability analysis (SMAA) [54] are also widely applied. Different MCDA approaches adopt different mathematical expressions for the aggregation, which means the same decision problems may generate distinct outcomes by using different MCDA methods. In order to structure a systematic decision-making problem, the practitioner needs to go through several steps for the alternatives screening and sorting, criteria evaluation, MCDA method selection and aggregation and ranking, which is shown in **Figure 2.3** [53].

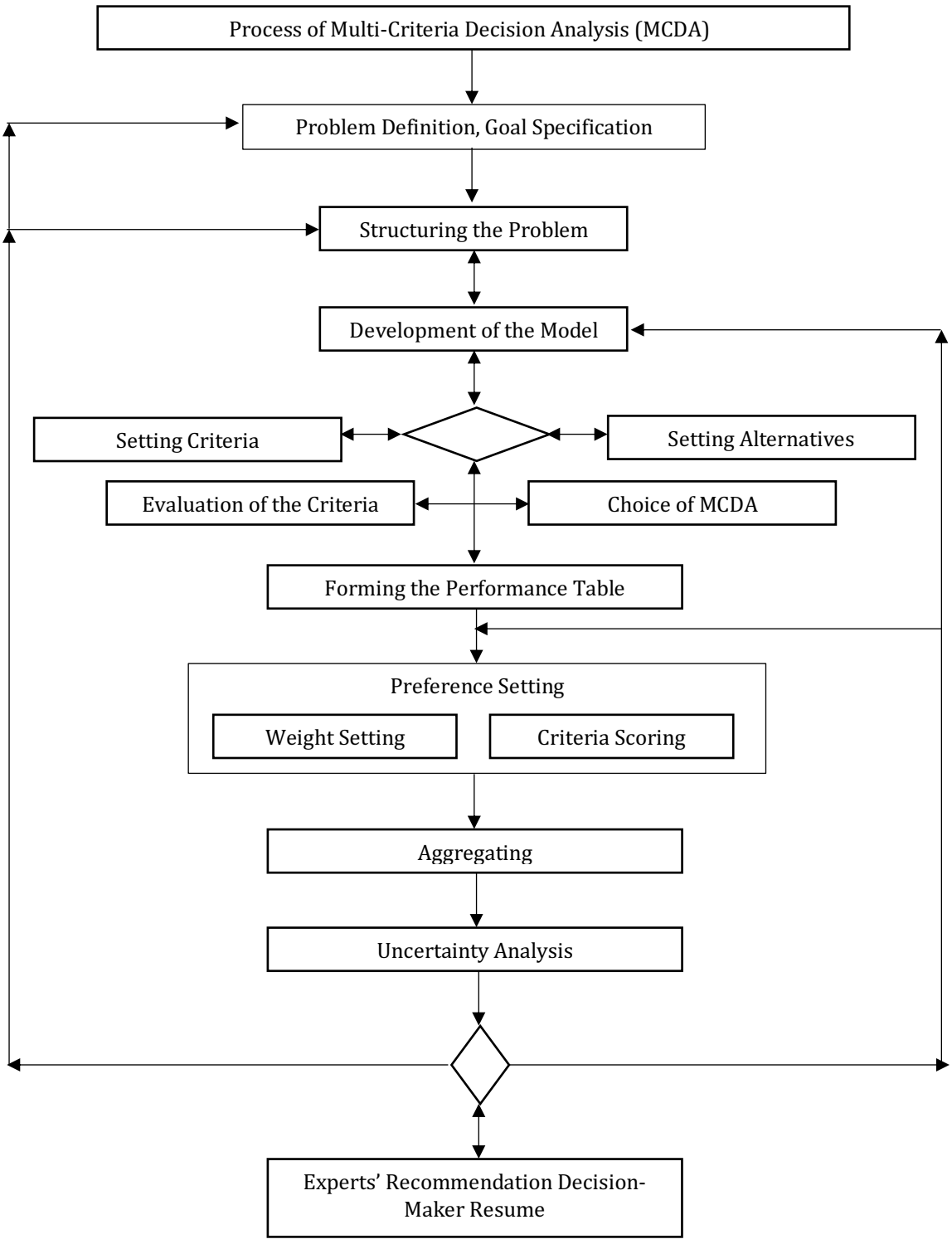

Figure 2.3. Aggregated scheme of the multi-criteria decision analysis process [53].

As listing the detail calculation of all the MCDA methods is not the major focus of this dissertation, only the two methods – MAUT and SMAA – that are applied in this study are described in detail. In MAUT, the final result is calculated as a total utility score by aggregating the performance for each attribute. In this current study, the most widely used additive utility function was executed for this evaluation, which can be seen as a weighted sum process [55]:

$$U(\boldsymbol{a}) = \Sigma \boldsymbol{w}_i \times u(\boldsymbol{a}_i) \quad (3)$$

In Equation (3), $U(\boldsymbol{a})$ is the total utility of alternative $\boldsymbol{a}$, $u(\boldsymbol{a}_i)$ is the utility of $\boldsymbol{a}$ on attribute i and $\boldsymbol{w}_i$ is the weighting factor for attribute i while $\boldsymbol{w}_i > 0$ and $\Sigma \boldsymbol{w}_i = 1$. Unlike MAUT, the SMAA deals with multi-objective problems in an inverse way by exploring the weight space based on the assumed utility function [56]. In SMAA, the alternatives' performance on each attribute is usually a stochastic variable. As a result, the utility score will be a probabilistic distribution estimated with all possible weight combinations. Here, to simplify, the deterministic case is used as an illustration. On the basis of Equation (3), the SMAA seeks to determine all the weight combinations $\boldsymbol{w}$ that yield an overall utility of alternative $\boldsymbol{a}$ greater than or equal to that of any other alternative:

$$U(\boldsymbol{a}) \geq U(\boldsymbol{b}), \forall \boldsymbol{b} \quad (4)$$

$$\Sigma \boldsymbol{w}_i \times u(\boldsymbol{a}_i) \geq \Sigma \boldsymbol{w}_i \times u(\boldsymbol{b}_i) \quad (5)$$

The set of the weight combinations $\boldsymbol{w}$ that will satisfy Equation (4) are called favorable weight vectors W_a, and an acceptability index A_i is defined as the volume of the favorable weight vectors divided by the volume of feasible weight vectors W where:

$$W = \{ \boldsymbol{w} \in R^n : \boldsymbol{w}_i > 0 \text{ and } \Sigma \boldsymbol{w}_i = 1 \} \quad (6)$$

$$W_a = \{ \boldsymbol{w} \in W : U(\boldsymbol{a}) \geq U(\boldsymbol{b}), \forall \boldsymbol{b} \} \quad (7)$$

$$A_i = vol(W_a) / vol(W) \quad (8)$$

The acceptability index represents the probability that certain alternatives will be ranked first. The alternative with the largest probability to be chosen based on their favorable weight vectors within the range of all feasible weight vectors can be determined by exploring the acceptability index for all alternatives. In this research, the method applied is SMAA-2 [57], which is similar to SMAA with the extension to calculate the acceptability index for all alternatives to be ranked not only first, but from best to worst.

2.5 Energy Storage Technologies

In recent years, the promotion of cleaner energy use by introducing renewable energy sources into the electric energy grid has encouraged the fast development of energy storage systems. Currently, there are various types of energy storage systems that could be used for large-scale applications. As specified by Liu et al. [58], energy storage systems can be classified into four types as mechanical, chemical, electric, and electrochemical energy storage, which is presented in **Figure 2.4**. Among them, electrochemical energy storage (EES) such as batteries has shown great potential to be implemented for real electricity grid application due to their sufficient efficiency and long cycle life [59]. Multiple types of battery storage technologies with different redox reactions have been developed such as lithium-ion batteries, sodium-ion batteries, and flow batteries. In this dissertation, flow batteries are the major technology evaluated for sustainability assessment.

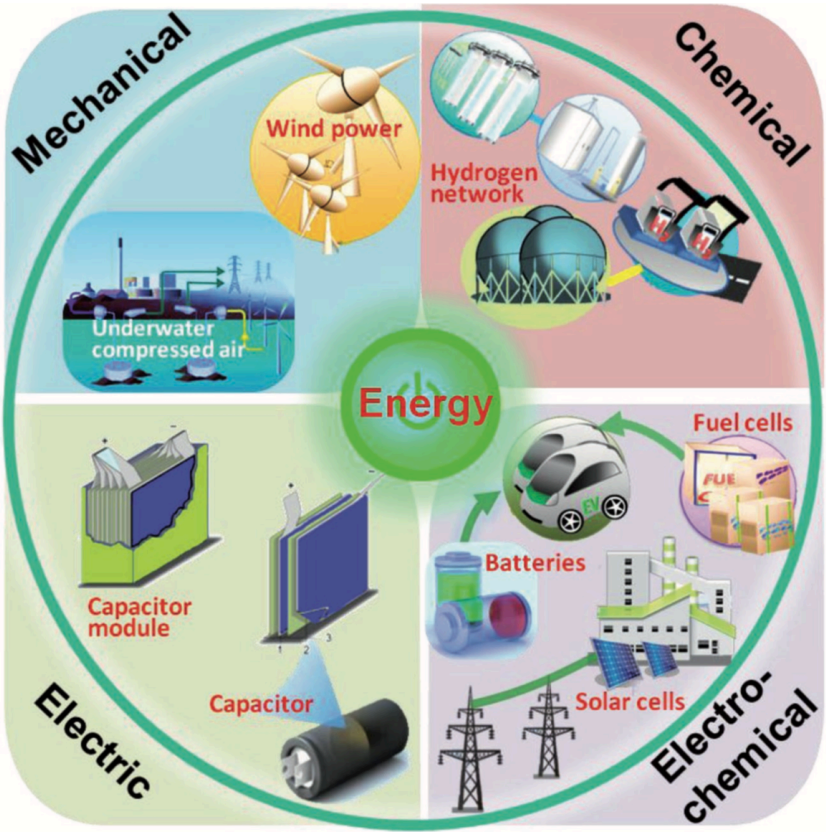

Figure 2.4. Classifications of energy storage systems [58].

2.5.1 Flow Battery Energy Storage Technologies

A flow battery is a rechargeable energy storage device that provides conversion between chemical to electrical energy by having the active species dissolved in liquid stored in two external electrolyte tanks and generally separated by membranes [29]. As a potential technology for energy storage, there are both advantages and disadvantages [29, 60] associated with the installation and operation of flow battery:

Pros:

1. Ability to store large amounts of power and energy.
2. Separation of power and energy.

3. Electrode only serves to provides electrochemically active surface.

4. Safety and thermal management qualities.

Cons:

1. Relatively low energy and power density.

2. High capital cost.

3. Potential for cross contamination.

4. Reduced round-trip efficiency due to pumping requirements.

In recent years, several flow battery technologies with different chemistries [61] have been developed, and some of them have been successfully applied for industry application. However, the related environmental impacts of this technology are rarely addressed, which means the adverse effects due to raw materials extraction, manufacturing, installation, operation and end-of-life has remained unrevealed. The most recent study published by Weil et al. [62] explored the life cycle environmental impact of the vanadium redox flow battery (VRFB) indicating there is a large impact on global warming potential and abiotic resource depletion due to the vanadium pentoxide production. In addition, Rydh [63] also performed an LCA for the VRFB, but the study was published on 1998, which means the data used and results generated are not up-to-date and may not be applicable anymore. Vogt et al. [64] investigated the associated environmental impact on applying the VRFB for stationary energy storage, but the data used are based on Rydh's research. Within our literature review, no other studies are found to investigate the sustainable development of the flow battery. Thus, the only method used for assessment is LCA, and all of these studies are limited to VRFB; flow batteries with different chemistries have not been considered.

Chapter 3: Flow Battery Production: Materials Selection and Environmental Impact

3.1 Abstract

Energy storage systems, such as flow batteries, are essential for integrating variable renewable energy sources into the electricity grid. While a primary goal of increased renewable energy use on the grid is to mitigate environmental impact, the production of enabling technologies like energy storage systems causes environmental impact. Thus, understanding the impact of producing energy storage systems is crucial for determining the overall environmental performance of renewable energy from a systems perspective. In this study, the environmental impact associated with the production of emerging flow battery technologies is evaluated in an effort to inform materials selection and component design decisions. The production of three commercially available flow battery technologies is evaluated and compared on the basis of eight environmental impact categories, using primary data collected from battery manufacturers on the battery production phase including raw materials extraction, materials processing, manufacturing and assembly. In the baseline scenario, production of all-iron flow batteries led to the lowest impact scores in six of the eight impact categories such as global warming potential, 73 kg CO_2 eq/kWh; and cumulative energy demand, 1090 MJ/kWh. While the production of vanadium redox flow batteries led to the highest impact values for six categories including global warming potential, 184 kg CO_2 eq/kWh; and cumulative energy demand, 5200 MJ/kWh. Production of zinc-bromine flow batteries had the lowest values for ozone depletion, and freshwater ecotoxicity, and the highest value for abiotic resource depletion. The analysis highlight that the relative environmental impact of producing the three flow battery technologies varies

with different system designs and materials selection choices. For example, harmonization of the battery system boundary led to freshwater eutrophication and freshwater ecotoxicity values for vanadium redox flow batteries lower than the values for zinc-bromine flow batteries. Regarding alternative material use strategies, we conclude that vanadium redox flow batteries exhibit the lowest potential in four of the eight impact categories including global warming potential at 61 kg CO_2 eq/kWh. In zinc-bromine flow batteries, the titanium-based bipolar plate contributes higher environmental impact compared to carbon-based materials, and the polymer resins used in all-iron flow batteries could be replaced with material with lower potential for ecotoxicity. Overall, the analysis reveals the sources of potential environmental impact, due to the production of flow battery materials, components and systems. The findings from this study are urgently needed before these batteries become widely deployed in the renewable energy sector. Furthermore, our results indicate that materials options change the relative environmental impact of producing the three flow batteries and provide the potential to significantly reduce the environmental impact associated with flow battery production and deployment.

3.2 Introduction

Reducing dependency on fossil fuels by introducing renewable energy such as wind and solar is fundamental to achieving climate mitigation goals [26, 65]. For example, the State of California expects to mitigate climate change through a comprehensive policy-driven initiative that requires 100% conversion of the electricity supply grid to low-carbon sources by the year 2045 with the goal to achieve an 80% decrease in economy-wide greenhouse gas (GHG) emissions by the year 2050 compared to 1990 levels [27, 28]. To maximize the utility

and increase the penetration of renewable energy, utility-scale energy storage is required. In recent years, several advanced energy storage technologies have been developed with battery storage systems seen as one of the most researched and successfully commercialized [58, 66, 67]. Among the various types of battery storage systems, flow batteries represent a promising technology for stationary energy storage due to scalability and flexibility, separation of power and energy, and long durability and considerable safety in battery management [29, 68, 69].

As an emerging battery storage technology, several different types of flow batteries with different redox reactions have been developed for industrial applications [62, 70, 71]. With extensive research carried out in recent years, several studies have explored flow batteries with higher performance and novel structural design [72-74]. Further, studies focused on the cost perspective have explored the economic feasibility of flow battery production [51, 75, 76]. In contrast, little to no assessment of the environmental impact due to flow battery production has been undertaken [62, 77]. Thus, environmental benefit associated with only the use phase of flow batteries in the electric grid could be inaccurately estimated, because detailed data on flow battery production, and corresponding environmental impact, are not available [64, 70, 78]. We know from the extensive literature that environmental impact assessment of lithium-ion battery production has been well documented [79-82]. These early studies established the foundation for future assessments and provided important guidance for both the design of future lithium-ion battery technologies and the evaluation of alternative chemistries [82-84].

Early evaluation of novel flow battery technologies and chemistries could likewise inform better materials selection and system designs before the market becomes well-

established. To fill this gap in established knowledge, the present study focuses on using life cycle assessment to evaluate the environmental impact associated with the industrial-scale production of emerging flow battery energy storage technologies and the corresponding sensitivity to materials selection decisions. As such, this study contributes to the concept of cleaner production in two key ways. First, by providing the environmental impact data necessary to inform sustainability assessments, the development and deployment of flow battery technologies in the energy grid can be guided by data-supported metrics. Second, by providing an understanding of the materials and production methods that contribute disproportionately to high environmental impact, manufacturers can identify the need for selecting alternative material sets or production pathways to improve the environmental impact profile of their technology.

3.3 Material and Methods

The goal of this study is to understand the potential environmental impact associated with the production of flow batteries using life cycle assessment as the methodology for evaluation (see Chapter 2, Section 2.2). We have systematically evaluated three different state-of-the-art flow battery technologies: vanadium redox flow batteries (VRFB), zinc-bromine flow batteries (ZBFB) and all-iron flow batteries (IFB). Eight impact categories are considered, and the contribution by battery component is evaluated. To more deeply evaluate the environmental impact of the materials, energy, and resources used for each component, we investigated the upstream unit processes required for battery production. Sensitivity analysis is included in an effort to inform materials selection decisions and system design.

3.3.1 Flow Battery Technologies

Flow batteries have three major components: cell stack (CS), electrolyte storage (ES), and auxiliary parts or 'balance-of-plant' (BOP) (see **Figure 3.1**) [61]. The cell stack determines the power rating for the system and is assembled from several single cells stacked together. The stack is supported by accessories such as current collectors, gaskets and stack shells or end plates [70, 85-87]. A single cell usually consists of a bipolar plate, electrode, membrane and cell frame [61, 69, 86]. Liquid electrolytes, stored in tanks, determine the energy capacity of the flow battery. The balance of plant includes several peripheral components that support the operation of the battery including recirculation loops consisting of pump and pipes, a battery management system (BMS) for operational control, a power conditioning system (PCS) for current conversion, and other structural supporting accessories [60]. The accessories used in the cell stack and peripheral components included in the balance of plant can vary for different flow batteries.

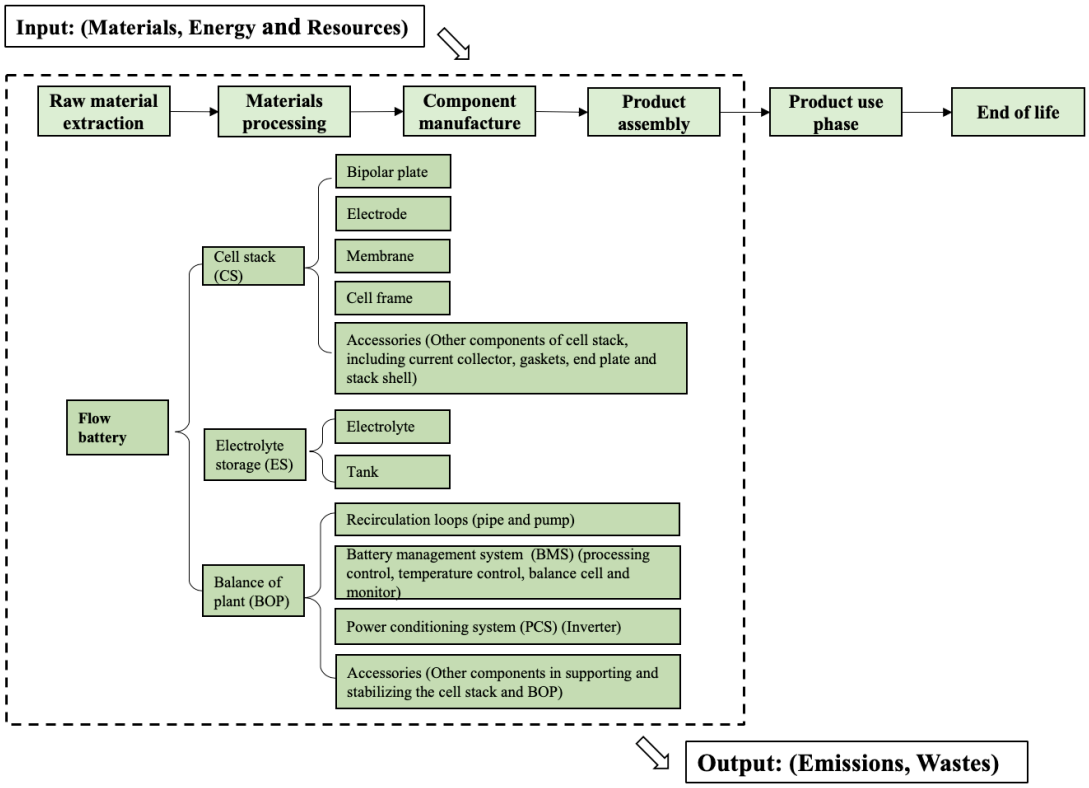

Figure 3.1. The system boundary and classification of flow battery components used in this study are shown schematically. Note that the use phase and end-of-life phase are beyond the scope.

In the current study, we investigated three types of flow batteries: VRFB, ZBFB, and IFB. Their design configurations are presented in **Figure 3.2**, and the corresponding chemical reactions are provided below.

Vanadium Redox Flow Battery (VFRB):

Cathode: $VO^{2+} + H_2O - e^- \rightleftharpoons VO_2^+ + 2H^+$

Anode: $V^{3+} + e^- \rightleftharpoons V^{2+}$

Cell: $VO^{2+} + H_2O + V^{3+} \rightleftharpoons VO_2^+ + V^{2+} + 2H^+$

Zinc-bromine Flow Battery (ZBFB):

Cathode: $2Br^- - 2e^- \rightleftharpoons Br_2$

Anode: $Zn^{2+} + 2e^- \rightleftharpoons Zn$

Cell: $2Br^- + Zn^2 \rightleftharpoons Zn + Br_2$

All-iron Flow Battery (IFB):

Cathode: $2Fe^{2+} - 2e^- \rightleftharpoons 2Fe^{3+}$

Anode: $Fe^{2+} + 2e^- \rightleftharpoons Fe$

Cell: $3Fe^{2+} \rightleftharpoons Fe + 2Fe^{3+}$

The design of VRFB can be categorized as a full-flow system in which all the reacting chemicals are dissolved in a liquid phase, while the ZBFB and IFB are hybrid systems since metal forms as a solid phase deposited on the electrode surface [60, 69]. Typically, a membrane is inserted in each cell to maintain two separate flow paths, as seen in **Figure 3.2** for VRFB and IFB. This is not the case for ZBFB because the cell stack in this battery only requires one flow path, which avoids the use of a membrane and additional storage tanks. More specifically, as specified by the manufacturer, the bipolar plate and electrode in ZBFB is not manufactured from more traditional carbon-based materials [70] but instead is produced from titanium metal. The titanium plate is processed as one integrated conductive board in ZBFB with injection molded polyethylene as the cell frame. In contrast, for VRFB and IFB, the bipolar plate, electrode, membrane and cell frame are compacted together as separate layers in VRFB and IFB with a traditional bipolar plate design. **Table 3.1** provides further details on the battery components and the materials from which they are made.

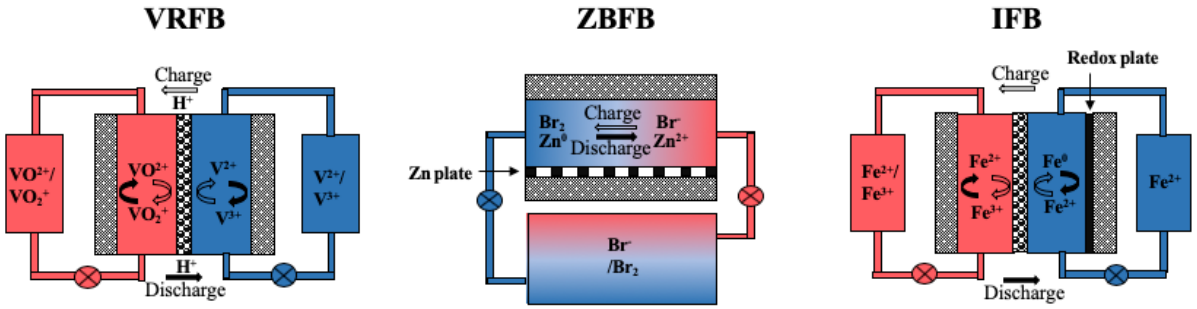

Figure 3.2. The chemical reactions and system design for the three flow battery technologies are illustrated in this schematic. Flow battery types include: VRFB = vanadium redox flow battery; ZBFB = zinc-bromine flow battery; and IFB = all-iron flow battery.

Table 3.1. The component breakdown and materials used in the three flow batteries.

Component	Vanadium redox flow battery	Zinc-bromine flow battery	All-iron flow battery
Cell stack			
Bipolar plate	Graphite	Titanium	Graphite
	Polyethylene	Polyethylene	Vinyl ester
Electrode	Carbon fiber felt	/	Carbon fiber felt
Membrane	Nafion®	/	Polyethylene
Cell frame	Glass fiber	Polyethylene	Glass fiber reinforced polymer
	Polypropylene		
Accessories			
Current collector	Copper	Titanium	Aluminum
Gasket		Polyethylene	Ethylene propylene diene
Supporting shell and frame	Steel	Steel	Steel
		Polyethylene	

	Chlorinated polyvinyl chloride		
Electrolyte storage			
Electrolyte	Hydrochloric acid	Zinc bromide	Ferrous chloride
	Sulfuric acid	Bromide	Potassium chloride
	Vanadium pentoxide	Water	Manganese chloride
	Water		Water
Tank	Polyethylene	Polyethylene	Isophthalic polyester
		Steel	
Balance of plant			
Recirculation loop			
Pump	/	/	/
Pipe	Polyethylene	Polyethylene	Polyvinyl chloride
Battery management system			
Process control system	Electronics	Electronics	Electronics
			Carbon fiber felt
Thermal management system	Fan	Fan	Fan
	Heat exchanger	Heat exchanger	
Power conditioning system	Inverter	Inverter	Inverter
Accessories	Titanium	Polyethylene	/
	Polyvinylidene fluoride	Steel	
		Titanium	
		Aluminum	

3.3.2 System Description and Life Cycle Inventory

The goal of this study is to conduct a detailed environmental impact assessment of flow battery production and to evaluate the sensitivity of the results to materials selection and system design choices. The battery production phase is comprised of raw materials

extraction, materials processing, component manufacturing, and product assembly, as shown in **Figure 3.1**. As this study focuses only on battery production, the battery use and end-of-life phases are not within the scope of the study. Supply chain transportation is also excluded from the scope due to the high level of uncertainty associated with the materials and components, which can be produced in different parts of the world. The functional unit for the production phase is one kWh energy capacity stored in one battery package.

The materials and processing methods associated with each component in the three flow batteries, which were established on the basis of primary inventory data collected from battery manufacturers, are shown in **Figures A1 – A3** in Appendix A**.** These components are further aggregated into the three subsystems mentioned above: cell stack (CS), electrolyte storage (ES) and balance of plant (BOP). The Ecoinvent database provided the reference life cycle inventory (LCI) datasets for materials used [88], including primary extraction (mining), refining, and fabrication. In cases where reference life cycle inventory datasets were not available in Ecoinvent, we relied on published peer-reviewed literature for materials production such as vanadium pentoxide [62, 89, 90], carbon fiber felt [91, 92] and battery membrane materials [93]. We used 'global' (GLO) or 'rest of world' (RoW) data in Ecoinvent in the absence of regional or country-specific data. A complete constitution of the life cycle inventory is provided in detail in the Appendix B.

3.3.3 Impact Assessment

We selected eight midpoint environmental impact categories for characterizing the environmental impact of producing the three flow battery technologies, using SimaPro software [94]. Global warming potential (GWP), ozone depletion potential (ODP), fine

particulate matter (PM), acidification potential (AP) and freshwater eutrophication potential (EP) are calculated using the ReCiPe midpoint 2016 (ReCiPe) method [95]. Freshwater ecotoxicity potential is based on the USETox® model (potentially affected fraction of species (PAF)) using the 'recommended' characterization factors [44-46], the characterization factors for abiotic resource depletion potential are determined using the CML-IA method [36], and fossil fuel energy use is calculated using the cumulative energy demand included in the Ecoinvent database [96]. To fully account for the environmental impact of the materials, energy, and resources used for each component, we also investigated the unit processes in Ecoinvent representing the upstream production activities. The contributions of the unit processes are distributed into five categories: 'materials production', 'energy consumption', 'resource use', 'waste treatment', and 'other related'. To avoid an excessive number of unit processes in the contribution analysis, those unit processes contributing less than 1% to the total impact score are not included in the contribution analysis.

3.3.4 Uncertain Issues and Sensitivity Analysis

While primary data for battery manufacturing is preferable over modeled data, the collection of primary data revealed variability among manufacturers. Specifically, the level of detail in the data was not consistent from manufacturer to manufacturer, especially for the accessories and balance of plant, which provided us with the opportunity to explore the impact of component selection on environmental impact results. Also, with the goal to evaluate the impact of materials selection decisions and potentially guide future flow battery design, the production methods for three select materials are explored in greater depth. Thus, a series of scenarios are considered here to quantify these uncertainties.

To harmonize the different datasets submitted by the manufacturers, we adopted a harmonized battery system boundary with comparable sets of components, and we applied a two-step modification to the life cycle inventory (see details in Appendix C). For the first step, the accessories associated with the cell stack and balance of plant are subtracted from the system. These components are influenced mainly by the design choices of particular flow battery units and are not necessarily core attributes of a given battery technology. Secondly, the life cycle inventory for battery management system and power conditioning system in the balance of plant are harmonized for the three flow batteries to make sure the devices considered for comparison are equivalent. More specifically, these are modified to evaluate production of devices, including electronic systems, not just materials, as was provided by the manufacturer of ZBFB. See Appendix C for details. Hereafter, we refer to this as the 'harmonized system boundary.' Since it is a more harmonized boundary, we use it as the basis for the materials selection based scenario analyses described below.

In an effort to look more deeply into the effect of materials selection and processing choices on the comparative environmental impact of flow battery production, various core materials, specifically vanadium pentoxide, Nafion®, and carbon fiber felt, are explored. Three sets of scenarios are applied, as outlined in **Table 3.2** (additional details are provided in Appendix D). For vanadium pentoxide production, different production processes are considered, as well as different data sources and different allocation methods. For membrane materials, an alternative material, Daramic®, is evaluated; and for the carbon fiber felt, different precursors are considered as well as different data sources. These three materials were selected for the scenario analysis because alternative production methods

and / or materials were readily identifiable but not yet recorded in standardized life cycle inventory databases.

Table 3.2. Scenarios for evaluating uncertainty on select materials in the flow batteries.

Scenarios	Description
Vanadium pentoxide	
Scenario A1	The vanadium pentoxide production from blast furnace crude steel making process based on manufacturing data from PAN. Steel, Sichuan, China (Chen et al., 2015).
Scenario A2	The vanadium pentoxide production from the electric arc furnace steelmaking process based on literature data (Weber et al., 2018).
Scenario A2*	The vanadium pentoxide production plus the allocated impact from the electric arc furnace steelmaking process based on literature data. The steel manufacturing modeling is modified from Ecoinvent and monetary value is used for allocation (Weber et al., 2018).
Scenario A3	The vanadium pentoxide production based on manufacturing data from granulate generated in power plant burning crude oil (Jungbluth and Eggenberger, 2018).
Scenario A4	The vanadium pentoxide production based on stoichiometric calculation from fly ash generated in power plant burning crude oil (Jungbluth and Eggenberger, 2018).
Membrane	
Scenario B1	The Nafion® membrane production based on literature data, the manufacturing modeling is modified from Ecoinvent (Weber et al., 2018).
Scenario B2	The Daramic® membrane production based on literature data, the manufacturing modeling is modified from Ecoinvent (Mohammadi and Skyllas-Kazacos, 1995).
Carbon fiber felt	
Scenario C1	The carbon fiber felt production using polyacrylonitrile (PAN) as a precursor based on modeling data (Romaniw, 2013).
Scenario C2	The carbon fiber felt production using polyacrylonitrile (PAN) as a precursor based on manufacturing data from SGL Carbon SE (Minke et al., 2017).
Scenario C3	The carbon fiber felt production using Rayon as a precursor based on manufacturing data from SGL Carbon SE (Minke et al., 2017).

3.4. Results and Discussion

With the battery technology and assessment framework specified, we begin with a baseline environmental impact assessment of flow battery production using the original data provided by manufacturers. This analysis is followed by the analysis of production impacts

for the harmonized system boundary, and then subsequently by the sensitivity analysis relative to options for vanadium pentoxide production, membrane materials, and carbon fiber felt production methods.

3.4.1 Baseline Environmental Impact Assessment

The results of the baseline environmental impact assessment for the production of the three flow batteries, distributed by component and by unit process, are presented in **Figure 3.3 and 3.4**, respectively. The IFB system exhibits the lowest impact scores in six of the eight impact categories, except ozone depletion potential and freshwater ecotoxicity potential. The ZBFB system has the lowest impact scores for ozone depletion potential and freshwater ecotoxicity potential, but the highest for abiotic resource depletion potential. The VRFB system exhibits the highest impact scores for global warming potential, ozone depletion potential, fine particulate matter, acidification potential, freshwater eutrophication potential, and cumulative energy demand. As shown in **Figure 3.3**, the distribution of impacts contributed by production of individual components varies among the three flow battery technologies, but consistent major contributors are the cell stack (CS) or the electrolyte storage (ES) components, except for the impact categories of freshwater eutrophication potential and abiotic resource depletion potential, which are driven by the balance of plant. The results in **Figure 3.4** help to clarify the reason for these distributions, since the environmental impact is generally driven by the materials and production processes associated with these components. In **Figure 3.4**, the boundary between the gray and colored portions of the bar indicates the 1% cut-off threshold and the corresponding pie charts show the detailed distribution for unit processes included in the portion above the 1% cut-off threshold. Select materials that are major contributors to certain impact

categories are separated out as independent sub-categories in the pie charts to highlight their contributions to the total. For example, production of the vanadium pentoxide (V_2O_5) used in VRFB triggers high impacts for global warming potential, acidification potential, fine particulate matter, and cumulative energy demand, and the production of the tetrafluoroethylene used as a processing material for the Nafion® membrane triggers high impact for ozone depletion potential [63, 96, 97]. For ZBFB, production of the titanium used in the bipolar plate contributes to global warming potential, ozone depletion potential, acidification potential, fine particulate matter, cumulative energy demand, and freshwater ecotoxicity potential; and production of the bromine used as a core chemical in the electrolyte dominates the high abiotic resource depletion potential. For IFB, the production of resin used in the glass fiber reinforced polymer cell frame leads to the high freshwater ecotoxicity potential. Considering each impact category individually, the results show a few trends. For instance, ozone depletion potential and abiotic resource depletion potential are triggered primarily by raw materials production, whereas freshwater eutrophication potential is triggered primarily by waste treatment. Comparing the triggers for the different battery chemistries, for the global warming potential and acidification potential impact categories, the primary triggers for VRFB and IFB are unit processes associated with materials production, while for ZBFB energy consumption during production is more important. For fine particulate matter, energy consumption and resource use contribute more than materials production for ZBFB and IFB, but not for VRFB.

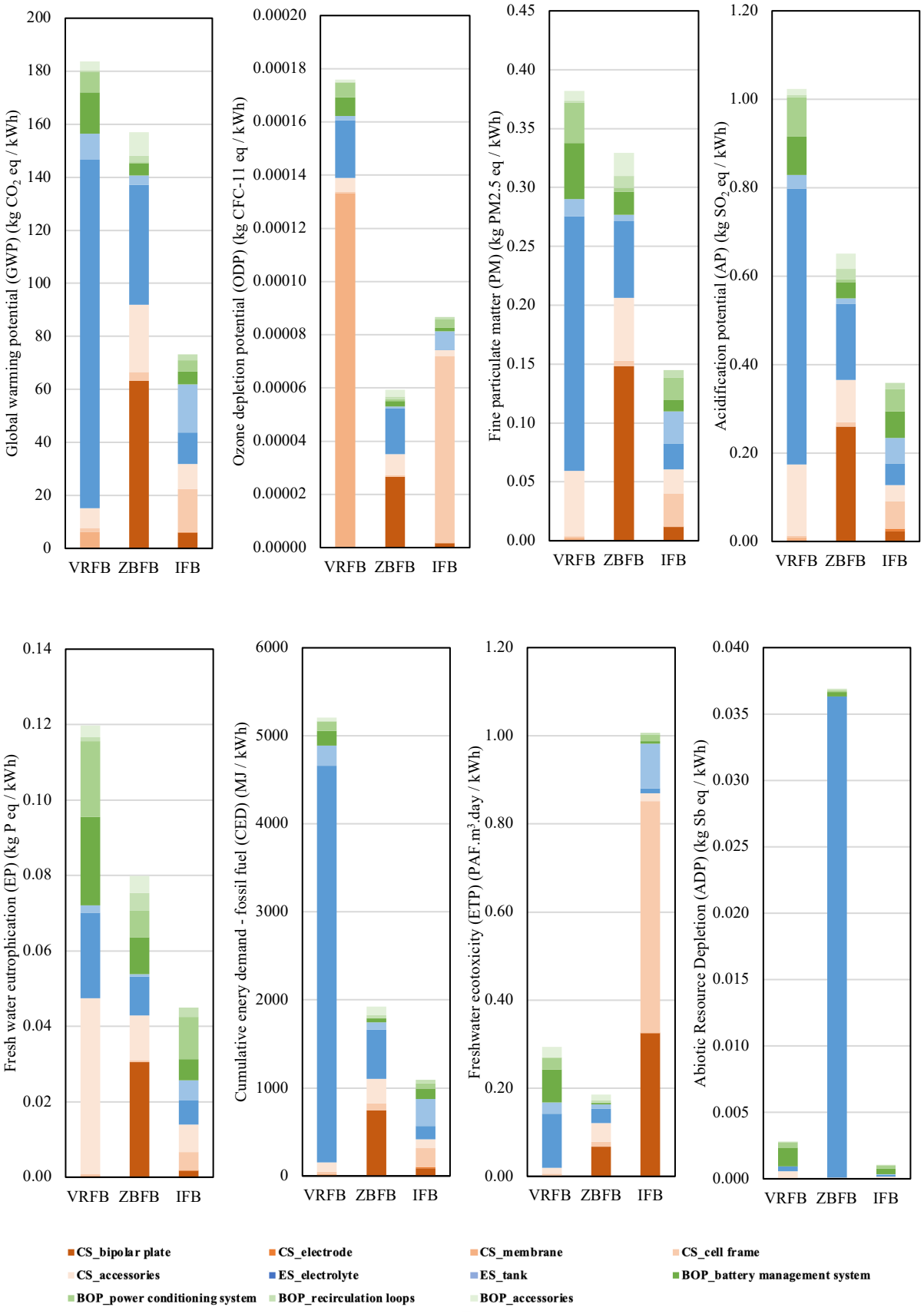
Global warming potential (GWP) (kg CO_2 eq / kWh)
Ozone depletion potential (ODP) (kg CFC-11 eq / kWh)
Fine particulate matter (PM) (kg PM2.5 eq / kWh)
Acidification potential (AP) (kg SO_2 eq / kWh)
Fresh water eutrophication (EP) (kg P eq / kWh)
Cumulative enery demand - fossil fuel (CED) (MJ / kWh)
Freshwater ecotoxicity (ETP) (PAF.m^3.day / kWh)
Abiotic Resource Depletion (ADP) (kg Sb eq / kWh)
VRFB ZBFB IFB
CS_bipolar plate
CS_electrode
CS_membrane
CS_cell frame
CS_accessories
ES_electrolyte
ES_tank
BOP_battery management system
BOP_power conditioning system
BOP_recirculation loops
BOP_accessories

Figure 3.3. The potential environmental impact of flow battery production is shown, as distributed by battery component. Flow battery types include: VRFB = vanadium redox flow battery; ZBFB = zinc-bromine flow battery; and IFB = all-iron flow battery. Flow battery components include: cell stack (CS), electrolyte storage (ES) and balance of plant (BOP).

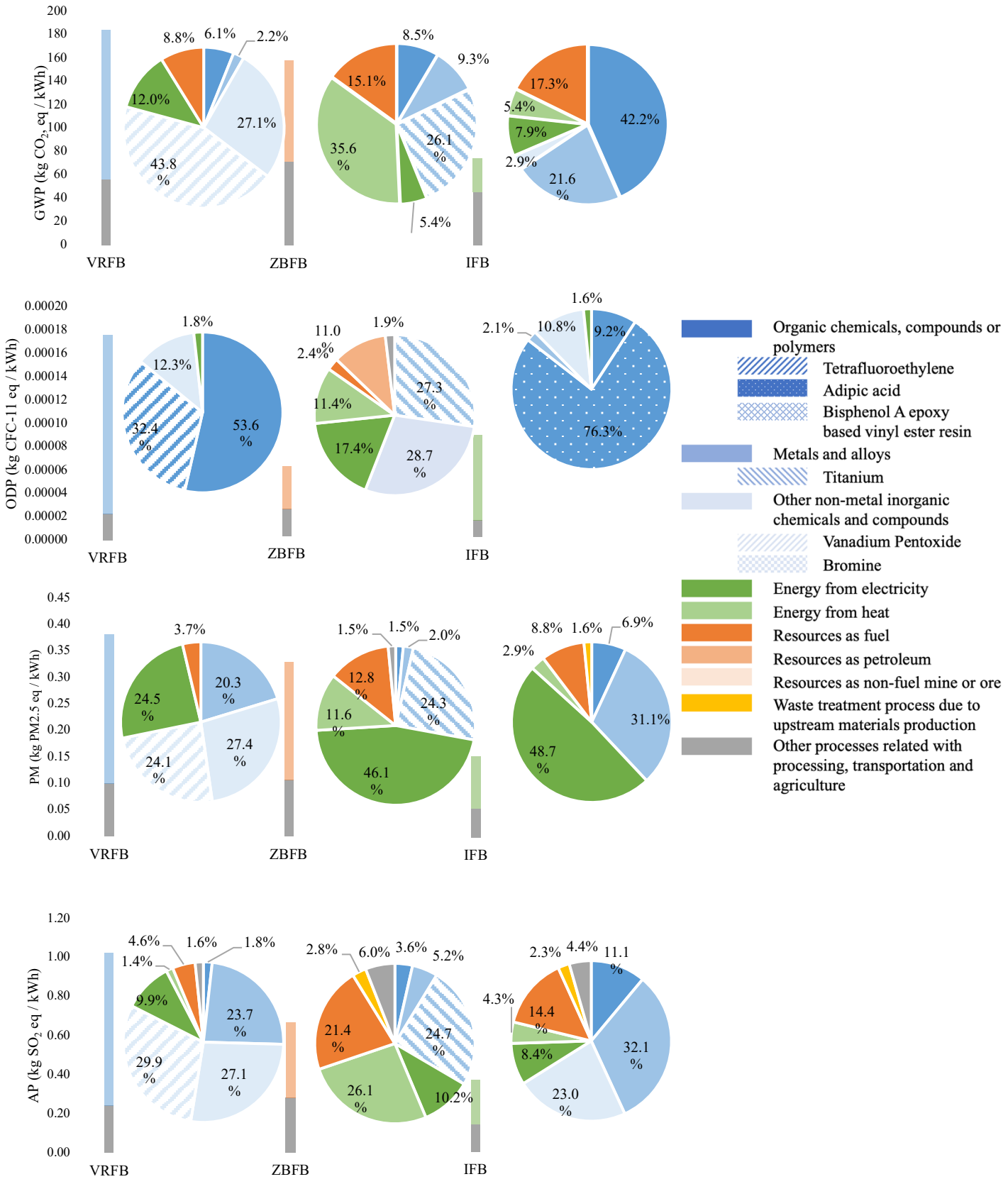
GWP (kg CO_2, eq / kWh)
200
180
160
140
120
100
80
60
40
20
0
8.8%
6.1%
2.2%
12.0%
27.1%
43.8 %
8.5%
9.3%
15.1%
35.6 %
26.1 %
5.4%
17.3%
5.4%
7.9%
2.9%
42.2%
21.6 %
VRFB
ZBFB
IFB
ODP (kg CFC-11 eq / kWh)
0.00020
0.00018
0.00016
0.00014
0.00012
0.00010
0.00008
0.00006
0.00004
0.00002
0.00000
1.8%
12.3%
32.4 %
53.6 %
11.0
2.4%
1.9%
11.4%
27.3 %
17.4%
28.7 %
1.6%
2.1%
10.8%
9.2%
76.3%
VRFB
ZBFB
IFB
PM (kg PM2.5 eq / kWh)
0.45
0.40
0.35
0.30
0.25
0.20
0.15
0.10
0.05
0.00
3.7%
24.5 %
20.3 %
24.1 %
27.4 %
1.5%
1.5%
2.0%
12.8 %
11.6 %
24.3 %
46.1 %
8.8%
1.6%
6.9%
2.9%
31.1%
48.7 %
VRFB
ZBFB
IFB
AP (kg SO_2 eq / kWh)
1.20
1.00
0.80
0.60
0.40
0.20
0.00
4.6%
1.6%
1.8%
1.4%
9.9%
23.7 %
29.9 %
27.1 %
2.8%
6.0%
3.6%
5.2%
21.4 %
24.7 %
26.1 %
10.2%
2.3%
4.4%
11.1 %
4.3%
14.4 %
8.4%
32.1 %
23.0 %
VRFB
ZBFB
IFB
Organic chemicals, compounds or polymers
Tetrafluoroethylene
Adipic acid
Bisphenol A epoxy based vinyl ester resin
Metals and alloys
Titanium
Other non-metal inorganic chemicals and compounds
Vanadium Pentoxide
Bromine
Energy from electricity
Energy from heat
Resources as fuel
Resources as petroleum
Resources as non-fuel mine or ore
Waste treatment process due to upstream materials production
Other processes related with processing, transportation and agriculture

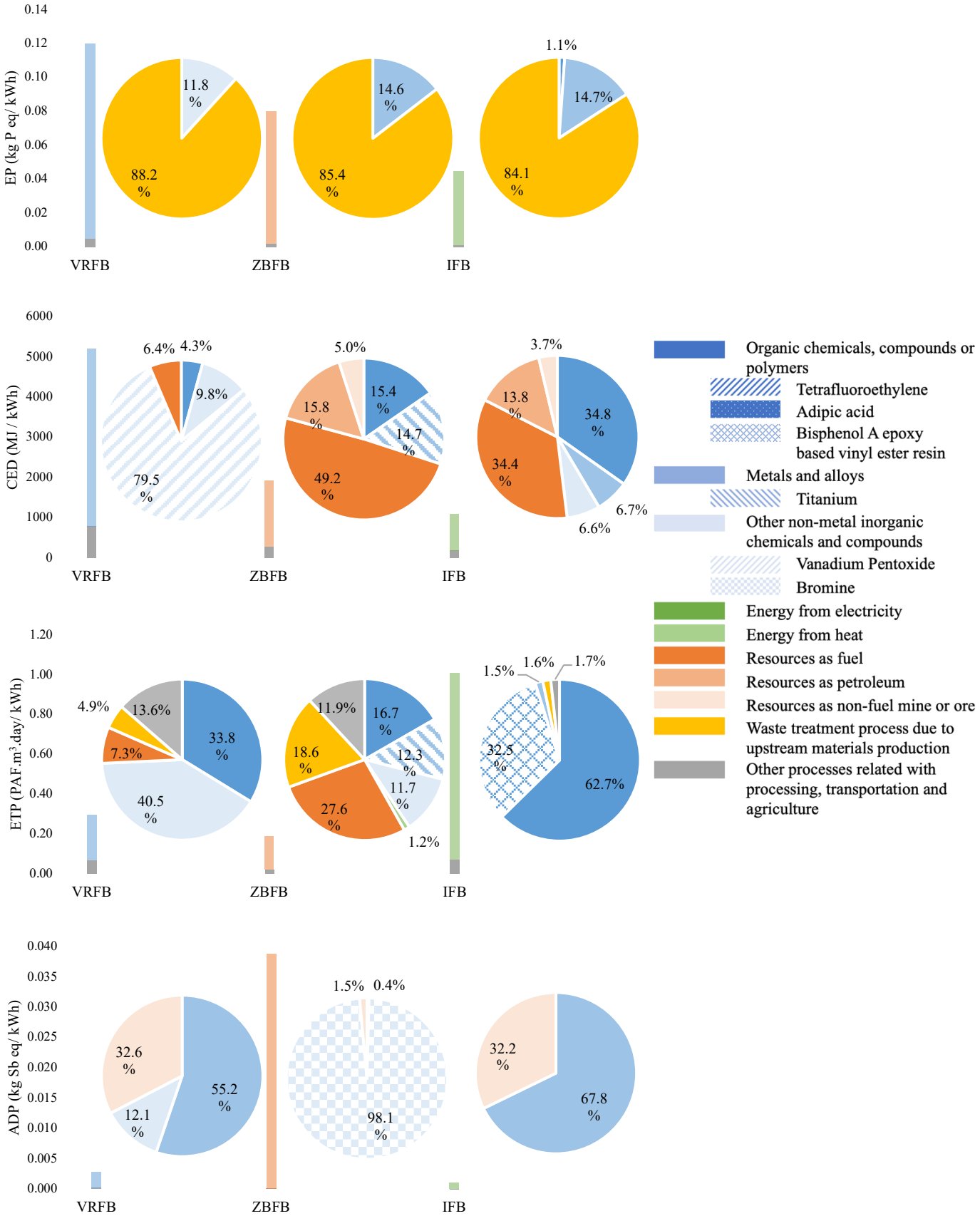
EP (kg P eq/ kWh)
0.14
0.12
0.10
0.08
0.06
0.04
0.02
0.00
11.8 %
88.2 %
14.6 %
85.4 %
1.1%
14.7%
84.1 %
VRFB
ZBFB
IFB
CED (MJ / kWh)
6000
5000
4000
3000
2000
1000
0
6.4%
4.3%
9.8%
79.5 %
5.0%
15.4 %
15.8 %
14.7 %
49.2 %
3.7%
13.8 %
34.8 %
34.4 %
6.7%
6.6%
ETP (PAF.m3.day/ kWh)
1.20
1.00
0.80
0.60
0.40
0.20
0.00
4.9%
13.6%
33.8 %
7.3%
40.5 %
11.9%
16.7 %
18.6 %
12.3 %
11.7 %
27.6 %
1.2%
1.5%
1.6%
1.7%
32.5 %
62.7%
ADP (kg Sb eq/ kWh)
0.040
0.035
0.030
0.025
0.020
0.015
0.010
0.005
0.000
32.6 %
55.2 %
12.1 %
1.5%
0.4%
98.1 %
32.2 %
67.8 %
Organic chemicals, compounds or polymers
Tetrafluoroethylene
Adipic acid
Bisphenol A epoxy based vinyl ester resin
Metals and alloys
Titanium
Other non-metal inorganic chemicals and compounds
Vanadium Pentoxide
Bromine
Energy from electricity
Energy from heat
Resources as fuel
Resources as petroleum
Resources as non-fuel mine or ore
Waste treatment process due to upstream materials production
Other processes related with processing, transportation and agriculture

Figure 3.4. The contributions to the eight impact categories are shown, distributed by materials use, energy consumption, resource use, waste treatment, and other processes, and based on the analysis of unit processes adopting a 1% cut-off value of total contribution for production of the three flow batteries, with tetrafluoroethylene, adipic acid, bisphenol A epoxy-based vinyl ester resins, titanium, vanadium pentoxide, and bromine, highlighted separately as major triggers for at least one or more impact categories.

We also highlight findings for global warming potential, freshwater ecotoxicity potential, and abiotic resource depletion potential. The high total impact of global warming potential for VRFB is primarily due to production of the electrolyte, which accounts for 72% of the total score. For ZBFB, production of the bipolar plate is the highest contributor at 40%, followed by production of the electrolyte (29%). For the IFB, the impact is largely due to production of the storage tank (39%) and the cell frame (22%). Looking closely at the unit process analysis for global warming potential, for VRFB and ZBFB, the products derived from metallurgical processes contribute more to the higher global warming potential than do other materials used in the flow battery system. For example, the high global warming potential of electrolyte production in VRFB is due to the use of V_2O_5, which is a by-product of steel manufacturing [93]. The bipolar plate for ZBFB contains titanium, the production of which generates a higher global warming potential than that of the graphite-based materials used in the other two flow batteries. For IFB, production of several organic substances used as processing materials for the storage tank and cell frame correspond to high global warming potential scores causing these two components to be the highest contributors to

global warming potential. Results on fine particulate matter and acidification potential follow similar trends.

For freshwater ecotoxicity potential, the IFB system has the highest impact score due to production of the cell frame (52%) and the bipolar plate (32%), and the unit process analysis from **Figure 3.4** indicates that this is primarily due to the production of organic compounds especially the bisphenol-A epoxy-based vinyl ester resin. In contrast, for VRFB and ZBFB, their bipolar plates are made of graphite and titanium, respectively, and the cell frames are made of polyethylene - both of which do not require production of materials with high freshwater ecotoxicity potential. Instead, the relatively low freshwater ecotoxicity potential value for VRFB is caused primarily by the production of non-metal inorganic materials. For ZBFB, which has the lowest freshwater ecotoxicity potential value, the titanium bipolar plate is the component generating the highest freshwater ecotoxicity potential due to the production of titanium. Interestingly, the ZBFB system has a significantly larger abiotic resource depletion potential than VRFB and IFB. From the results in **Figure 3.4** we find the production of bromine contributes to a much higher resource depletion potential than any of the other materials. The remainder is then due to the production of metals such as copper and gold contained in electronic devices, which is consistent with the results for VRFB and IFB.

3.4.2 Harmonized Battery System Boundary Environmental Impact Assessment

The modifications to the battery system boundary are intended to harmonize the different datasets provided by the battery manufacturers. The previously defined battery system boundary for the baseline results was modified to a harmonized battery system by

eliminating the accessories and modifying the battery management system and power conditioning system components. Further details are provided in Section 2.4. The results from the harmonized battery system boundary analysis are compared to the baseline results in **Figure 3.5** (detailed distributions by component, which are analogous to those in **Figure 3.3**, are presented in **Figure C1** in Appendix C). Due to the nature of this harmonization, the impact values for VRFB and IFB are reduced in all cases because the system boundary has been curtailed for these two battery systems. The subtraction of the accessories has the greatest effect on these impact reductions, compared to the effect of modifying the balance of plant components, suggesting that these components could perhaps be better designed to minimize the impact caused by the production of these accessories. The most significant effect of subtracting the accessories is seen for the freshwater eutrophication potential value for VRFB; fine particulate matter and acidification potential values for VRFB are also noticeably changed. The changes for IFB are consistently small.

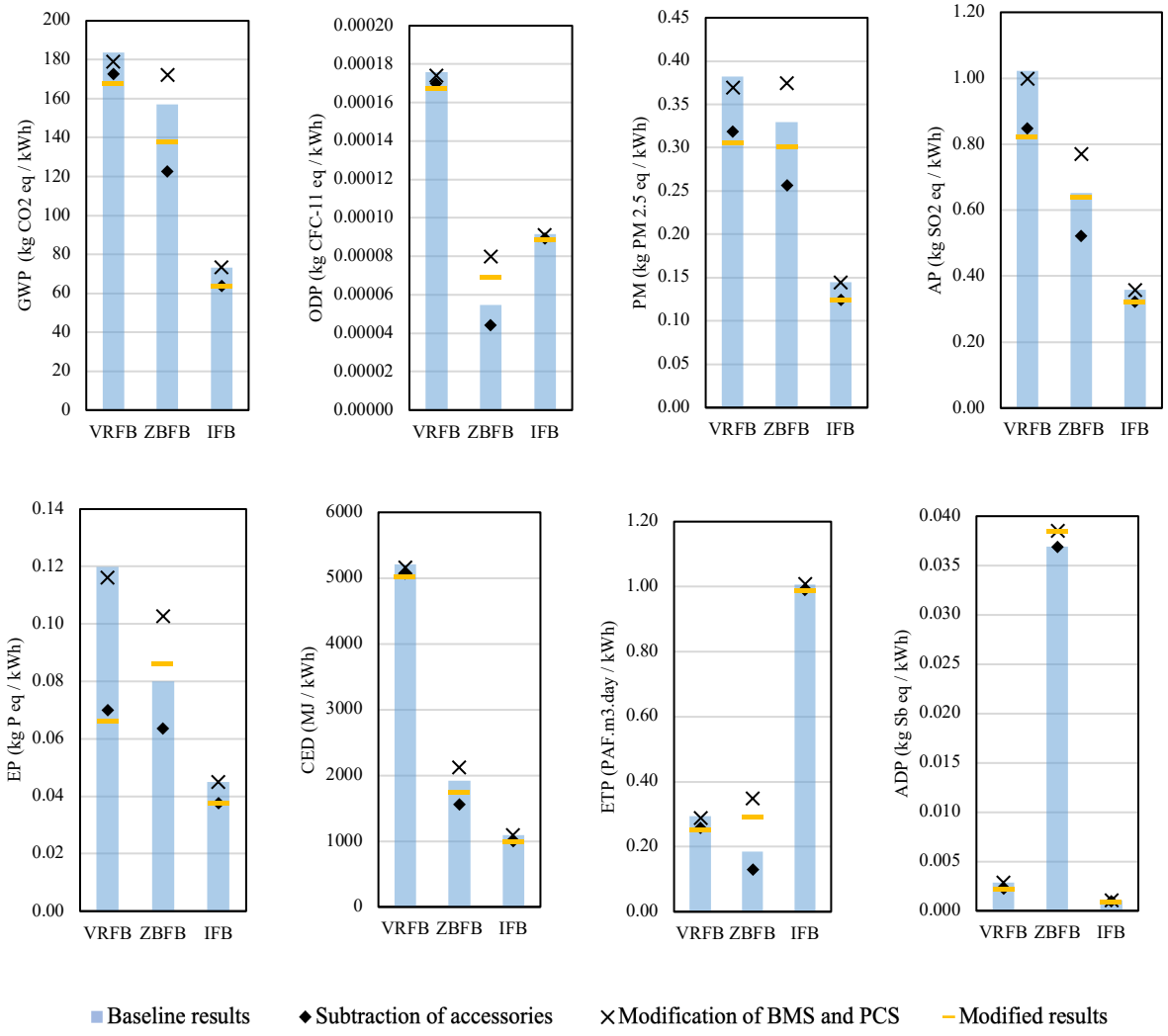

Figure 3.5. The change in environmental impact results are shown for production of the three flow batteries given the modifications to the battery system boundary to harmonize across the three battery types, which includes subtracting the accessories and modifying the battery management system and power conditioning system components.

For ZBFB, the potential environmental impacts are mixed. Subtracting the accessories reduces the impact, especially for global warming potential, fine particulate matter, acidification potential, and freshwater eutrophication potential. However, the modification of the balance of plant leads to increased impact values for all impact categories, because the

battery system boundary has been expanded in this case to include production of electronic devices, not just materials, suggesting that the role of the electronic devices should not be neglected for these battery systems. When the two modifications are combined, the results for ZBFB lead to net increases in ozone depletion potential, freshwater eutrophication potential, freshwater ecotoxicity potential and abiotic resource depletion potential, and net decreases in the other categories (global warming potential, fine particulate matter, and acidification potential). Importantly, this harmonization lead to changes in the relative rankings of the three flow battery technologies for a few of the impact categories: ZBFB is now the worst for freshwater eutrophication potential, second for freshwater ecotoxicity potential and essentially equal to VRFB for fine particulate matter; which highlights the importance of this sensitivity analysis in comparing the production of the three flow battery systems. The exclusion of the accessories and the modifications to the balance of plant represent a battery system boundary that highlights the core functional components in the flow batteries, therefore, we used the results after this harmonization for the remaining sensitivity analyses (noted by the yellow bars in **Figure 3.5** and **Figure C1** in Appendix C).

3.4.3 Sensitivity Analysis on Materials Selection and Processing

In this section, the relative environmental impact associated with production of different materials selection options was investigated in an effort to highlight that the use of alternative materials may reduce overall environmental impact of flow battery production.

3.4.3.1 Vanadium Pentoxide

The results shown in **Figure 3.3 – 3.5**, support the conclusion that V_2O_5 production plays an important role in several impact categories including global warming potential, fine particulate matter, acidification potential and especially cumulative energy demand for the VRFB system. Of the four processing routes investigated in this scenario analysis, the V_2O_5 produced in Scenarios A1 and A2 (and A2*) is a by-product of steel production, but for Scenarios A3 and A4, it is produced from crude oil burning residues. **Figure 3.6** presents the environmental impact results for V_2O_5 production normalized to per kg for each of the five scenarios listed in **Table 3.2.** Significant variations are observed. In general, the V_2O_5 produced from crude oil corresponds to less environmental impact than the V_2O_5 produced from steel production. Also, the differences between the two crude oil scenarios are relatively small, whereas there are substantial differences seen for the various scenarios based on steel production. Scenario A1 is based on actual production data, whereas Scenario A2 uses simulated data, and the process conditions are different. The large differences in global warming potential and cumulative energy demand values for these two scenarios correspond to the different production methods, as the steel in Scenario A1 is made using a blast furnace which consumes large amounts of hard coals (see Appendix D), while in Scenario A2, the steel is made using an electric arc furnace. The higher fine particulate matter and freshwater eutrophication potential values for Scenario A2 are due to the emission of sulfur dioxide calculated based on the stoichiometric calculation, while for Scenario A1, there is a desulphurization process reported as a pretreatment which reduces the sulfur dioxide emissions. Also, comparing the results of Scenario A2 and Scenario A2*, the allocated impacts from the steel production contribute to a rather high impact score, especially for global

warming potential, ozone depletion potential, freshwater eutrophication potential, and cumulative energy demand. Overall, the results for Scenario A2* are the highest, except for the impact category of cumulative energy demand, for which Scenario A1 is highest. These wide variations in estimated potential environmental impact associated with V_2O_5 production are influenced by multiple factors such as extraction sources, processing routes and allocation rules. Given the variations described here, there is clearly a need for a unified and systematic life cycle inventory data set for V_2O_5 production.

The effect of these changes in V_2O_5 production not only affect the environmental impact categories directly, as described above, but they also translate to corresponding effects on the environmental impact associated with producing the VRFB flow battery system, as shown in **Figure 3.7**; the earlier results for ZBFB and IFB (taken from **Figure 3.5**) are included for comparison. For many of the impact categories, the different scenarios lead to changes in the relative ranking among the three flow battery technologies. For instance, if V_2O_5 produced from crude oil burning residue is assumed (Scenarios A3 or A4), production of VRFB no longer corresponds to the highest global warming potential, fine particulate matter, acidification potential, and cumulative energy demand values, and actually ranks lowest for global warming potential and cumulative energy demand under Scenario A3. If Scenario A2 is used, production of VRFB no longer corresponds to the highest values for global warming potential and cumulative energy demand, but presents increased values for fine particulate matter and acidification potential. For the impact categories of ozone depletion and abiotic resource depletion potential, however, the flow battery rankings are independent of the scenarios. When adopting Scenario A2*, which is the only scenario that considers the allocated emissions from the steel production, the impact values increase for

global warming potential, ozone depletion potential, fine particulate matter, acidification potential, freshwater eutrophication potential, and freshwater ecotoxicity potential, but decrease for cumulative energy demand; these changes do not, however, result in changes in rank.

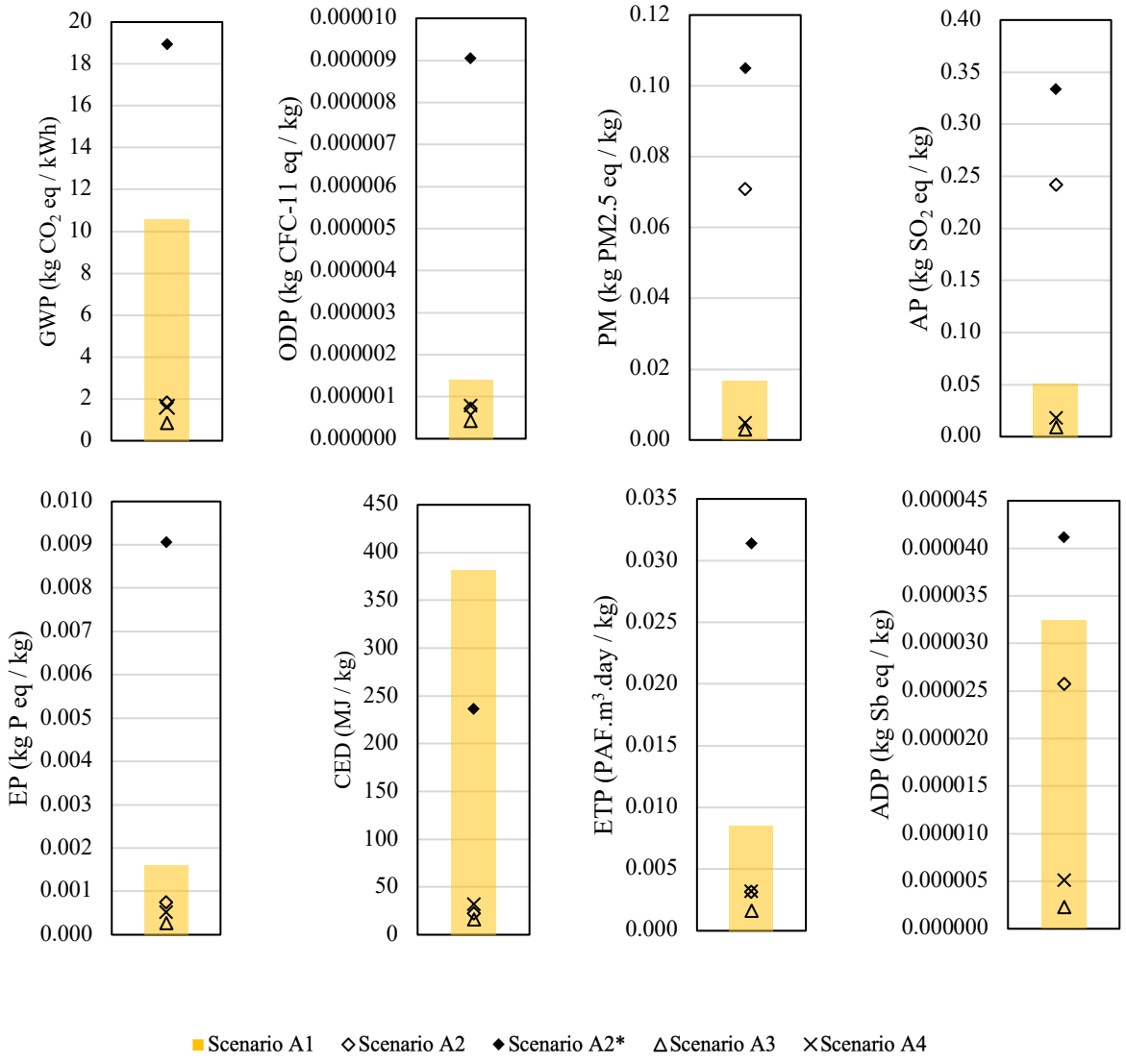

Figure 3.6. Variations in environmental impact per kg of vanadium pentoxide production are shown, assuming different scenarios for extraction sources and processing routes.

3.4.3.2 Membrane Materials

The second scenario analysis focuses on the membrane materials used for the flow batteries. Although Nafion® is commonly used as the membrane material in flow batteries, various alternative membrane materials have also been developed for battery use. As described in a recent publication by Shi et al., [98], newly developed membrane materials have been tested with higher ion conductivity and stability that could improve the battery performance, however, the associated production data are not yet complete for a comprehensive impact assessment. Nafion®, a sulfonated fluorocarbon polymer, is currently the most widely applied membrane material in [99, 100]. From the results shown in **Figure 3.3**, the major contributor to ozone depletion potential for VRFB production is the Nafion® membrane, which corresponds to 76% of the total ozone depletion potential. A recent life cycle assessment study on VRFB compared the Nafion® membrane with sPEEK, another sulfonated membrane, the results of which indicate that production of Nafion® would trigger a much higher environmental impact than sPEEK [62]. Here, with Scenario B2, we consider production of a non-sulfonated alkane-based alternative membrane material, Daramic®, the data for which are derived from a literature review (see details provided in Appendx F). The results presented in **Figure D1** (in Appendix D) show that the environmental impact associated with production of a Nafion® membrane is substantially larger than that for a Daramic® membrane. Whereas the Daramic® membrane consists primarily of polyethylene and silica, the higher impact for Nafion® are caused by the complex synthesis processes including fluorination and sulfonation with the use of several high impact polymers such as tetrafluoroethylene (TEF) [62, 97, 101]. The results for Scenario B2 are translated into impacts values for VRFB production, as shown by the yellow

circles in **Figure 3.7**. Notably, the ozone depletion potential value is significantly reduced, to the point that VRFB is now ranked lowest for this impact category.

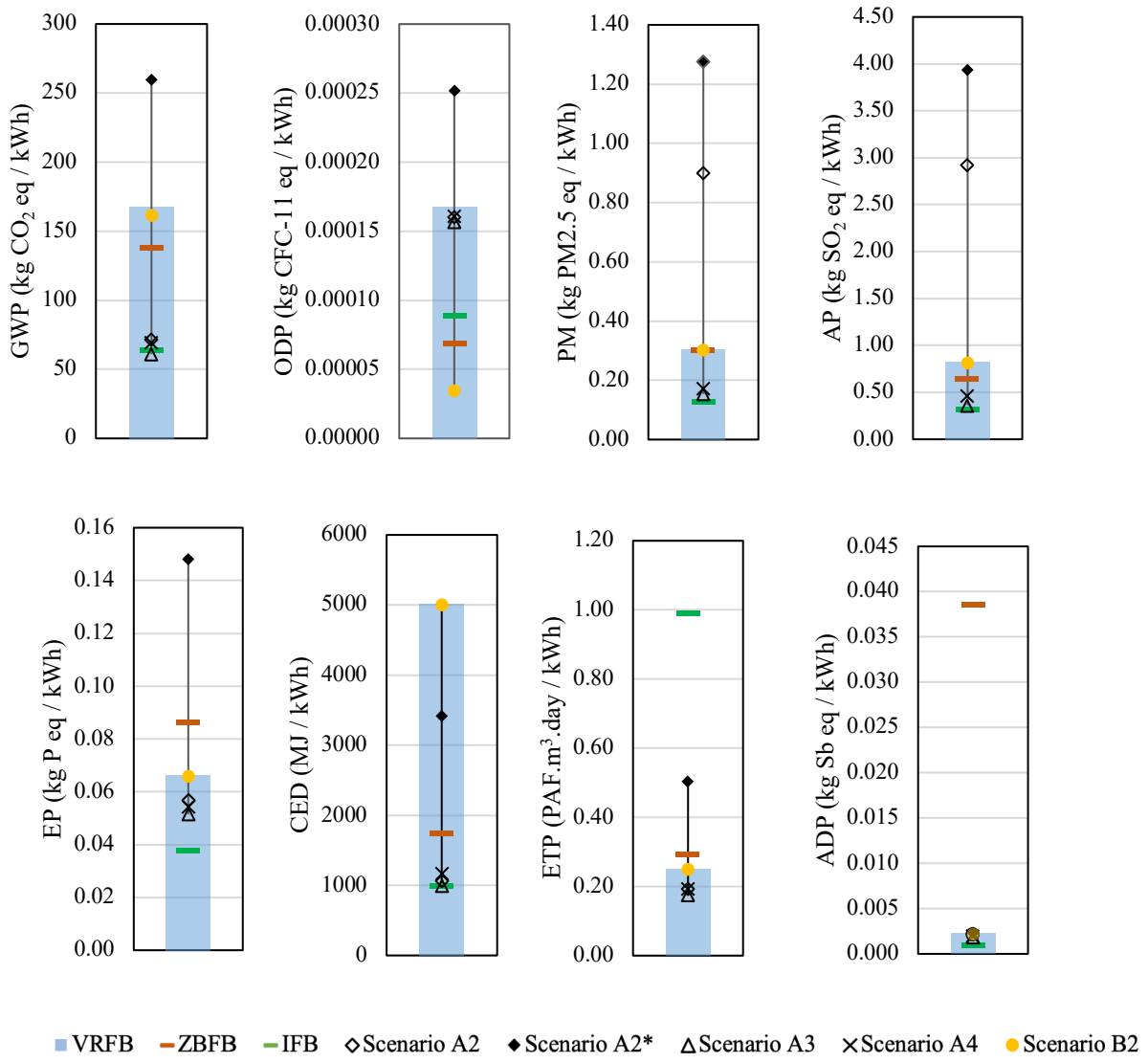

Figure 3.7. The environmental impact results for flow battery production are compared, given the various scenarios for vanadium pentoxide produced from electric arc furnace (Scenario A2 and Scenarios A2*) and crude oil (Scenarios A3 and A4). The results corresponding to production of alternative membrane materials are also investigated (Scenario B2).

3.4.3.3 Carbon Fiber Felt

The use of carbon fiber felt as electrodes in flow batteries is becoming increasingly popular due to good electrical conductivity, light weight and high electrochemical stability [102]. Although the amount of carbon fiber felt used in a flow battery system is small and does not significantly influence the total environmental impact, the relatively high energy consumption for carbon fiber felt production is considered here as the high-temperature pyrolysis may trigger high environmental impact [91, 92]. In our battery systems, the carbon fiber felt is used as electrodes for VRFB and IFB. The scenario analysis considers three different carbon fiber felt production methods (see **Table 3.2**, as well as more detailed information provided in Appendix D). The results per kg felt, shown in **Figure D2** in Appendix D, indicate that production of the rayon-based carbon felt results in higher impact than that for the PAN-based carbon felt. However, there are still uncertainties associated with the PAN-based carbon felt, especially for fine particulate matter, acidification potential and freshwater eutrophication potential, as seen when comparing Scenarios C1 and C2, which are based on modeling data and manufacturing data, respectively. Despite the significant variations seen in **Figure D3** (in Appendix D), when translated to the impact assessment for producing the flow battery systems, as shown in **Figure D3** (in Appendix D), the effect becomes negligible due to the small overall impact of the carbon fiber felt electrodes. In addition, it is noted that another electrode material - graphite felt, can be prepared from carbon fiber felt with one more step – graphitization [103]. However, the impact of graphite felt production is not considered because this material was not specified by the manufacturers that provided data for this assessment, and choosing graphite felt

instead of carbon felt is unlikely to significantly change the total impact results given the small amount and minor impact of carbon fiber felt used in the battery system.

3.5 Conclusions

The investigation into the production of three flow batteries provides important guidance on potential environmental impact associated with battery component manufacturing, upstream production activities, battery system designs, and materials selection choices, given state-of-the-art commercial technologies. In particular, the findings and conclusions of this study are as follows: While the environmental impact clearly depends on the flow battery chemistry, especially the selection of electrolyte and cell stack materials, it also depends on the balance of plant design and production methods. Furthermore, for VRFB, because the vanadium pentoxide is the primary driver for five impact categories, alternative production routes can significantly reduce the potential impact. Also, the high ozone depletion associated with production of the Nafion® membrane can be avoided if alternative materials such as Daramic® can be used while achieving equivalent performance. In ZBFB, production of the titanium-based bipolar plate corresponds to higher environmental impact compared to production of carbon-based materials, and the polymer resins used in IFB could potentially be replaced with lower ecotoxicity materials. The results of this study also highlight that some of the environmental impact is associated with materials selection and production options that could be difficult to modify. For example, the bromine used in ZBFB electrolytes triggers a much higher abiotic resource depletion value compared to the electrolytes used in VRFB and IFB. Also, although the integrated titanium bipolar plate installed in ZBFB avoids the use of additional membranes and electrodes, which

avoids potential impacts such as the high ozone depletion triggered by the Nafion® in the VRFB, the processes used for titanium production lead to higher values for global warming potential, fine particulate matter, acidification potential, and freshwater eutrophication potential. In the current landscape, the materials used to produce IFB exhibit better environmental impact performance due to the use of low impact iron-based electrolyte and carbon-based cell stack. While flow batteries do offer some use-phase advantages such as long cycle life and separation of power and energy when compared to alternatives such as lithium-ion systems, the IFB, ZBFB, and VRFB systems considered here all exhibit similar use-phase efficiencies. Thus, the differences in the environmental impact profile between these flow battery technologies are due to the materials selection and battery production aspects. Tradeoffs between the use-phase benefits and production phase impacts are, however, not yet well understood and are the topic of an ongoing study investigating the net environmental benefits of flow batteries as a technology class for grid applications by considering various temporal and geographical characteristics and dynamic renewable resource profiles.

More broadly, this study highlights 1) that materials selection choices, even within the same technology, can significantly affect the environmental impact of production, 2) that significant uncertainty exists in the environmental impact data for the materials and production processes used to fabricate energy storage systems. Further, this study contributes new data on the life cycle environmental impacts of emerging flow battery production and their distribution across material choices and production pathways. This enables 1) flow battery manufacturers to make informed decisions about the selection of materials and methods used to fabricate their products and 2) environmental impact

assessments to account for uncertainty associated with materials selection and production pathways. Conventionally, environmental impact is only one of many factors influencing materials selection decisions. Considerations such as material cost and level of performance are often prioritized above environmental impact considerations, yet tradeoffs may exist between these criteria. Therefore, further research into developing materials and production methods that simultaneously yield improvements relative to all criteria, e.g., low-cost, high-performance, and low environmental impact options, is needed. With evolving technologies, batteries with newly developed materials, designs and production methods, which correspond to lower environmental impact, should be pursued.

Chapter 4: Human Health Toxicity Assessment of Substances in Energy Storage Batteries

4.1 Abstract

Battery storage technologies such as redox flow batteries (RFBs) and lithium-ion batteries (LIBs) are appealing candidates for large scale energy storage requirements to support the integration of renewable energy into electricity grids. To ensure that their environmental benefits outweigh the negative impacts of producing battery storage systems, it is vital to assess the potential toxicity hazard and health impacts of battery materials and waste emissions during production. Here, we present a case study based on integrating life cycle impact assessment (LCIA) and chemical hazard assessment (CHA) approaches to characterize the toxicity hazard and health impacts associated with the production of six types of battery storage technologies including three RFBs: vanadium redox flow battery (VRFB), zinc-bromine flow battery (ZBFB), and the all-iron flow battery (IFB) alongside three LIBs: lithium iron phosphate (LFP), lithium nickel cobalt manganese hydroxide (NCM), and lithium manganese oxide (LMO). We used materials inventory data from manufacturers for RFBs, and from published sources for LIBs. GreenScreen® for Safer Chemicals v1.4 (GreenScreen®) and USETox® v2.0 (USETox®) were used for CHA and LCIA, respectively. The results show that LIBs use higher numbers of hazardous chemicals, whereas RFBs use higher amounts of hazardous chemicals, probably due to the relatively low energy density of RFBs. The vanadium pentoxide used in VRFB and lithium nickel cobalt manganese hydroxide used in NCM are chemicals of high concern. There were no hazard endpoints identified for the

materials used in LFP and LMO due to a lack of toxicity data. The assessment of chemicals used in the manufacturing process showed many chemicals of high concern, which indicated an opportunity for reducing the environmental impacts by substituting safer alternatives. We found higher impacts on human health outcomes for LIBs than for RFBs, noting that uncertainties associated with the characterization factors demand caution in interpreting the results. This study's comprehensive evaluation of toxicity hazard and life cycle impacts for materials, components, and systems associated with the six battery energy storage technologies provides an important foundation for the identification of safer alternatives to ensure that the environmental benefits outweigh the costs of deploying batteries in the electricity grid to support the integration of renewable energy resources.

4.2 Introduction

Concerns about environmental issues such as climate change, air pollution, and water pollution have motivated the deployment of alternative energy resources and the technologies that support them. For example, California is pioneering solutions through implementing policies such as the Renewables Portfolio Standard (RPS) and Senate Bill 100 which requires 60 percent of retail electricity sales to be sourced from renewable resources by 2025 and 100% of the electric demand to be met by zero-carbon electricity resources by 2045 [27, 28]. Meeting the RPS and SB 100 goals will likely depend strongly on the use of wind and solar energy. However, these resources can cause mismatching of electricity demand and supply due to the variability of their electricity generation profile. Energy storage can be an effective way to compensate for this mismatch and enable a high renewable penetration level on the electric grid, and in particular, battery storage

technologies provide a solution towards this end. Currently, various battery technologies are being considered to fulfill such a role such as lithium-ion batteries and redox flow batteries. Between these two battery technologies, lithium-ion batteries are currently ubiquitous due to their high energy density enabling use in portable applications and gradually lower cost [104]. In addition to enabling the proliferation of electric vehicles, lithium-ion batteries are also suitable for large scale grid-connected energy storage [64]. Although flow batteries are figured to have lower energy density compared to lithium-ion batteries, they have the potential to more easily scale up to the large energy storage capacities required to support the RPS due to their ability to independently configure their power capacity and energy capacity. These benefits render flow batteries as a potential key component of renewable energy system design as well.

While renewable energy systems are considered to have lower environmental impacts compared to non-renewable alternatives, the manufacturing of batteries to enable their use is not burden-free. Sustainability assessment fulfills the key role of identifying the environmental trade-offs associated with the deployment of renewable energy systems, yet most of the efforts have focused on their functional performance and economic feasibility [47, 52, 72-74]. Fortunately, research projects focusing on sustainability assessment of batteries are emerging under the pressure to promote cleaner energy use. For example, life cycle assessment has been done to investigate the environmental impact of implementing battery storage technologies [62, 81-82, 84]. Materials flow analysis has been applied to explore the resource criticality during the materials supply chain [83]. Risk assessment was conducted to study the physical hazards (e.g., flammablity) causing chemicals exposure [105, 106]. However, this base of literature does not contain a study that has systematically

evaluated the toxicity hazard and human health effects due to materials use through the whole production chains. Additionally, most of the literature has focused on relatively mature, commercially available technologies such as lead-acid batteries and conventional lithium-ion batteries. Therefore, there is a need to perform these assessments for emerging energy storage technologies such as advanced lithium-ion and flow batteries to better support decision-making regarding the development and deployment of grid-connected energy storage.

The goal of this study is to investigate the toxicity hazard and life cycle human health impact on the production of battery storage technologies to identify and minimize the associated adverse effects existed in the battery production chain. We systematically evaluated six types of battery storage technologies, which include three redox flow batteries (RFBs): vanadium redox (VRFB), zinc-bromine (ZBFB), and all-iron (IFB); and three lithium-ion batteries(LIBs): lithium iron phosphate (LFP), lithium nickel cobalt manganese hydroxide (NCM), and lithium manganese oxide (LMO). We built on previously published results of environmental impacts of the batteries [80, 81], and we considered opportunities to minimize the use of toxic chemicals and identification of safer alternatives through the combined applications of the chemical hazard assessment (CHA) and life cycle impact assessment (LCIA) methods to assess both the primary raw materials and processing chemicals used to manufacture flow batteries and lithium-ion batteries.

4.3 Material and Methods

4.3.1 Integrated Assessment Framework

As shown in **Figure 4.1(a)**, we integrated CHA and LCIA (see Sections 2.1 and 2.2 in Chapter 2) to assess the input chemicals and output emissions from different battery production stages such as raw materials extraction, materials processing, and component manufacturing. We started with assessing the primary materials directly applied in those battery technologies, then expanded our assessment to include the processing chemicals in the upstream production activities, battery components comprising of primary materials, and the complete battery systems. This integrative approach provides an opportunity to compare materials, components, and systems for different battery energy storage technologies. We used GreenScreen® for Safer Chemicals v1.4 (GreenScreen®), a CHA framework [13]; and USETox® v2.0 (USETox®), an LCIA methodology [44-46].

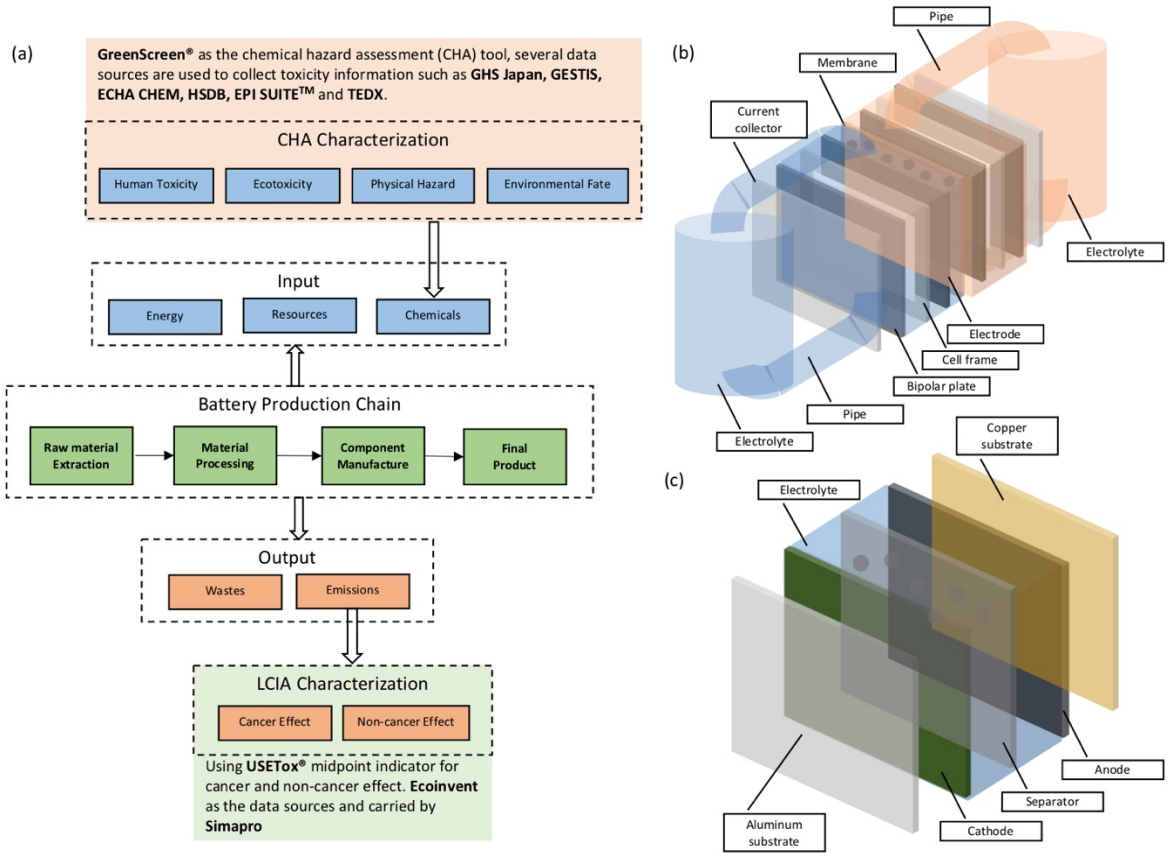

Figure 4.1. (a) The integrated assessment framework on toxicity hazard and health impact for battery storage technologies and the structure and component illustrations of (b) flow battery technology and (c) lithium-ion battery technology.

4.3.2 Manufacturing and Materials Use for Battery Storage Technologies

In **Figure 4.1(b)** and **(c)**, the diagram of the internal structures and major components are provided for redox flow batteries and lithium-ion batteries respectively. Additional details on battery material use are provided in **Table 4.1** and **4.2**. To highlight components that are correlated with the battery function, peripheral components such as battery management system, inverter, battery packaging, and accessories are not included in our assessments because they are independent modules. The configurations of the three lithium-ion batteries

are similar regardless of different material types. The components of cell stack for all the three lithium-ion batteries include electrodes categorized as cathode and anode, separator inserted to divide the two electrodes and electrolytes filled between cathode and anode [79-81]. Substrates used as current collectors are typically made of aluminum and copper [79-81]. redox flow batteries differ from lithium-ion batteries in that the electrolytes are stored in external tanks and connected to the cell stack via pipes and pumps, enabling physical separation of the power and energy capacity subsystems [70, 107]. Unlike lithium-ion batteries whose vital materials that conduct the redox reactions are embedded in their cathode, the active species for redox flow batteries are dissolved in electrolytes [70, 71, 107]. Other components inside the redox flow batteries cell stack consist of bipolar plate, cell frame, electrode, membrane, and current collector. Structural differences between the three selected redox flow batteries are shown in **Table 4.1**. The ZBFB does not include a supplemental electrode and membrane materials compared to VRFB and IFB due to the use of an integrated titanium bipolar plate instead of a more traditional carbon-based bipolar plate [107]. Additional information on redox flow batteries components is available in previously published reports [107]. The primary materials in redox flow batteries were collected from manufacturers and fully disclosed in **Table 3.1** in Chapter 3 and Appendix B. The main difference between the three redox flow batteries is the different active chemicals used as electrolytes. Manufacturers reported that material choices for the bipolar plate, cell frame, current collector, and tank also vary. The inventory of primary materials is derived from industrial-scale life cycle assessment (LCA) studies [107]. In **Table 4.2**, we report the use of different cathode active chemicals, which is distinctive for the three lithium-ion batteries. There are also different material choices for components such as the separator and

electrode binder and solvent. Interestingly, some of the chemicals are commonly used in lithium-ion batteries, such as those used as electrolytes, cathode and anode substrate. We focused on the types and numbers of chemicals used in the battery systems, and we assessed the toxicity hazards and life cycle health impacts associated with the weight of chemicals in terms of kg per kWh of battery energy capacity to highlight the various battery characteristics and performance parameters. We collected data on the weight percentage of each component for the six batteries as shown in Table 4.3 and 4.4, then calculated the energy density of each battery to convert the functional unit into per kWh based

Table 4.1. The detailed specifications on energy density, major components and materials use for the three flow batteries.

Details specification	**VRFB** [107]	**ZBFB** [107]	**IFB** [107]
Energy density	15.89 Wh/kg	33.38 Wh/kg	15.76 Wh/kg
Cell stack component			
Bipolar plate	Graphite	Titanium	Graphite
	Polyethylene	Polyethylene	Vinyl ester
Electrode	Carbon fiber felt	/	Carbon fiber felt
Membrane	Nafion®	/	Polyethylene
Cell frame	Glass fiber	Polyethylene	Glass fiber reinforced polymer
	Polypropylene		
Current collector	Copper	Titanium	Aluminum
Electrolyte storage component			
Electrolytes	Hydrochloric acid	Zinc bromide	Ferrous chloride
	Sulfuric acid	Bromine	Potassium chloride
	Vanadium pentoxide	Water	Manganese chloride
	Water		Water
Tank	Polyethylene	Polyethylene	Isophthalic polyester
Pipe	Polyethylene	Polyethylene	Polyvinylchloride

Table 4.2. The detailed specifications on energy density, major components and materials use for the three lithium-ion batteries.

Details specification	**LFP** [80]	**NCM** [80]	**LMO** [81]
Energy density	88.00 Wh/kg	112.00 Wh/kg	114.00 Wh/kg
Cell stack component			
Cathode	N-methyl-2-pyrrolidone	N-methyl-2-pyrrolidone	Latex
	Carbon black	Carbon black	Carbon black
	Polytetrafluoroethylene	Polytetrafluoroethylene	Lithium manganese oxide
	Lithium iron phosphate	Lithium nickel cobalt manganese hydroxide	
Cathode substrate	Aluminum	Aluminum	Aluminum
Anode	N-methyl-2-pyrrolidone	N-methyl-2-pyrrolidone	Latex
	Polytetrafluoroethylene	Polytetrafluoroethylene	Carbon black
	Graphite	Graphite	Graphite
Anode substrate	Copper	Copper	Copper
Electrolytes	Ethylene carbonate	Ethylene carbonate	Ethylene carbonate
	Lithium hexafluorophosphate	Lithium hexafluorophosphate	Lithium hexafluorophosphate
Separator	Polyethylene, low density	Polyethylene, low density	Silica sand
	Polypropylene	Polypropylene	Phthalic anhydride
			Acetone
			Polyethylene, low density
			Hexafluoroethane
			Polyvinyl fluoride

Table 4.3. The component weight percentages of the three flow batteries with peripheric components not considered for analysis highlighted in gray.

Battery weight percentage	**VRFB** [107]	**ZBFB** [107]	**IFB** [107]
Bipolar plate	0.51%	7.74%	3.59%
Electrode	0.03%	0.00%	0.05%
Membrane	0.02%	0.00%	0.07%
Cell frame	0.65%	2.94%	4.33%
Current collector	0.48%	0.80%	0.13%
Solutes	23.84%	32.58%	36.84%
Tank	4.08%	3.20%	4.73%
Pipes	0.05%	0.80%	0.91%
Battery management system	0.90%	1.60%	0.57%
Water	63.57%	26.44%	44.76%
Balance of Plant Accessories	5.39%	23.10%	3.90%

Table 4.4. The component weight percentages of the three lithium-ion batteries with peripheric components not considered for analysis highlighted in gray.

Battery weight percentage	**LFP** [81]	**NCM** [81]	**LMO** [82]
Cathode	24.80%	23.20%	15.10%
Cathode substrate	3.60%	3.60%	9.78%
Anode	8.00%	9.40%	14.52%
Anode substrate	8.30%	8.30%	15.98%
Electrolyte	12.00%	12.00%	13.62%
Separator	3.30%	3.30%	4.06%
External current collector	0.00%	0.00%	1.25%
Cell container	20.00%	20.10%	5.58%
Module and battery packaging	17.00%	17.00%	14.50%
Battery management system	3.00%	3.00%	5.60%

4.3.3 Chemical Hazard Assessment

We used GreenScreen® for Safer Chemicals version 1.4 (GreenScreen®) by Clean Production Action, (see Section 2.1 in Chapter 2) to assess chemicals based on their hazard endpoints, which are based on transparent and systematic benchmarking criteria [13, 14]. GreenScreen® is widely accepted in research fields, industries, non-governmental organizations, and government agencies, resulting in the publication of several case studies [32-34]. GreenScreen® includes information on 20 hazard endpoints (**Table 2.1**) including those related to human health, environmental toxicity and fate, and physical hazards. The selection and evaluation of these 20 hazard endpoints align with several national and international protocols such as the Globally Harmonized System of Classification and Labeling of Chemicals (GHS), the European Union's Registration, Evaluation, Authorization and Restriction of Chemicals (REACH), and the U.S. Environmental Protection Agency's Design for Environment Program [32-34, 108]. After completing the collection on toxicity information for those hazard endpoints, a benchmark (BM) decision logic with five possible BM scores are applied as follows: Chemical of High Concern (BM-1), Use but Search for Safer Alternatives (BM-2), Use but Still Opportunity for Improvement (BM-3), Safer Chemical (BM-4), and Unspecified due to Insufficient Data (BM-U). To conduct a GreenScreen® assessment, four steps specified in the guidance manual are strictly followed. In this study, we have evaluated the BM scores as well as the hazard endpoints for each battery technology from the perspectives of battery materials, components, and the whole battery system. Additionally, not only were the primary materials directly used for battery assembly assessed but also the processing chemicals used in the upstream battery production activities were investigated, which to our knowledge is among the few attempts that

incorporate a life cycle thinking into the CHA. We reviewed the published literature to gather information on processing chemicals: further details are provided in the Appendix E. The GreenScreen® method requires a minimum amount of hazard trait data to assign a BM score, otherwise BM-U is assigned due to data gaps. In the current study, a BM-U score is assigned when no information can be found for the given chemical. An official GreenScreen® assessment requires a third-party validation, which was not done here, therefore, these benchmark scores are currently designated as 'GreenScreen®-based'.

4.3.4 Life Cycle Impact Assessment

We conducted a life cycle impact assessment (LCIA) to evaluate the human health impacts associated with potentially hazardous emissions from the production of the six battery technologies. To construct the life cycle inventory (LCI), data compiled from the Ecoinvent database were used as input for the SimaPro LCA software to generate outcomes [94]. The functional unit is per kWh energy capacity of each battery type to enable a consistent comparison between the impact results. USETox® version 2.0 (USETox®) model, which is endorsed by the Society for Environmental Toxicology and Chemistry (SEATC), was chosen as the LCIA methodology for this study [44-46]. The main outputs of USETox® are sets of chemicals characterization factors (CFs) consisting of fate, exposure, and effect parameters. The mid-point indicator, which uses the number of disease cases as a comparative toxic unit, was adopted to assess cancer and non-cancer effects. Two sets of chemical CFs, including *recommended and interim*, were both considered to illustrate the associated sensitivity and uncertainty that exists in the current LCIA framework. Unlike the

recommended CFs on which a scientific consensus has been reached, the *interim* CFs still have high uncertainties related to the parameters describing fate and exposure due to insufficient data or flawed models [46]. Specific chemicals using *interim* CFs include metals, dissociating chemicals, and amphiphilics [46]. Additionally, we conducted a detailed analysis showing the impact contributors attributed to various battery components and materials to highlight the main drivers on human health impact.

4.4 Results and Discussion

4.4.1 Hazard Assessment on Primary Materials

In **Figure 4.2**, the GreenScreen®-based BM results for the six battery technologies are presented in terms of number and weight (kg per kWh energy capacity) of primary materials used. The associated contributions by number and weight percentage are also reported. Among the six selected battery technologies, the ZBFB uses four chemicals, and no BM-1 chemicals are identified. In contrast, the other five batteries all contain more than ten chemicals of which the LMO exhibits the highest number of chemicals used in the system with the highest number of BM-1 chemicals observed. However, the BM results based on the weight percentages indicate that instead of LMO, NCM shows the highest percentage of BM-1 chemicals. For the IFB, although the number and percentage of BM-1 chemicals in the system are not high, it has the second-highest number of chemicals used and the highest number and number percentage of BM-U chemicals. The higher the number of BM-U chemicals, the higher the associated uncertainty in chemical toxicity from the battery system. For example, the IFB could be the least preferred if all the BM-U chemicals are identified to

be BM-1 in the future. When normalizing the BM results based on unit weight of chemicals, the quantity of chemicals required for redox flow batteries is much higher than lithium-ion batteries due to their relatively low energy density. Among the three chosen redox flow batteries, the ZBFB uses the lowest weight of chemicals, but still over two times higher than any of the lithium-ion batteries. For the IFB, it demands the most weight of chemicals for each kWh of energy capacity, nevertheless, VRFB uses the highest amount of BM-1 chemicals and the weight percentage is close to 60% in the total battery system. Similarly, the weight percentage on BM-1 chemicals used in the NCM is also close to the value of VRFB, however, the corresponding absolute weight required is much lower owning to its high energy density. For LFP and LMO, although they show lower weight percentages on BM-1 chemicals compared to NCM, there is considerable uncertainty since the weight percentage of BM-U chemicals for LFP and LMO are among the highest. Therefore, it is not optimistic if those BM-U chemicals are later discovered to be BM-1 chemicals when future toxicity data is available.

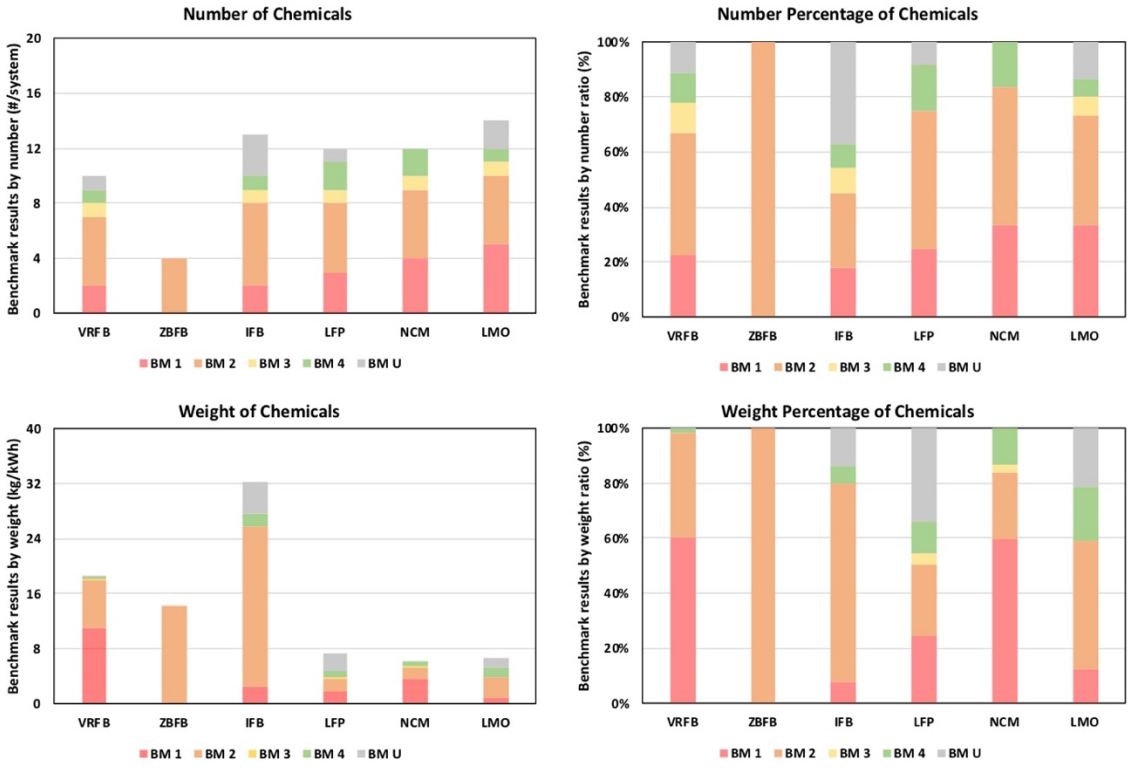

Figure 4.2. The GreenScreen®-based benchmark results on number and unit weight (kg per kWh energy capacity) of primary materials and their percentage contributions on the six battery storage technologies (VRFB = vanadium redox flow battery, ZBFB = zinc-bromine flow battery, IFB = all-iron flow battery, LFP = lithium iron phosphate, NCM = lithium nickel cobalt manganese hydroxide, and LMO = lithium manganese oxide).

The previous system-level comparison of BM scores provides a view of toxic chemicals used in each battery system. Subsequently, we focused on the BM scores attributed to different battery components (**Table 4.5** and **4.6**), including primary materials (BM results for each specific primary material are provided in Appendix F through **Table F1 – F6**). Information presented in **Table 4.5** shows that for redox flow batteries, only VRFB and IFB have components containing BM-1 chemicals, and all of them are used in the cell

frame and electrolytes. When considering the BM contribution by weight percentage shown **Table 4.6**, a system weight of 59% for VRFB is due to the electrolyte chemicals, in which vanadium pentoxide (**Table F1**) is responsible for the dominant amount of BM-1 chemicals. Unlike VRFB, the weight of BM-1 chemicals used in the IFB is much lower, since most of the electrolyte chemicals which comprise 70% of the system weight are categorized as BM-2. The only BM-1 chemical in the IFB in the electrolyte is manganese dioxide (**Table F3**), but this only accounts for 2% of the total system weight. For the ZBFB, all the components use BM-2 chemicals, and similar to the VRFB and the IFB, most of the system weight is due to electrolyte chemicals. Efforts to minimize the use of toxic chemicals and to identify safer alternatives should focus on chemical electrolytes. For the VRFB, the vanadium pentoxide is the active chemical necessary to the battery system and may be difficult to replace, therefore the only way to reduce the use of vanadium pentoxide is to improve the battery energy density and increase the associated production efficiency to avoid material loss. In contrast, replacing manganese dioxide for the IFB electrolytes is relatively easier because it is used to balance the solvent pH, and there could be alternative, potentially less toxic chemicals for the same function. For the ZBFB, although all the chemicals are identified to be BM-2, this doesn't mean there is no toxicity associated with the ZBFB system. The bromine used in ZBFB electrolytes (**Table F2**) is considered to be a highly volatile liquid with very high acute toxicity, protocols on process safety should be strictly followed to avoid the associated chemical exposure.

Table 4.5. The GreenScreen®-based benchmark results on the number of primary materials used in each component of the six battery energy storage technologies.

Flow battery coponent	Type	BM 1	BM 2	BM 3	BM 4	BM U	Total Chemicals Used
Bipolar plate	VRFB	0	1	0	1	0	2
	ZBFB	0	2	0	0	0	2
	IFB	0	0	0	1	1	2
Cell frame	VRFB	1	1	0	0	0	2
	ZBFB	0	1	0	0	0	1
	IFB	1	0	0	0	1	2
Electrode	VRFB	0	0	1	0	0	1
	ZBFB	/	/	/	/	/	/
	IFB	0	0	1	0	0	1
Membrane	VRFB	0	0	0	0	1	1
	ZBFB	/	/	/	/	/	/
	IFB	0	1	0	0	0	1
Current collector	VRFB	0	1	0	0	0	1
	ZBFB	0	1	0	0	0	1
	IFB	0	1	0	0	0	1
Electrolyte	VRFB	1	2	0	0	0	3
	ZBFB	0	2	0	0	0	2
	IFB	1	3	0	0	0	4
Tank	VRFB	0	1	0	0	0	1
	ZBFB	0	1	0	0	0	1
	IFB	0	0	0	0	1	1
Pipe	VRFB	0	1	0	0	0	1
	ZBFB	0	1	0	0	0	1
	IFB	0	1	0	0	0	1
Li-ion battery component	**Type**	**BM 1**	**BM 2**	**BM 3**	**BM 4**	**BM U**	**Total Chemicals Used**
Cathode	LFP	2	0	1	0	1	4
	NCM	3	0	1	0	0	4
	LMO	1	1	0	0	1	3
Cathode substrate	LFP	0	1	0	0	0	1
	NCM	0	1	0	0	0	1
	LMO	0	1	0	0	0	1
Anode	LFP	1	0	1	1	0	3
	NCM	1	0	1	1	0	3
	LMO	1	1	0	1	0	3
Anode substrate	LFP	0	1	0	0	0	1
	NCM	0	1	0	0	0	1
	LMO	0	1	0	0	0	1
Electrolyte	LFP	1	1	0	0	0	3
	NCM	1	1	0	0	0	3
	LMO	1	1	0	0	0	3
Separator	LFP	0	2	0	0	0	2
	NCM	0	2	0	0	0	2
	LMO	3	1	1	0	1	6

Table 4.6. The GreenScreen®-based benchmark results on the weight percentage of primary materials used in each component of the six battery energy storage technologies.

Flow battery coponent	Type	BM 1	BM 2	BM 3	BM 4	BM U	Chemicals weight ratio
Bipolar plate	VRFB	0.00%	0.12%	0.00%	1.61%	0.00%	1.73%
	ZBFB	0.00%	15.18%	0.00%	0.00%	0.00%	15.18%
	IFB	0.00%	0.00%	0.00%	5.95%	1.05%	7.00%
Cell frame	VRFB	0.44%	1.75%	0.00%	0.00%	0.00%	2.19%
	ZBFB	0.00%	5.76%	0.00%	0.00%	0.00%	5.76%
	IFB	5.34%	0.00%	0.00%	0.00%	3.56%	8.90%
Electrode	VRFB	0.00%	0.00%	0.17%	0.00%	0.00%	0.17%
	ZBFB	/	/	/	/	/	/
	IFB	0.00%	0.00%	0.09%	0.00%	0.00%	0.09%
Membrane	VRFB	0.00%	0.00%	0.00%	0.00%	0.06%	0.06%
	ZBFB	/	/	/	/	/	/
	IFB	0.00%	0.14%	0.00%	0.00%	0.00%	0.14%
Current collector	VRFB	0.00%	1.61%	0.00%	0.00%	0.00%	1.61%
	ZBFB	0.00%	1.67%	0.00%	0.00%	0.00%	1.67%
	IFB	0.00%	0.99%	0.00%	0.00%	0.00%	0.99%
Electrolyte	VRFB	58.90%	21.41%	0.00%	0.00%	0.00%	80.31%
	ZBFB	0.00%	58.47%	0.00%	0.00%	0.00%	58.47%
	IFB	2.23%	69.66%	0.00%	0.00%	0.00%	71.89%
Tank	VRFB	0.00%	13.76%	0.00%	0.00%	0.00%	13.76%
	ZBFB	0.00%	6.28%	0.00%	0.00%	0.00%	6.28%
	IFB	0.00%	0.00%	0.00%	0.00%	9.32%	9.23%
Pipe	VRFB	0.00%	0.18%	0.00%	0.00%	0.00%	0.18%
	ZBFB	0.00%	1.57%	0.00%	0.00%	0.00%	1.57%
	IFB	0.00%	1.77%	0.00%	0.00%	0.00%	1.77%
Li-ion battery component	**Type**	**BM 1**	**BM 2**	**BM 3**	**BM 4**	**BM U**	**Chemicals weight ratio**
Cathode	LFP	11.83%	0.00%	2.87%	0.00%	31.19%	45.89%
	NCM	40.39%	0.00%	2.70%	0.00%	0.00%	43.09%
	LMO	0.87%	0.33%	0.00%	0.00%	20.29%	21.49%
Cathode substrate	LFP	0.00%	5.20%	0.00%	0.00%	0.00%	5.20%
	NCM	0.00%	5.22%	0.00%	0.00%	0.00%	5.22%
	LMO	0.00%	12.81%	0.00%	0.00%	0.00%	12.81%
Anode	LFP	3.23%	0.00%	0.57%	10.98%	0.00%	14.78%
	NCM	3.82%	0.00%	0.68%	12.95%	0.00%	17.45%
	LMO	0.64%	0.75%	0.00%	19.74%	0.00%	21.13%
Anode substrate	LFP	0.00%	12.00%	0.00%	0.00%	0.00%	12.00%
	NCM	0.00%	12.04%	0.00%	0.00%	0.00%	12.04%
	LMO	0.00%	20.94%	0.00%	0.00%	0.00%	20.94%
Electrolyte	LFP	15.27%	2.09%	0.00%	0.00%	0.00%	17.36%
	NCM	15.32%	2.10%	0.00%	0.00%	0.00%	17.42%
	LMO	15.68%	2.14%	0.00%	0.00%	0.00%	17.82%
Separator	LFP	0.00%	4.76%	0.00%	0.00%	0.00%	4.76%
	NCM	0.00%	4.78%	0.00%	0.00%	0.00%	4.78%
	LMO	2.78%	1.87%	0.13%	0.00%	1.02%	5.80%

Compared to redox flow batteries, the lithium-ion batteries use more BM-1 chemicals in their batteries' components. In **Table 4.5**, we report that the lithium-ion batteries cathode, anode, electrolytes, and separator all contain BM-1 chemicals, especially for the NCM electrolytes and LMO separator because both of them contain three BM-1 chemicals. The results presented in **Table 4.6** show that the weight of the components is more uniformly distributed for lithium-ion batteries, with LFP and NCM leaning more weight on their cathode. The BM-1 chemicals used in those lithium-ion batteries components (**Table S4 – S6**), show that ethylene carbonate, a commonly used organic solvent, is identified in all the three lithium-ion batteries with a very close weight percentage around 15% – 16% to the battery system. There are newly developed electrolytes solvent chemicals for lithium-ion batteries [109, 110] which may support the sustainable selection of safer alternatives. Compared to LFP and LMO, the higher weight percentage of BM-1 chemicals in NCM is contributed by the battery cathode due to the use of lithium nickel cobalt manganese hydroxide as the cathode active material. However, the cathode active material for LFP and LMO that respectively corresponds to 31% and 20% of the system weight is classified as BM-U. This highlights the data gaps for the CHA, which call for future studies of toxicity assessment of emerging cathode active materials. Additionally, the BM-1 chemicals observed in the anode for all the three lithium-ion batteries and the separator for LMO have relatively small weights rendering them unlikely to affect human health as severely as the previously mentioned materials used in high amounts in battery manufacturing.

4.4.2 Analysis of Hazard Endpoints

Here we report the results of hazard endpoints to determine the hazard traits underlying BM scores. In **Figure 4.3** and **4.4**, frequencies on the 20 hazard endpoints by number and unit weight (kg per kWh) of chemicals are provided for each of the six battery technologies where the toxicity data are aggregated from their corresponding primary materials. To differentiate the level of severity, a hazard classification categorized as Low (L), Moderate (M), High (H), and Very High (vH) is applied to each hazard endpoint. From the results shown in **Figure 4.3** and **4.4**, it is clear that the distributions of hazard endpoints vary among different battery technologies. The frequencies of hazard endpoints for the ZBFB is less than the other five batteries due to the lowest number of chemicals used in the system. When normalized by weight, the weight of chemicals for the redox flow batteries could be much higher than that for the lithium-ion batteries in some of the hazard endpoints (noting the different y-axis scale for redox flow batteries and lithium-ion batteries in **Figure 4.4**). Interestingly, this phenomenon doesn't necessarily apply to all of the hazard endpoints because the redox flow batteries show little to no hazards in some endpoints.

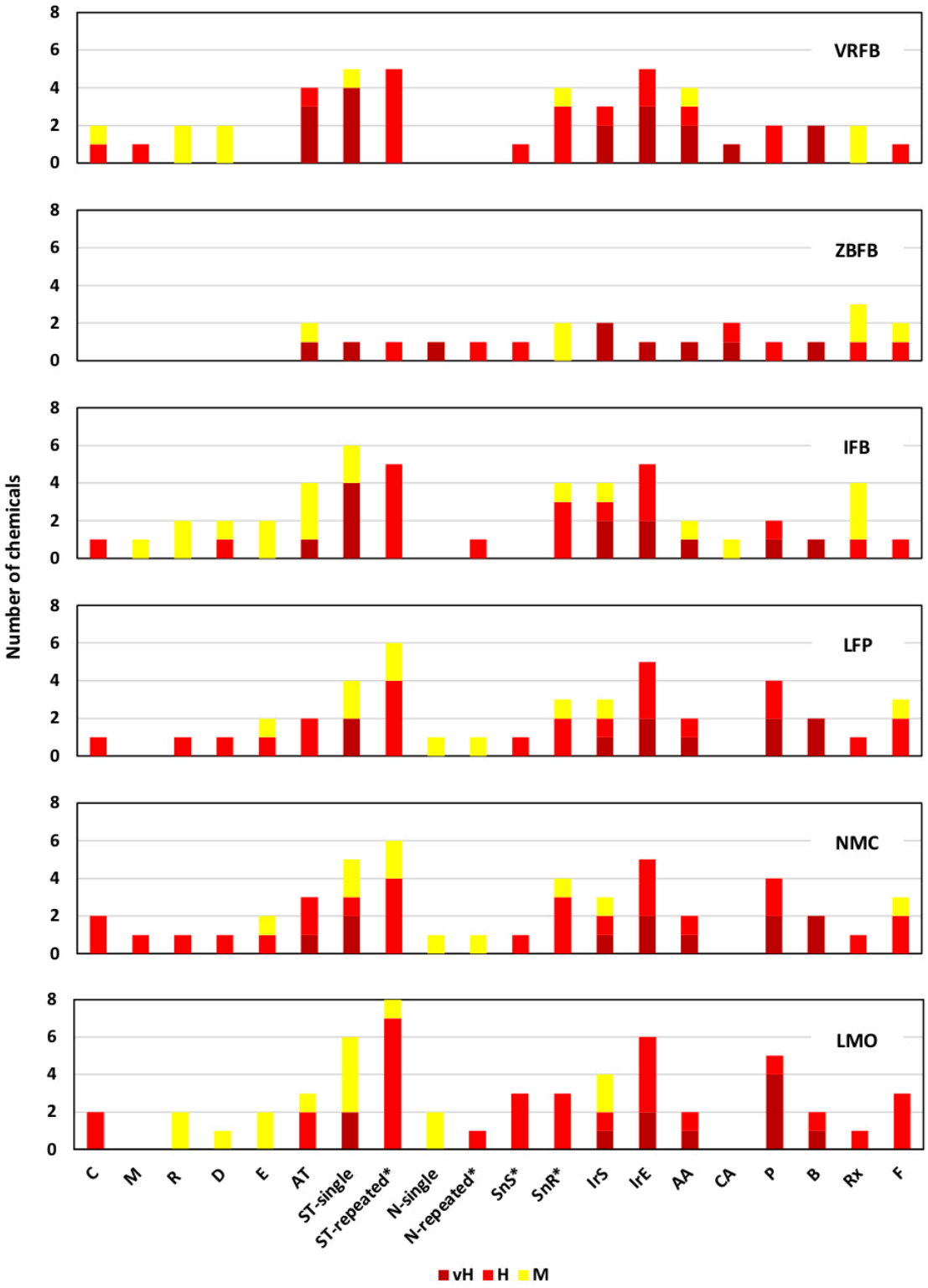

Figure 4.3. Distribution of twenty different hazard endpoints specified in GreenScreen® by number of chemicals used in the six battery energy storage technologies.

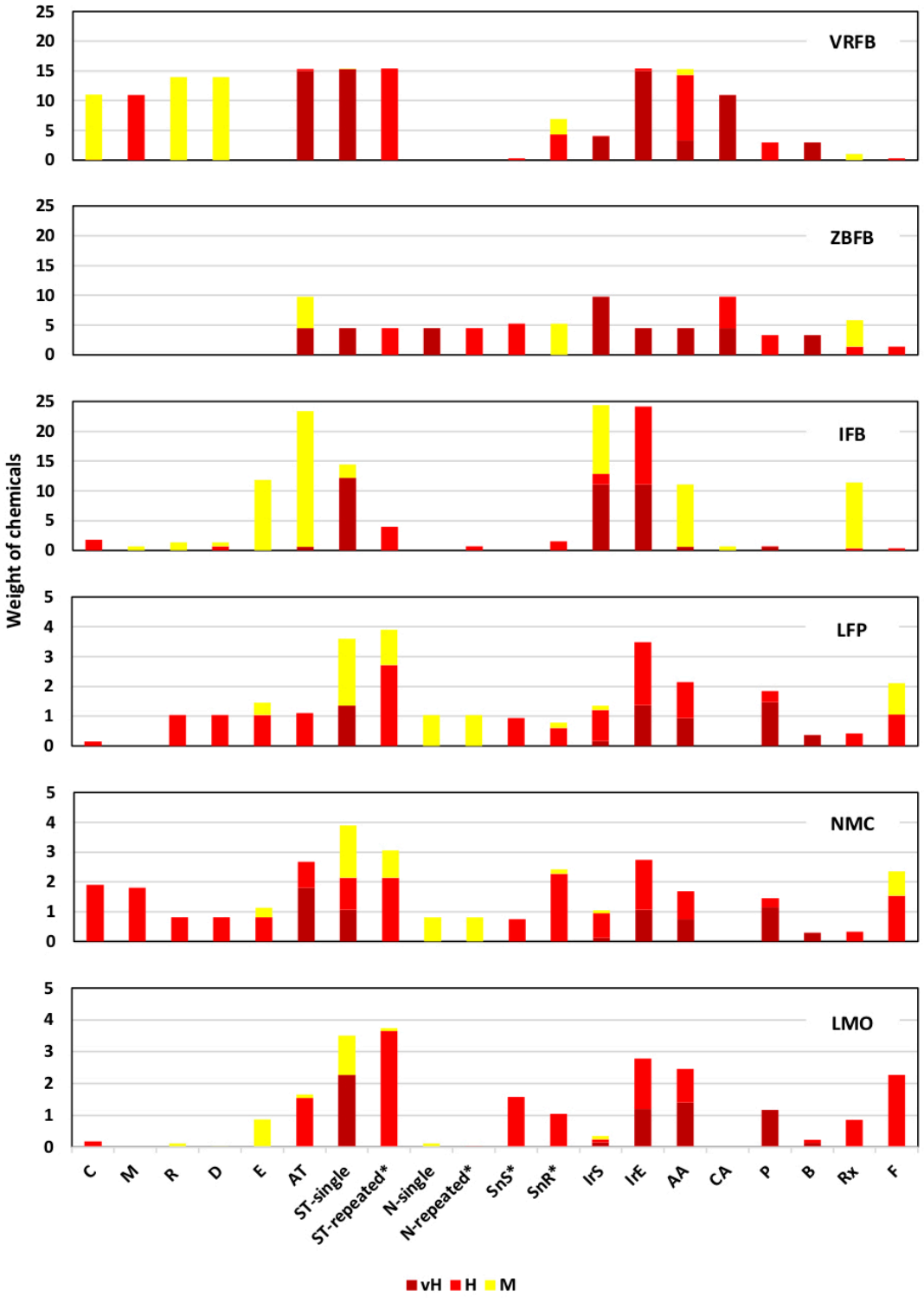

Figure 4.4. Distribution of twenty different hazard endpoints specified in GreenScreen® by weight of chemicals per kWh energy capacity used in the six battery energy storage systems.

Starting with hazard endpoints belonging to human health group I, which is of particular concern in the GreenScreen® decision logic, we observed that lithium-ion batteries trigger more human health group I hazard endpoints than redox flow batteries based on the number of chemicals. When compared by the weight of chemicals, the redox flow batteries and lithium-ion batteries are also comparable though the energy density of lithium-ion batteries is much higher (which means the required unit weight for lithium-ion batteries is much lower). The NCM is the only battery type that possesses high hazards on all of the human health group I hazard endpoints, followed by is LFP which exhibits four of them. LMO is among the best in these three lithium-ion batteries as it only has high carcinogenicity (C) with a small amount of triggering chemicals. For the VFRB, the weight of triggering chemicals in human health group I is much higher than other batteries even though it only has a high hazard for mutagenicity (M). In contrast, the performance of the ZBFB and the IFB is better with the ZBFB showing no human health group I hazard endpoints. For human health group II hazard endpoints, we focused on acute toxicity (AT) because it refers to serious adverse health effects (i.e. lethality) through oral, dermal, or inhalation exposure [106] which requires exceeding caution over other hazard endpoints in this category.

Among the six battery technologies, the VRFB shows the highest number and unit weight of chemicals triggering very high or high AT which indicates the associated hazards through its production could be the highest. For the IFB, although it appeared to have the highest AT hazard based on the weight of chemicals, its use of the very high hazard chemicals is small. Most of the chemicals receive a classification of medium hazard which means their thresholds of lethal dose are relatively high. Compared to redox flow batteries, the

performance of lithium-ion batteries on AT is better since their relative weights use per kWh capacity are lower and NCM is the only one using very high AT chemicals. It should be noted that for other human health group II hazard endpoints, the performance variances for each specific battery technology are large, and trade-offs exist when considering those hazard endpoints by number or by the unit weight of chemicals. For example, while the VRFB is identified to have a higher hazard on AT, it has little to no hazards associated with neurotoxicity (N) and skin sensitization (SnS). The IFB exhibits the highest hazards on eye irritation (IrE) when considered by the unit weight of chemicals used, however, the LMO is the least preferred instead when considered by the number of chemicals used. Regarding those hazard endpoints belonging to ecotoxicity and environmental fate, the performance of those battery technologies also varies in terms of number and unit weight of chemicals. But compared to lithium-ion batteries, only redox flow batteries use chemicals with chronic aquatic toxicity (CA). Lastly, regarding flammability (F) in the category of physical hazard. The performance of lithium-ion batteries tends to be worse regardless of the number or unit weight of chemicals used. This indicates that redox flow batteries show superior properties on physical hazards over lithium-ion batteries, which the latter is commonly criticized for their potential on flammability due to thermal runaway [111].

4.4.3 Toxicity Hazard of Upstream Processing Chemicals

We first provide an approach to identify the associated production hazards for primary materials that are classified as BM-U from the previous analysis. Secondly, for complex polymers and composite materials used in the battery systems, we explore

opportunities for safer alternatives through various production routes. In **Figure 4.5**, we present the BM scores and unit weight (kg per kWh) of the processing chemicals required to produce those primary materials that are vital to the battery systems. Specifically, they are electrolyte active chemicals for redox flow batteries and cathode active chemicals for lithium-ion batteries. Due to the relatively low energy density of redox flow batteries, the unit weight of processing chemicals required to produce vital materials for redox flow batteries are larger than those for lithium-ion batteries. However, the processing chains of these materials in lithium-ion batteries are longer than redox flow batteries since the production of active cathode materials of lithium-ion batteries undergoes more complex synthesis routes. For redox flow batteries, electrolyte chemicals can be produced using simpler operations. In terms of the production hazards, there were more BM-1 chemicals used for the production of vital materials in the three lithium-ion batteries. For example, several intermediate lithium compounds such as lithium carbonate and lithium hydroxide are classified as BM-1 chemicals. Further, it is observed that those nickel, cobalt, and manganese compounds used to manufacture the NCM and LMO vital materials are also BM-1 chemicals. In contrast, we found fewer hazards for those processing chemicals used in the redox flow batteries as most of them received a BM-2 with less severe hazard endpoints identified.

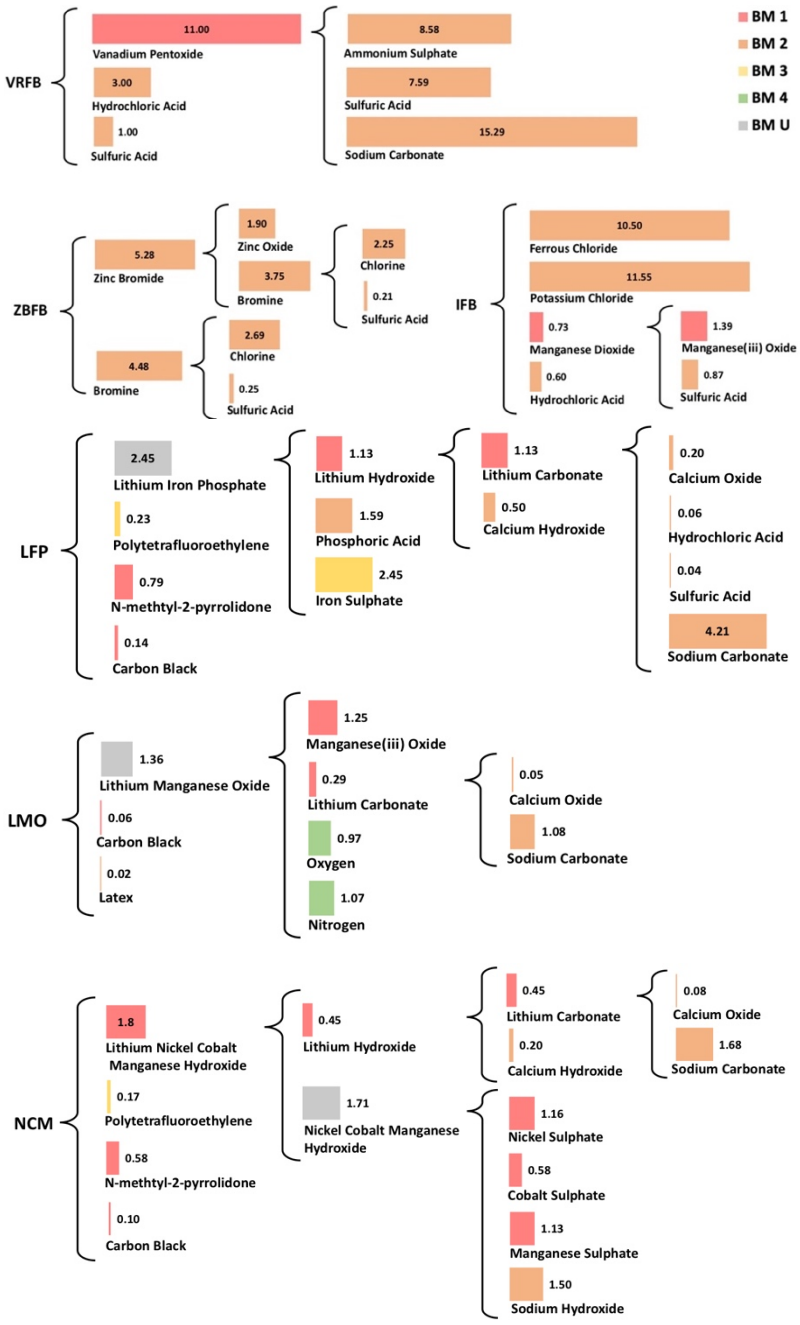

Figure 4.5. The GreenScreen®-based benchmark results for the core functional materials and the associated processing chemicals used in the six battery energy storage systems, which are electrolyte materials for flow batteries and cathode materials for lithium-ion batteries. The quantitative number corresponds to kg of chemicals needed per kWh energy capacity.

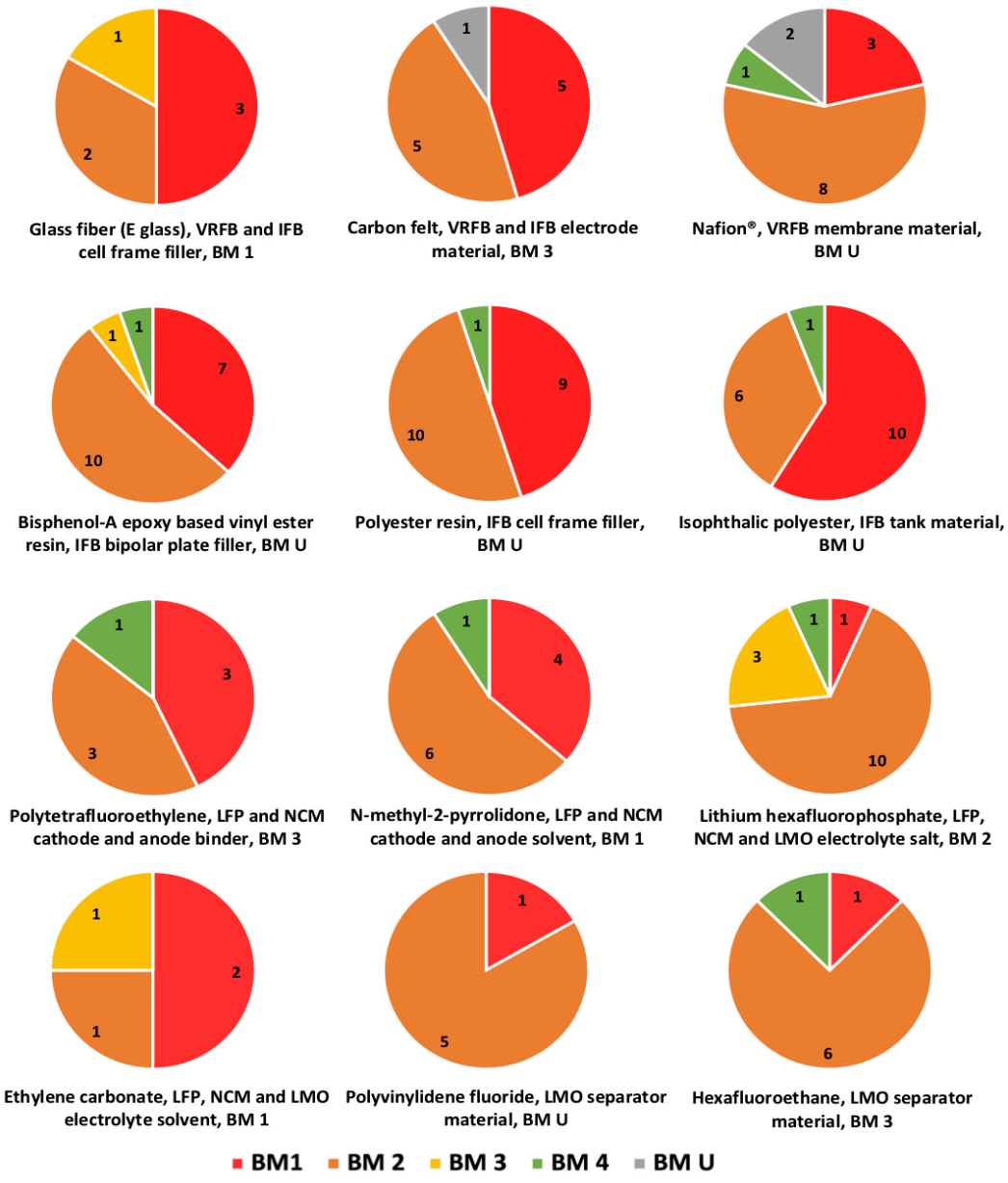

Figure 4.6. The GreenScreen®-based benchmark score distribution for the processing materials used in different components of the six battery energy storage systems.

In addition to vital materials, we also assessed twelve polymers and complex composite materials used in other battery components. As shown in **Figure 4.6**, the distributions of BM scores for processing chemicals are provided along with the information on their corresponding primary materials. These results indicate that many of the processing materials used in the twelve selected primary materials are chemicals of high concern. Each processing chemical used in one primary chemical is only counted once to avoid double-counting, although the processing chemicals can potentially be used several times in different processing routes.

There are eleven processing materials used to manufacture the carbon fiber felt, five of them receive BM-1 (45%), five of them receive BM-2 (45%), and one of them receives BM-U (5%). In contrast, if solely looking at the carbon fiber felt, it is classified as a BM-3 chemical, which indicates the use of carbon fiber felt during the assembly and use-phase of the flow battery only presents minor adverse effects. However, people working to manufacture carbon fiber felt production may be exposed to a highly hazardous environment as several of the processing chemicals are chemicals of high concern and the use of them should be avoided. For the Nafion® membrane, eight of the processing chemicals are BM-2, which accounts for 57% of the total chemicals used; three chemicals are assigned as BM-1. The bisphenol-A epoxy-based vinyl ester resin, polyester resin, and isophthalic acid based unsaturated polyester used in the IFB are both classified as BM-U as they are complex polymer resins with no toxicity information available. When broken down into the processing chemicals, a large number of BM-1 and BM-2 chemicals are identified. In terms of those primary materials used in lithium-ion batteries, the breakdown of polytetrafluoroethylene indicates that three of the seven processing chemicals are BM-1

chemicals; and three of them are assigned as BM-2. The LFP and NCM electrode solvent, N-methyl-2-pyrrolidone, which itself is already classified as BM-1 chemical, consists of four BM-1 (36%) and six BM-2 (55%) processing chemicals through its production chain. For lithium hexafluorophosphate, which is a commonly used lithium-ion batteries electrolyte salt, ten of the processing chemicals are classified as BM-2; but only one BM-1 chemical are reported to be used. There are also BM-1 chemicals used to produce polymers applied as LMO separator, however, most of the processing chemicals associated with the separator production are categorized as BM-2. More details on the BM results for processing chemicals are provided in the Appendix F, **Table F7**.

4.4.4 Life Cycle Impact Assessment of Chemicals in Battery Storage Technologies

In this section, we present the results of the human health impacts based on the fate, exposure, and effect factors associated with the chemical emissions during battery production. The assessment focused on cancer and non-cancer effects with *recommended and interim* CFs. The *interim* factors include chemicals with CFs with no universal consensus and for simplification; metals are the major materials characterized using i*nterim* CFs due to their high use in the six battery technologies.

In **Figure 4.7**, we present the normalized LCIA results by disease case per kWh. The results show that lithium-ion batteries have impact scores higher than redox flow batteries though the energy density of lithium-ion batteries is much higher. The results based on *recommended* CFs and *interim* CFs show the impact of the non-cancer effect is approximately one magnitude higher than cancer effects with LMO showing the highest impact score and

IFB showing the lowest. The relative ranking of the six battery technologies remains unchanged. The results with the *recommended* CFs solely applied show that cancer and non-cancer effects are on the same scale with the LFP and NCM showing higher impact scores. Interestingly, LMO is now ranked to be the lowest among the six battery technologies in contrast to the previous results using *recommended and interim* CFs.

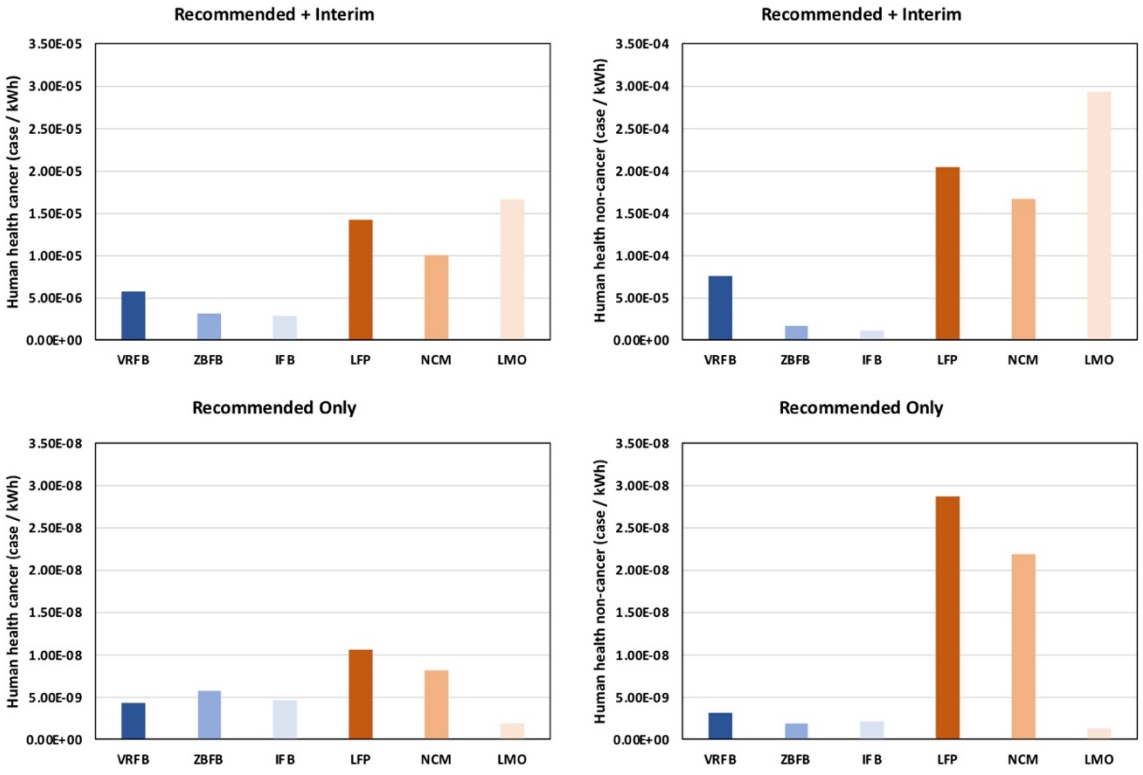

Figure 4.7. The USETox® results on human health cancer and non-cancer effect for the six battery energy storage systems considering the *recommended* and *interim* characterization factors and *recommended* characterization factors only.

The uncertainties associated with the results based on different CFs warrants exploration. Since various CFs are directly correlated with their corresponding materials, we investigated the detailed contributions attributed to different battery components and each specific material. The results are presented in **Figure 4.8** and these flow charts show the percentage contribution of each battery component with the accompanying materials, which the components and materials with a contribution less than 0.5% are merged into the categories of other components and other materials in order to highlight the major contributors.

We first focus on the findings for LMO due to the large variations observed in the previous LCIA results. When considering both the *recommended and interim* CFs, copper is the highest contributor dominating the health impact, especially for the non-cancer effect. Since the CFs for copper are categorized as *interim* CFs, this explains the large impact reduction of LMO when only using the *recommended* CFs. The cause of high impact on copper is due to its high CFs over other materials as the LCIA results contributed by copper for the VRFB, LFP and NCM are also pretty high though their weight use of copper is smaller than LMO. For the VRFB, another important contributor to human health impact (especially for cancer effect) is vanadium pentoxide which is the vital active materials used to a large extent in the VRFB system. When considering the results based on *recommended* CFs, the impact contributed by Nafion® membrane increases. The major contributing materials for the ZBFB are titanium, zinc bromide, and bromine regardless of what types of CFs were applied. For the IFB, the impact results are more uniformly distributed to each component and material, while the impact contribution of several polymer resins that are not relevant to the battery functional performance is slightly higher. For LFP and NCM, the contributing components

and materials are similar since the original data for these batteries were extracted from the same study. Interestingly, the major contributors for LFP and NCM, no matter what types of CFs considered, are not the cathode active materials. When considering the scenario using both *recommended and interim* factors, copper is among the highest contributor. However, when considering only the *recommended* CFs, polytetrafluoroethylene, which is used as the electrode binder, tends to be the highest contributor for both of the two batteries.

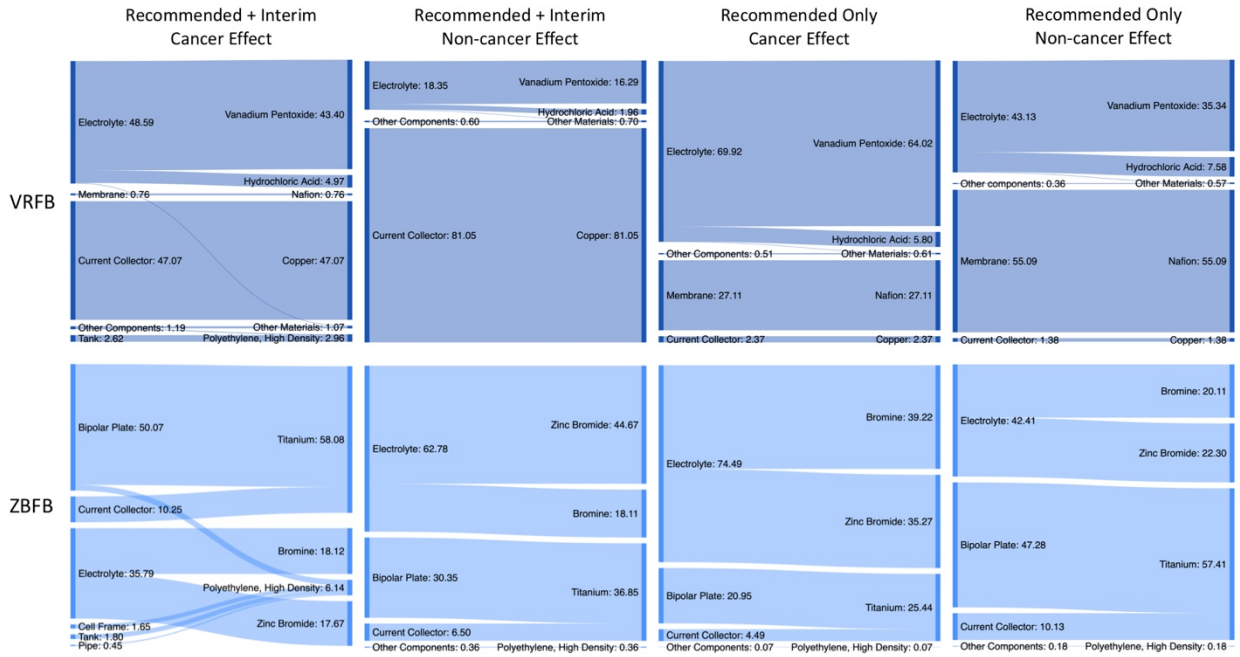

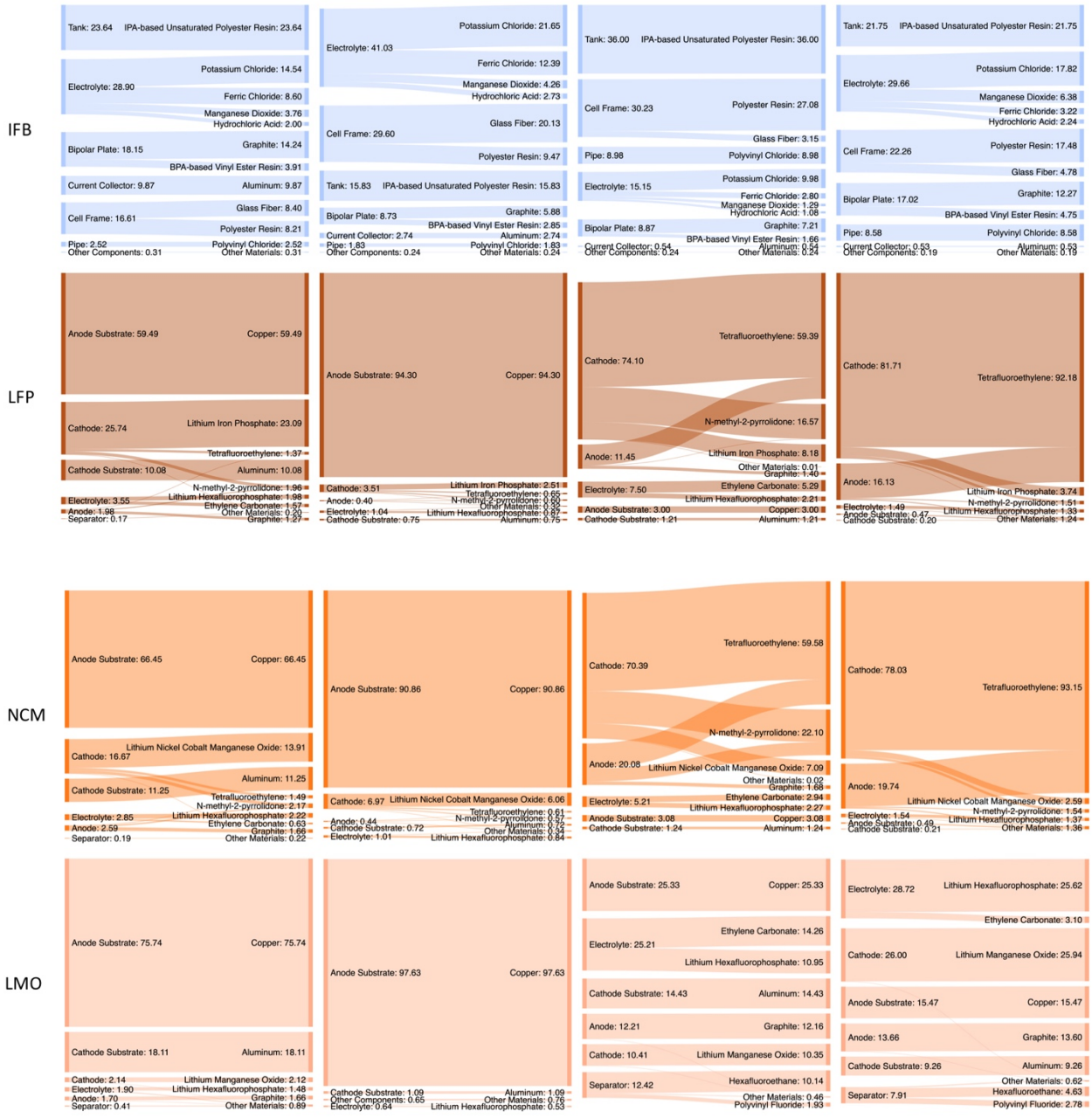

Figure 4.8. The percentage distribution of the USETox® results on human health cancer and non-cancer effect for the six battery energy storage systems considering the *recommended and interim* characterization factors and *recommended* characterization factors only.

4.5 Conclusions

In this case study, the toxicity hazard and life cycle health impact associated with the production of flow batteries and lithium-ion batteries was investigated. Through CHA, we characterized the inherent hazard potential of the input chemicals, despite data gaps that impede robust hazard classification. The collection of the toxicity information is transparent. Although LCIA provided quantitative results on human health impact for comparison across battery types, there are also gaps and uncertainties in characterization factors that caution the interpretation of the results. The GreenScreen®-based benchmark score and hazard endpoints results on primary materials used in these batteries clearly indicate that lithium-ion batteries use more chemicals of concern, while flow batteries use more mass of chemicals of concern. Specifically, the vanadium pentoxide used in VRFB and lithium nickel cobalt manganese hydroxide used in LMO are BM-1 chemicals. When evaluating the upstream processing chemicals, it is observed that the intermediate processing lithium compounds and several complex polymer resins and composites use BM-1 chemicals during the production process. The USETox® results on human health cancer and non-cancer effects varied significantly when considering different characterization factors, which indicates that a more standardized methodology is needed. In summary, battery design parameters and materials selection determine the toxicity potential and health impacts. For some battery types, environmental and human health impacts are attributable to essential components (e.g., vanadium pentoxide for VRFB; lithium nickel cobalt manganese hydroxide for NCM). However, there are materials that are not essential for battery performance yet show high hazard potentials, which indicate opportunities exist to identify safer alternatives.

Chapter 5: Techno-economic Analysis on Materials Cost of Flow Batteries Production

5.1. Introduction

Increasing concerns about environmental issues such as climate change, air pollution, and resource depletion have motivated the introduction of alternative energy resources and the deployment of energy storage technologies that support the adoption of renewable resources. California is pioneering solutions through the reinforcement of policies and laws such as the Renewables Portfolio Standard (RPS) and Senate Bill 100 (SB 100) which require 60 percent of retail electricity sales to be sourced from renewable resources by 2025 and 100% of the electric demand to be met by fossil-fuel-free electricity by 2045 [27, 28]. Meeting the RPS and SB 100 goals will strongly depend on the use of renewable energy such as wind and solar. However, the drawback of using renewable resources is the mismatch of electricity demand and supply due to the intermittency of their electricity generation profile. Energy storage can be an effective way to compensate for this mismatch and enable a high renewable penetration level on the electric grid, and in particular, electrochemical energy storage technologies are highly rated among other energy storage technologies. Compared to the current prevailing battery technologies on the market, flow batteries can be more easily expanded in power or energy capacity due to their physical separation between charging/discharging and storage subsystems. Additional advantages of flow batteries include a large depth of discharge, minimal degradation, and a long lifespan. These benefits help to promote flow batteries as a key potential component for renewable energy system design.

The cost and revenue associated with the redox flow battery (RFB) systems are critical to their widespread application. Researchers have focused on analyzing the potential for cost reduction in redox flow batteries and identifying possible practices for enhancing the revenue of redox flow batteries operation. This chapter focuses on assessing the economic cost of flow battery production. A techno-economic analysis (TEA) approach is applied by considering material prices. With data on material prices, a component cost distribution is provided for each flow battery type assessed in this project.

5.2. Methodology

5.2.1. Techno-economic Analysis Model

To perform the analysis of cost sensitivities and their behavior relative to changes in environmental impact, the methods of techno-economic analysis (TEA) were employed [112-115] (see Section 2.3 in Chapter 2). The goal is to investigate and understand the major cost contributors for flow battery systems since these technologies are relatively early in their commercial deployment compared to alternatives such as lithium-ion batteries. Therefore, this section focuses on materials cost since these costs will be fundamental to each flow battery type, while the other costs (e.g., utilities, labor, and fixed costs) will vary from manufacturer to manufacturer and will depend on business strategy, which are not easily assessed with current data availability. Thus, for this project, the TEA is focused on material costs and is based on the product specifications (see **Table 5.1**) and the materials inventory data provided by the flow battery manufacturers (see **Table 3.1**), which were used in Chapter 3 for the LCA study. The cost assessment is performed for the three flow batteries based on this materials inventory and the unit materials cost searched from various sources.

The cost distribution by battery component is determined to highlight the major cost drivers in the battery system. For comparison, the normalized dollar value per kWh battery capacity for the three flow batteries are also evaluated.

Table 5.1. The performance parameters for the three flow batteries.

PRODUCT SPECIFICATIONS			
Product Name	VRFB	ZBFB	IFB
Product Weight (kg)	32,287	3,844	26,232
Energy Capacity (kWh)	500	125	400
Rated power (kW)	125	25	100
Discharge Time (hour)	4	5	4
Energy Density (Wh/kg)	15.49	32.52	15.25

5.2.2. Materials Cost Data and Uncertainty

For the TEA model, data on the prices of key materials used in the flow battery systems are required. Gathering material cost information that complies with data quality and reliability standards, however, can be difficult. The cost of materials is subject to the dynamics of global markets and trade, causing these values to vary over time. Additionally, materials such as the Nafion® membrane and glass fiber reinforced polymer cell frame are complex synthetic materials that are protected by patents as private products, therefore prices for these have to be estimated. The sources for price information in our case can be classified into four types: 1) international market prices, 2) United States (US) import prices, 3) literature prices, and 4) retail prices.

The ‘international market price’ is suitable for materials that are traded as bulk commodities, where their prices are continuously monitored and updated in international trade, such as metals like copper and aluminum. The international market price, however, may not be representative of the prices paid in a specific geographical area as different countries have different exchange rates and policies as well as local tariffs.

The ‘US import price’ is collected based on the price of goods imported to the U.S. These are well documented by several U.S. governmental institutes and databases such as the United States Geological Survey (USGS) and Statista. The import price is converted into a dollar value for the U.S. case, which is equal to the world price plus any transport, tariff and other costs that customers would bear for importing the material to the U.S. [116]. The import price may also not be an accurate prediction as the manufacturers’ purchase source is not disclosed.

The ‘literature price’ is based on price values found in the published literature for the materials cost of flow battery production. The advantage of using literature data is that the cost information is complete even for materials that are difficult to track to a market, and these data are peer-reviewed. Due to the lack of original studies and primary data in these studies, however, much of the cost information in literature studies are predicted values, while some are cited from previous publications. These values, therefore, may not capture the dynamic price variations to reflect the current situation.

The ‘retail price’ is the material price collected from the vendors who purchase those materials from upstream supply chains and sell them directly to the commercial end-users. These prices, however, may not be applicable to this study as flow battery manufacturers do not necessarily buy their materials from second-hand vendors.

Due to the dynamic nature of market price and the uncertainty associated with different sources, we clearly note the price sources collected for each material considering the requirement of transparency. Furthermore, due to the variations in the market prices for materials, a sensitivity analysis is conducted to explore the uncertainty in market price variability for selected materials, specifically: vanadium pentoxide, titanium, bromine and carbon fiber felt. The vanadium pentoxide is used as the electrolyte in the VRFB, the titanium and bromine are used in the bipolar plate and electrolyte, respectively, for ZBFB, and carbon fiber felt is the electrode used for VRFB and IFB but is also used in the IFB balance of plant as a rebalancing cell which is unique among the three batteries.

For these four materials, a three-point estimation is applied for estimation based on a pessimistic price (worst case), most likely price (current value) and optimistic price (best case). The three-point estimation creates an approximate probability distribution to predict the outcomes of future events, e.g. materials price, when only limited information is available. Usually, a beta or triangular distribution is assumed, and, in this study, a double-triangular distribution is used, as shown in **Figure 5.1**. The notation "a" is the optimistic price which represents the best case, "b" is the pessimistic price indicating the worst case, and "m" is the most likely price, which indicates the current price [117]. With the three value points determined, a weighted-average (E) as expected price and a standard deviation (SD) can be calculated as follows:

$$E = (a + 4m + b) / 6 \quad (9)$$

$$SD = (b - a) / 6 \quad (10)$$

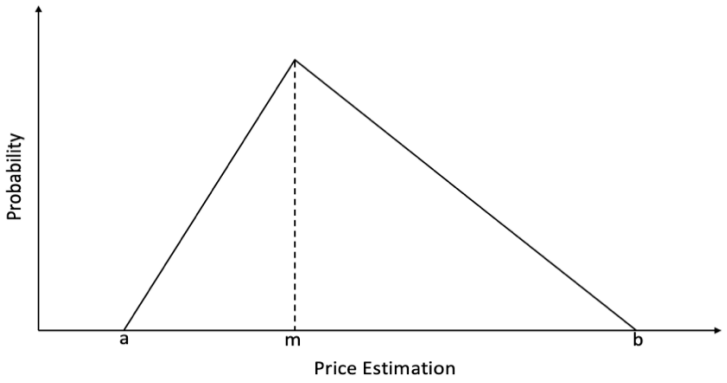

Figure 5.1. An example of probability distribution used for three-point estimation.

5.3. Results and Discussion

5.3.1. Material Pricing Data

The price of materials (in $/kg) used for the baseline cost analysis are provided in **Tables 5.2 – 5.4**. Prices per kW for the pumps and inverters are also included [47, 77]. Historical pricing data for vanadium pentoxide, titanium, bromine and carbon fiber felt are provided and discussed below.

Table 5.2. Material price information for materials used in the VRFB system.

Battery Technology	**VRFB**			
Component	**Price**	**Unit**	**Data type**	**Data source**
Bipolar Plate				
Graphite	1.58	$/kg	2015 MARKET AVERAGE	USGS [118]
Polyethylene, low density	1.22	$/kg	2017 IMPORT AVERAGE	STATISTA [119]
Cell frame				
Polypropylene	1.84	$/kg	2017 IMPORT AVERAGE	STATISTA [120]
Glass fiber	2	$/kg	ESTIMATED VALUE	Amirhossein et al. [121]
Electrode				
Carbon felt paper	237.6	$/kg	LITERATURE VALUE	Minke et al. [52]
Membrane				
Nafion®	937.53	$/kg	LITERATURE VALUE	Minke et al. [52]
Cell Stack Accessories				
Steel, low alloyed	0.69	$/kg	2019 MARKET AVERAGE	Worldsteelprice [122]
Copper	6.61	$/kg	2018 VENDOR VALUE	USGS [123]
Polyvinylchloride	0.97	$/kg	2019 MARKET AVERAGE	Investing.com [124]
Electrolyte				
Vanadium pentoxide	35.75	$/kg	2019 MARKET AVERAGE	USGS [125]
Hydrochloric acid	0.13	$/kg	2018 MARKET INSTANT	ICIS [126]
Sulfuric acid	0.06	$/kg	LITERATURE VALUE	Minke et al. [47]
Water	0.00241	$/kg	GOVERNMENT VALUE	[127]
Tank				
Polyethylene, high density	1.26	$/kg	2017 IMPORT AVERAGE	STATISTA [128]
Pipes				
Polyethylene, high density	1.26	$/kg	2017 IMPORT AVERAGE	STATISTA [128]
Pump	13.46	$/kW	LITERATURE VALUE	Minke et al. [129]
Inverter	112.13	$/kW	LITERATURE VALUE	Minke et al. [47]
Battery Management System				
Aluminum	2.54	$/kg	2018 IMPORT AVERAGE	USGS [130]
Titanium	30	$/kg	2019 MARKET INSTANT	TRICORMETALS [131]
Power Control System	150	$/kW	LITERATURE VALUE	Minke et al. [129]
Balance of Plant Accessories				
Steel, low alloyed	0.69	$/kg	2019 MARKET AVERAGE	Worldsteelprice [122]

Table 5.3. Material price information for materials used in the ZBFB system.

Battery Technology	**ZBFB**			
Component	**Price**	**Unit**	**Data Type**	**Data Source**
Bipolar Plate				
Titanium	30	$/kg	2019 MARKET INSTANT	TRICORMETALS [128]
Polyethylene, high density	1.26	$/kg	2017 IMPORT AVERAGE	STATISTA [127]
Cell frame				
Polyethylene, high density	1.26	$/kg	2017 IMPORT AVERAGE	STATISTA [126]
Cell Stack Accessories				
Steel, low alloyed	0.69	$/kg	2019 MARKET AVERAGE	Worldsteelprice [121]
Titanium	30	$/kg	2019 MARKET INSTANT	TRICORMETALS [128]
Polyethylene, high density	1.26	$/kg	2017 IMPORT AVERAGE	STATISTA [127]
Electrolyte				
Bromine	4.9	$/kg	2017 IMPORT AVERAGE	USGS [130]
Zinc	3.2	$/kg	2018 IMPORT AVERAGE	USGS [131]
Water	0.00246	$/kg	GOVERNMENT VALUE	[132]
Tank				
Polyethylene, high density	1.26	$/kg	2017 IMPORT AVERAGE	STATISTA [127]
Pipes				
Polyethylene, high density	1.26	$/kg	2017 IMPORT AVERAGE	STATISTA [130]
Pump	13.46	$/kW	LITERATURE VALUE	Minke et al. [47]
Inverter	112.13	$/kW	LITERATURE VALUE	Minke et al. [47]
Battery Management System				
Steel, low alloyed	0.69	$/kg	2019 MARKET AVERAGE	Worldsteelprice [121]
Aluminum	2.54	$/kg	2018 IMPORT AVERAGE	USGS [130]
Copper	6.61	$/kg	2018 VENDOR VALUE	USGS [132]
Power control system	150	$/kW	LITERATURE VALUE	Minke et al. [129]
Balance of Plant Accessories				
Steel, low alloyed	0.69	$/kg	2019 MARKET AVERAGE	Worldsteelprice [121]
Aluminum	2.54	$/kg	2018 IMPORT AVERAGE	USGS [130]
Titanium	30	$/kg	2019 MARKET INSTANT	TRICORMETALS [128]

Table 5.4. Material price information for materials used in the IFB system.

Battery Technology	**IFB**			
Component	**Price**	**Unit**	**Data type**	**Data source**
Bipolar Plate				
Graphite	1.58	$/kg	2015 MARKET AVERAGE	USGS [118]
Polypropylene	1.84	$/kg	2017 IMPORT AVERAGE	STATISTA [120]
Cell frame				
Polyester resin	3.36	$/kg	2017 IMPORT AVERAGE	STATISTA [133]
Glass fiber	2	$/kg	ESTIMATED VALUE	Amirhossein et al. [121]
Electrode				
Carbon felt paper	237.6	$/kg	LITERATURE VALUE	Minke et al. [52]
Membrane				
UHMW polyethylene	595.88	$/kg	2019 VENDOR VALUE	Sigma Aldrich [134]
Cell Stack Accessories				
Steel, low alloyed	0.69	$/kg	2019 MARKET AVERAGE	Worldsteelprice [122]
Aluminum	2.54	$/kg	2018 IMPORT AVERAGE	USGS [130]
EPDM Gasket	2.5	$/kg	LITERATURE VALUE	Viswanathan et al. [51]
Electrolyte				
Iron chloride	0.35	$/kg	2018 MARKET INSTANT	ICIS [135]
Potassium chloride	0.27	$/kg	2019 MARKET AVERAGE	Indexmundi [136]
Manganese dioxide	2.21	$/kg	2015 IMPORT AVERAGE	USGS [136]
Hydrochloric acid	0.13	$/kg	2018 MARKET INSTANT	ICIS [126]
Water	0.00186	$/kg	GOVERNMENT VALUE	[137]
Tank				
Polyester resin	3.36	$/kg	2017 IMPORT AVERAGE	STATISTA [133]
Pipes				
Polyvinylchloride	0.97	$/kg	2019 MARKET AVERAGE	Investing.com [124]
Pump	13.46	$/kW	LITERATURE VALUE	Minke et al. [129]
Inverter	112.13	$/kW	LITERATURE VALUE	Minke et al. [47]
Battery Management System				
Carbon felt paper	237.6	$/kg	LITERATURE VALUE	Minke et al. [52]
Power control unit	150	$/kW	LITERATURE VALUE	Minke et al. [129]
Balance of Plant Accessories	None			

5.3.1.1. Vanadium Pentoxide Price Data

Vanadium pentoxide is the major contributor to cost for the VRFB system as the electrolyte corresponds to more than 80% of the total cost and is also a primary driver of VRFB environmental impacts. The price of vanadium pentoxide is monitored by several organizations such as USGS. It is reported that the vanadium pentoxide produced in the US is based on secondary sources such as catalysts, ashes, and petroleum residues which are 100% import reliant [138]. The market price of vanadium pentoxide varies over time. **Figure 5.2** presents the variation in the monthly price, while **Figure 5.3** presents a year-to-year variation [139]. The prices for vanadium pentoxide have ranged from 20 – 50 $/kg in the past year and the peak price is observed from November to December 2018, when prices reached as high as 49.60 $/kg. For year-to-year prices, there are no clear trends. Before 2004, the price of vanadium pentoxide varied between 3 – 9 $/kg, while after 2004, the price seldom dropped below 10 $/kg and the price variability increased. It is also noted that the price of vanadium pentoxide increased sharply in certain years such as 2005 and 2008, with average prices of 38.60 $/kg and 32.50 $/kg respectively. According to USGS, the price spike in 2005 was attributed to strong demand in the steel and aerospace industries and the inability of the producers to increase production in a timely manner [140]. In the year 2008, the price increase was caused by a sharp reduction in production volume due to power shortages in South Africa and bad weather in China, which are both primary countries with vanadium reserves and production [141].

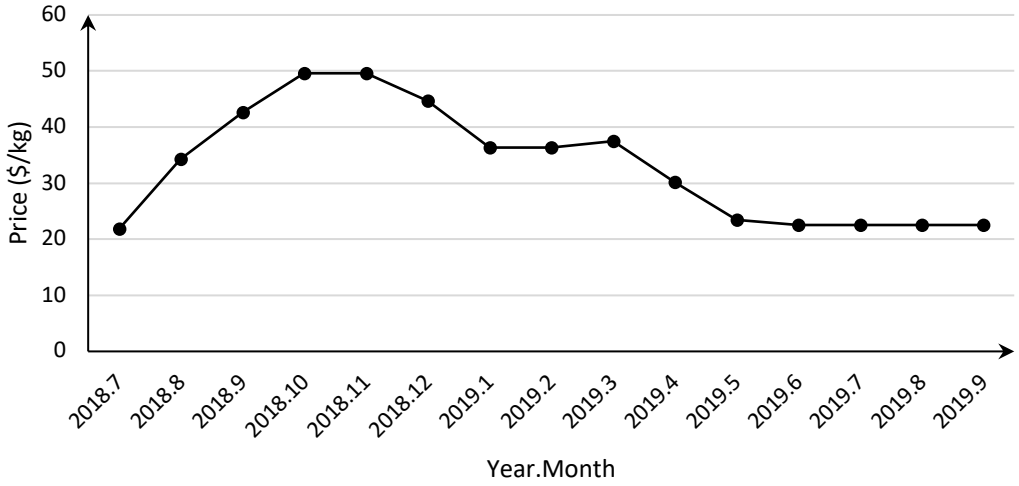

Figure 5.2 The monthly price of vanadium pentoxide during the past year [125].

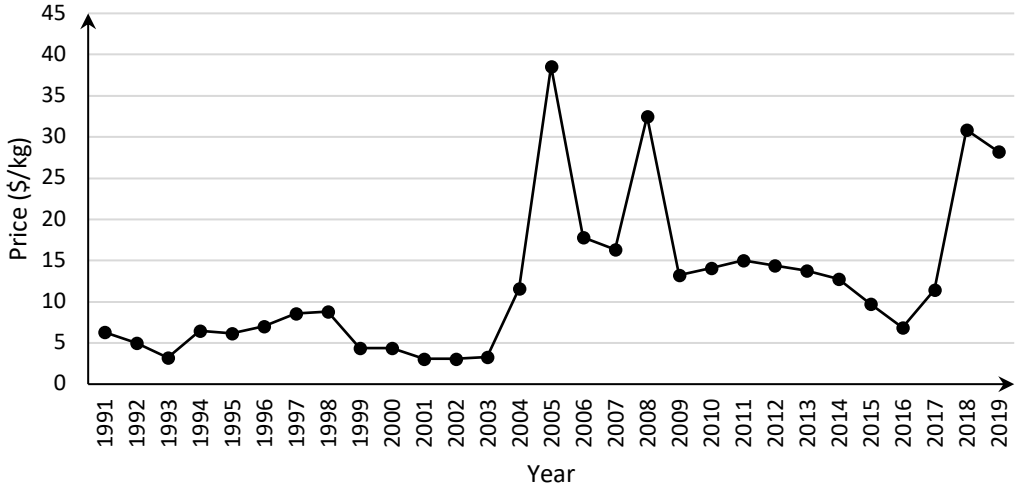

Figure 5.3 The average yearly price of vanadium pentoxide from 1991 – 2019 [139].

Due to the large variations, estimating a single point for the price of vanadium pentoxide may not be representative. With the application of the three-point estimation method, the current price is set to be 35.75 $/kg, which is the average price during the past year from July 2018 to June 2019. The pessimistic price is estimated to be 50 $/kg, which is

close to the highest price observed in October 2018. The optimistic price is chosen to be 8 $/kg, which is extracted from the literature [52] and closely matches the yearly price between 1991 – 2004.

5.3.1.2. Titanium Price Data

In the ZBFB, the titanium is a core material used to manufacture the bipolar plate that contributes about 22% of the total system cost. Titanium is also used in the cell stack accessories in support of the cell stack structure. The price of titanium products such as titanium mineral concentrates, titanium sponge, and titanium dioxide are monitored by USGS. However, the type of titanium products used in the ZBFB specifically is a titanium milled product for which price data over time are unavailable. Thus, the producer price index (PPI) for the titanium mill product is shown in **Figure 5.4** [142]. The PPI reflects the relative change in the market price of materials compared to the baseline year – the year 1982 in this case. From **Figure 5.4**, the current PPI value is close to 170 and the peak value is 355 in the year 2006. Our data search indicates that the current price for the titanium milled product is approximately 30 $/kg when the PPI is approximately 170 [142]. Based on the current price and the PPI index over the years, the pessimistic price is converted from the current price using the point when the PPI index was at its peak value of 355, and the optimistic price is determined at the point when PPI index is 100. Thus, pessimistic and optimistic prices are calculated to be 62.65 $/kg and 17.65 $/kg, respectively.

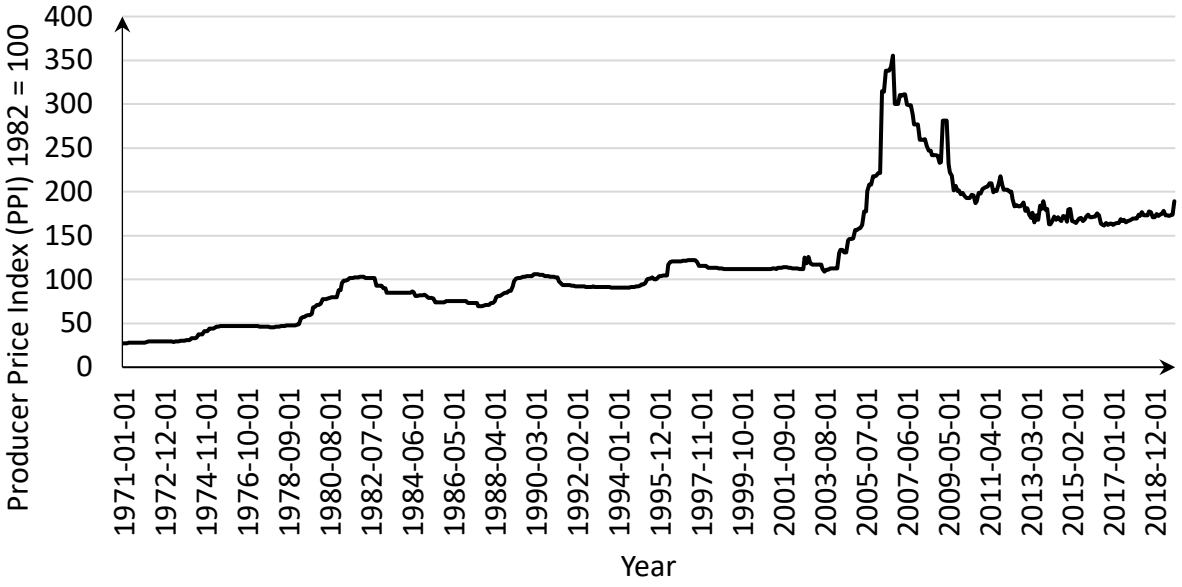

Figure 5.4. The producer price index of titanium milled production from 1971 to 2019 [142].

5.3.1.3. Bromine Price Data

Bromine is one of the active species used as the electrolyte in the ZBFB system, which also contributes to over 20% of the total system cost. Statistical information on bromine prices has been researched by the USGS. However, the price data are not kept up to date to protect company proprietary information, as the scale of the bromine market is relatively small and only a few suppliers are identified [143]. The yearly price for bromine from 1991 to 2017 is presented in **Figure 5.5** [143]. The current price used in the three-point estimation is set to be 4.90 $/kg, which is from the year 2017 – the most updated information available. The optimistic price is 1 $/kg since the market price had stagnated at a value of approximately 1 $/kg for a long period from 1991 – 2005. It is noted that the market price for bromine has slowly increased after the year 2006, and the peak price cannot be determined since no decreasing trend is observed. This renders estimation of pessimistic

price difficult as it is unknown how much higher the price of bromine can reach. To predict a possible future (pessimistic) price, a simple linear regression is performed (**Figure 5.6**) using price data from 2007 to 2017 as the price increase rate is relatively steady during this time. With the simulation, the pessimistic price is set to be 6 $/kg, corresponding to the predicted value in the year 2020.

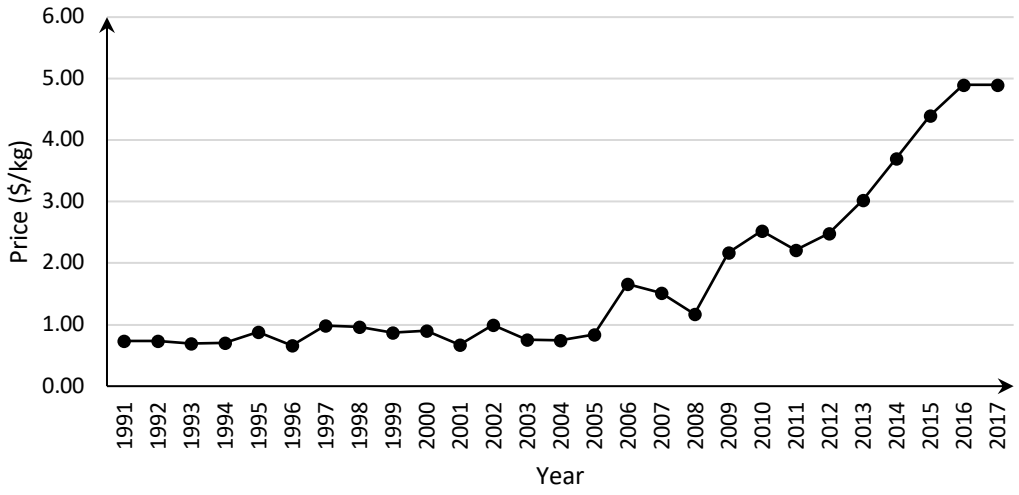

Figure 5.5. The average yearly price of bromine from 1991 – 2017 [143].

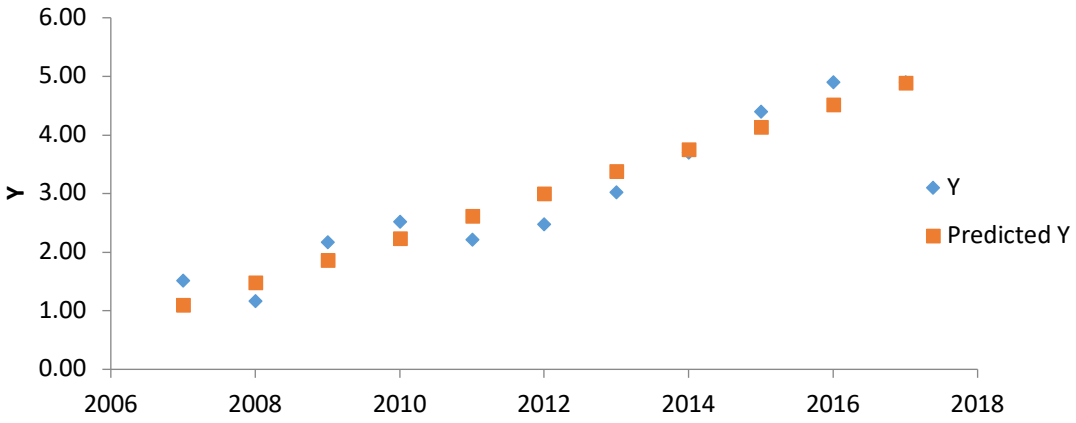

Figure 5.6. The regression analysis for bromine using price data from 2007-2017.

5.3.1.4. Carbon Fiber Felt Price Data

In this analysis, the carbon fiber felt is largely used in the IFB battery management system as a rebalancing cell and contributes strongly to the total system cost of the IFB system. The market price of carbon fiber felt is not continuously monitored since it is a material used in very specific applications and has a complex production chain. To acquire three price points for estimation, all the data are extracted from the literature. The current price is estimated to be 237.60 $/kg, the pessimistic price is set to be 280 $/kg, and the optimistic price is estimated to be 80 $/kg [52].

5.3.2. Baseline Cost Analysis

5.3.2.1. Vanadium Pentoxide Flow Battery

The material costs for the VRFB system, are calculated using the unit cost input data in **Table 5.2**. In **Figure 5.7**, the cost distribution by component is provided, along with an expanded view for the cell stack (power components) only. Due to the high cost of vanadium pentoxide and its use as the major species in the electrolyte, the cost of electrolyte accounts for 80% of the total cost. Other components related to energy capacity such as tanks, pipes, and pumps account for only 1% of total costs. The second-largest share of the total cost is the battery management system (BMS) costs at 9%, and the inverter, which also belongs to the balance of plant, contributes 6% of the total cost. Surprisingly, the cost of the whole cell stack, which is related to the power capacity, only contributes 4% to the total cost. When only considering the power capacity component, the Nafion® membrane is the highest contributor and accounts for 55% of the power capacity subsystem. The Nafion® membrane contributes 2% of the total cost. The electrode and cell stack accessories contribute 19% and

20% of the power capacity subsystem, respectively, but these are almost negligible relative to the total cost.

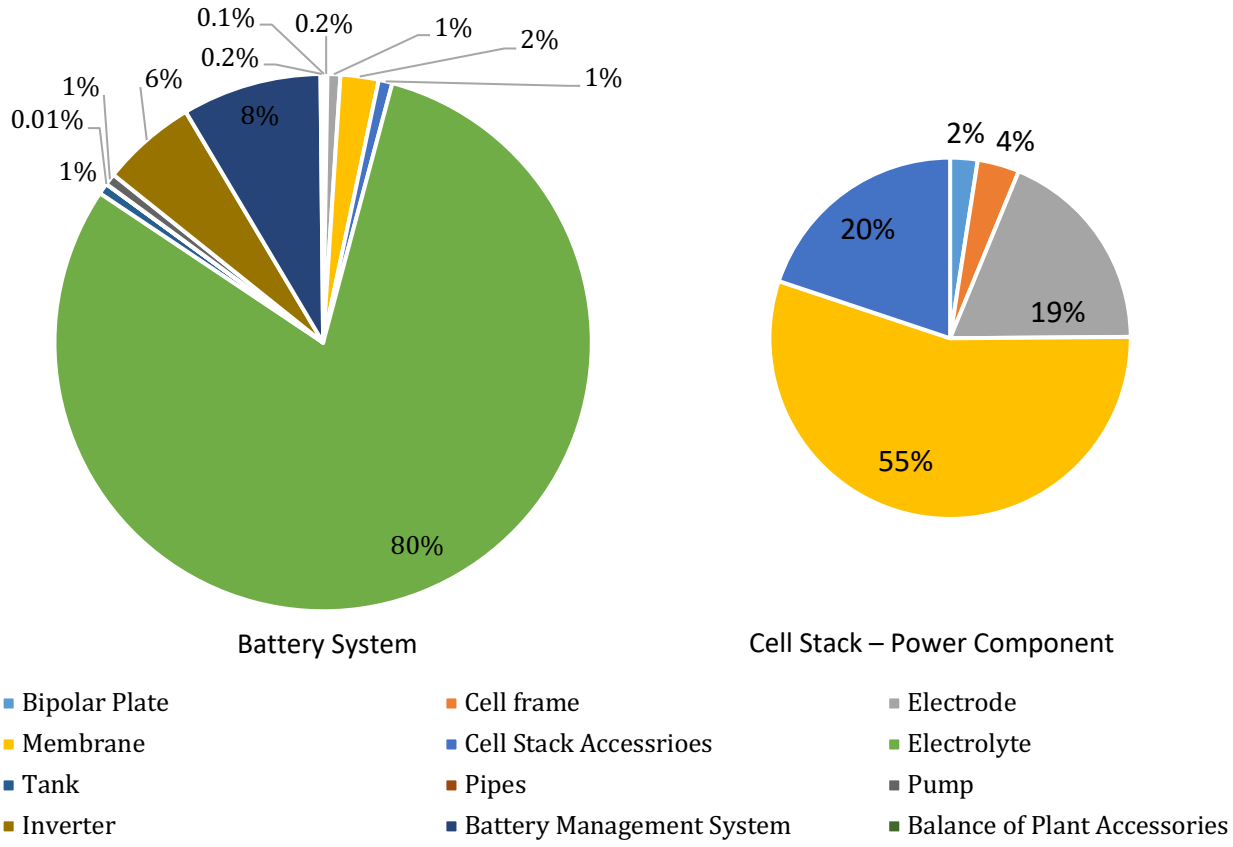

Figure 5.7. Materials cost distributed by component in the VRFB system.

5.3.2.2. Zinc-bromide flow battery

The cost of materials used for the ZBFB system is calculated using the unit cost input in **Table 5.3**. In **Figure 5.8**, the cost distribution by component is provided, along with an expanded view for the cell stack (power components) only. The power capacity components comprise the largest share of total costs as the cell stack accounts for 33% of the total cost, followed by components related to energy capacity with a share of 31% of the total cost. The BMS accounts for 20% of the total cost, and the percentage for the inverter is 14%. The

electrolyte and the bipolar plate are identified as cost drivers, as they account for 29% and 22% of the total cost, respectively. The materials with high prices associated with the bipolar plate and electrolyte are titanium and bromine, respectively. It is noted that the ZBFB electrolyte does not contribute as much to the total cost as the electrolyte in the VRFB system.

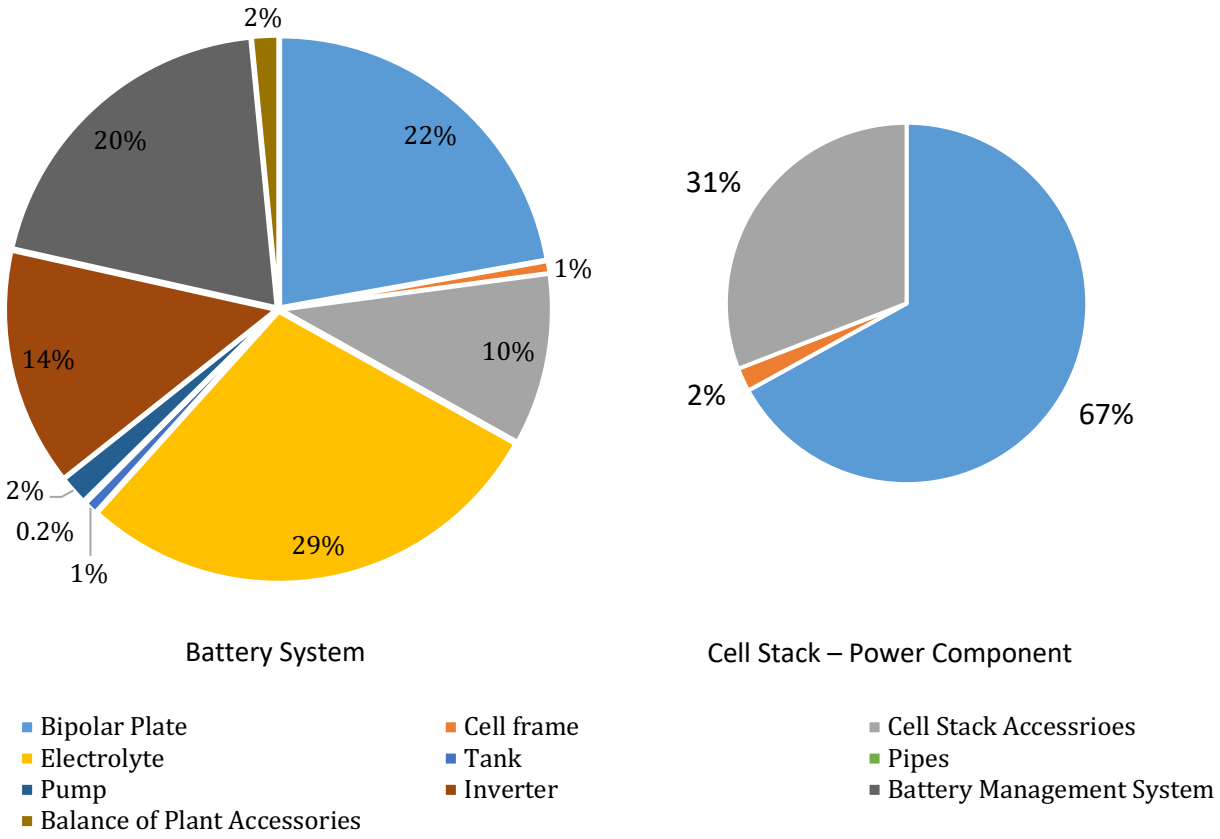

Figure 5.8. Materials cost distributed by component in the ZBFB system.

5.3.2.3. All-iron flow battery

The material costs for the IFB system are calculated using the unit cost input data in **Table 5.4**. In **Figure 5.9**, the cost distribution by component is provided, along with an expanded view for the cell stack (power components) only. Contrary to the VRFB and ZBFB,

the BMS in IFB contributes to the largest share of the cost at 49% of the total cost. The cell stack accounts for 25% of the total cost, while the electrolyte only accounts for 5%. Another supporting component, the inverter, accounts for 14% of the total cost. The cost distribution considering only the cell stack indicates that the membrane accounts for 55%, followed by the electrode and cell frame, which account for 15% and 14%, respectively.

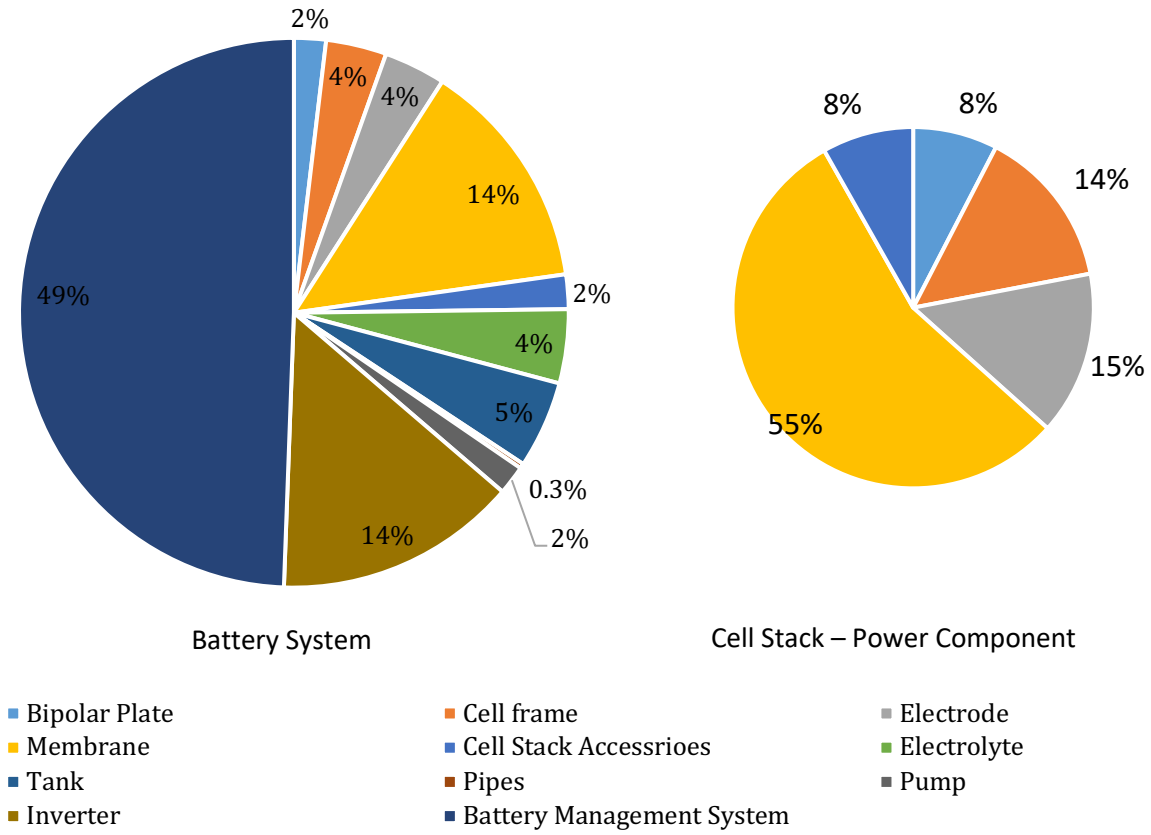

Figure 5.9. Materials cost distributed by component in the IFB system.

5.3.2.4. Comparison of the Three Flow Batteries

The material costs (and relative distribution by component) for the three battery systems normalized to per kWh energy capacity are compared in **Figure 5.10**. The cost per

energy capacity of VRFB is significantly higher than that of the other two flow batteries due to the large use of vanadium pentoxide and its corresponding high raw material cost. The primary cost drivers vary among the flow batteries. The VRFB cost is dominated by the electrolyte with a percentage cost of over 80%. The largest contributor for ZBFB is also the electrolyte with a share of 29% but only slightly higher than the bipolar plate, which corresponds to 22%. By contrast, the primary cost driver for IFB is the BMS at 49% due to the large amount of carbon fiber felt used as the rebalancing cell as specified by the manufacturer, which is unique in the IFB system, compared to 8% for VRFB and 20% for ZBFB. Another balance of plant component, the inverter, accounts for 6%, 14%, and 14% of total costs for the VRFB, ZBFB and IFB systems, respectively. These results align well with the literature results shown in **Table 5.1**, where the share of PCS varies from 8% to 25%. However, the cost comparison may be somewhat limited by the different scales and energy-to-power ratios for the flow battery systems. Further, with the fast development of newly designed battery systems, the technology readiness levels associated with different types of flow batteries may also vary. In our case, the design parameters are fixed by the manufacturer specifications.

Due to differences in the battery parameters provided by manufacturers, we have calculated the battery system cost with normalized parameters and performed a sensitivity analysis by varying the E/P ratio and energy capacity, so that proper comparison between the different battery types can be made. Four levels of E/P ratio and energy capacity are applied to change the amount of stored energy and discharging behavior, as the related power output is fixed once the E/P ratio and energy capacity are determined. The total

battery system cost associated with different E/P ratios and energy capacities for the three different flow battery types are provided in **Figure 5.10**.

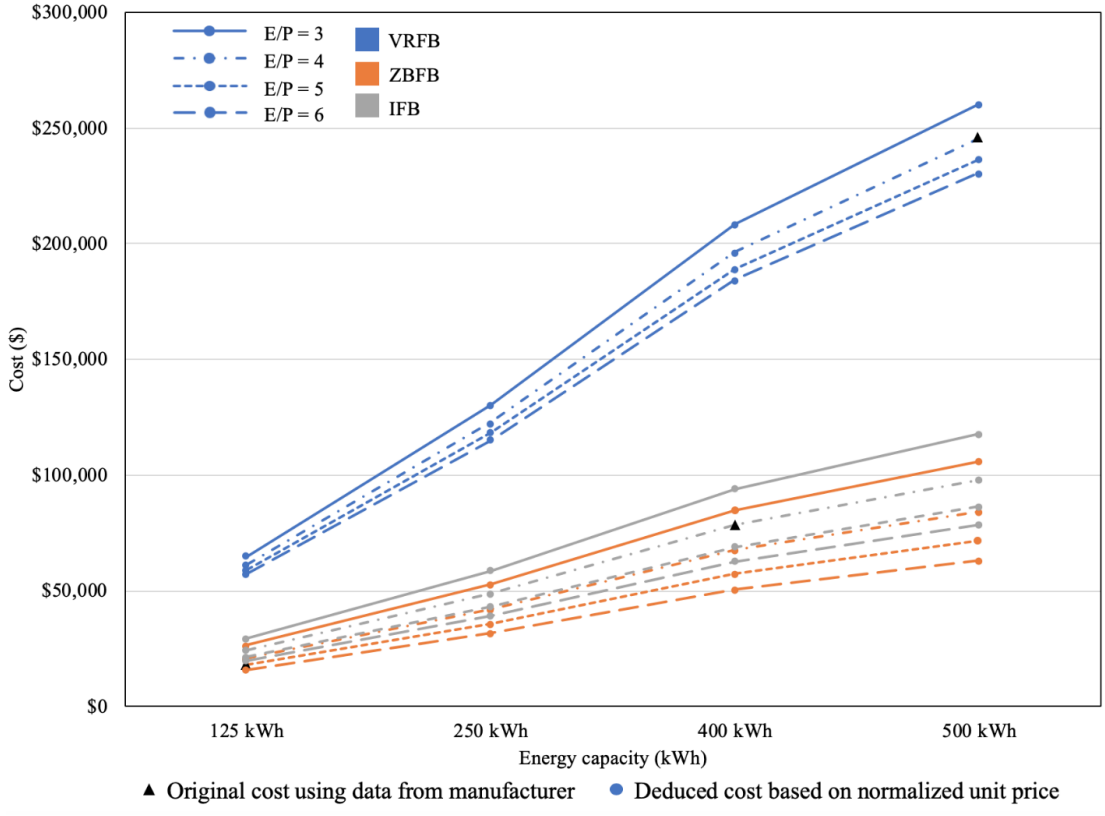

Figure 5.10. Total battery system cost for different E/P ratios and energy capacities.

The costs using the raw data and default battery parameters from manufactures are highlighted as black triangles, while other data points are deduced from the original data using unit cost per kWh or per kW for different components multiplying with the energy capacity and power output for various assumed battery systems. For example, since the cell stacks are primarily associated with the power output, the cost of cell stacks should be scaled up using unit data per kW. On the contrary, the electrolyte and tank determine the energy capacity, therefore the total cost of these two in the battery should be calculated using unit

data per kWh. For BOP, both the power control system, pump, and inverter are categorized as power components as they are closely related to the power output, while the BOP accessories and rebalancing cells in IFB are seen as energy subsystem components to contain and balance the electrolyte system.

From **Figure 5.10**, it is observed that with the data available for this study, the cost of the VRFB system is always higher than the ZBFB and IFB system, regardless of energy capacity and E/P ratio. Further, the increase in cost for VRFB is significantly higher when increasing the energy capacity of the battery system due to the high unit price and use of vanadium pentoxide compared to the electrolyte of the ZBFB and IFB. The cost of the ZBFB and IFB could vary depending on the different battery parameters. At similar energy capacities and E/P ratios, the cost of the IFB would be slightly higher than that for the ZBFB and for a 125 kWh system, the costs of IFB and ZBFB are close and comparable. Interestingly, the cost of the battery system is very sensitive to the E/P ratio when the energy capacity is fixed. The smaller the E/P ratio, the higher the power output and the influence of power output on ZBFB is more significant than for the VRFB and IFB, especially when the energy capacity is high. For example, the increase in cost for the ZBFB from E/P = 4 to E/P =3 is higher than VRFB and IFB for a 500 kWh system. This is attributed to the high cost of the titanium bipolar plate in the cell stack as a power component for the ZBFB compared to the graphite-based bipolar plate in VRFB and IFB. This could explain why the ZBFB is designed to be smaller in energy capacity as the effect of E/P ratio is not that insignificant for a 125 kWh system.

5.3.3. Sensitivity Analysis due to Material Price Variations

The economic cost analyses presented in this study are driven by material prices, however, the price of raw materials used in the three flow battery systems have been subject to historical variations due to fluctuations in the global markets for these materials. Therefore, in this section, a sensitivity analysis focused on variations in raw material prices based on historical fluctuations is performed.

The three-point estimation values (described in Section 5.2.2) are summarized in **Table 5.5** for the four materials assessed. With the three price points determined, a weighted average (E) as the expected market price is calculated with a standard deviation available to reflect the variations. The larger the price gap between the pessimistic and optimistic price, the larger the standard deviation identified.

Table 5.5. The price estimation for the selected materials used in the flow battery.

Price Information ($/kg)	Vanadium pentoxide	Titanium	Bromine	Carbon fiber felt
Current	35.75	30.00	4.90	237.60
Pessimistic	50.00	62.65	6.00	280.00
Optimistic	8.00	17.65	1.00	80.00
Weighted average (E)	32.33	33.38	4.43	218.40
Standard deviation (SD)	7.00	7.50	0.83	33.33

The results of the sensitivity analysis are presented in **Figure 5.11**. The material cost of the VRFB system due to the variations in vanadium pentoxide price (**Figure 5.11(a)**) ranges between 185.5$/kWh and 647.5 $/kWh when using different price points. The expected price value is estimated to be 466.0 $/kWh with a standard deviation value of 77.0 $/kWh. Thus, changes in the price of vanadium pentoxide will greatly affect the VRFB system

cost. The baseline value, 491 $/kWh, is near the upper value in the range, reflecting that recent prices for this material have been higher than historical values.

The influence of titanium and bromine prices on the ZBFB cost is shown in **Figure 5.11(b)** and **5.11(c)**, respectively. The expected ZBFB cost (157.8 $/kWh) is higher than the baseline estimated value (153.2 $/kWh), relative to titanium sensitivity, whereas, the expected cost for the bromine scenario (149.3 $/kWh) is lower than the baseline estimation, but these differences are relatively small. The system cost deviations due to variations on titanium price are larger than the case of bromine, and both of them are relatively small compared to the vanadium pentoxide for VRFB.

For the IFB, the variations in cost due to price changes for carbon fiber felt are provided in **Figure 5.11(d)**. The expected system cost (190.7 $/kWh) is slightly lower than the baseline estimated value (196.1 $/kWh). The decrease in cost using the optimistic price is larger than the increase in cost when using a pessimistic value, which indicates the future price is likely to further lower the cost.

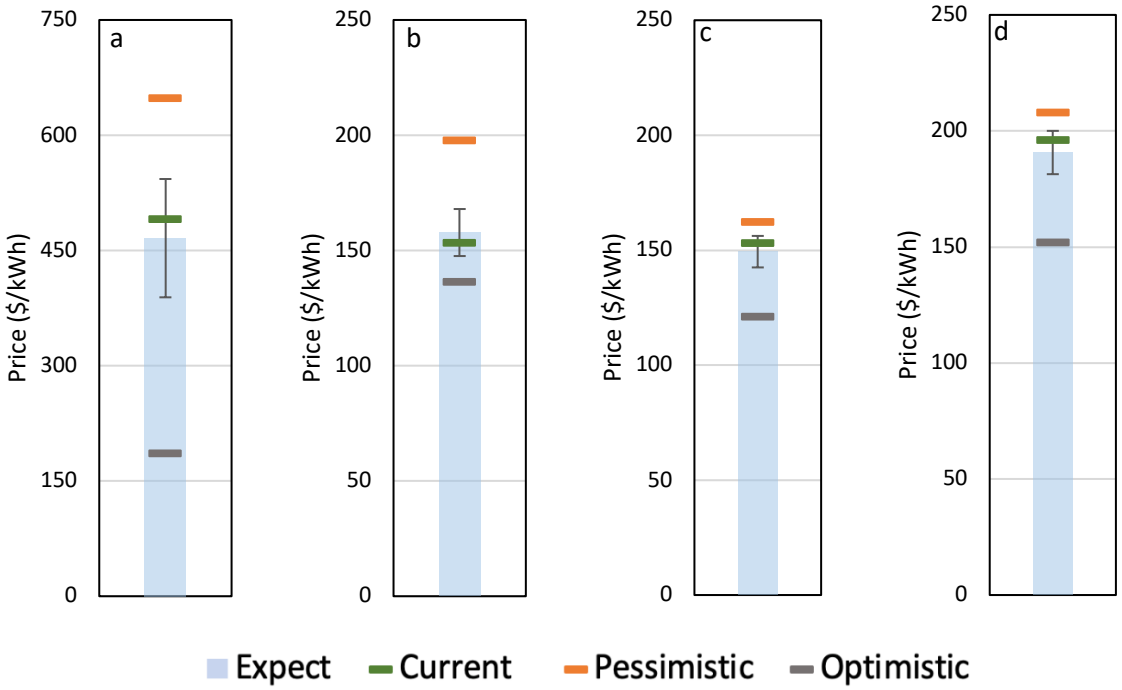

Figure 5.11. The sensitivity of flow battery cost due to variations in the material price: (a) vanadium pentoxide for VRFB, (b) titanium and (c) bromine for ZBFB, and (d) carbon fiber felt for IFB.

5.4. Summary

A techno-economic assessment was conducted on three different flow battery types to determine: 1) the cost of energy storage capacity for each flow battery type based on material prices that are endemic to each type, 2) the main drivers of the total cost for each flow battery type, 3) the sensitivity of total cost for flow battery energy storage to fluctuations in material and component prices, and 4) comparison of cost and environmental impact among the three flow battery types. These objectives were accomplished by compiling an inventory of material and component price data from literature and public

sources for the materials used in the flow battery systems as specified by their manufacturers and conducting a techno-economic assessment for each type.

Chapter 6: The Role of Data Source Selection in Chemical Hazard Assessment: A Case Study on Organic Photovoltaics

6.1 Abstract

Chemical hazard assessment (CHA), designed to evaluate the inherent hazard of chemicals used in everyday consumer products, is gaining in popularity and rigor. Although CHA is being more commonly used by industry and government organizations, there is limited information in the academic literature on the merits and limitations of CHA methods. In the current study, the significance of the need to use multiple data sources to successfully complete a CHA is explored. Specifically, a case study approach is used in which more than one hundred organic substances used in the synthesis of organic solar cells are evaluated using the GreenScreen® for Safer Chemicals framework as the basis for the CHA. Seven data sources, including three chemical-oriented, two hazard-trait-oriented, and two predictive data sources, are utilized to minimize data gaps and allow for complete assessments for most of the chemicals of interest. Findings from sensitivity analysis using single data sources and combinations of data sources highlight that the CHA outcomes can vary considerably as a function of data sources used, which highlights the importance of identifying and/or creating more comprehensive and standardized data sources.

6.2 Material and Methods

In an effort to understand the process for conducting a CHA, and the implications of data source selection on CHA results, a case study on the process chemicals used to fabricate low bad gap polymers (LBGPs) in organic photovoltaic solar cells (OPVs) is presented. OPVs

is a promising technology for energy storage due to its flexibility and large-scale manufacturing ability. Of several CHA tools and decision frameworks, the GreenScreen® for Safer Chemicals (GreenScreen®) is selected as the base framework to assess the chemical hazard (see Section 2.1 in Chapter 2).

6.2.1 Low Band Gap Polymers Used in Organic Photovoltaics

The chemicals used in the photoactive layer of organic solar cells were selected for the case study because this is still an emerging technology. **Figure 6.1** illustrates the general structure for an organic solar cell. Absorption of a photon leads to the formation of an excited state, which travels to the photoactive layer where the charges are separated and transported through the hole conductor to the cathode or anode electrodes [144]. The organic cell is placed onto a transparent glass substrate to give further stability. The most important layer in a solar cell is the photoactive layer because it creates the pathway for the electricity to make its way to the electrodes to convert solar energy into electricity. To accomplish this, two different materials, an electron donor and electron acceptor, are combined [145]. This donor material is the focus of the current study. The most popular substance used as the donor material is poly(3-hexylthionphene) (P3HT), with power conversion efficiency (PCE) values of approximately 5%. However, P3HT is not a good electron donor for the photoactive layer due to its high band gap that does not allow it to absorb a wide range of the solar spectrum [146]. Thus, research efforts have focused on the laboratory development and testing of polymers with lower band gaps, which allow for more photon absorption and potentially higher PCEs [147].

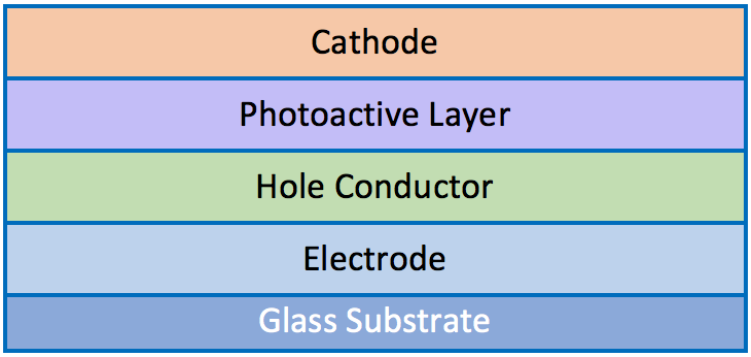

Figure 6.1. General structure of an organic solar cell.

There have been many new substances synthesized as possible LBGPs for the donor material in the active layer, but not all provide adequate efficiencies and therefore have lower probability of being commercialized. Krebs et. al. [146] explained that to be commercially produced, organic solar cells must exhibit PCEs of at least 10%, thus an arbitrary threshold of 7% was used as the basis for selecting the polymers to be evaluated in the current study. A total of thirteen polymers were investigated: PDTP-DFBT, PBDTT-DPP, PBDTT-SeDPP, PCPDTFBT, PDTSTPD, PDPP5T, PCDTBT, PBTTPD, PBnDT-DTffBT, PBDTTPD, PTB7, PSiF-DBT, and PDTGTPD. The risks of environmental releases of and direct human exposure to these polymers is lower than for the monomers and other materials used in their synthesis [148], which can be released during their production, transport, use and disposal, including as residuals remaining in the finished polymer; therefore, the chemicals used to synthesize the LBGPs were assessed. A complete list of the polymers and the chemicals used in their synthesis is provided in **Table 6.1**.

Table 6.1. Low Band Gap Polymers - Full Names and Power Conversion Efficiencies.

Polymer	Full Name	Power conversion efficiency
PDTP-DFBT	Poly[2,7-(5,5-bis-(3,7-dimethyloctyl)-5H-dithieno[3,2-b:2′,3′-d]pyran)-alt-4,7-(5,6-difluoro-2,1,3benzothiadiazole)]	10.6% [149]
PBDTT-DPP	poly{2,6′-4,8-di(5-ethylhexylthienyl)benzo[1,2-b;3,4-b]dithiophene-alt-5-dibutyloctyl-3,6-bis(5-bromothiophen-2-yl)pyrrolo[3,4-c]pyrrole-1,4-dione}	8.6% [150]
PBDTT-SeDPP	poly{2,6′-4,8-di(5-ethylhexylthienyl)benzo[1,2-b;3,4-b]dithiophene-alt-2,5-bis(2-butyloctyl)-3,6-bis(selenophene-2yl)pyrrolo[3,4-c]pyrrole-1,4-dione}	9.5% [151]
PCPDTFBT	Poly[2,6-(4,4-bis-(2-ethylhexyl)-4*H*-cyclopenta [2,1-*b*;3,4-*b*′]dithiophene)-*alt*-4,7(2,1,3-benzothiadiazole)]	8.2% [152]
PDTSTPD	Poly[(5,6-dihydro-5-octyl-4,6-dioxo-4*H*-thieno[3,4-*c*]pyrrole-1,3-diyl)[4,4-bis(2-ethylhexyl)-4*H*-silolo[3,2-*b*:4,5-*b*′;]dithiophene-2,6-diyl]]	7.3% [153]
PDPP5T	diketopyrrolopyrrole–quinquethiophene alternating copolymer	7.0% [154]
PCDTBT	Poly[*N*-9′-heptadecanyl-2,7-carbazole-*alt*-5,5-(4′,7′-di-2-thienyl-2′,1′,3′-benzothiadiazole)]	7.0% [155]
PBTTPD	Poly[[5-(2-ethylhexyl)-5,6-dihydro-4,6-dioxo-4*H*-thieno[3,4-*c*]pyrrole-1,3-diyl](4,4′-didodecyl[2,2′-bithiophene]-5,5′-diyl)]	8.6% [156]
PBnDT-DTffBT	Poly(benzo[1,2-b:4,5-b′]dithiophene)-(5,6-difluoro-4,7-dithien-2-yl-2,1,3-benzithiadiazole)	7.2% [157]
PBDTTPD	Poly[[5-(2-ethylhexyl)-5,6-dihydro-4,6-dioxo-4*H*-thieno[3,4-c]pyrrole-1,3-diyl][4,8-bis[(2-ethylhexyl)oxy]benzo[1,2-b:4,5-b′]dithiophene-2,6-diyl]]	7.3% [158]
PTB7	Poly({4,8-bis[(2-ethylhexyl)oxy]benzo[1,2-*b*:4,5-b′]dithiophene-2,6-diyl}{3-fluoro-2-[(2-ethylhexyl)carbonyl]thieno[3,4-*b*]thiophenediyl})	9.2% [159]
PSiF-DBT	Poly(2,7-silafluorene)-alt-(4,7-di-2-thienyl-2,1,3-benzothiadiazole)	7.73% [160]
PDTGTPD	Poly(dithienogemole-alt-thienopyrrolodione)	7.3% [161]

6.2.2 Data Sources for Hazard Assessment

Various data sources are recommended for completing a GreenScreen® assessment [13]. For this study, we use the following sources: the Globally Harmonized System of Classification and Labeling (GHS) [108], GESTIS [162], Sigma-Aldrich safety data sheets (SDSs) [163], California Proposition 65 [164], TEDX [165], VEGA [166] and EPI Suite™ [167]. GHS, an internationally agreed upon system created by the United Nations, was designed to replace the various hazard classification systems in different countries by using a consistent set of criteria. GHS-Japan [168], currently the largest GHS-based database containing information on approximately 3000 chemicals, was used in this study. The GESTIS substances database is maintained by the Institute for Occupational Safety and Health of the German Social Accident Insurance (IFA). It provides GHS classifications that may not have been found in GHS-Japan. Sigma-Aldrich (St. Louis, Missouri), which is a producer of commercial chemicals, provides an extensive set of publicly available SDSs. We define these three data sources as 'chemical-oriented data sources' as they are collections of various hazard traits associated with certain chemicals, arranged by chemical.

The chemical-oriented data sources do not cover all the hazard traits used in GreenScreen®, thus additional data sources were needed. The second type of data sources used are labeled as 'hazard-trait-oriented data sources' because these sources provide information on specific hazard traits and list the chemicals that exhibit the hazard traits. For example, California Proposition 65 provides a publicly available list of chemicals known to the State of California to cause cancer and reproductive or developmental effects. Another source, TEDX, known as the Endocrine Disruption Exchange, assesses and compiles evidence for substances that interfere with development and reproductive function, and provides a

limited, but complementary, data set for substances that are suspected or known to be endocrine disruptors.

The last two data sources used in this study, EPI Suite™ and VEGA, are labeled as 'predictive data sources'. Instead of direct reference to experimental toxicological test results, both predictive data sources use structure-activity relationships to estimate the toxicity of the chemical of interest. They both start from a molecular structure represented using Simplified Molecular-Input Line-Entry System (SMILES) notation and use group contribution or linear free energy relationships to predict hazard traits. EPI Suite™, an estimation program developed by the US EPA and Syracuse Research Corporation, was chosen because it provides physical and chemical properties of an organic substance as well as information on environmental fate [167]. VEGA, a package of estimation programs focused on environmental fate and human toxicity endpoints such as mutagenicity, provides detailed information and analysis to support the toxicity predictions, allowing the user to evaluate the reliability of the prediction. Utilizing all of the above resources allows for the assignment of a benchmark score for each of the chemicals of interest in the case study (described below).

6.3 Results and Discussion

6.3.1 Chemical Hazard Assessment Results

In this study, 'GreenScreen®-based' chemical hazard assessments using the seven previously mentioned data sources were successfully completed for the 149 process chemicals used to fabricate the 13 active-layer LBGPs of interest (details of the 'GreenScreen®-based' benchmark score for each processing chemical are provided in

Appendix G). The CHA results for each LBGP are summarized by benchmark score in **Table 6.2**, where the distribution both by number of chemicals and by percent of chemicals are listed, along with the best/worst performance highlighted for each column. All 13 LBGPs had a relatively high percentage of BM-1 chemicals and the percentage of BM-1 plus BM-2 chemicals is always greater than 70%. Comparatively, the percentages of BM-3, BM-4, and BM-U chemicals are relatively low. **Figure 6.2** illustrates the distribution in benchmark scores for all 149 chemicals aggregated together indicating that 37% are BM-1 chemicals, 38% are BM-2 chemicals, 12% are BM-3 chemicals, 8% are BM-4 chemicals, and 5% are BM-U chemicals. These results demonstrate that the majority of the chemicals assessed are chemicals of concern.

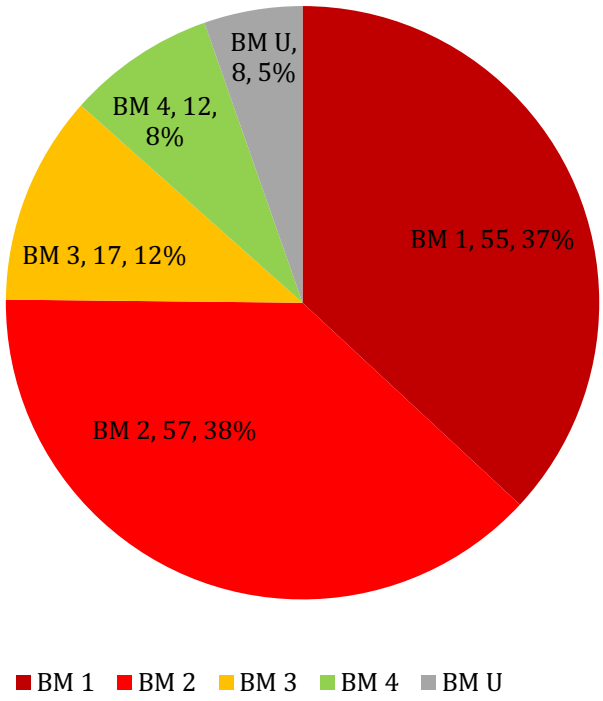

Figure 6.2. 'GreenScreen®-based' results for the 149 chemicals used to process the 13 LBGPs studied.

Table 6.2. Number and Percentage of 'GreenScreen®-Based' Benchmark Scores for each LBGP.

Polymer	BM-1		BM-2		BM-3		BM-4		BM-U		Total Chemicals Used
PDTP-DFBT	14	47%	8	27%	5	17%	1	3%	2	7%	30
PBDTT-DPP	7	41%	7	41%	2	12%	1	6%	0	0%	17
PBDTT-SeDPP	10	48%	6	29%	3	14%	1	5%	1	5%	21
PCPDTFBT	17	43%	15	38%	5	13%	2	5%	1	3%	40
PDTSTPD	12	50%	7	29%	2	8%	2	8%	1	4%	24
PDPP5T	10	40%	8	32%	2	8%	5	20%	0	0%	25
PCDTBT	13	37%	13	37%	5	14%	4	11%	0	0%	35
PBTTPD	13	45%	11	38%	1	3%	4	14%	0	0%	29
PBnDT-DTffBT	9	35%	11	42%	1	4%	4	15%	1	4%	26
PBDTTPD	14	45%	10	32%	2	7%	4	13%	1	3%	31
PTB7	18	42%	19	44%	2	5%	3	7%	1	2%	43
PSiF-DBT	17	52%	10	30%	3	9%	3	9%	0	0%	33
PDTGTPD	11	42%	10	39%	2	8%	2	8%	1	4%	26

The hazard traits that triggered each BM-1, BM-2 and BM-3 chemical, in accordance with the decision logic described above, are noted in **Table 6.3**. Looking closer, endocrine activity (E) was the hazard trigger for 12 of the 55 BM-1 chemicals; persistence (P) and carcinogenicity (C) were the hazard triggers for 11; reproductive toxicity (R), mutagenicity (M) and bioaccumulation (B) were the next most common hazard triggers for BM-1 chemicals. For BM-2 chemicals, high eye irritation (IrE) and skin irritation (IrS) were the hazard traits that triggered most of the BM-2 scores, whereas systematic toxicity and organ

effects (ST) was the third most common trigger. Flammability (F) and acute aquatic toxicity (AA) were also common hazard triggers for BM-2 scores. For the BM-3 chemicals, the main hazard trigger was IrS.

Table 6.3. Hazard Traits that Trigger the 'GreenScreen®-Based' Benchmark Scores.

Hazard Trait	BM-1	BM-2	BM-3
C	11	1	0
M	6	0	0
R	7	3	0
D	2	0	0
E	12	0	0
N	0	6	0
AT	0	9	2
IrE	0	27	4
IrS	0	21	5
ST	0	17	2
SnS	0	4	0
SnR	0	2	0
AA	0	10	4
CA	0	1	4
P	11	4	2
B	6	3	1
Rx	0	1	0
F	0	12	4

6.3.2 Data Source Sensitivity Analysis

The results shown above were generated using seven data sources, which collectively provide insight into the relative hazard associated with the 149 process chemicals used to make LBGPs. The purpose of this section is to evaluate the sensitivity of these results to the various data sources used. To do so, we conduct the following sensitivity analyses between data sources used and resulting benchmark scores: (1) benchmark scores if only one data source is used, considering each source one at a time; and (2) benchmark scores if all but one data source is used, removing one source at a time. Sensitivity of hazard triggers to the data source(s) used is also explored.

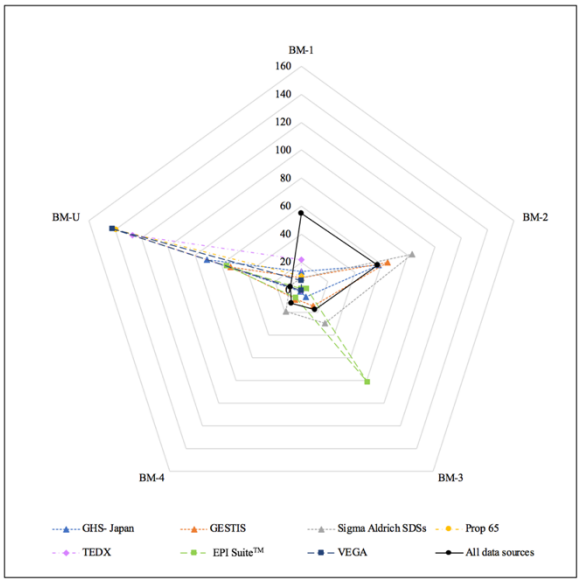

Figure 6.3. Sensitivity of the 'GreenScreen®-based' benchmark score results for the 149 LBGP process chemicals to applying single data sources compared with using all data sources.

We first consider the sensitivity of the assessed benchmark if only one data source is used, considering each source one at a time, and compare this to the results shown above that utilize all seven data sources. We note that an official GreenScreen® assessment requires the use of more than one data source [13]. These sensitivity results (see **Figure 6.3**) clearly illustrate that multiple data sources are required to capture the BM-1 and minimize the BM-U chemicals. Although GHS-Japan, GESTIS and Sigma-Aldrich SDSs sources are more comprehensive than the others in the number of hazard traits accounted for, they do not include data on E, P, and B, which are important potential hazard traits that can result in a BM-1 score. Thus, the additional hazard-oriented and predictive data sources are key to not only reducing the number of BM-U chemicals, but also in appropriately placing chemicals into BM-1. The Sigma-Aldrich SDSs data source is particularly useful in placing BM-2 chemicals because it has abundant hazard trait information on Physical Hazards and Human Health Group II Hazards (i.e., F, IrE and IrS) for more chemicals. In contrast, using only EPI Suite™ will increase the number of BM-3 chemicals because this data source only contains information on environmental fate such as P and B without toxicity information (T).

We next consider the sensitivity of the benchmark scores to scenarios in which all but one data source is used, removing one data source at a time. This analysis is not simply the inverse of the previous analysis, because multiple hazard classifications are generally required to assign a benchmark score. The results (see **Figure 6.4**) indicate that with one fewer data source (regardless of which one) the number of BM-1 chemicals tends to decrease and the numbers of BM-3 and BM-U chemicals tend to increase or remain the same. The trends for BM-2 and BM-4 chemicals are less clear and depend on the data source removed. It is observed, however, that when any of the hazard-oriented or predictive data sources are

not used, the number of BM-2 chemicals increases due to the fact that these data sources had placed the chemicals in the BM-1 category. These data sources contain information on additional chemicals and additional hazard traits not contained within the chemical-oriented data sources. Of these four data sources, the contributions of EPI Suite™ and TEDX to successfully assigning BM scores are higher than those of Prop 65 and VEGA. Among the chemical-oriented data sources, the contribution of Sigma-Aldrich SDSs is the highest because it provides information that can move many BM-U chemicals to scored benchmark chemicals. The major contribution of GHS-Japan is that it provides information that can convert certain BM-3 chemicals into BM-1 and BM-2 chemicals. The benchmark results are not sensitive to the removal of GESTIS as a data source, because most of the hazard information in GESTIS overlaps with the data in GHS-Japan and Sigma-Aldrich SDSs.

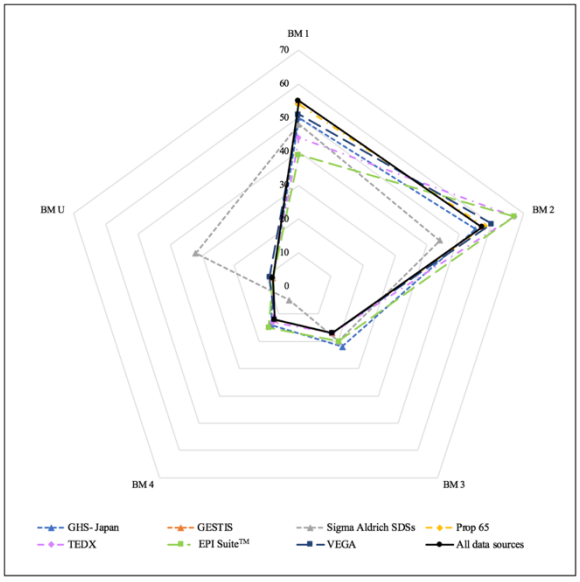

Figure 6.4. Sensitivity of the 'GreenScreen®-based' benchmark score results for the 149 LBGP process chemicals to extracting one data source at a time compared with using all data sources.

The next sensitivity analysis is focused on the relationship between data source and the hazard traits that trigger the benchmark scores. There are two components to this analysis. In the first component, we investigated the hazard traits that trigger BM-1, BM-2 and BM-3 chemicals by separately applying each of the three chemical-oriented data sources. In the second component, we created three combinations (Combination 1: chemical-oriented data sources; Combination 2: chemical-oriented data source plus hazard-trait-oriented data sources; and Combination 3: chemical-oriented data sources plus hazard-trait-oriented data source plus predictive data sources) to compare the hazard traits that trigger the different benchmark scores.

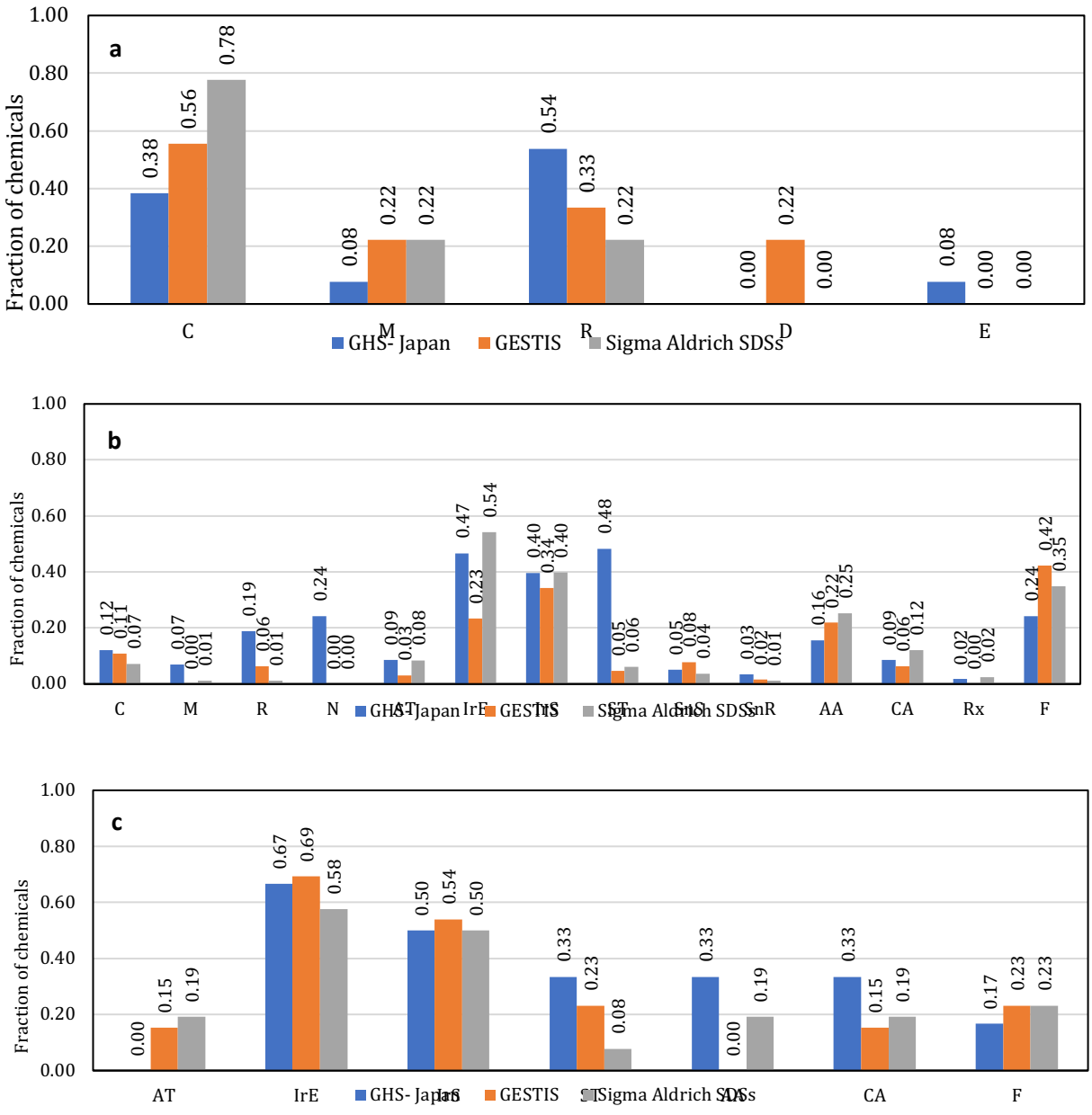

Figure 6.5. The fraction of chemicals triggered by each hazard trait when applying different chemical-oriented data sources for: (a) BM-1, (b) BM-2, and (c) BM-3 chemicals.

The results for the first component of this sensitivity analysis are shown in **Figure 6.5**. A ratio value is used to represent the frequency of the hazard traits that trigger the benchmark scores because the number of chemicals assigned a given benchmark score varies

depending on the data sources used (as illustrated above). The benchmark score of a chemical can be triggered by multiple hazard traits, consequently the sum of the ratio values is not always equal to 1. For BM-1 chemicals (see **Figure 6.5(a)**), the most common trigger in GHS-Japan is R, while in GESTIS and Sigma-Aldrich SDSs, the most common trigger is C. Also, note that there are limited BM-1 chemicals triggered by the hazard traits M, D and E. A BM-2 score can be triggered by a wider range of hazard traits, therefore, the results are more sensitive to the data source used, as seen in **Figure 6.5(b)**. For GHS-Japan, the most common trigger is ST, followed by IrE and IrS; for GESTIS, the top three triggers are F, IrS and IrE; and for Sigma-Aldrich SDSs, they are IrE, IrS and F. Also, the analysis highlights that some hazard traits such as N, ST and R are found in GHS-Japan, but are rarely included in the GESTIS and Sigma-Aldrich SDSs data sources. For BM-3 chemicals (see **Figure 6.5(c)**), there is less variation and the top triggers for all three data sources are IrS and IrE. These results highlight that while GHS-Japan has more data on ST, AA, and CA, the GESTIS and Sigma-Aldrich SDSs have more data on AT and F. The data in **Figure 6.5** show that the hazard traits that trigger the benchmark scores are indeed sensitive to the data source even though these three chemical-oriented data sources each contain data that are based on the GHS framework.

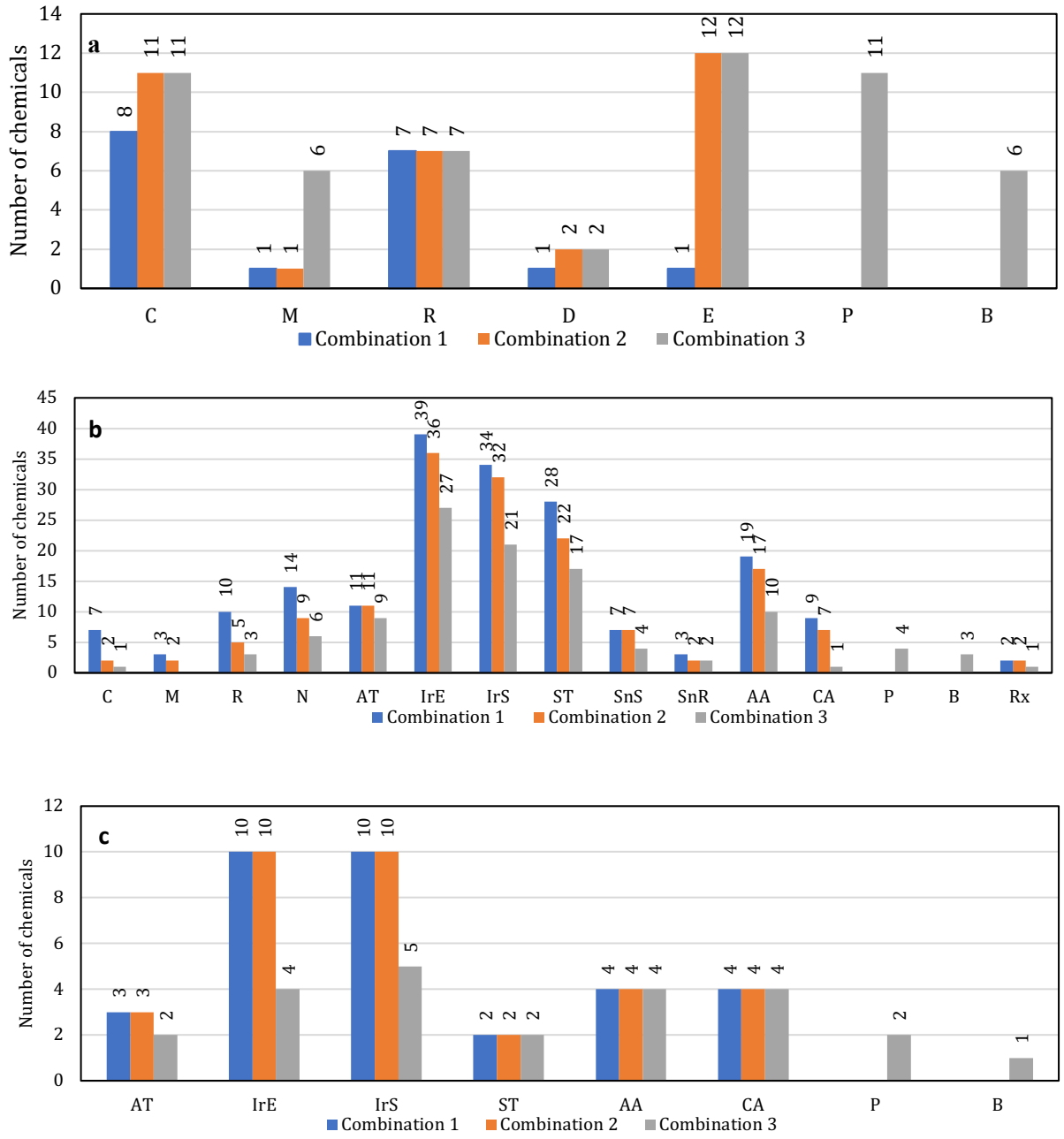

Figure 6.6. The number of (a) BM-1, (b) BM-2 and (c) BM-3 chemicals triggered by each hazard trait when applying different combinations of data sources (Combination 1: Chemical-Oriented Data Sources, Combination 2: Chemical-Oriented Data Sources and Hazard-Trait-Oriented Data Sources, and Combination 3: Chemical-Oriented Data Sources, Hazard-Trait-Oriented Data Sources, and Predictive Data Sources).

The purpose of the second component of this sensitivity analysis is to explore the contribution of hazard-trait-oriented and predictive data sources to the hazard trait triggers. As previously noted, the inclusion of these additional data sources leads to more chemicals being identified as BM-1 chemicals, thus, the results in **Figure 6.6** are provided as absolute numbers rather than fractions. For the BM-1 chemicals shown in **Figure 6.6(a)**, the addition of hazard-trait-oriented data sources (Combination 2) leads to an increase in the hazard trait triggers C and E. The addition of predictive data sources (Combination 3) leads to an increase in the hazard trait triggers M, P and B. As the number of BM-1 chemicals increases for data source combinations 2 and 3, the number of BM-2 and BM-3 chemicals must decrease, making the effect of hazard trait triggers more difficult to interpret for BM-2 and BM-3 chemicals. Except for the hazard trait triggers of P and B, the number of other hazard trait triggers for BM-2 scores tend to decrease (see **Figure 6.6(b)**), because the addition of these data sources leads to the reclassification of some BM-2 chemicals into BM-1 chemicals. For BM-3 chemicals, shown in **Figure 6.6(c)**, the only change is that the predictive data sources (applied in Combination 3) will add the potential hazard trait triggers of P and B, while also transferring chemicals to BM-1 or BM-2, because of the combination rules for P, B and T stated earlier in the decision logic. Overall, by adding hazard-trait-oriented and predictive data sources to the chemical-oriented data sources, the additional hazard traits of E, P, B and M can trigger different benchmark scores.

6.4. Conclusions

The current study evaluated the role of data source selection on the outcome of a chemical hazard assessment (CHA). The GreenScreen® for Safer Chemicals framework was

used as the basis to assign benchmark scores to more than 140 organic chemicals used as process chemicals in the synthesis of low band gap polymers for organic photovoltaic solar cells. With the application of multiple hazard / toxicity data sources, almost all of these chemicals were successfully assessed. Key hazard traits that trigger each assessment result were identified. Although by using multiple data sources, as well as multiple types of data sources, we avoided having chemicals assigned as 'Benchmark Unknown', the selection of data source(s) strongly influenced the hazard trait triggers and the corresponding CHA outcome, as evaluated through a series of sensitivity analyses. Thus, the findings from this study strongly indicate that for CHA to be successfully and broadly used for targeting chemicals of concern in products and processing, the development and open access of standardized, complete, and comprehensive chemical hazard and toxicity data sources are greatly needed.

Chapter 7: Multicriteria Decision Analysis Characterization of Chemical Hazard Assessment Data Sources

7.1 Abstract

Chemical Hazard Assessment (CHA), which aims to investigate the inherent hazard potential of chemicals, has been developed with the purpose of promoting safer consumer products. Despite the increasing use of CHA in recent years, finding adequate and reliable toxicity data required for CHA is still challenging due to issues regarding data completeness and data quality. Also, collecting data from primary toxicity reports or literature can be time consuming, which promotes the use of secondary data sources instead. In this study, we evaluate and characterize numerous secondary data sources on the basis of five performance attributes: reliability, adequacy, transparency, volume and ease of use. We use GreenScreen® for Safer Chemicals v1.4 as the CHA framework, which defines the endpoints of interest used in this analysis. We focused upon thirty-four data sources reflecting three types of secondary data: chemical-oriented data sources, hazard-trait-oriented data sources and predictive data sources. To integrate and analyze the evaluation results, we applied two multi-criteria decision analysis (MCDA) methodologies – multi-attribute utility theory (MAUT) and stochastic multi-objective acceptability analysis (SMAA). Overall, the findings in this research program allow us to explore the relative importance of performance criteria and the data source quality for effectively conducting CHA.

7.2 Introduction

With the world-wide promotion of green chemistry practices and safer consumer and industrial products, there is an increased need to facilitate the selection of safer chemicals

with well-designed decision tools and corresponding data sources [32-34]. Among currently available CHA frameworks, GreenScreen® for Safer Chemicals version 1.4 (GreenScreen®), created by Clean Production Action, is a decision framework developed to screen chemicals on the basis of their hazard traits using transparent and systematic benchmarking criteria (13). GreenScreen® has become widely accepted and utilized in industry, non-governmental organizations and government alike. In GreenScreen®, information on 20 hazard endpoints (**Table 7.1** as listed in Chapter 2, Section 2.1) is reviewed, including those related to human health, environmental toxicity and fate, and physical hazards. Although several data sources are recommended for conducting GreenScreen® assessments [13], finding adequate and reliable hazard trait data for all 20 endpoints is not easy, due to challenges associated with data completeness and data quality, which ultimately limits the credibility and robustness of the hazard assessment. This problem exists not only with GreenScreen®, but also applies to other CHA tools and frameworks, as noted in the recent report released by The National Academies, which summarized issues with data gaps, and uncertainty in CHA, and the reasons for this level of complexity [9].

In many cases, the results of a hazard assessment are not dictated by the CHA methods and tools themselves, but rather the data sources used for the assessment [169]. Discrepancies can occur because hazard data derived from different test methods do not always agree due to differences in experimental method and/or interpretation and variances in experimental conditions in different studies [170]. Also, a vast number of data sources can be used to acquire toxicity information [171]; some of them are primary data sources and some are secondary data sources. Primary data sources are peer-reviewed toxicity reports or research articles prepared by the scientists who conducted the toxicity tests; secondary

data sources are created by organizations, the purposes of which are to describe, interpret, evaluate, analyze and/or aggregate data from the primary data [172]. While primary data sources are considered more authoritative and usually disclose more details, the information from secondary data sources is more abundant and easier to access, especially for non-experts.

The selection of proper secondary data sources for CHA can be challenging, raising a series of important research questions: Which attributes of a given data source determine if the data source will be useful in a CHA? Can exceptional performance in one attribute compensate for poor performance in another attribute? Should all of these performance attributes be assumed to have equal importance? The purpose of this study is to investigate these research questions. To do so we use multi-criteria decision analysis (MCDA) which is explained in our Chapter 2, Section 2.4. Our MCDA approach to evaluate data sources for CHA is a quantitative approach that extends methods used in previous studies that utilized various qualitative decision-theory based methodologies, such as those based on qualitative weight of evidence (WoE) [173-175] and systematic review [174, 176-178] to evaluate toxicological and epidemiological data sources. These methods require the reviewer to examine large amounts of information and make decisions for prioritizing information based on their performance in each attribute. In Linkov's study [175], the WoE approach divides performance attributes into seven categories, including: listing evidence, best professional judgement, causal criteria, logic, scoring, indexing and quantification; with the 'quantification' category being seen as the most quantitative and transparent category. The study by Klimisch et al. [176], which is one of the few well-recognized efforts to evaluate toxicity data sources, applied three terms, reliability, relevance and adequacy, to assess

primary toxicity data by listing criteria and answering question sets, and the final evaluation was integrated into four levels. This approach can be categorized as a combination of causal criteria and indexing. We build our own study on this approach, but directed at *secondary* data sources, which are structured quite differently than *primary* data sources and thus require a modified assessment strategy, and aimed at moving toward the 'quantification' category mentioned above. More specifically, our extension into MCDA methods to evaluate the performance attributes of *secondary* data sources, which is to our the knowledge the first such effort, thus allows for a quantitative evaluation of the data sources themselves while taking into account the influence of compensatory weighting schemes for the performance attributes, thereby addressing the research questions defined above.

7.3 Material and Methods

To evaluate the various data sources and their respective value in conducting a CHA, a systematic and quantitative model was established using MCDA. The process flow for the model was organized as follows: 1. selection of the *CHA framework(s)*; 2. selection of the *alternatives* (i.e., *data sources*); 3. identification of the *performance attributes*; 4. *evaluation* of each data source on the basis of each performance attribute; 4. application of MCDA to *aggregate* the evaluation results into a single value indicator, and 5. application of *weight sensitivity analysis* and *acceptability index analysis* to evaluate the sensitivity of the results to uncertainty in weighting schemes.

GreenScreen® was chosen as the baseline CHA framework (see Section 2.1 in Chapter 2), as it is commonly applied for government, non-government and industry-based assessments [13] and is transparent in its methodology and accessible to the public free of

charge. The selection of GreenScreen® dictates the hazard traits of interest (see **Table 7.1**), which influences the type of data needed for the CHA. Actual GreenScreen® assessments were not conducted as part of this study on data source selection. The data sources, described below, were evaluated on the basis of performance relative to five attributes: reliability, adequacy, transparency, volume and ease of use. To accommodate the MCDA model, a two-step evaluation of the data sources was performed: *characterization* and *quantification*. The characterization refers to the review of each data source on the basis of the five performance attributes, whereas, in the quantification step, the characterization results are converted into numerical values that can be used as the input values for the MCDA. Two MCDA methods, multi-attribute utility theory (MAUT) [55, 56, 177] and stochastic multi-objective acceptability analysis (SMAA) [54, 57], were applied to integrate the evaluation results (see Section 2.4 in Chapter 2). Lastly, we explored the weighting factors assigned to each performance attribute through the application of weight sensitivity analysis (for MAUT) and acceptability index analysis (for SMAA). Further details on each of these methodological steps are provided below.

7.3.1 Secondary Data Sources Evaluation

In total, 34 secondary data sources were selected for this research, the full names for which are listed in **Table 4.1**. To ensure a wide range of data sources for CHA, sources were chosen from different types of organizations including governmental bodies, research institutes, non-profit organizations and industry (such as chemical and manufacturing companies). The specified lists and the information sources suggested by GreenScreen® were used as the primary basis for data source selection [13]. Data sources were also

identified through a search of two database portals: the eChemPortal [178] and the Toxicology Data Network® (TOXNET®) [179]. The eChemPortal is a global portal, operated by the European Commission in collaboration with various European Union Agencies, that collects the physical properties, environmental fate and behavior, ecotoxicity, and toxicity information on chemicals [178]. TOXNET®, which is maintained by the U.S. National Library of Medicine (NLM) in their Toxicology and Environmental Health Information Program (TEHIP), also includes several databases providing hazard information for chemicals [179]. In this study, all of the data sources were accessed via the Internet.

To ensure that the data sources could be evaluated in a systematic and relatively unbiased way, the data sources were divided into three types: "chemical-oriented data sources," "hazard-trait-oriented data sources," and "predictive data sources." [169]. Chemical-oriented data sources refer to data sources that are organized by chemical, providing information on various hazard traits associated with each chemical. Hazard-trait-oriented data sources are organized on the basis of specific hazard traits and list chemicals suspected of exhibiting these specified hazard traits. The three predictive data sources provide toxicity data that are generated computationally, rather than on the basis of experimental data or case studies. The quantitative structure-activity relationship (QSAR) is one typical predictive model gaining popularity in the toxicity research field [10, 180, 181]. In QSAR, the physical/chemical properties, toxicology and the environmental fate of chemicals can be predicted on the basis of the chemical structure, based upon structural similarities to well investigated chemicals [181]. Due to the unique characteristics of predictive data sources compared with the chemical-oriented and hazard-trait oriented

types of data sources, we also investigated the appropriateness of using the selected performance attributes to evaluate the predictive data sources.

Table 7.1. The full names and categorization of the 34 secondary data sources used in this study are provided below.

Chemical-oriented data sources
• European Chemical Agency's Dissemination portal with information on chemical substances registered under REACH (ECHA CHEM)
• GHS Classification Results by the Japanese Government (GHS-Japan)
• Databases on hazardous substances under the Institute for Occupational Safety and Health of the German Social Accident Insurance (GESTIS)
• Joint Substance Data pool of the German Federal Government and the German Federal States (GSBL)
• Australia's National Industrial Chemical Notification and Assessment Scheme's Inventory Multi-tiered Assessment and Prioritisation framework (NICNAS IMAP)
• New Zealand Hazardous Substances and New Organisms Chemical Classification Information Database (HSNO CCID)
• Hazardous Substances Data Bank (HSDB®)
• Public Classification and Labelling (C&L) Inventory according to the European Union (EU) CLP Regulation (EC) No 1272/2008 (ECHA C&L Inventory)
• Sigma-Aldrich Materials Safety Data Sheets (Sigma-Aldrich MSDSs)
• Organisation for Economic Cooperation and Development Existing Chemicals Database (OECD HPV)
• Canada's Existing Substances Assessment Repository (CESAR)
• The Pesticide Action Network Pesticide Database (PAN)
• Data Bank of Environmental Properties of Chemicals (EnviChem)
• Canadian Categorization Results (CCR)
• The International Chemical Secretariat's Substitute it Now! List (ChemSec Sin)
• ChemIDplus® A TOXNET (Toxicology Data Network) Database (ChemIDplus®)
• Japan CHEmicals Collaborative Knowledge database (J-CHECK)
• The High Production Volume Information System (HPVIS)

Hazard-trait-oriented data sources

- The California Proposition 65 (CA Prop 65)
- Chemical Carcinogenesis Research Information System (CCRIS)
- Genetic Toxicology (GENE-TOX)
- The Pocket Guide from the National Institute for Occupational Safety and Health (NIOSH)
- The Endocrine Disruption Exchange (TEDX)
- The Maximum Workplace Concentration (MAK)
- The Toxicant and Disease Database under the Collaborative on Health and the Environment (CHE)
- The Carcinogenic Potency Database (CPDB)
- The Aquatic Life Benchmarks for Pesticide Registration (EPA OPPALB)
- The Human Health Benchmarks for Pesticides (EPA HHBP)
- The Comparative Toxicogenomics Database (CTD™)
- International Toxicity Estimates of Risk (ITER)
- United States Environmental Protection Agency Integrated Risk Information System (US EPA IRIS)

Predictive data sources

- The Danish (Q)SAR Database ((Q)SAR)
- The Estimation Program Interface Suite™ (EPI SUITE™)
- Virtual models for property Evaluation of chemicals within a Global Architecture (VEGA)

In **Figure 7.1**, five performance attributes (reliability, adequacy, transparency, volume and ease of use) were used for this study. These attributes were selected on the basis of various previous studies [176. 182-184] and are briefly described here. Further details on the definition, characterization and quantification of these attributes are available in the Appendix H. “Reliability” and “adequacy” were originally from Klimisch’s study [176] on assessing primary data sources, but they are revised here to adapt to the evaluation of secondary data sources. The term “reliability” refers to two aspects of the data source – the test methods used to acquire the data and the organizations responsible for the data collection. For the test methods, the reliability level is classified per the data hierarchy discussed in a recent USEPA report on flame retardants [182]; reliability values were also

assigned for different types of organizations. The term "adequacy" was designed to represent the performance of each data source relative to its ability to determine the hazard endpoints in GreenScreen®, i.e., the fraction of the endpoints for which there are data (see the Appendix H for details and an example). To evaluate how transparent each data source is for CHA, the attribute "transparency" evaluates four sub-attributes [185]: (1) the level of detail provided in the description of the hazard identification process, (2) the citation for the original publication of the data, (3) the data collection protocol, and (4) evidence of peer review or comments on the data sources. Further, we use the term "volume" in reference to the number of chemicals contained in each data source. Lastly, the term "ease of use" refers to the characterization of the data sources based on: (a) their input and output information, (b) if access is free or not, and (c) if special user expertise is required. This attribute description is derived from the OECD Substitution and Alternatives Assessment Tool Selector [183] and Gauthier et al.'s study [184], which illustrates the importance of convenience in finding data sources particularly for people who are not experts in the toxicology field.

For each data source, the performance attributes were characterized and quantified by the authors, the results of which are shown in **Table H1 – H5** in the Appendix H. For qualitative terms such as "reliability", "transparency" and "ease of use", a semi-quantification method was adopted with which each attribute is converted to a 4-point maximum-possible score, as described in Table B6 in the Appendix H and then normalized to a scale of 0-1. For the quantitative attributes "adequacy" and "volume," a mathematical approach was applied to again generate a 0-1 normalized scale, as described in detail in the Appendix H.

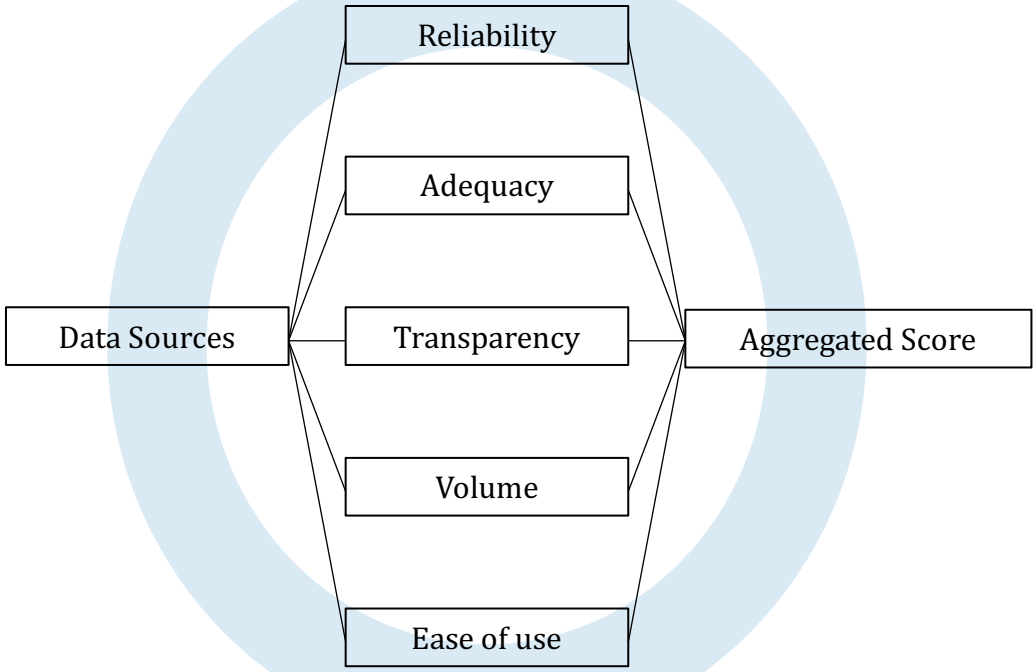

Figure 7.1. The performance attribute referred for data sources evaluation.

7.3.2 The MCDA Methodologies

Two MCDA methodologies were applied in this study: MAUT and SMAA (details provided in Chapter 2, Section 2.4). The MAUT was applied through *Decerns MCDA*, a software including a set of MCDA methods with the ability to conduct a weight sensitivity analysis [53]. The SMAA was carried out via *JSMAA*, another MCDA software developed only for the SMAA based methods [186]. The computational structures of the two MCDA methods indicate that the final rank of an alternative will not only be affected by their performance on each attribute, but also the weighting factors assigned. For MAUT, an equal weight for each attribute was adopted for this study as the baseline for the initial data source

evaluation, followed by a weight sensitivity analysis to see the effect of changes in relative weighting factors on the total utility score. Further, the application of SMAA allowed us to explore the acceptability index of each data source without setting predetermined weighting factors through the software modeling process.

7.4 Results and Discussion

7.4.1 The MAUT Evaluation of Secondary Data Sources

Through MAUT, the total utility score for each data source is aggregated by summing up their weighted utility scores on the five performance attributes (note that the raw data for the characterization and quantification are presented in the Appendix H in Tables H1 – H5). **Figure 7.2** presents the rank order and calculated total utility score for each of the 34 secondary data sources by adopting equal weighting factors as the baseline scenario. The implication of the equal weighting is that the maximum contribution of a given performance attribute to the utility score is 0.20, as noted in **Figure 7.2** for several of the data sources. **Figure 7.2** is divided into three sub-figures, to separate the three types of data sources for clearer performance comparisons. **Figure 7.2(a)** includes the results for the chemical-oriented data sources; **Figure 7.2(b)** includes those for the hazard-trait-oriented data sources; and **Figure 7.2(c)** includes those for the predictive data sources. Generally speaking, the chemical-oriented data sources show higher utility scores compared with the hazard-trait-oriented data sources and predictive data sources. Among all the data sources, the ECHA CHEM, GHS-Japan and GESTIS, all of which are chemical-oriented data source, are the top three data sources, with each receiving a total utility score higher than 0.8. The CTD™ and California Prop 65 are the top two hazard-trait-oriented data sources with utility scores

between 0.65-0.7. For all three predictive data sources, their utility scores are very close in value, ranging from 0.52-0.57. The data sources with the lowest total utility scores are EPA OPPALB and EPA HHBP, both of which are hazard-trait-oriented data sources.

Although the high total utility scores for most of the chemical-oriented data sources are derived from relatively good performance on all five performance attributes, there are some exceptions. For instance, ECHA C&L Inventory and Sigma-Aldrich MSDSs have relatively low scores for transparency because these data sources do not clearly disclose the scientific basis for their classifications, but these are compensated for by the high scores for volume. Likewise, ChemIDPlus has low scores for both adequacy and transparency, but again a high score for volume. All of the 18 chemical-oriented data sources perform fairly well in both reliability and ease of use. The lower total utility scores for hazard-trait-oriented data sources are generally due to the poor performance on adequacy and volume, which are the result of the fact that these data sources focus on specific hazard traits and therefore typically include a smaller number of chemicals. Some of the hazard-trait-oriented data sources also have low scores for transparency, but most perform well in terms of reliability and ease of use. For the predictive data sources, the better performance on volume compensates somewhat for the low performance on adequacy, transparency, reliability and ease of use. As the predictive data sources generate the toxicity information based on the structure similarity and physical-chemical properties of existing chemicals, their reliability cannot compete with the data sources based on strict experimental tests, and predictive data sources require high user expertise for use. The low adequacy for predictive data sources is due to the nature of those quantitative or logical approaches, which are suitable for predicting certain hazard endpoints especially environmental fate, such as the

bioaccumulation and persistence, but are not precise enough for other endpoints. While acquiring data through predictive methods, it can be very difficult for the user to extract the original data, prediction routes and to validate their quality due to the modeling complexity, which results in a low transparency score for predictive data sources (Puzyn et al. 2010). It is important to note here that predictive data sources are the most dynamic category of data sources at this point in time, and the associated scores could therefore need to be revised periodically as the methods continue to evolve.

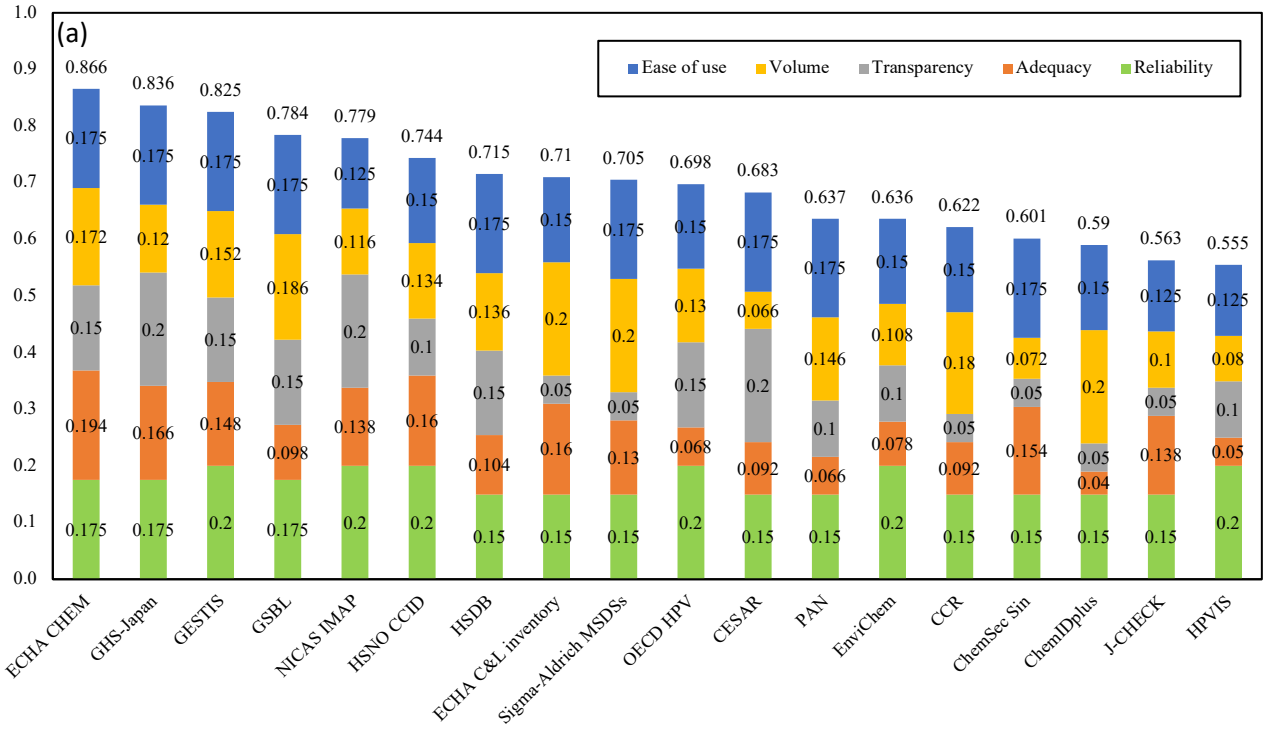

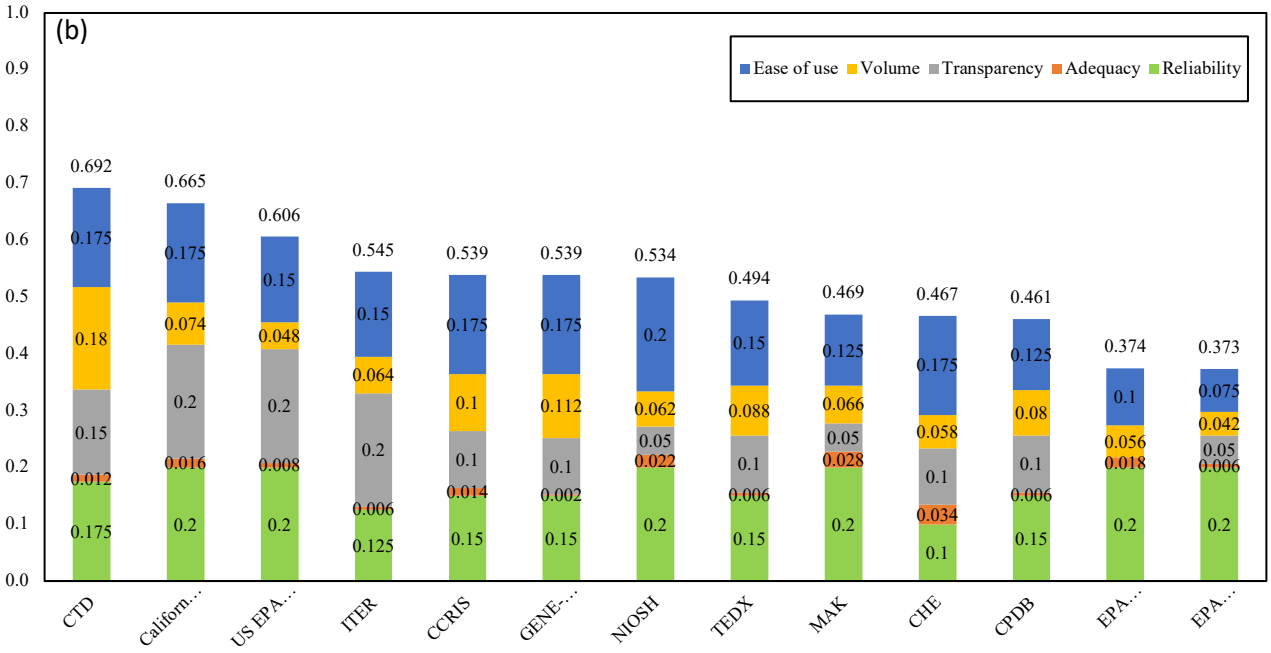

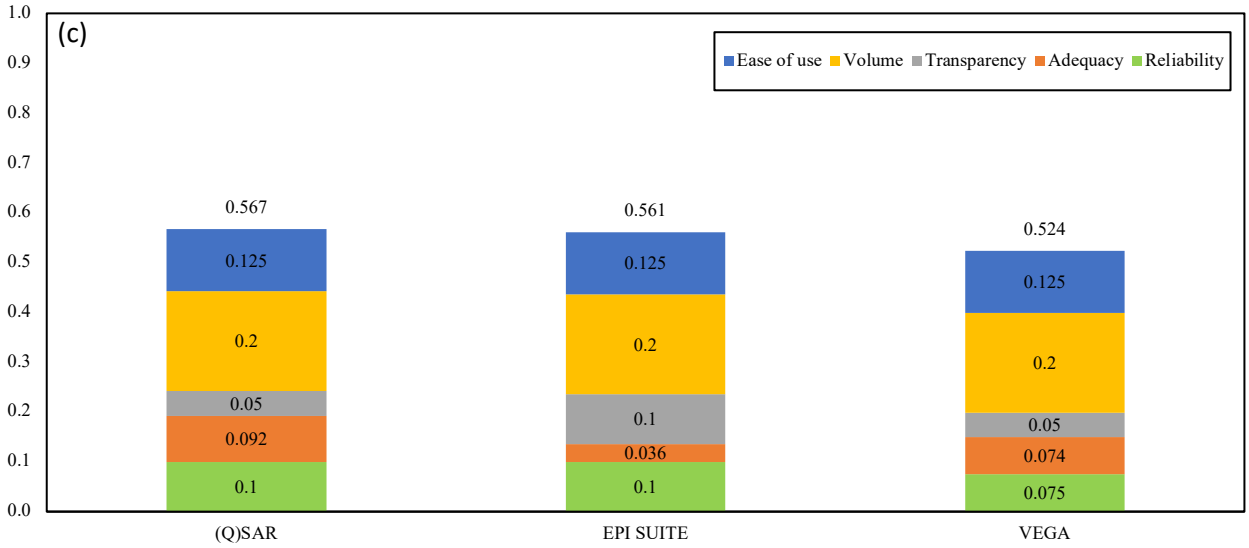

Figure 7.2. The total utility score of the (a) chemical-oriented data sources, (b) hazard-trait-oriented data sources and (c) predictive data sources based on their performance on each attribute assuming equal weight from MAUT.

7.4.2 Weight Sensitivity Analysis

With the aid of *Decerns MCDA*, a weight sensitivity analysis was conducted to explore the relationship between weighting factors and the total utility scores. In the MAUT results presented in **Figure 7.2**, each performance attribute was assumed to be of equal importance in the evaluation of a given data source, and therefore each attribute was weighted equally. As the weighting factors can be varied to reflect variable priority for the performance attributes, here the weighting factors for each attribute were changed linearly, one at a time, to explore the effect on the total utility scores. During this process, the weighting factors for the other four attributes were changed concurrently at a consistent rate. The weight sensitivity results relative to each of the five attributes are presented in **Figure 7.3**, noting the three types of data sources. The lower and upper limit of each error bar reflect the data source's total utility score when the weight on this attribute is assigned values of 0 or 1, respectively. The dots in between these limits are the total utility score when adopting equal weighting per the baseline scenario shown in **Figure 7.2**. The color of these dots indicates if the total utility will increase (green) or decrease (red) when increasing the weight. To clarify the methodology, we highlight one example. For ECHA CHEM, when the weight of adequacy is increased from 0 to 1, the total utility score changes from 0.84 to 0.97, respectively. The score of 0.84 is the total utility without considering adequacy (adequacy term is weighted as 0), whereas the score of 0.97 is equal to the single utility when adequacy has a weight of 1 (and no other performance attributes are considered). The green dot indicates that as the weight of adequacy increases the overall utility increases, which is consistent with the baseline results in **Figure 7.2** in which the contribution of adequacy to the total utility score

(0.194 out of 0.866 total) is greater than that from each of the other performance attributes (maximum = 0.175) for this data source.

The results shown in **Figure 7.3** indicate that the total utility scores of any given data source are very sensitive to the weighting factors (or priority) assigned to the different performance attributes. Furthermore, the extent of sensitivity is highly variable, although some important trends are observed. When varying the weight for reliability, the hazard-trait-oriented data sources tend to be more sensitive compared to chemical-oriented data sources, which means the performance of hazard-trait-oriented data sources are more easily influenced by this attribute, which is also the case for adequacy and ease of use. For predictive data sources, the fluctuations relative to each attribute are quite small for all attributes except volume and transparency.

For some of the data sources, under select weighting scheme scenarios, a total utility score of 1.0 can be achieved. For instance, several chemical-oriented and hazard-trait-oriented data sources achieve this score when reliability is weighted 100%. This result is a reflection of these data sources performing at the highest level possible in terms of reliability. A similar result is observed relative to transparency and volume. For the three predictive data sources, a total utility score of 1.0 can only be achieved if volume is weighted at 100%, and only one data source, MAK, achieves such a total utility score when ease of use is the single attribute of interest. It is interesting to note that none of the data sources can achieve a total utility score of 1.0 when adequacy is the only attribute of interest, which reflects the important reality that none of the data sources contain all of the data required to assess the 20 hazard endpoints necessary to complete a GreenScreen® – based CHA; multiple data

sources are always necessary, as noted in our previous publication on organic photovoltaics (He et al. 2018).

These results suggest that the baseline (and common default) scenario of weighting performance attributes equally does not provide a robust assessment of the relative performance of a given data source for use in a CHA. Furthermore, when using these secondary data sources to conduct a CHA, practitioners should make an effort to be explicit about the performance attributes they value and their relative priority in data source selection. Even if a quantitative MCDA is not conducted, it is important to acknowledge that the relative weighting (prioritization given by a practitioner) of performance attributes will affect the practitioner's potential selection of data sources and can therefore potentially bias the CHA results as the hazard trait information in each data source may include different data on various chemicals with different levels of reliability, transparency, etc.. For example, if a practitioner considers the performance attribute "volume" to be most important, they may choose to only use data sources that contain a high number of chemicals, but in these data sources the "adequacy" performance attribute, which characterizes the abundance of the hazard endpoints for chemicals in a given data source, may not be well addressed. Without enough hazard endpoints for the CHA, more data gaps can exist, thus potentially biasing the results.

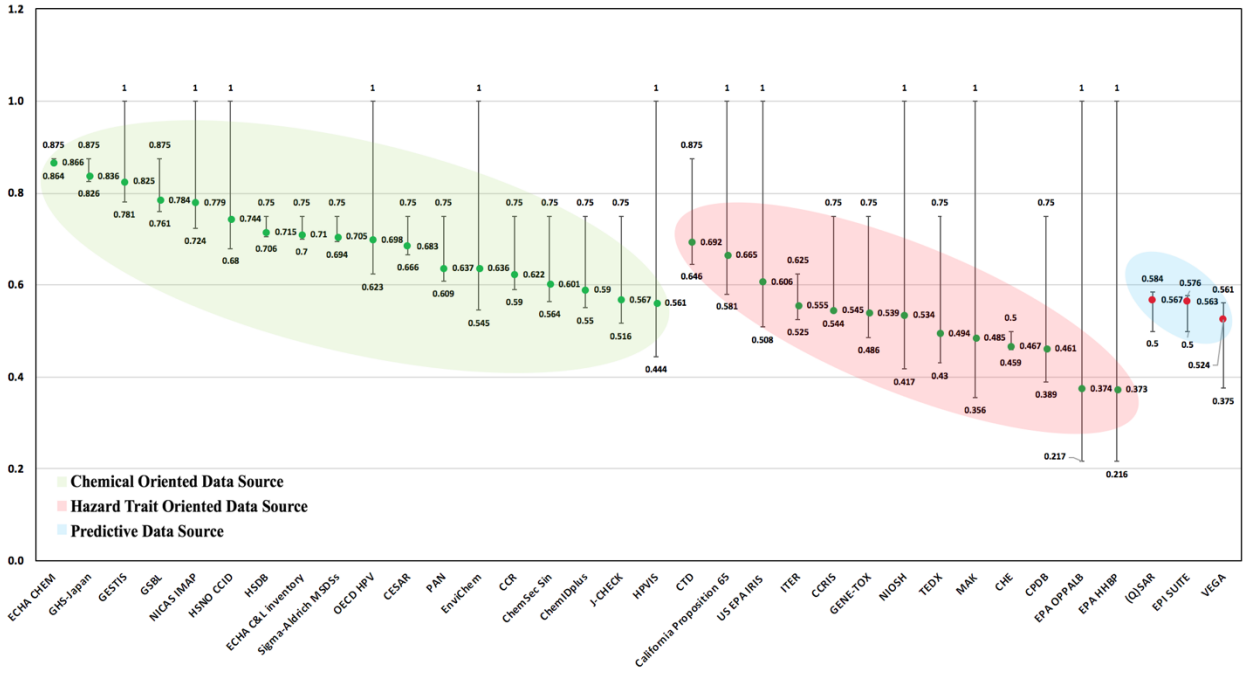
Chemical Oriented Data Source
Hazard Trait Oriented Data Source
Predictive Data Source
ECHA CHEM
GHS-Japan
GESTIS
GSBL
NICAS IMAP
HSNO CCID
HSDB
ECHA C&L Inventory
Sigma-Aldrich MSDSs
OECD HPV
CESAR
PAN
EnviChem
CCR
ChemSec Sin
ChemDplus
J-CHECK
HPVIS
CTD
California Proposition 65
US EPA IRIS
ITER
CCRIS
GENE-TOX
NIOSH
TEDX
MAK
CHE
CPDB
EPA OPPALB
EPA HHBP
(Q)SAR
EPI SUITE
VEGA

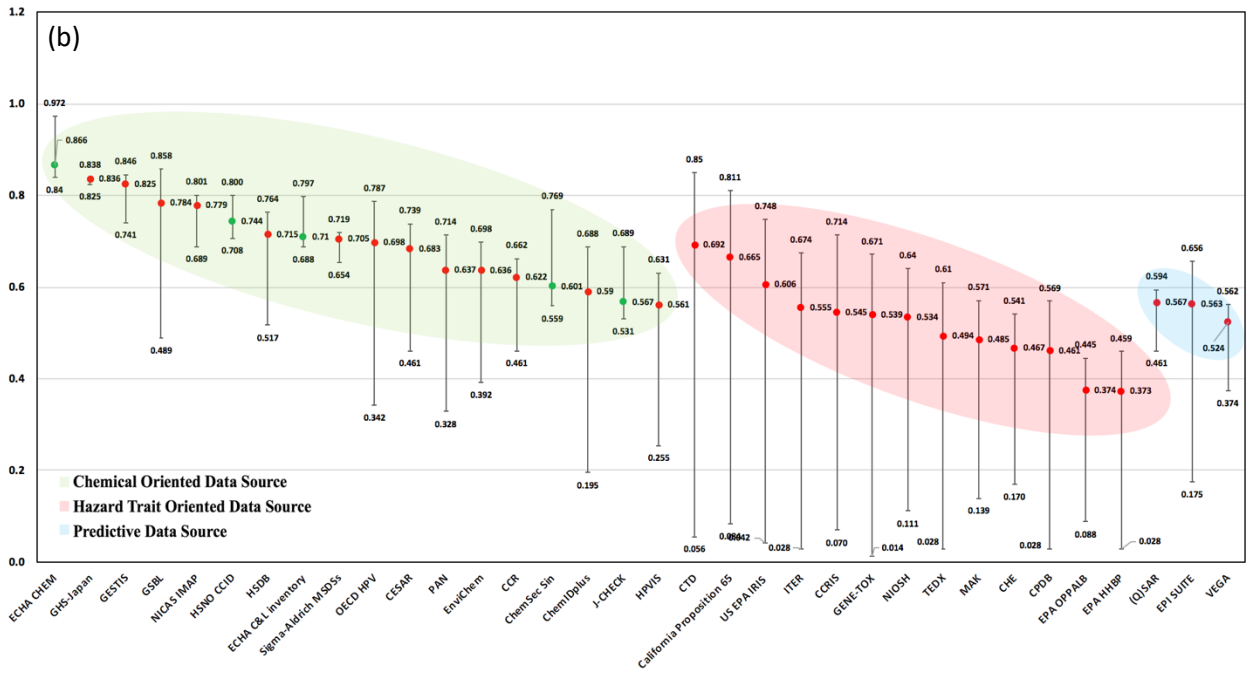
(b)
Chemical Oriented Data Source
Hazard Trait Oriented Data Source
Predictive Data Source
ECHA CHEM
GHS-Japan
GESTIS
GSBL
NICAS IMAP
HSNO CCID
HSDB
ECHA C&L Inventory
Sigma-Aldrich MSDSs
OECD HPV
CESAR
PAN
EnviChem
CCR
ChemSec Sin
ChemDplus
J-CHECK
HPVIS
CTD
California Proposition 65
US EPA IRIS
ITER
CCRIS
GENE-TOX
NIOSH
TEDX
MAK
CHE
CPDB
EPA OPPALB
EPA HHBP
(Q)SAR
EPI SUITE
VEGA

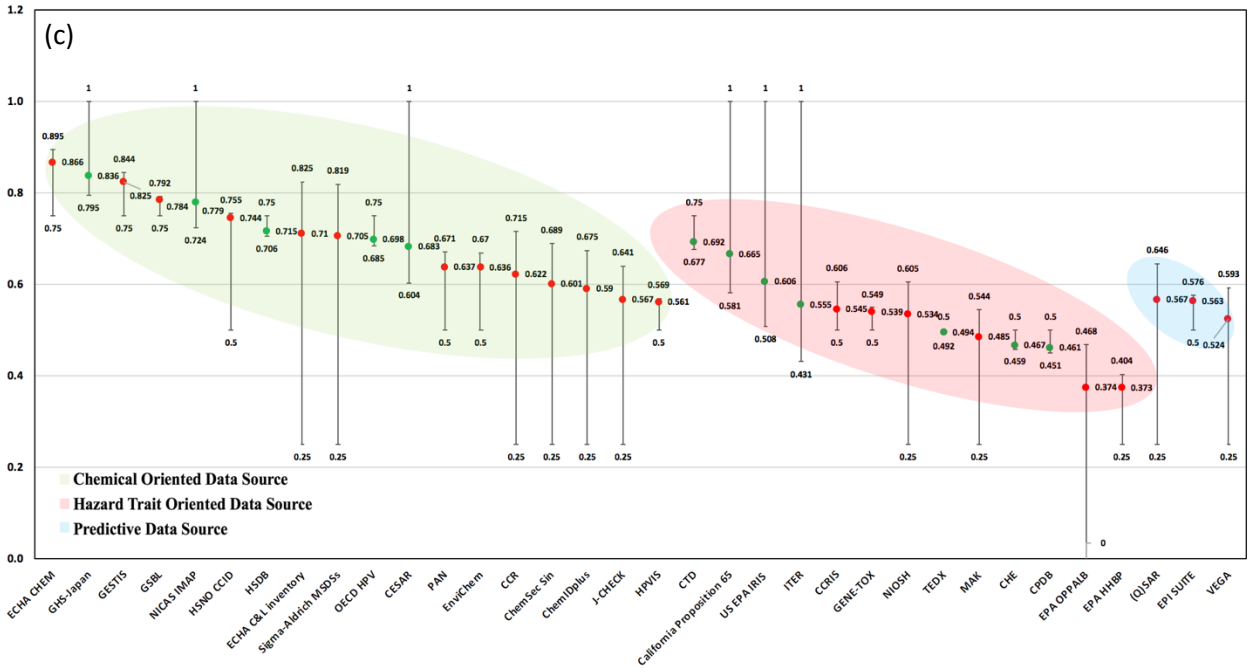
(c)
Chemical Oriented Data Source
Hazard Trait Oriented Data Source
Predictive Data Source
ECHA CHEM
GHS-Japan
GESTIS
GSBL
NICAS IMAP
HSNO CCID
HSDB
ECHA C&L Inventory
Sigma-Aldrich MSDSs
OECD HPV
CESAR
PAN
EnviChem
CCR
ChemSec Sin
ChemIDplus
J-CHECK
HPVIS
CTD
California Proposition 65
US EPA IRIS
ITER
CCRIS
GENE-TOX
NIOSH
TEDX
MAK
CHE
CPDB
EPA OPPALB
EPA HHBP
(Q)SAR
EPI SUITE
VEGA

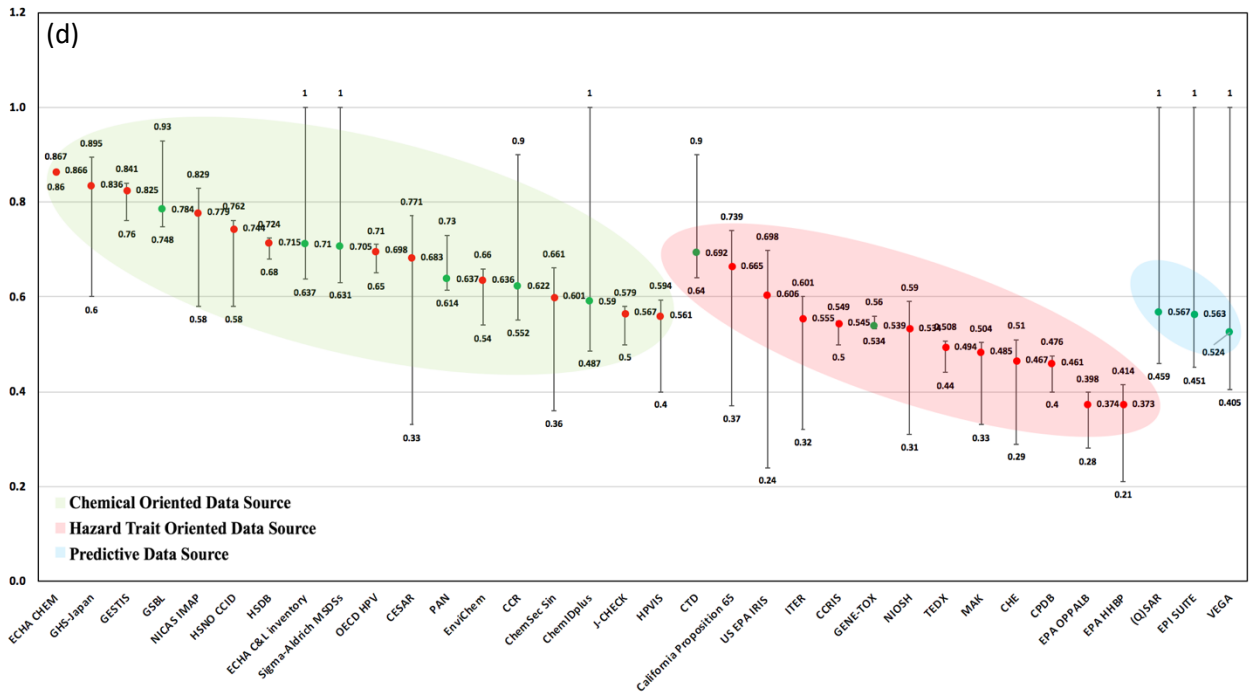
(d)
Chemical Oriented Data Source
Hazard Trait Oriented Data Source
Predictive Data Source
ECHA CHEM
GHS-Japan
GESTIS
GSBL
NICAS IMAP
HSNO CCID
HSDB
ECHA C&L Inventory
Sigma-Aldrich MSDSs
OECD HPV
CESAR
PAN
EnviChem
CCR
ChemSec Sin
ChemIDplus
J-CHECK
HPVIS
CTD
California Proposition 65
US EPA IRIS
ITER
CCRIS
GENE-TOX
NIOSH
TEDX
MAK
CHE
CPDB
EPA OPPALB
EPA HHBP
(Q)SAR
EPI SUITE
VEGA

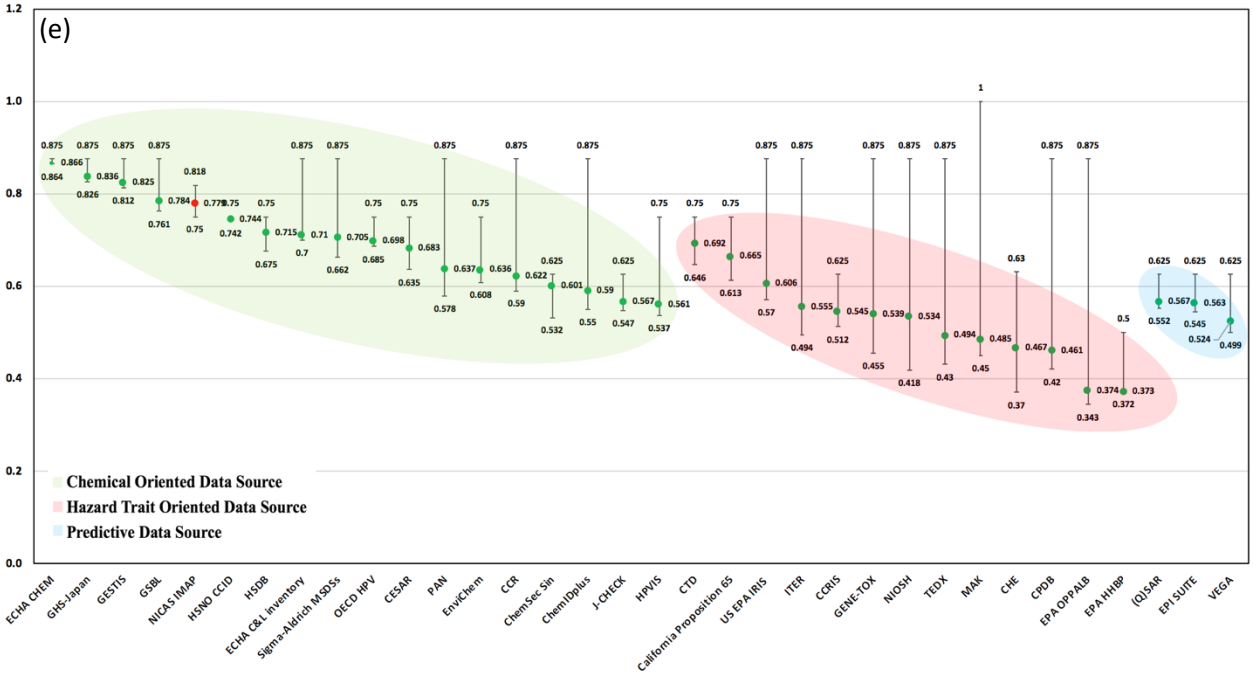

Figure 7.3. The variations in the total utility score for each data source by changing the weighting factor values from 0 to 1 for each performance attribute: (a) reliability, (b) adequacy, (c) transparency, (d) volume and (e) ease of use.

For some of the data sources, under select weighting scheme scenarios, a total utility score of 1.0 can be achieved. For instance, several chemical-oriented and hazard-trait-oriented data sources achieve this score when reliability is weighted 100%. This result is a reflection of these data sources performing at the highest level possible in terms of reliability. A similar result is observed relative to transparency and volume. For the three predictive data sources, a total utility score of 1.0 can only be achieved if volume is weighted at 100%, and only one data source, MAK, achieves such a total utility score when ease of use is the single attribute of interest. It is interesting to note that none of the data sources can achieve a total utility score of 1.0 when adequacy is the only attribute of interest, which reflects the

important reality that none of the data sources contain all of the data required to assess the 20 hazard endpoints necessary to complete a GreenScreen® – based CHA.

7.4.3 Acceptability Index Analysis through SMAA

Figure 7.4 presents the SMAA results for the three types of data sources. The vertical axis is the acceptability index; along the horizontal axis from front to back, the results represent the probability of each data source being selected for a given rank relative to the other data sources; and along the other horizontal axis from left to right, represents the probability distribution for a given data source to be ranked from first to last. For ease of comparison, the data sources are arranged by their MAUT baseline utility scores. To illustrate the interpretation of the results, we begin with the predictive data sources, as shown in **Figure 7.4(a)**. Of the three predictive data sources, the relative ranking is the same when derived with MAUT as with SMAA. However, the ranking scheme in SMAA is not presented as a total utility score like in MAUT but the relative probability of a data source to be selected in each rank. The three triangles in **Figure 7.4(a)** provide a graphical representation of the relative probabilities (i.e., acceptability index values) for each of the three predictive data sources to be ranked first, second, and third, respectively. The (Q)SAR and EPI SUITE™ have much higher acceptability index values (53% and 47%) and are therefore ranked first over VEGA (0%). The probability for each data source to be ranked second is 47% for (Q)SAR, 27% for EPI SUITE™, and 26% for VEGA. VEGA has the highest acceptability index (74%) associated with being ranked third, while there is no probability for (Q)SAR to be ranked third. Looking closer at (Q)SAR, as it always receives the highest

acceptability index for both first and second rankings, it is preferred over the other two data sources regardless of the values chosen for weighting factors.

Similar to the results for the predictive data sources, the SMAA results in **Figure 7.4(b)** are consistent with the MAUT baseline utility scores for the hazard-trait-oriented data sources that rank either high or low. Interestingly, there are large discrepancies for the data sources ranked in the middle, specifically ITER, CCRIS, GENE-TOX, NIOSH, TEDX and MAK. In **Figure 7.5**, we extracted the SMAA results for these six data sources, and two different modes of distribution were observed. In the first mode, the acceptability index is concentrated in a narrower rank range with a single peak shaped distribution, which is the case for CCRIS, NIOSH and TEDX. The ITER, GENE-TOX and MAK belong to the second mode where the acceptability index for these data sources is more uniformly distributed across the various rank levels. The final rank of these data sources is difficult to determine by SMAA as their acceptability index distribution varies significantly when compared to their scores in MAUT, which are shown in **Table 7.2**.

Table 7.2. The calculated baseline MAUT results (total and for each performance attribute) for selected hazard-trait-oriented data sources. The data sources are organized on the basis of the total MAUT score, from highest to lowest. The data sources in bold follow the first mode distribution and the remaining data sources follow the second mode distribution.

Data sources	Total	Reliability	Adequacy	Transparency	Volume	Ease of use
ITER	0.545	0.125	0.006	0.200	0.064	0.150
CCRIS	**0.539**	**0.150**	**0.014**	**0.100**	**0.100**	**0.175**
GENE-TOX	0.539	0.150	0.002	0.100	0.112	0.175
NIOSH	**0.534**	**0.200**	**0.022**	**0.050**	**0.062**	**0.200**
TEDX	**0.494**	**0.150**	**0.006**	**0.100**	**0.088**	**0.150**
MAK	0.469	0.200	0.028	0.050	0.066	0.125

For chemical-oriented data sources, shown in **Figure 7.4(c)**, data sources that received high scores in MAUT are also among the top ranked in SMAA, while the data sources with a low MAUT baseline utility score rank low. There is almost no overlap in the acceptability index distributions for these groups of data sources, which indicates that the top ranked data sources will always be preferred over the lowest ranked data sources regardless of the choice of weighting factors. The variation in acceptability index for data sources ranked in the middle is expanded but, unlike for the hazard-trait-oriented data sources, no obvious peak shape distribution was observed. Overall, we found that the ranks in SMAA are consistent with the MAUT results when the number of data sources used for comparison is small. When increasing the number of data sources assessed, the SMAA results are quite similar with the MAUT results for the data sources ranked high or low, however,

for the data sources ranked in the middle, the SMAA results tend to show a relatively larger performance variance for each data source compared to that observed for the MAUT results.

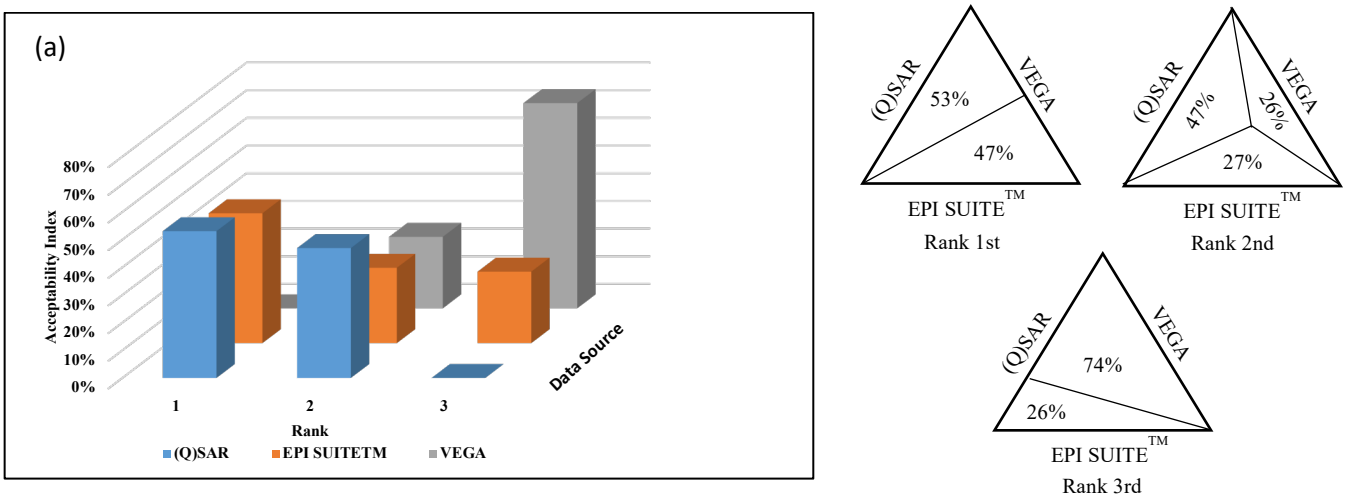

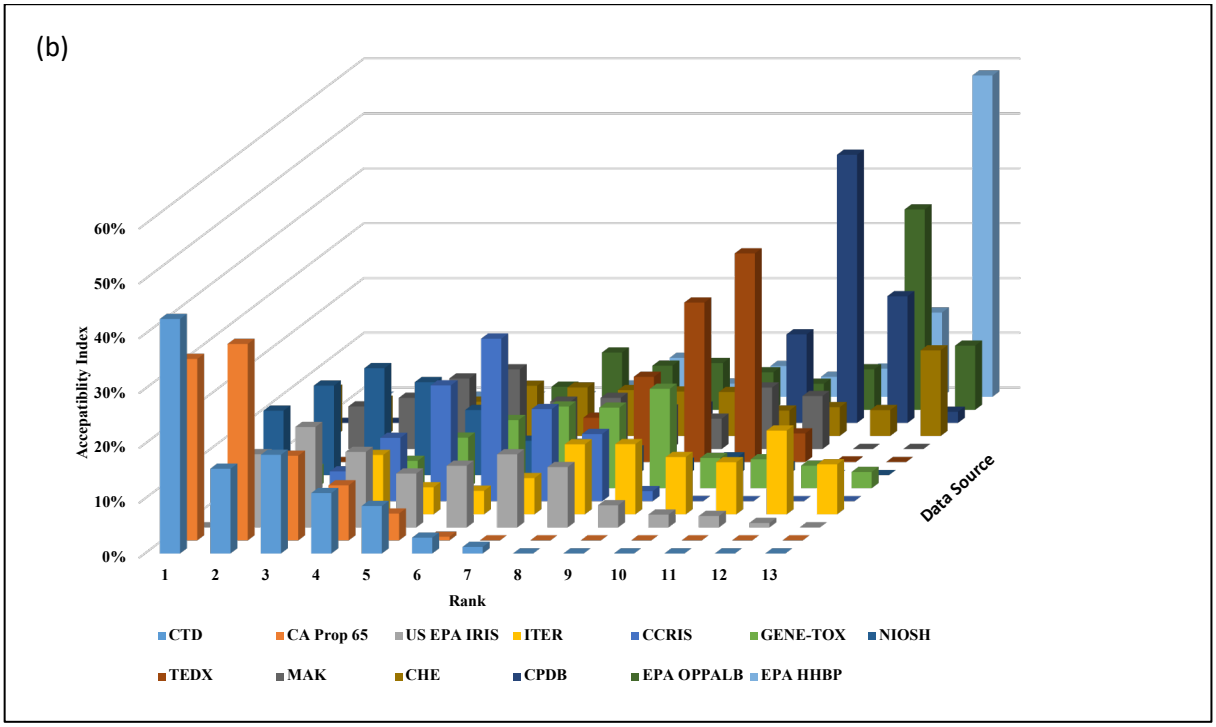

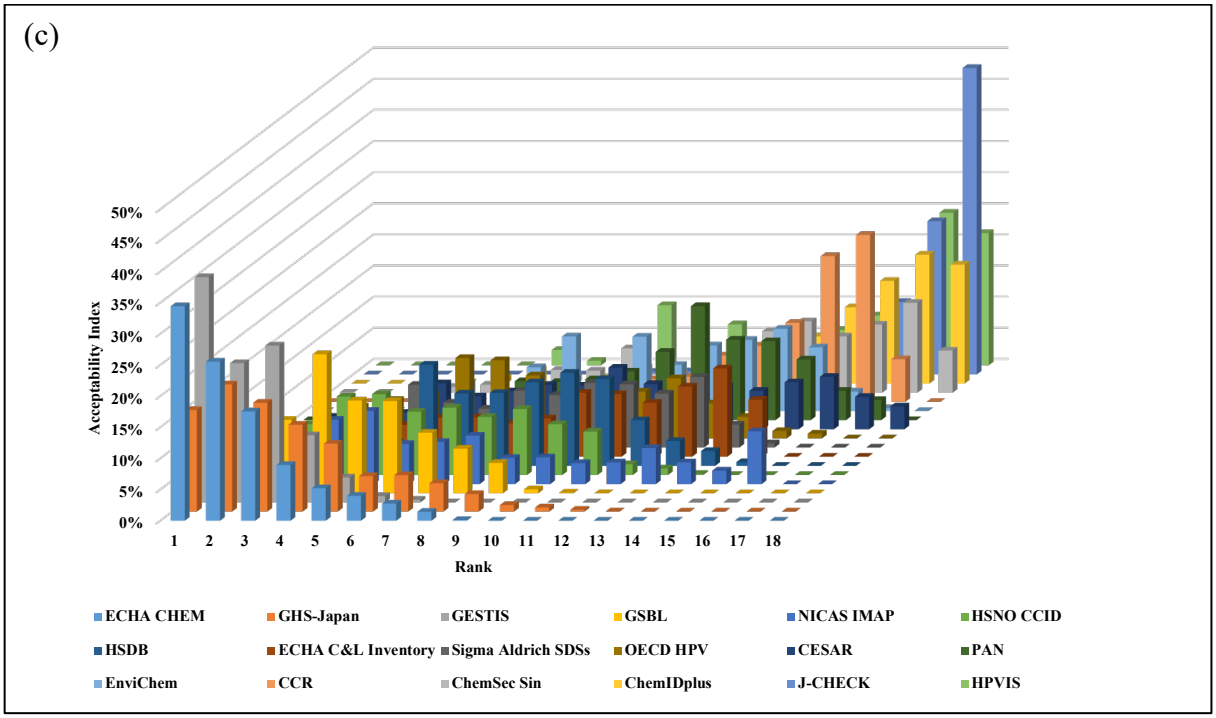

Figure 7.4. The SMAA results for the three types of data sources.

7.4.4 Comparison and Tradeoffs between MAUT and SMAA

The application of SMAA is complementary with the MAUT and it can be beneficial for decision making by using these two methods as a combination. For example, in MAUT (see **Figure 7.2(a)**), the HSDB, ECHA C&L Inventory, Sigma-Aldrich MSDSs, OECD HPV and CESAR received relatively high baseline utility scores (ranking between 7 to 11) among the data sources ranked in the middle (ranking between 5 to 15) but were very close in value, whereas with SMAA (see **Figure 7.6**), their acceptability index values exhibit a wider spread, which helps to further distinguish the performance of each data source and provides more justification for one data source to be ranked higher than the others. However, the MAUT and SMAA results can also present very different results. In **Table 7.2**, we see the CCRIS and GENETOX received the same utility score in MAUT and the only difference is their

performance on two attributes where CCRIS is 0.012 higher on adequacy and 0.012 lower on volume compared to GENETOX. This minor difference triggers a larger variance in the SMAA results, as shown in **Figure 7.5** where CCRIS consistently ranks higher than GENETOX as its acceptability index is almost always higher than the eighth rank and its peak is at the sixth rank, while the peak for GENETOX is at the ninth rank.

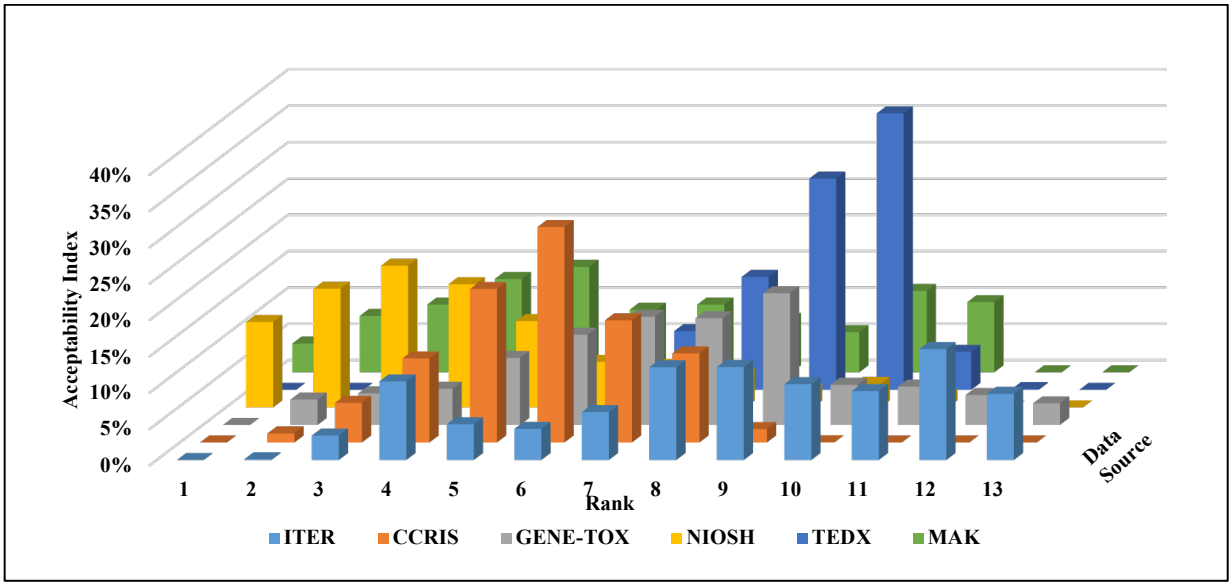

Figure 7.5. The SMAA results for the six hazard-trait-oriented data sources ranked in the middle of Figure 4.5, the sequence of which is determined by their performance from high to low in the MAUT baseline results.

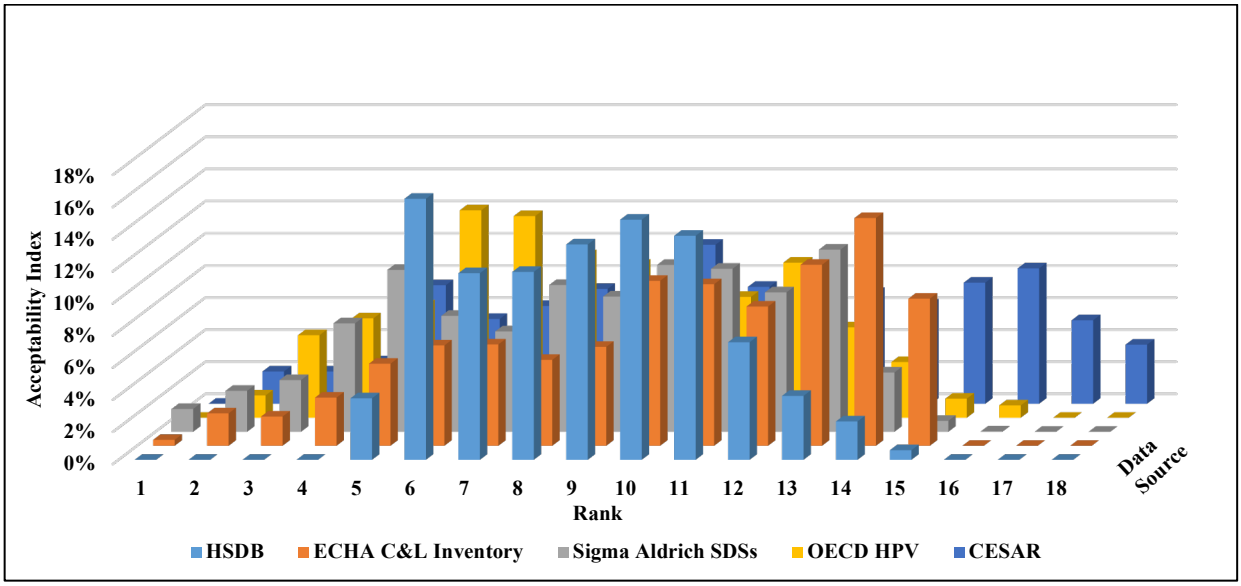

Figure 7.6. The SMAA results (extracted from Figure 4.5) for the five chemical-oriented data sources receiving similar utility scores in the MAUT baseline analysis.

The variations in the results presented by MAUT and SMAA are due to their differences in methodology [177]. The random weights applied in SMAA can accommodate higher uncertainty, which is useful in our case as weighting factors for the five performance attributes are difficult to determine. In MAUT, the total utility scores are aggregated from the single data source performance on each attribute, which are aggregated independent of any interrelation between data sources. In contrast, the SMAA results provide a more robust interpretation of the relative preference of the alternative data sources, which is often ignored by other MCDA methods. In the current study, we see it can be difficult to choose the better data source if both of them receive similar MAUT utility scores. This is not likely to happen with SMAA, as the acceptability index among those ranks will more clearly distinguish the performance variance between the data sources. Thus, the results from SMAA can be more persuasive for decision making as the preference for each data source is

reflected by their distribution in the acceptability index, which is internally determined by their relative performance on each attribute. However, it is foreseeable that SMAA loses some transparency because it hides the details of a data source's performance relative to each attribute. Though two complementary MCDA approaches are implemented, bias still cannot be fully eliminated, even in SMAA where the weighting is explored randomly. As the entire weight space always equals the value of one and is shared by all alternative data sources, the data source with extraordinary performance on certain attributes will take up more weight space, while the data sources that have similar performance on those attributes will squeeze the weight space for each other [57]. This is also part of the reason for the various acceptability distributions for hazard-trait-oriented data sources in the middle range of ranks. Though their cumulative total utility scores are similar in MAUT, the extraordinary performance on certain attributes for some data sources raise their ranks in SMAA, when compared with others.

7.5 Conclusions

As access and use of appropriate data sources are key to conducting a CHA, the selection of proper data sources will directly determine the credibility and robustness of the hazard assessment. We applied two MCDA approaches to evaluate select data sources relative to five performance attributes (i.e., reliability, adequacy, transparency, volume and ease of use). With the MAUT evaluation, the analysis has provided a clear aggregated utility score reflecting the performance of each data source and illuminating the challenges associated with developing a reasonable weighting scheme among the performance attributes. Thus, as a compromise in this current study, equal weight is set to each attribute

as the baseline. Through the weight sensitivity analysis, the influence of weighting factors on the utility score for the five performance attributes is observed, however, the weighting factors in the sensitivity analysis are not completely independent as the weight for the other attributes changes concurrently when varying a given attribute. Through the SMAA, random weight combinations are assigned to each attribute to explore the weight space for each data source, and the results on acceptability index indicate the relative rank preference of each data source, which further distinguish the performance variance of each data source. The use of these two approaches are complementary with each other and will improve the robustness of decision making when jointly applied.

Through the characterization results, we found the three types of data sources have their own strengths and shortcomings with respect to the five performance attributes. The predictive data sources perform well in terms of volume, but perform poorly in reliability, adequacy and transparency; the hazard-trait-oriented data sources perform well in terms of reliability and ease of use, but perform poorly in adequacy and volume; and the chemical-oriented data sources with high utility score perform well in all performance attributes, but the data sources with lower utility score can be poorly in adequacy, transparency and volume. It is also observed that the top-ranking chemical-oriented data sources such as ECHA CEHM, GHS-Japan and GESTIS always perform better no matter what combinations of weight scheme are selected for the five performance attributes. Although some of these relative strengths and weaknesses are inherent to the type of data source, our quantitative methodology provides deeper and more systematic comparisons than would be provided by other methods such as expert judgment. From the perspective of evaluating the five

performance attributes, improvements can still be made, especially for evaluating adequacy, transparency and volume.

Overall, our findings suggest that in order to establish CHA as a robust and reproducible decision making tool for comparing chemicals and their alternatives, it will be critical for practitioners to carefully select their data sources and to explicitly identify the performance attributes of interest in selecting those data sources. In the current study, we chose five performance attributes, but perhaps these are not the only, nor the best five, for every CHA. Our study also assumes some level of compensatory performance among the attributes, such that if a data source performs well with respect to one performance attribute, this can compensate for poor performance in another performance attribute, thus still yielding a high total utility score. Perhaps this type of compensatory weighting is not appropriate for selecting data sources for CHA, especially if only a few data sources are applied. Moreover, the significant sensitivity to the weighting schemes observed in this study suggests that a high total utility score is also not the best approach to selecting data sources. Thus, we conclude that: (a) multiple data sources are necessary to adequately provide the data needed for a CHA, (b) these data sources should be selected such that they complement each other in their high-performing performance attributes such that all performance attributes are 'maximized' by at least one data source, and (c) the selection of data sources should be deliberate and explicit, taking into account performance relative to identifiable performance attributes. Lastly, more complete, transparent and standardized data sources would alleviate the need for careful data source selection.

Chapter 8: Conclusions

8.1. Summary and Conclusions

A comprehensive sustainability assessment on three flow batteries – vanadium pentoxide flow battery (VRFB), zinc-bromine flow battery (ZBFB), and all-iron flow battery (IFB), were conducted to secure sustainable production of future energy storage systems before they are widely deployed. In Chapter 3, a life cycle impact assessment approach was applied to evaluate eight environmental impact categories associated with battery production with highlights on battery component design and material selection choices. In the baseline scenario, it is observed that the performance of the three flow batteries vary a lot when considering different impact categories with IFB showing the lowest impact on six impact categories and VRFB showing the highest impact on six impact categories. However, further sensitivity analysis on component design and material choices indicates large potential on impact reduction when optimized scenarios were applied. Specifically, the various sources of vanadium pentoxide production could lead the VRFB with lowest impact in several categories. In Chapter 4, chemical hazard assessment (CHA) and life cycle human health analysis were jointly applied to six battery energy storage systems to identify chemicals of concern with their inherent hazard to human health and the environment. In comparison with the three emerging flow batteries, three relatively well-developed lithium-ion batteries were also assessed. Both the primary chemicals and processing chemicals were analyzed in order to investigate the potential health impact on upstream production activities. From our analysis, the vanadium pentoxide used in VRFB and several lithium compounds used in lithium-ion batteries are chemicals of high concern. Though able to show the toxicity hazard and health impact with a full list of material inventories, constraints also exist in those

methodologies such as data gaps and uncertainties. In Chapter 5, the materials cost on the production of the three flow batteries was investigated through a techno-economic analysis approach. The market price of each material used in the battery systems were identified from the literature, with sensitivity analysis performed on those materials with fluctuating prices. Based on the original battery configurations provided from manufacturers, the production cost of VRFB was among the highest, while ZBFB was the lowest. When optimizing the energy capacity and energy/power ratio of a unit battery system, the costs of ZBFB and IFB could be comparable. However, the cost of VRFB is always higher than the other two batteries due to the much higher cost of vanadium pentoxide, which is the core electrolyte material and is therefore unlikely to be replaced. The comprehensive evaluations on the environmental impact, toxicity hazard, human health impact and materials cost provide important guidance to battery manufacturers and decision-makers. As one important life cycle stage, the production phase of flow batteries could contribute to negative environmental impact, thus the environmental benefit gained from the deployment of energy storage systems should be judged through an integrated approach considering both the production and use phases. However, sustainability assessment on the production of flow batteries has not been previously performed, which could lead to partial or even incorrect analysis when determining the overall benefits due to a lack of detailed production data. Hence, the analysis on flow battery production provided in this dissertation could be a great supplement in advancing sustainability assessment on energy storage systems.

As mentioned, the current framework of sustainability assessment still has quite a few uncertainty issues associated with data sources that impede the robustness of the assessment results. In Chapters 6 and 7, we have explored the influence of data source

selection choices on CHA. In Chapter 6, a case study on low band gap polymers in organic photovoltaics is used to show how different data sources could affect the CHA results. Seven different toxicity data sources categorized as chemical-oriented data sources, hazard-trait-oriented data sources, and predictive data sources were jointly and separately applied to evaluate the sensitivity of the CHA results. Further, we have applied a multi-criteria decision analysis (MCDA) approach in Chapter 7 to evaluate an expanded list of thirty-four toxicity data sources to identify proper data sources that could enhance the results of CHA. We have chosen five evaluation criteria as reliability, adequacy, transparency, volume, and ease of use and ranked the performance of each data source using two MCDA methods. The results in both Chapters 6 and 7 indicate various types of toxicity data sources should be used in CHA to increase the validity of CHA results, which could be important for future case studies.

8.2. Future Work

Energy storage systems for stationary applications might be boosted with the increasing penetration of renewable energy sources into the electric grid. As such, the environmental benefits should be comprehensively evaluated considering all the life cycle stages. Besides the production of flow batteries covered in this dissertation, future work should also address the upstream raw materials, use phase, and end-of-life stages with more sophisticated analysis. In the past, analysis of upstream materials processing for energy storage systems solely relied on existing life cycle inventory data. More complete and detailed studies should be carried out to evaluate the associated flow of materials and energy through the supply chain considering various factors such as market, location, and policy. For use phase analysis, though already addressed in the literature, further analysis considering the temporal and

geographical variance are still urgent, since many of the studies were built based on analytical models. Also, the lack of updated production data due to the fast development of energy storage systems also limit the current use phase studies, for which advanced analysis that is able to capture dynamic changes are needed. Further, the end-of-life strategy is also one important next step that requires comprehensive assessment. Currently, there are very limited studies that considered the end-of-life strategies for flow batteries. With the promotion of circular economy in effort to enhance the life span of products through repair, reuse, remanufacture and recycling, it might be critical for energy storage systems to have viable end-of-life strategies that could largely offset the impact from production. Lastly, customized sustainability assessment approaches should also be explored given the uncertainties and data gaps we encountered in our analysis.

REFERENCES

[1] United Nations General Assembly, 1987. Report of the World Commission on Environmental and Development: Our Common Future. (accessed: November 19/2018).

[2] Sheldon, R.A., 2017. Metrics of green chemistry and sustainability: past, present, and future. ACS Sustain. Chem. Eng. 6.1, 32-48.

[3] International Standard ISO 14040, 1997. Environmental management - life cycle assessment—principles and framework.

[4] Environmental management – Life cycle assessment – Principles and framework, 2006.

[5] Finnveden, G.; Hauschild, M.Z.; Ekvall, T.; Guinée, J.; Heijungs, R.; Hellweg, S.; Koehler, A.; Pennington, D.; Suh, H., 2009. Recent developments in life cycle assessment. J. Environ. Manag. 91.1, 1-21.

[6] Jørgensen, A.; Le Bocq, A.; Nazarkina, L.; Hauschild, M., 2008. Methodologies for social life cycle assessment. Int. J. Life. Cycle. Assess. 13.2, 96.

[7] Hendrickson, C. T.; Lave, L. B.; and Matthews, H. S, 2005. Environmental Life Cycle Assessment of Goods and Services: An Input-Output Approach, Resources for the Future Press.

[8] [NRC] National Research Council, 2014. A framework to guide selection of chemical alternatives. Washington, DC: National Research Council, National Academies Press.

[9] Malloy, T.F.; Zaunbrecher, V.M.; Batteate, C.M.; Blake, A.; Carrol Jr, W.F.; Corbett, C.J.; Hansen, S.F.; Lampert, R.J.; Linkov, I.; Mcfadden, R.; Moran, K.D.; Olivetti, E.; Ostrom, N.K.; Romero, M.; Schoenung, J.M.; Seager, T.; Sinsheimer, P.; Thayer, K.A., 2017(a). Advancing alternative analysis: integration of decision science. Environ. Health. Perspect. 125(6).

[10] Malloy, T.; Zaunbercher, V.; Beryt, E.; Judson. R.; Tice, R.; Allard, P.; Blake, A.; Cote, I.; Godwin, H.; Heine, L.; Kerzic, P.; Kostal, J.; Marchant, G.; McPartland, J.; Moran, K.; Nel, A.; Oguseitan, O.A.; Rossi, M,; Thayer, K.; Tickner, J.; Whittaker, M.; Zarker, K., 2017(b). Advancing alternatives analysis: the role of predictive toxicology in selecting safer chemical products and processes. Integr. Environ. Assess. Manag. 13(5), 915-925.

[11] Hester, R. E.; Harrison, R. M.; Eds., 2013. Chemical alternatives assessments, Vol. 36, Royal Society of Chemistry, Cambridge, U.K.

[12] OECD Hazard Assessment. http://www.oecd.org/env/ehs/risk-assessment/hazardassessment.htm. (accessed: November 19, 2018).

[13] Greenscreen® for safer chemicals. https://www.greenscreenchemicals.org/learn/learn-about-greenscreen (accessed: November, 19, 2018).

[14] Alternative Assessment Guide. http://theic2.org/alternatives_assessment_guide. (accessed: November, 19, 2018).

[15] BizNGO Chemical Alternatives Assessment Protocol. http://www.bizngo.org/static/ee_images/uploads/resources/BizNGOChemicalAltsAssessmentProtocol_04_12_12.pdf. (accessed: November 19, 2018).

[16] OECD Hazard Assessment. http://www.oecd.org/env/ehs/risk-assessment/hazardassessment.htm. (accessed: November 19, 2018).

[17] Greco, S.; Figueira, J.R.; Ehrgott, M., 2016. Multiple criteria decision analysis. 2nd ed. New York: Springer's International series.

[18] Linkov, I.; Ramadan, A.B., 2004. Comparative risk assessment and environmental decision making, Vol. 38. Springer Science & Business Media.

[19] Linkov, I.; Seager, T.P., 2011. Coupling multi-criteria decision analysis, life-cycle assessment, and risk assessment for emerging threats. Environ. Sci. Technol. 45(12), 5068-5074.

[20] Giove, S.; Brancia, A.; Satterstrom, F.K.; Linkov. I., 2009. Decision support systems and environment: Role of MCDA. Boston (MA): Springer.

[21] Cinelli, M.; Coles, S.R.; Kirwan. K., 2014. Analysis of the potentials of multi criteria decision analysis methods to conduct sustainability assessment. Ecol. Indic. 46, 138-148.

[22] Khan, R.A.; Anand, A.; Wani, M.F., 2018. A holistic framework for environment conscious based product risk modeling and assessment using multi criteria decision making. J. Clean. Prod. 174, 954-965.

[23] Kiker, G.A.; Bridges, T.S.; Varghese, A.; Seager, T.P.; Linkov, I., 2005. Application of multicriteria decision analysis in environmental decision making. Integr. Environ. Assess. Manag. 1(2), 95-108.

[24] Jacobs, M. M.; Malloy, T.F.; Tickner, J. A.; Edwards, S., 2016. Alternatives assessment frameworks: research needs for the informed substitution of hazardous chemicals. Environ. Health. Perspect. 124(3), 265-280.

[25] Malloy, T.F.; Sinsheimer, P.J.; Blake, A.; Linkov, I., 2013. Use of multi-criteria decision analysis in regulatory alternative analysis: a case study of lead free solder. Integr. Environ. Assess. Manag. 9(4), 652-664.

[26] Chu, S.; Majumdar, A., 2012. Opportunities and challenges for a sustainable energy future. Nat. 488(7411), 294-303.

[27] Senate Bill No. 100, California Renewable Portfolio Standard Program: emissions of greenhouse gases.

https://leginfo.legislature.ca.gov/faces/billNavClient.xhtml?bill_id=201720180SB100. (accessed: November 19, 2018).

[28] Assembly Bill 32. California Air Resource Board. https://www.arb.ca.gov/cc/ab32/ab32.htm. (accessed: November 19, 2018).

[29] Wang, W.; Luo, Q.; Li, B.; Wei, X.; Li, L.; Yang, Z., 2013Recent progress in redox flow battery research and development. Adv. Funct. Mater. 23(8), 970-986.

[30] Kear, G.; Shah, A.A.; Walsh, F.C., 2012. Development of the all-vanadium redox flow battery for energy storage: a review of technological, financial and policy aspects. Int. J. Energy. Res. 36(11), 1105-1120.

[31] Perry, M.L.; Weber, A.Z., 2016. Advanced redox-flow batteries: a perspective. J. Electrochem. Soc. 163(1), A5064-A5067.

[32] Regulation, E. C., 1999. No 1907/2006 of the European Parliament and of the Council of 18 December 2006, concerning the Registration." Evaluation, Authorisation and Restriction of Chemicals (REACH), establishing a European Chemicals Agency, amending Directive. 45 1-849.

[33] Chemicals under the Toxic Substances Control Act (TSCA). https://www.epa.gov/chemicals-under-tsca (accessed June 10, 2016).

[34] Safer Consumer Products. http://www.dtsc.ca.gov/SCP/index.cfm (accessed November 24, 2015).

[35] Goedkoop, M.; Heijungs, R.; Huijbregts, M.; De Schryver, A., 2009. ReCiPe 2008. A life cycle impact assessment method which comprises harmonised category indicators at the midpoint and the endpoint level.

[36] Guinée, J., 2001. Handbook on life cycle assessment—operational guide to the ISO standards. Int. J. Life. Cycle. Assess. 6(5), 255-255.

[37] Jolliet, O.; Margni, M,; Charles, R.; humbert, S.; Payyet, J.; Rebitzer, G.; Rosenbaum, R., 2003. IMPACT 2002+: a new life cycle impact assessment methodology. Int. J. Life. Cycle. Assess. 8(6), 324.

[38] Bare, J.C., 2002. TRACI: The tool for the reduction and assessment of chemical and other environmental impacts. J. Ind. Ecol. 6(3-4), 49-78.

[39] Ekvall, T.; Azapagic, A.; Finnveden, G.; Rydberg, T.; Weidema, B.P.; Zamagni, A., 2016. Attributional and consequential LCA in the ILCD handbook. Int. J. Life. Cycle. Assess. 21(3), 293-296.

[40] Rebitzer, G.; Ekvall, T.; Frischknect, R.; Hunkeler, D.; Norris, G.; Rydberg, T.; Schmidt, W.P.; Suh, S.; Weidema, B.P.; Pennington, D.W., 2004. Life cycle assessment: Part 1: Framework, goal and scope definition, inventory analysis, and applications. Environ. Int. 30(5), 701-720.

[41] Hauschild, M.Z.; Huijbregts, M.A., 2015. Introducing life cycle impact assessment. Life Cycle Impact Assessment. Springer, Dordrecht, 1-16.

[42] Pennington, D. W.; Potting, J.; Finnveden, G.; Lindeijer, E.; Jolliet, O.; Rydberg, T.; Rebitzer, G., 2004. Life cycle assessment Part 2: Current impact assessment practice. Environ. Int. 30(5), 721-739.

[43] International Standard ISO 14040; 1997. Environmental management - life cycle assessment—principles and framework.

[44] Hauschild, M.Z.; Huijbregts, M.; Jolliet, O.; MacLeod, M.; Margni, M.; van de Meent, D.; Rosenbaum, R.K.; McKone, T.E., 2008. Building a model based on scientific consensus for

life cycle impact assessment of chemicals: the search for harmony and parsimony. Environ. Sci. Technol. 42, 7032-7037

[45] Henderson, A.D.; Hauschild, M.Z.; van de Meent, D.; Huijbregts, M.A.; Larsen, H.F.; Margni, M.; McKone, T.E.; Payet, J.; Rosenbaum, R.K.; Jolliet, O., 2011. USEtox fate and ecotoxicity factors for comparative assessment of toxic emissions in life cycle analysis: sensitivity to key chemical properties. Int. J. LCA. 16(8), 701.

[46] Rosenbaum, R.K.; Bachmann, T.M.; Gold, L.S.; Huijbregts, M.A.; Jolliet, O.; Juraske, R.; Koehler, A.; Larsen, H.F.; MacLeod, M.; Margni, M.; McKone, T.E., 2008. USEtox—the UNEP-SETAC toxicity model: recommended characterisation factors for human toxicity and freshwater ecotoxicity in life cycle impact assessment. Int. J. LCA. 13(7), 532.

[47] Minke, C.; Kunz, U.; Turek, T., 2017. Techno-economic assessment of novel vanadium Redox flow batteries with large-area cells. J. Power Sources. 361, 105-114.

[48] Mellentine, J.A., Performance Characterization and Cost Assessment of an Iron HybridFlow Battery. PhD Dissertation.

[49] Ha, S.; Gallagher, K.G., 2015. Estimating the system price of redox flow batteries for grid storage, J. Power Sources, 296, 122–132.

[50] Zheng, M.; Sun, J.; Meinrenken, C.J.; Wang, T., 2019. Pathways toward enhanced techno-economic performance of flow battery systems in energy system applications. *J. Electrochem. Energy Convers. Storage*. 16(2).

[51] Viswanathan, V.; Crawford, A.; Stephenson, D.L.; Kim, S.; Wang, W.; Li, B.;Coffey, G.; Thomsen, E.; Graff, G.; Balducci, R.; Kintner-Meyer, M., 2014. Cost and performance model for redox flow batteries," J. Power Sources. 247, 1040–1051.

[52] Minke, C.; Turek, T., 2018. Materials, system designs and modelling approaches in

techno-economic assessment of all-vanadium redox flow batteries – A review, J. Power Sources. 376, 66–81.

[53] Yatsalo, B.; Didenko, V.; Gritsyuk, S.; Sullivan, T., 2015. Decerns: a framework for multi-criteria decision analysis. Int. J. Comput. Int. Sys. 8(3), 467-489.

[54] Lahdelma, R.; Hokkanen, J.; Salminen, P., 1998. SMAA-stochastic multiobjective acceptability analysis. Eur. J. Oper. Res.106(1), 137-143.

[55] Sanayei, A.; Mousavi, S.F.; Abdi, M.R.; Mohaghar, A., 2008. An integrated group decision-making process for supplierselection and order allocation using multi-attribute utility theory and linear programming. J. Franklin I. 345(7), 731-747.

[56] Dyer, J.S., 2005. MAUT-multiattribute utility theory, multiple criteria decision analysis: state of the art surveys. New York (NY): Springer. 265-292.

[57] Lahdelma, R.; Salminen, P., 2001. SMAA-2: Stochastic multicriteria acceptability analysis for group decision making. Operations Research. 49(3), 444-454.

[58] Liu, J.; Wang, J.; Xu, C.; Jiang, H.; Li, C.; Zhang, L.; Lin, J.; Shen, Z.X., 2018. Advanced energy storage devices: basic principles, analytical methods, and rational materials design. Adv. Sci. 5(1), 1700322.

[59] Lawder, M.T.; Suthar, B.; Northrop, P.W.; De, S.; Hoff, C.M.; Leitermann, O.; Crow, M.L.; Santhanagopalan, S; Subramanian, V.R., 2014. Battery energy storage system (BESS) and battery management system (BMS) for grid-scale applications. Proc. IEEE. 102(6), 1014-1030.

[60] Chalamala, B.R., et al. 2014. Redox flow batteries: an engineering perspective. Proc. the IEEE 102(6), 976-999.

[61] Noack, J.; et al. 2015. The chemistry of redox-flow batteries. Angew. Chem. Int. Ed. 54(34), 9776-9809.

[62] Weber, S.; Peters, J.F.; Baumann, M.; Weil, M., 2018. Life Cycle Assessment of a Vanadium Redox Flow Battery. Environ. Sci. Technol. 52(18), 10864-10873.

[63] Rydh, C.J., 1999. Environmental assessment of vanadium redox and lead-acid batteries for stationary energy storage. J. Power Sources. 80,(1-2), 21-29.

[64] Hiremath, M.; Derendorf, K.; Thomas Vogt, T., 2015. Comparative life cycle assessment of battery storage systems for stationary applications. Environ. Sci. Technol. 49(8), 4833.

[65] Sáez-Martínez, F. J.; Lefebvre, G.; Hernández J. J.; Clark, J. H., 2016. Drivers of sustainable cleaner production and sustainable energy options. J. Clean. Prod. 138, 1-7.

[66] Luo, X.; Wang, J.; Dooner, M.; Clarke, J., 2015. Overview of current development in electrical energy storage technologies and the application potential in power system operation. Appl. Energy. 137, 511-536.

[67] Mehrjerdi, H; Hemmati, R., 2019. Modeling and optimal scheduling of battery energy storage systems in electric power distribution networks. J. Clean. Prod. 234, 810-821.

[68] Mehrjerdi, H; Hemmati, R., 2019. Modeling and optimal scheduling of battery energy storage systems in electric power distribution networks. J. Clean. Prod. 234, 810-821.

[69] Leung, P.; Li, X.; De León, C.P.; Berlouis, L.; Low, C.J.; Walsh, F.C., 2012. Progress in redox flow batteries, remaining challenges and their applications in energy storage. RSC Adv. 2(27), 10125-10156.

[70] Park, M.; Ryu, J.; Wang, W.; Cho, J., 2017. Materials design and engineering of next generation flow-battery technologies. Nat. Rev. Mater. 2(1), 16080.

[71] Ulaganathan, M.; Aravindan, V.; Yan, Q.; Madhavi, S.; Skyllas-Kazacos, M.; Lim, T.M., 2016. Recent advancements in all-vanadium redox flow batteries. Adv. Mater. Interfaces. 3(1), 1500309.

[72] Davies, T.J.; Tummino, J.J., 2018. High-Performance Vanadium Redox Flow Batteries with Graphite Felt Electrodes. Carbon. 4(1), 8

[73] Yin, C.; Gao, Y.; Guo, S.; Tang, H. A, 2014. A coupled three dimensional model of vanadium redox flow battery for flow field designs. Energy. 74, 886-895.

[74] Yuan, Z.; Duan, Y.; Zhang, H.; Li, X.; Zhang, H.; Vankelecom, I., 2016. Advanced porous membranes with ultra-high selectivity and stability for vanadium flow batteries. Energy Environ. Sci. 9(2), 441-447.

[75] Dmello, R.; Milshtein, J.D.; Brushett F.R.; Smith, K.C., 2016. Cost-driven materials selection criteria for redox flow battery electrolytes. J. Power Sources. 330, 261-272.

[76] Ha, S.; Gallagher, K.G., 2015. Estimating the system price of redox flow batteries for grid storage. J. Power Sources. 296, 122-132.

[77] L'Abbate, P.; Dassisti, M.; Olabi, A.G., 2019. Small-Size Vanadium Redox Flow Batteries: An Environmental Sustainability Analysis via LCA, in: Basosi, R.; Cellura, M.; Longo, S.; Parisi, M.L. (Eds.), Life Cycle Assessment of Energy Systems and Sustainable Energy Technologies; Springer: Cham, Swetzerland, pp. 61-78.

[78] Schmidt, T.; Beuse, M.; Xiaojin, Z.; Steffen, B.; Schneider, S.F.; Pena-Bello, A.; Bauer, C.; Parra, D., 2019. Additional emissions and cost from storing electricity in stationary battery systems. Environ. Sci. Technol. 53(7), 3379-3390.

[79] Ellingsen, L.A.; Majeau-Bettez, G.; Singh, B.; Srivastava, A.K.; Valøen, L.O.; Strømman, A.H., 2014. Life cycle assessment of a lithium-ion battery vehicle pack. J. Ind. Ecol. 18(1), 113-124.

[80] Majeau-Bettez, G.; Hawkins, T.R.; Strømman, A.H., 2011. Life cycle environmental assessment of lithium-ion and nickel metal hydride batteries for plug-in hybrid and battery electric vehicles. Environ. Sci. Technol. 45(10), 4548-4554.

[81] Notter, D.A.; Gauch, M.; Widmer, R.; Wager, P.; Stamp, A.; Zah, R.; Althaus, H.J., 2010. Contribution of Li-ion Batteries to the Environmental Impact of Electric Vehicles. Environ. Sci. Technol. 44, 6550-6556.

[82] Dunn, J.B.; Gaines, L.; Kelly, J.C.; James, C.; Gallagher, K.G., 2015. The significance of Li-ion batteries in electric vehicle life-cycle energy and emissions and recycling's role in its reduction. Energy Environ. Sci. 8(1),158-168.

[83] Olivetti, E.A.; Ceder, G.; Gaustad, G.G.; Fu, X., 2017. Lithium-ion battery supply chain considerations: analysis of potential bottlenecks in critical metals. Joule. 1(2), 229-243.

[84] Peters J.F. and Weil M, 2018. Providing a common base for life cycle assessments of Li-in batteries. J. Clean. Prod. 171, 704-713.

[85] Lachuriya, A.; Kulkarni, R.D.; 2017. Stationary electrical energy storage technology for global energy sustainability. ICNTE. Cl1-6.

[86] Cunha, Á.; Martins, J.; Rodrigues, N.; Brito, F.P., 2015. Vanadium redox flow batteries: a technology review. Int. J. Energy Res. 39(7), 889-918.

[87] Dinesh, A.; Olivera, S.; Venkatesh, K.; Santosh, M.S.; Priya, M.G. Asiri, A.M.; Muralidhara, H.B., 2018. Iron-based flow batteries to store renewable energies. Environ. Chem. Lett. 16(3), 683-694.

[88] Wernet, G.; Bauer, C.; Steubing, B.; Reinhard, J.; Moreno-Ruiz, E.; Weidema, B., 2016. The ecoinvent database version 3 (part I): overview and methodology. Int. J. LCA. 21(9),1218-1230.

[89] Chen, S.; Fu, X.; Chu, M.; Liu, Z.; Tang, J., 2015. Life cycle assessment of the comprehensive utilisation of vanadium titano-magnetite. J. Clean. Prod. 101, 122-128.

[90] Jungbluth, N.; Eggenberger S, 2018. Life Cycle Assessment for Vanadium Pentoxide (V_2O_5) from secondary resources. ESU-services Ltd. http://esu-services.ch/data/abstracts-of-lcis/#c154 (accessed November 11, 2018).

[91] Minke, C.; Kunz, U.; Turek, T., 2017. Carbon felt and carbon fiber – A techno-economic assessment of felt electrodes for redox flow battery applications. J. Power Sources. 342, 116-124.

[92] Romaniw, Y. A., 2013. The relationship between light-weighting with carbon fiber reinforced polymers and the life cycle environmental impacts of orbital launch rockets. PhD Dissertation. Georgia Institute of Technology, Atlanta, GA.

[93] Mohammadi, T.; Skyllas-Kazacos, M., 1995. Characterization of novel composite membrane for redox flow battery applications. J. Membr. Sci. 98(1-2), 77-87.

[94] SimaPro, Pre-sustainability. https://network.simapro.com (accessed November 18, 2017)

[95] Huijbregts, M.; Steinmann, Z.J.; Elshout, P.M.; Stam, G.; Verones, F.; Vieira, M.; Zijp, M.; Hollander, A.; Van Zelm, R., 2017. ReCiPe2016: a harmonised life cycle impact assessment method at midpoint and endpoint level. Int. J. LCA. 22(2), 138-147.

[96] Frischknecht, R.; Jungbluth, N.; Althaus, H.J.; Bauer, C.; Doka, G.; Dones, R.; Hischier, R.; Hellweg, S.; Humbert, S.; Köllner, T.; Loerincik, Y.; Margni, M.; Nemecek, T., 2007.

Implementation of Life Cycle Impact Assessment Methods, ecoinvent report No. 3, v2.0; Swiss Centre for Life Cycle Inventories, Dübendorf.

[97] Banerjee, S.; Curtin, D.E., 2004. Nafion® perfluorinated membranes in fuel cells. J. Fluor. Chem. 125(8), 1211-1216

[98] Shi, Y.; Eze, C.; Xiong, B.; He, W.; Zhang, H.; Lim, T. M.; Ukil, A.; Zhao, J., 2019. Recent development of membrane for vanadium redox flow battery applications: A review. Appl. Energy. 238, 202-224.

[99] Prifti, H. Parasuraman, A.; Winardi, S.; Lim, T.M.; Skyllas-Kazacos, M., 2012. Membranes for redox flow battery applications. Membranes. 2(2), 275-306.

[100] Schwenzer, B. Zhang, J.; Kim, S.; Li, L.; Liu, J.; Yang, Z., 2011. Membrane development for vanadium redox flow batteries. ChemSusChem. 4(10), 1388-1406.

[101] Sayler, T.S., 2012. Preparation of perfluorinated ionomers for fuel cell applications. PhD Dissertation. The University of Alabama, Tuscaloosa, AL.

[102] Meng, F.; McKechnie, J.; Turner, T.; Wong, K.H.; Pickering, S.J., 2017. Environmental aspects of use of recycled carbon fiber composites in automotive applications. Environ. Sci. Technol. 51(21), 12727-12736.

[103] Castañeda, L. F.; Walsh, F. C.; Nava, J. L.; de Leon, C. P., 2017. Graphite felt as a versatile electrode material: Properties, reaction, environment, performance and applications. Electrochim. Acta. 258,1115-1139.

[104] Li, M., Lu, j., Chen, Z., Amine, K., 2018. 30 years of lithium-ion batteries. Adv. Mater. 30(33), 1800561.

[105] Kang, D. H. P.; Chen, M., Ogunseitan, O. A., 2013. Potential environmental and human health impacts of rechargeable lithium batteries in electronic waste. Environ. Sci. Technol. 47(10), 5495-5503.

[106] Lebedeva, N. P.; Boon-Brett, L., 2016. Considerations on the Chemical Toxicity of Contemporary Li-Ion Battery Electrolytes and Their Components. J. Electrochem. Soc. 163(6), 821-830.

[107] He, H.; Tian, S.; Tarroja, B.; Ogunseitan, O. A.; Samuelsen, S.; Schoenung, J. M.; 2020. Flow battery production: Materials selection and environmental impact. J. Clean. Prod. 269, 121740.

[108] Globally Harmonized System of Classification and Labelling of Chemicals. http://www.unece.org/trans/danger/publi/ghs/ghs_rev02/02files_e.html (accessed September 13, 2018).

[109] Chen, S.; Wen, K; Fan, J.; Bando, Y.; Golberg, D., 2018. Progress and future prospects of high-voltage and high-safety electrolytes in advanced lithium batteries: from liquid to soild electrolytes. J. Mater. Chem. A. 6(25), 11631-11663.

[110] Kaloff, J.; Eshetu, G. G.; Bresser, D. Passerini, S., 2015. Safer electrolytes for lithium-ion batteries: state of the art and perspectives. ChemSusChem. 8(13), 2154-2175.

[111] Wang, W.; Ping, P.; Zhao, X.; Chu, G.; Sun, J.; Chen, C., 2012. Thermal runaway caused fire and explosion of lithium ion battery. J. Power Sources. 208, 210-224.

[112] Kang, H. Y.; Schoenung, J. M.; 2006. Economic Analysis of Electronic Waste Recycling: Modeling the Cost and Revenue of a Materials Recovery Facility in California. Environ. Sci. Technol. 40(5), 1672–1680.

[113] Ye, J; Schoenung, J. M., 2004. Technical Cost Modeling for the Mechanical Milling at

Cryogenic Temperature (Cryomilling). Adv. Eng. Mater. 6(8), 656–664.

[114] Field, F.; Kirchain, R.; Roth, R.; 2007. Process cost modeling: Strategic engineering and

economic evaluation of Materials technologies. JOM. 59(10) 21–32.

[115] Isaacs, J. A.; Tanwani, A.; Healy, M. L.; Dahlben, L. J., 2010. Economic assessment of single-walled carbon nanotube processes. J. Nanoparticle Res. 12(2)551–562, 2010.

[116] Parr, G., ANNUAL FORUM 2005 Trade and Uneven Development: Opportunities and Challenges Import Parity Pricing: A Competitive Constraint or a Source of Market Power? TIPS FORUM 2005 _____ Import Parity Pricing: A Competitive Constraint or a Source of Market Power?"

[117] ProjectManagement.com - 3-Points Estimating. [Online]. Available: https://www.projectmanagement.com/wikis/368763/3-Points-Estimating. (Accessed: 06-Jan-2020)

[118] Olson, D. W., USGS 2016 Minerals Yearbook – Graphite.

[119] LLDPE (Linear Low-Density Polyethylene): Production, Price and its Properties. [Online]. Available: https://www.plasticsinsight.com/resin-intelligence/resin-prices/lldpe/. (Accessed: 06-Jan-2020)

[120] Polypropylene Production Capacity, Market and Price. [Online]. Available: https://www.plasticsinsight.com/resin-intelligence/resin-prices/polypropylene/. (Accessed: 06-Jan-2020)

[121] Glass fiber - Wikipedia. [Online]. Available: https://en.wikipedia.org/wiki/Glass_fiber. (Accessed: 06-Jan-2020)

[122] Latest Free Steel Prices -. [Online]. Available: https://worldsteelprices.com/.

(Accessed: 06-Jan-2020)

[123] USGS 2019 Mineral Commodity Summaries - Copper. [Online]. Available: http://dx.doi.org/10.3133/fs20143004. (Accessed: 14-Jan-2020)

[124] Polyvinyl Chloride Futures Historical Prices - Investing.com. [Online]. Available: https://www.investing.com/commodities/pvc-com-futures-historical-data. (Accessed: 06-Jan-2020)

[125] Vanadium Statistics and Information. [Online]. Available: https://www.usgs.gov/centers/nmic/vanadium-statistics-and-information. (Accessed: 06-Jan-2020)

[126] Price and market trends: US hydrochloric acid supply poised to tighten | ICIS. [Online]. Available: https://www.icis.com/explore/resources/news/2018/02/01/10189415/price-and-market-trends-us-hydrochloric-acid-supply-poised-to-tighten/. (Accessed: 06-Jan-2020)

[127] Commercial Water Rates - Utilities | seattle.gov. [Online]. Available: https://www.seattle.gov/utilities/businesses-and-key-accounts/water/rates/commercial-water-rates. (Accessed: 06-Jan-2020)

[128] HDPE Production Capacity, Price and Market. [Online]. Available: https://www.plasticsinsight.com/resin-intelligence/resin-prices/hdpe/. (Accessed: 06-Jan-2020)

[129] Minke, C.; Dorantes Ledesma, M. A., 2018. Impact of cell design and maintenance strategy on life cycle costs of vanadium redox flow batteries. J. Energy Storage, 21, 571–580.

[130] USGS 2018 Mineral Commodity Summaries – Aluminium. 2013. [Online]. Available:

https://www.usitc.gov/publications/332/pub4703.pdf. (Accessed: 14-Jan-2020)

[131] Titanium Cost Comparison - Tricor Metals. [Online]. Available: https://www.tricormetals.com/cost-comparison.html. (Accessed: 06-Jan-2020)

[132] COPPER (Data in thousand metric tons of copper content unless otherwise noted).

[133] Polyester Production, Price and Market Forecast." [Online]. Available: https://www.plasticsinsight.com/resin-intelligence/resin-prices/polyester/. (Accessed: 06-Jan-2020)

[134] Polyethylene - U.H.M.W. (UHMW PE), sheet, thickness 2 mm, size 500 × 500 mm | Sigma-Aldrich. [Online]. Available: https://www.sigmaaldrich.com/catalog/product/aldrich/gf36466623?lang=en&region=US. (Accessed: 06-Jan-2020])

[135] US Ferric Chloride Producers Raise Prices in Healthy Market | ICIS. [Online]. Available: https://www.icis.com/explore/resources/news/2001/08/27/145944/us-ferric-chloride-producers-raise-prices-in-healthy-market/. (Accessed: 06-Jan-2020)

[136] Potassium Chloride - Monthly Price - Commodity Prices - Price Charts, Data, and News - IndexMundi. [Online]. Available: https://www.indexmundi.com/commodities/?commodity=potassium-chloride&months=12 [45] USGS 2015 Minerals Yearbook - Manganese. https://prd-wret.s3-us-west-2.amazonaws.com/assets/palladium/production/atoms/files/myb1-2015-manga.pdf. (Accessed: 06-Jan-2020)

[137] Potassium Chloride - Monthly Price - Commodity Prices - Price Charts, Data, and News - IndexMundi. [Online]. Available: https://www.indexmundi.com/commodities/?commodity=potassium-

chloride&months=12 [45] USGS 2015 Minerals Yearbook - Manganese. https://prd-wret.s3-us-west-2.amazonaws.com/assets/palladium/production/atoms/files/myb1-2015-manga.pdf. (Accessed: 06-Jan-2020)

[138] Polyak, E., USGS 2016 Minerals Yearbook - Vanadium. https://s3-us-west-2.amazonaws.com/prd-wret/assets/palladium/production/mineral-pubs/vanadium/myb1-2016-vanad.pdf .

[139] USGS 2019 Mineral Commodity Summaries - Vanadium Pentoxide."=https://prdwret.s3-us-west 2.amazonaws.com/assets/palladium/production/atoms/files/mcs-2019-vanad.pdf.

[140] USGS 2006 Mineral Commodity Summaries - Vanadium Pentoxide. https://s3-us-west-2.amazonaws.com/prd-wret/assets/palladium/production/mineral-

[141] USGS 2009 Mineral Commodity Summaries - Vanadium Pentoxide. https://s3-us-west-2.amazonaws.com/prd-wret/assets/palladium/production/mineral-pubs/vanadium/mcs-2009-vanad.pdf

[142] Producer Price Index by Commodity for Metals and Metal Products: Titanium and Titanium Base Alloy Mill Shapes. [Online]. Available: https://www.quandl.com/data/FRED/WPU10250505-Producer-Price-Index-by-Commodity-for-Metals-and-Metal-Products-Titanium-and-Titanium-Base-Alloy-Mill-Shapes. (Accessed: 06-Jan-2020)

[143] USGS 2018 Mineral Commodity Summaries - Bromine. [Online]. Available: https://s3-us-west-2.amazonaws.com/prd-wret/assets/palladium/production/mineral-pubs/bromine/mcs-2018-bromi.pdf. (Accessed: 06-Jan-2020)

[144] Günes, S.; Neugebauer, H.; Sariciftci, N.S., 2007. Conjugated polymer-based organic solar cells, Chem. Rev.107(4),1324-1338.

[145Darling, S.B.; You, F., 2013. The case for organic photovoltaics, Rsc. Adv. 3(39), 17633-17648.

[146] Huo, L.; Huo, J. ; Chen, H.; Zhang, S. ; Jiang, Y.; Chen, T. L. ; Yang, Y. , 2009. Bandgap and Molecular Level Control of the Low-Bandgap Polymers Based on 3,6-Dithiophen-2-yl-2,5-dihydropyrrolo[3,4-c]pyrrole-1,4-dione toward Highly Efficient Polymer Solar Cells. Macromolecules. 42(17), 6564-6571.

[147] Bundgaard, W.; Krebs, F.C., 2007. Low Band Gap Polymers for Organic Photovoltaics, Sol. Energy Mater. Sol. Cells. 91(11), 954-985.

[148] Lithner, D.; Larsson, Å.; Dave, G. , 2011. Environmental and Health Hazard Ranking and Assessment of Plastic Polymers based on Chemical Composition. Sci. Total Environ. 409(18), 3309-3324.

[149] You, J.; Dou, L.; Yoshimura, K.; Kato, T.; Ohya, K.; Moriarty, T.; Emery, K.; Chen, C.; Gao, J.; Li, G.; Yang, Y., 2-13. A Polymer Tandem Solar Cell with 10.6% Power Conversion Efficiency, Nat. Commun. 4,1446.

[150] Dou, L.; You, J.; Yang, J.; Chen, C.; He, Y.; Murase, S.; Moriarty, T.; Emery, K.; Li, G.; Yang, Y., 2012. Tandem polymer solar cells featuring a spectrally matched low-bandgap polymer[J. Nat. Photonics. 6(3), 180-185.

[151] Dou, L.; Chang, W.; Gao, J.; Chen, C.; You, J.; Yang, Y, 2013. A Selenium-Substituted Low-Bandgap Polymer with Versatile Photovoltaic Applications. Adv. Mater. 25(6), 825-831.

[152] Zhang, Y.; Zou, J.; Cheuh, C.; Yip, H.; Jen, A.K., 2012. Significant Improved Performance of Photovoltaic Cells Made from a Partially Fluorinated Cyclopentadithiophene/Benzothiadiazole Conjugated Polymer, Macromolecules. 45(13), 5427-5435.

[153] Chu, T.; Lu, J.; Beaupré, S.; Zhang, Y.; Pouliot, J.; Wakim, S.; Zhou, J.; Leclerc, M.; Li, Z.; Ding, J.; Tao, Y., 2011. Bulk Heterojunction Solar Cells Using Thieno[3,4-c]pyrrole-4,6-dione and Dithieno[3,2-b:2',3'-d]silole Copolymer With a Power Conversion Efficiency of 7.3%, J. Am. Chem. Soc. 133(22), 4250-4253.

[154] Li, W.; Roelofs, W.S.C.; Weink, M.M.; Janssen, R. A. J., 2012. Enhancing the Photocurrent in Diketopyrrolopyrrole-Based Polymer Solar Cells via Energy Level Control. J. Am. Chem. Soc.134(33),13787-13795.

[155] Blouin, N.; Michaud, A.; Leclerc, M., 2007. A Low-Bandgap Poly(2,7-Carbazole) Derivative for Use in High-Performance Solar Cells. Adv. Mater. 19(17), 2295-2300.

[156] Yuan, M.; Chiu, M.; Liu, S.; Chen, C.; Wei, K., 2010. A Thieno[3,4-c]pyrrole-4,6-dione-Based Donor-Acceptor Polymer Exhibiting High Crystallinity for Photovoltaic Applications. Macromolecules. 43, 6936-6938

[157] Zhou, H.; Yang, L.; Stuart, A.C.; Price, S.C.; Liu, S.; You, W., 2011. Development of Fluorinated Benzothiadiazole as a Structural Unit for a Polymer Solar Cell of 7 % Efficiency. Angew. Chem. Int. Ed.123(13), 3051-3054.

[158] Zhou, Y.; Najari, A.; Berrouard, P.; Beaupré, R.; Aïch, B.R.; Tao, Y.; Lerclerc, M.A., 2010. Thieno[3, 4-c]pyrrole-4, 6-dione Based Copolymer for Efficient Solar Cells. J. Am. Chem. Soc. 132, (15), 5330-5331.

[159] Liang, Y.; Feng, D.; Wu, Y.; Tsai, S.; Li, G.; Ray, C.; Yu, L., 2009. Highly Efficient Solar Cell Polymers Developed via Fine-Tuning of Structural and Electronic Properties. J. Am. Chem. Soc. 131(22). 7792-7799.

[160] Wang, E.; Lan, L.; Chen, J.; Peng, J.; Cao, Y., 2008. Development of Si-bridged Conjugated Donor Polymers for High- Efficiency Bulk-Heterojunction Photovoltaic Devices. Organic Photovoltaics. 11(23), 24.

[161] Amb, C.M.; Chen, S.; Graham, K.R.; Subbiah, J.; Small, C.E.; So, F.; Reynolds, J.R., 2011. Dithienogermole as a Fused Electron Donor in Bulk Heterojunction Solar Cells. J. Am. Chem. Soc. 133(26), 10062-10065.

[162] GESTIS. http://www.dguv.de (accessed September 14, 2018).

[163] Safety Data Sheet. http://www.sigmaaldrich.com/united-kingdom/technical-services/material-safety-data.html (accessed September 13, 2018).

[164] Proposition 65. http://www.oehha.org/prop65 (accessed July 13, 2018).

[165] Endocrine Disruptor Exchange. http://endocrinedisruption.org/ (accessed July 17, 2018).

[166] VEGA HUB – Virtual Models for Property Evaluation of Chemicals within a Global Architecture. https://www.vegahub.eu (Accessed August 13, 2018)

[167] EPI Suite™-Estimation Program Interface. https://www.epa.gov/tsca-screening-tools/epi-suitetm-estimation-program-interface (accessed July 15, 2018).

[168] Globally Harmonized System of Classification and Labeling. http://www.safe.nite.go.jp. (accessed September 13, 2018).

[169] He, H.; Gutierrez, Y,; Young, T.M.; Schoenung. J.M., 2019. The role of data source selection in chemical hazard assessment: A case on organic photovoltaics. J. Hazard. Mater. 365, 227-236

[170] Luechtefeld, T.; Maertens, A.; Russo, D.P.; Rovida, C.; Zhu, H.; Hartung, T.; 2016. Analysis of publically available skin sensitization data from REACH registration 2008 – 2014. ALTEX. 33(2),135.

[171] Judson, R.; Richard, A.; Dix, D.J.; Houck, K.; Marting, M.; Kavlock, R.; Dellarco, V.; Henry, T.; Holderman, T.; Sayre, P.; Tan, S; Carpenter, T.; Smith, E., 2009. The toxicity data landscape for environmental chemicals. Environmental Health Perspective. 117(5), 685-695.

[172] Hox, J.J.; Boeije, H.R.; 2005. Data collection, primary versus secondary. Encyclopedia of Social Measurement. 593-599.

[173] Gough, D., 2007. Weight of evidence: a framework for the appraisal of the quality and relevance of evidence. Res. Pap. Educ. 22(2), 213-228.

[174] Ågerstrand, M.; Beronius A., 2016. Weight of Evidence evaluation and Systematic Review in EU chemical risk assessment: Foundation is laid but guidance is needed. Environ. Int.92: 590-596.

[175] Linkov, I.; Loney, D.; Cormier, S.; Satterstrom, F.K.; Bridges, T., 2009. Weight-of-evidence evaluation in environmental assessment: review of qualitative and quantitative approaches. Sci.Total Environ. 407(19), 5199-5205.

[176] Higgins, J.P.; Green, S., 2011. Cochrane handbook for systematic reviews of interventions Vol. 4. John Wiley & Sons.

[177] Mandrioli, D,; Silbergeld, E.K,. 2016. Evidence from toxicology: the most essential science for prevention. Environ. Health Perspect.124(1), 6.

[178] Thayer, K.A.; Wolfe, M.S.; Rooney, A.A.; Boyles, A.L.; Bucher, J.R.; Birnbaum, L.S., 2014. Intersection of systematic review methodology with the NIH reproducibility initiative. Environ. Health Perspect.122(7), A176.

[176] Klimisch, H.J.; Andreae, M.; Tillmann, U.. 1997. A systematic approach for evaluating the quality of experimental toxicological and ecotoxicological data. Regul. Toxicol. Pharmacol. 25(1), 1-5.

[177] Velasquez, M.; Hester, P.T., 2011. An analysis of multi-criteria decision making methods. Int. J. Prod, Res. 49(6), 1669-1683.

[178] Organisation for Economic Cooperation and Development. 2016b. The global portal to information on chemical substances. Organisation for Economic Cooperation and Development; https://www.echemportal.org/echemportal/index.action. (accessed August 27, 2017).

[179] States National Library of Medicine. 2016. Toxicology Data Network. United States National Library of Medicine; https://toxnet.nlm.nih.gov. (accessed September 3, 2017).

[180] Luechtefeld, T.; Hartung, T., 2017.Computational approaches to chemical hazard assessment. Alternatives to Animal Experimentation. ALTEX. 34(4), 459-478.

[181] European Chemicals Agency. 2016. Practical guide – how to use and report (Q)SARs. European Chemicals Agency; https://echa.europa.eu/documents/10162/13655/pg_report_qsars_en.pdf. (accessed December 29, 2017).

[182] United States Environmental Protection Agency. 2015. Flame Retardants in Printed Circuit Boards. Washington, DC: United States Environmental Protection Agency; https://www.epa.gov/sites/production/files/2015-08/documents/pcb_final_report.pdf. (accessed July 26, 2017).

[183] Organisation for Economic Cooperation and Development. 2016a. OECD Substitution and Alternatives Assessment Tool Selector. Organisation for Economic Cooperation and Development; http://www.oecdsaatoolbox.org/Home/Tools. (accessed July 26, 2017).

[184] Gauthier, A.M.; Fung, M.; Panko, J.; Kingsbury, T.; Perez, A.L.; Hitchcock, K.; Ferracini, T.; Sahmel, J.; Banducci, A.; Jacobsen, M.; Abelmann, A.; Shay, E., 2015. Chemical assessment state of the science: Evaluation of 32 decision-support tools used to screen and prioritize chemicals. Int. Environ. Assess. Manag. 11(2), 242-255.

[185] Lowell Center for Sustainable Production, 2011. A compendium of methods and tools for chemical hazard assessment. Lowell Center for Sustainable Production. Lowell (MA): University of Massachusetts Lowell.

[186] Tervonen T., 2014. JSMAA: Open source software for SMAA computations. Int. J. of Syst. Sci. 45(1), 69-81.

APPENDIX A: The Processing Flow on The Production of The Three Flow Batteries

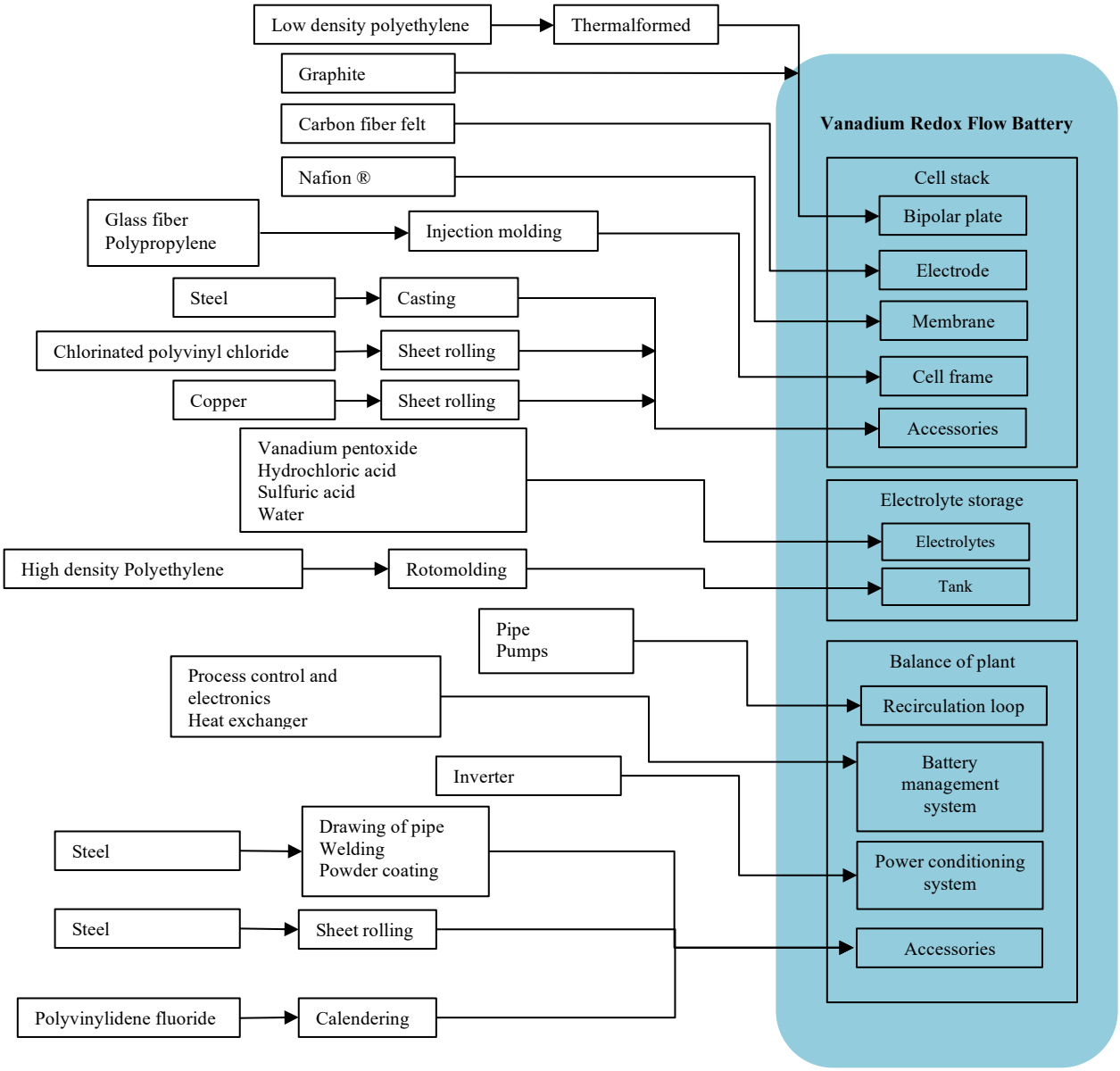

Figure A1. The process flow diagram for producing a vanadium redox flow battery.

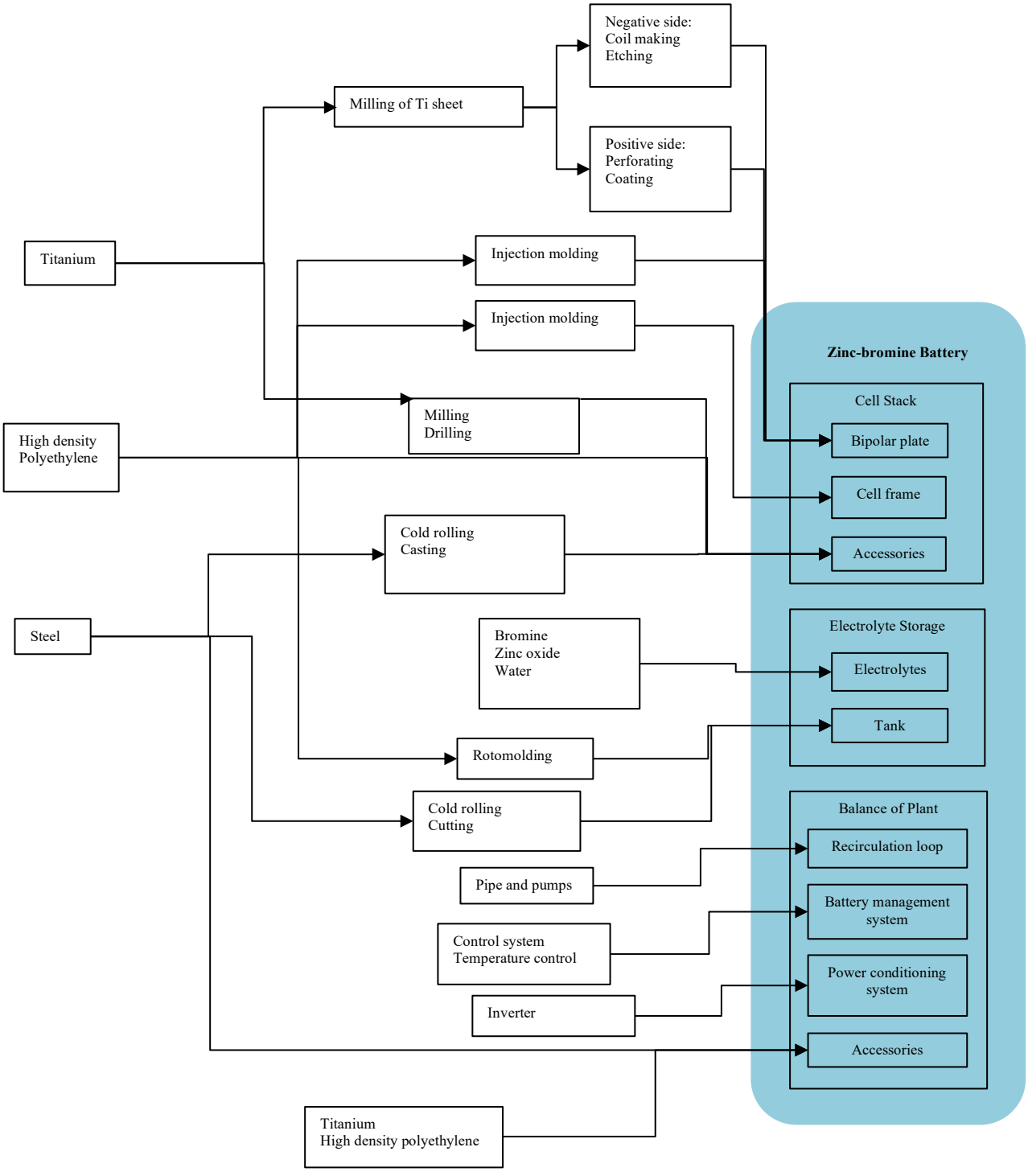

Figure A2. The process flow diagram for producing a zinc-bromine flow battery.

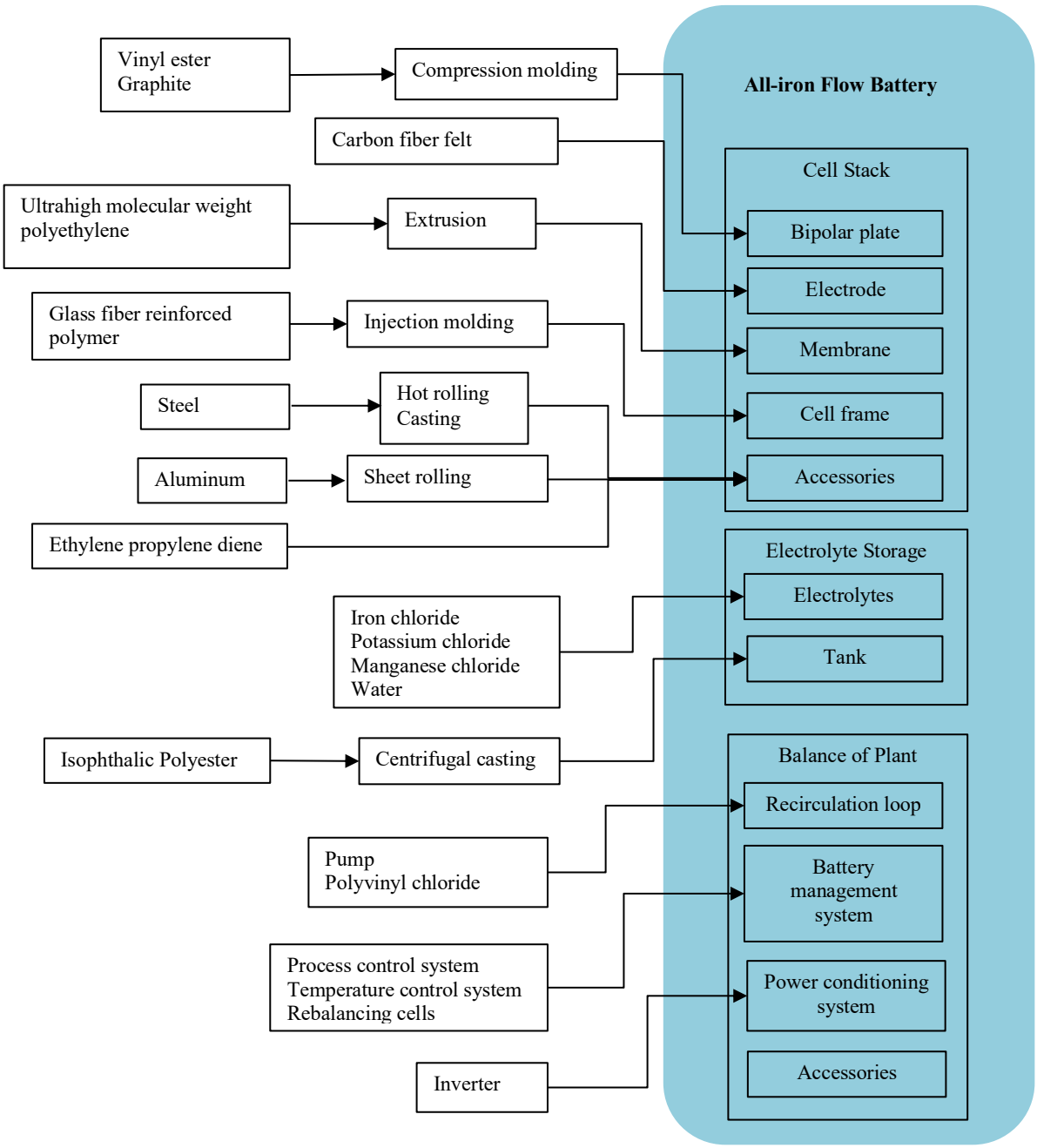

Figure A3. The process flow diagram for producing an all-iron flow battery.

APPENDIX B: Life Cycle Inventory of Flow Batteries Production

The constructed life cycle inventory (LCI) is organized based on the three subsystems categorized as cell stack, electrolyte storage and balance of plant. The cell stack (CS) is assembled from several single cells and supporting structures. Each single cell often consists of bipolar plate, electrode, membrane and cell frame [1]. The electrolyte storage (ES) includes the electrolyte, which is stored in tanks. The balance of plant (BOP) includes the peripheral components such as recirculation loops, battery management system (BMS), power conditioning system (PCS) and other accessories [1]. Due to the variations in system design, the components and accessories can be different in different flow batteries. The original LCI information was sourced from three manufacturers; and the Ecoinvent Database Version 3.4 was used as the characterization data source [2]. As the regional or country-specific data may not be found in Ecoinvent for the manufacturing processes, the rest of world (RoW) and global (GLO) data are used as substitutions. If required data are not found in Ecoinvent, the most relevant and recent LCA studies in the academic and industrial literature were used for references.

B1.1 Cell Stack

B1.1.1 Bipolar Plate

The bipolar plate is the critical component in the cell stack which provides the structural support as well as serving as a conductor [3]. For a suitable bipolar plate, the materials used must maintain good stability and conductivity when exposed to the electrolyte. Thus, carbon-based materials such as graphite are often selected [4]. According to the manufacturers' specifications, the VRFB and IFB both apply graphite-based

compounds for the bipolar plate, while for the ZBFB, an integrated titanium-based bipolar plate is reported to be used. The detailed LCI information on the bipolar plate for the three flow batteries is provided in **Tables B1-B3**. One note on the ZBFB bipolar plate is that the processing methods for titanium (Ti) such as milling, drilling, coating and sheet rolling are not directly characterized in Ecoinvent. The LCI constructed for the titanium processing was therefore modified due to lack of information. For instance, the Ti removed by milling was modified on the basis of the Ecoinvent process for "aluminium removed by milling" [5] in which the impact is calculated for the metal residues peeled during the machining process, and a removal rate of 23% is assumed. Similarly, the Ti removed by drilling was modified on the basis of the Ecoinvent process "aluminium removed by drilling" [6] with a removal rate of 25%. The Ti coating process was modified on the basis of the "selective coat, stainless steel" [7] available in Ecoinvent due to lack of alternative information; hydrochloric and sulfuric acid were the etching agents considered. Lastly, the Ti sheet rolling was modified on the basis of the Ecoinvent process "sheet rolling, aluminium" [8].

Table B1. Inventory for 1 kg bipolar plate production for VRFB.

Process	Source	Amount	Unit
Unit Output			
VRFB Bipolar Plate		1	kg
Materials and Assemblies			
Graphite {RoW}| production	Ecoinvent	0.93	kg
Polyethylene, low density, granulate {RoW}| production	Ecoinvent	0.07	kg
Processes			
Thermoforming of plastic sheets {RoW}| processing	Ecoinvent	0.07	kg

Table B2. Inventory for 1 kg bipolar plate production for ZBFB[1].

Process	Source	Amount	Unit
Unit Output			
ZBFB Bipolar Plate		1	kg
Materials and Assemblies			
Polyethylene, high density, granulate {RoW}| production	Ecoinvent	0.52	kg
Titanium primary, triple-melt {GLO}| production	Ecoinvent	0.48	kg
Processes			
Ti removed by milling {RoW}| processing	Ecoinvent*	0.11	kg
Ti removed by drilling, conventional {RoW}| processing	Ecoinvent*	0.12	kg
Ti coating {RoW}| processing	Ecoinvent*	0.03	m^2
Ti sheet rolling {RoW}| processing	Ecoinvent*	0.48	kg
Injection molding {RoW}| processing	Ecoinvent	0.52	kg

[1] The * here means the data are not directly applied but modified on the basis of other processes included in Ecoinvent

Table B3. Inventory for 1 kg bipolar plate production for IFB.

Process	Source	Amount	Unit
Unit Output			
IFB Bipolar Plate		1	kg
Materials and Assemblies			
Graphite {RoW}| production	Ecoinvent	0.85	kg
Bisphenol A epoxy based vinyl ester resin {RoW}| production	Ecoinvent	0.15	kg
Processes			
Injection molding {RoW}| processing	Ecoinvent	1	kg

B1.1.2 Electrode

In this study, both VRFB and IFB use the carbon fiber felt as the electrode material, the LCI for which is shown in **Table B4**. Since the ZBFB integrates the electrode into the bipolar plate in their design, there is no extra information presented. For the production of carbon fiber felt, there are no existing LCI data included in the Ecoinvent Database, hence literature data were used. Carbon fiber felt is produced by a pyrolysis process with the use of polymer precursors such as the polyacrylonitrile (PAN) [9]. The LCI data extracted in our study are based on a study analyzing the carbon fiber manufacturing through several modeling processes, in which the raw felt production processes are represented by three primary steps: stabilization, carbonization and graphitization, with three auxiliary steps called stretching, cooling and spooling [10]. No other data for further texturing are included due to lack of information. The processing data for the production of 1 kg carbon felt are shown on **Table B5**. The production of PAN is derived from Weber et. al.'s [11] study, where the processing data for acrylonitrile are based on the Ecoinvent dataset "Sohio process" [12], and the polymerization process is approximated with the "polyacrylamide production" [11, 13]. Some of the uncertainties associated with the data for carbon fiber felt production are addressed.

Table B4. Inventory for 1 kg electrode production for VRFB and IFB.

Process	Source	Amount	Unit
Unit Output			
VRFB and IFB Electrode		1	kg
Materials and Assemblies			
Acrylonitrile, Sohio process {GLO}| production	Ecoinvent	1.72	kg
Polyacrylamide {GLO}| production	Ecoinvent	1.72	kg
Carbon fiber felt | production	Literature	1	kg

Table B5. The detailed inventory information on carbon fiber felt production [10].

Unit: 1 kg Carbon fiber felt production	
Input	**Amount**
Energy, unspecified	215 MJ
Polyacrylonitrile	1.72 kg
Air	206.19 kg
N_2	23.81 kg
Output	
CO_2 to air	2 kg
CO to air	0.05 kg
H_2O to water	0.41 kg
H_2 to air	0.02 kg
HCN to air	0.28 kg
NH_3 to air	0.08 kg
N_2 to air	184.80 kg
O_2 to air	43.14 kg
Ar to air	2.06 kg
Methane to air	0.03 kg

B1.1.3 Membrane

As an ideal membrane for flow battery, the selected materials should possess low permeability, high ionic conductivity, low persistence and good chemical stability [14, 15]. The LCI information for the membrane production on VRFB and IFB is shown in **Tables B6** and **B7**. Nafion®, a sulfonated fluorocarbon polymer, is currently the most widely applied membrane for flow batteries [9], which is implemented in our assessment of the VRFB system. There are very limited processing data disclosed for the production of Nafion® membrane, and our reference LCI is extracted based on a recent LCA study on VRFB with the data on transportation excluded [11]. Scenarios that consider alternative membrane materials to Nafion® are noted in the Chapter 3, Section 3.4.3. For the IFB, the membrane used is reported to be ultra-high-molecular-weight polyethylene, for which the production data are simulated from the production of high-density polyethylene [16] and extrusion of plastic film [17] using Ecoinvent. For ZBFB, there are no membranes required due to its specific design.

Table B6. Inventory for 1 kg membrane production for VRFB.

Process	Source	Amount	Unit
Unit Output			
VRFB Membrane		1	kg
Materials and Assemblies			
Nafion® membrane | production	Literature	1	kg

Table B7. Inventory for 1 kg membrane production for IFB.

Process	Source	Amount	Unit
Unit Output			
IFB Membrane		1	kg
Materials and Assemblies			
Polyethylene, high density, granulate {RoW}| production	Ecoinvent	1	kg
Processes			
Extrusion, plastic film {RoW}| production	Ecoinvent	1	kg

B1.1.4 Cell Frame

Each single cell is surrounded by the cell frame, which provides the supporting structure to house all of the components in a cell. The cell frames used in the three flow batteries are injection molded using either polymers or organic compounds. The LCI details are provided in **Tables B8-B10**.

Table B8. Inventory for 1 kg cell frame production for VRFB.

Process	Source	Amount	Unit
Unit Output			
VRFB Cell frame		1	kg
Materials and Assemblies			
Polypropylene, granulate {RoW}| production	Ecoinvent	0.8	kg
Glass fiber {RoW}| production	Ecoinvent	0.2	kg
Processes			
Injection molding {RoW}| processing	Ecoinvent	1	kg

Table B9. Inventory for 1 kg cell frame production for ZBFB.

Process	Source	Amount	Unit
Unit Output			
ZBFB Cell Frame		1	kg
Materials and Assemblies			
Polyethylene, high density, granulate {RoW}| production	Ecoinvent	1	kg
Processes			
Injection molding {RoW}| processing	Ecoinvent	1	kg

Table B10. Inventory for 1 kg cell frame production for IFB.

Process	Source	Amount	Unit
Unit Output			
IFB Cell Frame		1	kg
Materials and Assemblies			
Glass fiber reinforced plastic, polyester resin, hand lay-up {RoW}| production	Ecoinvent	1	kg
Processes			
Injection molding {RoW}| processing	Ecoinvent	1	kg

B1.1.5 Cell Stack Accessories

The accessories used in the cell stacks support the functionality of the flow batteries. Accessories include the current collector that ensures the uniform distribution of electric current, the gasket applied between each cell preventing the electrolytes from leakage, and other supporting frames such as the end plates, load spreaders, stack shells and other standard parts in order to mechanically stabilize the cell stacks and keep connectivity with

the electrolyte storage and balance of plant. **Tables B11-B13** present the LCI on the cell stack accessories for the three flow batteries.

Table B11. Inventory for 1 kg cell stack accessories production for VRFB.

Process	Source	Amount	Unit
Unit Output			
VRFB Cell Stack Accessories		1	kg
Materials and Assemblies			
Steel, unalloyed {RoW}| production	Ecoinvent	0.54	kg
Copper {RoW}| production	Ecoinvent	0.10	kg
Polyvinylchloride, bulk polymerized {RoW}| production	Ecoinvent	0.34	kg
Processes			
Sheet rolling, copper {RoW}| processing	Ecoinvent	0.10	kg
Thermoforming of plastic sheets {RoW}| processing	Ecoinvent	0.54	kg

Table B12. Inventory for 1 kg cell stack accessories production for ZBFB.

Process	Source	Amount	Unit
Unit Output			
ZBFB Cell Stack Accessories		1	kg
Materials and Assemblies			
Steel, unalloyed {RoW}| production	Ecoinvent	0.92	kg
Titanium primary, triple-melt {GLO}| production	Ecoinvent	0.04	kg
Polyethylene, high density, granulate {RoW}| production	Ecoinvent	0.04	kg
Processes			
Sheet rolling, steel {RoW}| processing	Ecoinvent	0.92	kg
Ti removed by milling {RoW}| processing	Ecoinvent*	0.01	kg
Ti removed by drilling, conventional {RoW}| processing	Ecoinvent*	0.01	kg

Table B13. Inventory for 1 kg cell stack accessories production for IFB.

Process	Source	Amount	Unit
Unit Output			
IFB Cell Stack Accessories		1	kg
Materials and Assemblies			
Steel, unalloyed {RoW}| production	Ecoinvent	0.94	kg
Aluminum, primary, ingot {RoW}| production	Ecoinvent	0.03	kg
Synthetic rubber {RoW}| production	Ecoinvent	0.03	kg
Processes			
Hot rolling, steel {RoW}| processing	Ecoinvent	0.94	kg
Sheet rolling, aluminum {RoW}| processing	Ecoinvent	0.03	kg

B1.2 Electrolyte Storage

B1.2.1 Electrolyte

As the core part that determines the energy capacity of the whole flow battery system, the electrolytes used in the selected three flow batteries each represent distinct reactions with different active species providing chemical energy during the redox process. In the VRFB system, the active material in its electrolyte is the vanadium pentoxide (V_2O_5); the additional hydrochloric acid (HCl) and sulfuric acid (H_2SO_4) are used to improve the solubility and stability of the vanadium ions in the electrolyte systems, which corresponds to the mixed-acid VRFB system described in Wang et al.'s [18] study. Though V_2O_5 plays an important role as the active material, there are no established LCI databases that have information on V_2O_5 production. According to our literature review, most of the V_2O_5 is produced as a by-product during the steel production process [19]. It is noted that the related reduction and electrolysis processes used to prepare the battery electrolyte for use in battery operation, such as discussed in the literature [20], are not included due to lack of specific data for industrial-scale production. The LCI on V_2O_5 production is collected based on a research paper published in the year 2015 referring to the production at an actual steel plant in Sichuan, China (CN-SC) [21] where the production of V_2O_5 is extracted as a by-product of the crude steel production process using vanadium titano-magnetite (VTM). After mining and dressing, the VTM concentrate obtained is partly mixed with coal, coke and limestone to produce the sinter ores while the rest of the material is mixed with bentonite to produce pellet ores. Both of them are put into blast furnace production of pig iron. After that, a desulphurization process is applied, and the pig iron is put into the basic oxygen furnace plant for crude steel production with the vanadium-bearing slag extracted for the

further vanadium pentoxide production. It is reported that for 1000 kg crude steel production, the required iron ore is 4533 kg and the associated vanadium-bearing slag output is 28 kg. The slag ultimately yields 2.395 kg vanadium pentoxide [21]. Based on this ratio, the relative vanadium concentration is calculated to be 1.28% without considering material loss. Our modeling LCI mostly focuses on the vanadium pentoxide production plant, while the materials and energy input for vanadium-bearing slag production (28 kg) is allocated from the steel making process based on the weight ratio compared to the production of crude oil (1000 kg), which indicates that only 2.72% of the impacts associated with the materials use and energy is considered. The related processing chain and resulting emissions of steel production is not modeled due to the lack of specific data. The details for the vanadium-containing slag and the vanadium pentoxide production LCI are provided in **Table B14** and **Table B15**. Alternative scenarios for vanadium pentoxide production are evaluated in the Chapter 3, Section 3.4.3.

For ZBFB, the reported electrolyte is a mixture of bromine and zinc bromide ($ZnBr_2$), which are stored in one tank as two layers due to density differences. There are no direct data for the production of $ZnBr_2$, instead, the processing chemicals bromine and zinc oxide are used based on stoichiometric calculations. The only active material in IFB is ferrous chloride, while the addition of potassium chloride and manganese chloride ($MnCl_2$) is used for electrolyte stabilization and pH control to avoid the formation and precipitation of ferric hydroxide and gas generated through side reactions. As no data can be found for the $MnCl_2$ production in Ecoinvent, the production process is replaced by the reaction of manganese dioxide and hydrochloric acid. The LCI details on the electrolyte production for all three flow batteries are presented in **Tables B16-B18**.

Table B14. The detailed inventory information on vanadium-bearing slag production.

Unit: 1 kg Vanadium-bearing slag	
Input	**Amount**
Electricity, high voltage {CN-SC}	0.24 kWh
Coal, feedstock, 26.4 MJ per kg	1.04 kg
Vanadium contained Iron ores (1.28% vanadium concentration)	4.41 kg
Limestone	0.40 kg
Clay, bentonite	0.0068 kg
Fluorspar	0.0060 kg

Table B15. The detailed inventory information on vanadium pentoxide production.

Unit: 1 kg Vanadium Pentoxide Production	
Input	**Amount**
Electricity, high voltage {CN-SC}	2.59 kWh
Vanadium-bearing slag	11.69 kg
Ammonium sulfate {RoW}| production	0.78 kg
Salt, unspecified	0.58 kg
Sulfuric acid {RoW}|production	0.69 kg
Soda ash {GLO}| production	1.49 kg
Output	
CO_2 to air	5.09 kg
SO_2 to air	0.02 kg
Dust to air	0.39 kg

Table B16. Inventory for 1 kg electrolyte production for VRFB.

Process	Source	Amount	Unit
Unit Output			
VRFB Electrolyte		1	kg
Materials and Assemblies			
Hydrochloric acid, in solution state {RoW}| production	Ecoinvent	0.05	kg
Sulfuric acid {RoW}| production	Ecoinvent	0.02	kg
Vanadium Pentoxide {CN-SC| production	Literature	0.2	kg
Water, deionised {RoW}| production	Ecoinvent	0.73	kg

Table B17. Inventory for 1 kg electrolyte production for ZBFB.

Process	Source	Amount	Unit
Unit Output			
ZBFB Electrolyte		1	kg
Materials and Assemblies			
Bromine {RoW}| production	Ecoinvent	0.45	kg
Zinc oxide {RoW}| production	Ecoinvent	0.11	kg
Water, deionized {RoW}| production	Ecoinvent	0.44	kg

Table B18. Inventory for 1 kg electrolyte production for IFB.

Process	Source	Amount	Unit
Unit Output			
IFB Electrolyte		1	kg
Materials and Assemblies			
Iron (II) chloride {GLO}| production	Ecoinvent	0.20	kg
Potassium chloride {RoW}| production	Ecoinvent	0.22	kg
Manganese dioxide {GLO}| production	Ecoinvent	0.01	kg
Hydrochloric acid, in solution state {RoW}| production	Ecoinvent	0.01	kg
Water, deionized {RoW}| production	Ecoinvent	0.56	kg

B1.2.2 Tank

The tank serves as the container for the electrolyte in the flow battery systems. **Tables B19-B21** provide the LCI for the tank production. The processing method for all three flow batteries should be rotomolding. However, no detailed production data on rotomolding can be found in Ecoinvent nor through literature review, thus the Ecoinvent data set "blow molding" was applied as a proxy [22].

Table B19. Inventory for 1 kg tank production for VRFB.

Process	Source	Amount	Unit
Unit Output			
VRFB Tank		1	kg
Materials and Assemblies			
Polyethylene, high density, granulate {RoW}| production	Ecoinvent	1	kg
Processes			
Blow molding {RoW}| processing	Ecoinvent	1	kg

Table B20. Inventory for 1 kg tank production for ZBFB.

Process	Source	Amount	Unit
Unit Output			
ZBFB Tank		1	kg
Materials and Assemblies			
Polyethylene, high density, granulate {RoW}| production	Ecoinvent	1	kg
Processes			
Blow molding {RoW}| processing	Ecoinvent	1	kg

Table B21. Inventory for 1 kg tank production for IFB.

Process	Source	Amount	Unit
Unit Output			
IFB Tank		1	kg
Materials and Assemblies			
Isophthalic acid based unsaturated polyester resin {RER}| production	Ecoinvent	1	kg
Processes			
Blow molding {RoW}| processing	Ecoinvent	1	kg

B1.3 Balance of Plant

With regard to balance of plant (BOP), some of the data provided by the manufacturers are based on material weight and some are based on power output or just number of units for the standard parts. Thus, we were unable to normalize the LCI into per kg output, hence the data provided below are organized as one unit installed in a given flow battery system. Also, due to the design variances, the data provided for BOP are very

different for each flow battery with high uncertainty and some of the data are hard to define explicitly since the manufacturers purchase these parts from other suppliers. Some of these uncertainties are addressed in the Chapter 3, Section 3.4.2.

B1.3.1 Recirculation Loops

The recirculation loops considered in this study include the pumps and pipes. The pumps are used to pump the electrolyte into the cells from the storage tank. In Ecoinvent, the reference data for 1-unit pump production indicates a water pump with 40 W power output [23]. Thus, the pumps installed in each flow battery are calculated based on the total power required for the pumping system, and the number needed is the total power divided by the reference value. According to the data provided by the manufacturer, the VRFB and ZBFB both use polyethylene as the pipe material, and for IFB, the material is reported to be polyvinylchloride. The reference process “extrusion, plastic pipes” [24] in Ecoinvent is applied as the processing method for pipe production. The detailed LCI for recirculation loops are provided in **Tables B22-B24**.

Table B22. Inventory for 1-unit recirculation loop production for VRFB.

Process	Source	Amount	Unit
Unit Output			
VRFB Recirculation Loop		1	p
Materials and Assemblies			
Polyethylene, high density, granulate {RoW}| production	Ecoinvent	66.64	kg
Processes			
Pump, 40 W {RoW}| production	Ecoinvent	82.40	p
Extrusion, plastic pipes {RoW}| processing	Ecoinvent	66.64	kg

Table B23. Inventory for 1-unit recirculation loop production for ZBFB.

Process	Source	Amount	Unit
Unit Output			
ZBFB Recirculation Loop		1	p
Materials and Assemblies			
Polyethylene, high density, granulate {RoW}| production	Ecoinvent	30.00	kg
Processes			
Pump, 40 W {RoW}| production	Ecoinvent	24.00	p
Extrusion, plastic pipes {RoW}| processing	Ecoinvent	20.00	kg
Blow molding {RoW}| production	Ecoinvent	10.00	kg

Table B24. Inventory for 1-unit recirculation loop production for IFB.

Process	Source	Amount	Unit
Unit Output			
IFB Recirculation Loop		1	p
Materials and Assemblies			
Polyvinylchloride, bulk polymerized {RoW}| production	Ecoinvent	230.00	kg
Processes			
Pump, 40 W {RoW}| production	Ecoinvent	37.50	p
Extrusion, plastic pipes {RoW}| processing	Ecoinvent	230.00	kg

B1.3.2 Battery Management System

The battery management system (BMS) plays an important role in the flow battery system, and in our study, the BMS considered includes the process control system and thermal management system. The data for the BMS in each flow battery tend to be very different based on the manufacturer's specifications. In VRFB, several metals are reported to be used as the fan and heat exchanger for the thermal management system; the processing methods for those metals are not disclosed so the standard processes for metal working in Ecoinvent are utilized here. Additionally, there are electronics used as the process control system, which includes printed wiring board, cable and control units. For ZBFB, the thermal management system including the heat exchanger and fan and the process control system including cables and sensors are provided by the materials breakdown as steel, aluminum and copper. This information is acknowledged to be an approximation, and the processing methods for these metals are approximated using "metal working" in Ecoinvent. In IFB, the process control system is described by parts, some of which can be directly found in

Ecoinvent such as printed wiring board, resistor and circuit. However, some parts like electrical conduit and relay are not collected in Ecoivent; instead, the processes "chromium steel pipe" [25] are used to replace the conduit and "brass production" [26] and "wire drawing, copper" [27] are used to replace relay. In addition, carbon fiber felt is used as a rebalancing cell in the thermal management system while no other components for thermal management are reported. The detailed LCI information used for the battery management system for the three flow batteries is provided in **Tables B25-B27**.

Table B25. Inventory for 1-unit battery management system production for VRFB.

Process	Source	Amount	Unit
Unit Output			
VRFB Battery Management System		1	p
Materials and Assemblies			
Aluminum, primary, ingot {RoW}| production	Ecoinvent	133	kg
Printed wiring board, for power supply unit, Pb containing {GLO}| production	Ecoinvent	30	kg
Titanium primary, triple-melt {GLO}| production	Ecoinvent	50	kg
Electronics, for control units {RoW}| production	Ecoinvent	50	kg
Cable, unspecified {GLO}| production	Ecoinvent	20	kg
Processes			
Metal working, average for aluminum product {GLO}| processing	Ecoinvent	133	kg
Metal working, average for metal product {GLO}| processing	Ecoinvent	50	kg
Sheet rolling, aluminum {RoW}| processing	Ecoinvent	133	kg

Table B26. Inventory for 1-unit battery management system production for ZBFB.

Process	Source	Amount	Unit
Unit Output			
ZBFB Battery Management System		1	p
Materials and Assemblies			
Aluminum, primary, ingot {RoW}| production	Ecoinvent	20	kg
Steel, unalloyed {RoW}| production	Ecoinvent	20	kg
Copper {RoW}| production	Ecoinvent	20	kg
Processes			
Metal working, average for aluminum product {GLO}| processing	Ecoinvent	20	kg
Metal working, average for steel product {RoW}| processing	Ecoinvent	20	kg
Metal working, average for copper product {RoW}| processing	Ecoinvent	20	kg

Table B27. Inventory for 1-unit battery management system production for IFB.

Process	Source	Amount	Unit
Unit Output			
IFB Battery Management System		1	p
Materials and Assemblies			
Carbon fiber felt | production	Ecoinvent	100	kg
Printed wiring board, for power supply unit, Pb containing {GLO}| production	Ecoinvent	0.44	kg
Resistor, auxiliaries and energy use {GLO}| market	Ecoinvent	20	kg
Integrated circuit, logic type {GLO}| production	Ecoinvent	0.22	kg
Chromium steel pipe {GLO}| production	Ecoinvent	18	kg
Brass {RoW}| production	Ecoinvent	5	kg
Processes			
Wire drawing, copper {RoW}| processing	Ecoinvent	5	kg

B1.3.3 Power Conditioning System

The power conditioning system (PCS) converts the direct current power from the cell stacks into alternating current power for the flow battery to be applied on the grid and vice versa (*2*). The inverter is the major component in the PCS and is found in Ecoinvent [28]. The reference process for inverter production is based on power output of 500 kW, not weight. Thus, the number of inverters needed is normalized based on the power output of the flow battery system compared to the reference inverter in Ecoivent. The LCI data on PCS for the three flow batteries are not provided at the same level because of differences in the data provided by the manufacturers. For VRFB, there is an inner transformer and outer inverter used, as noted in **Table B28**. For ZBFB, details on the inverter are not provided as the

inverter is not installed inside this flow battery system but is an add-on, thus only the data on connectors using copper are provided as noted in **Table B29**. Table S30 provides the LCI information on PCS for IFB.

Table B28. Inventory for 1-unit power conditioning system for VRFB.

Process	Source	Amount	Unit
Unit Output			
VRFB Power Conditioning System		1	p
Materials and Assemblies			
Transformer, high voltage use {GLO}| production	Ecoinvent	66	kg
Inverter, 500 kW {GLO}| market	Ecoinvent	1	p

Table B29. Inventory for 1-unit power conditioning system for ZBFB.

Process	Source	Amount	Unit
Unit Output			
ZBFB Power Conditioning System		1	p
Materials and Assemblies			
Copper {RoW}| production	Ecoinvent	5	kg
Processes			
Wire drawing, copper {RoW}| processing	Ecoinvent	5	kg
Metal working, average for copper product {RoW}| processing	Ecoinvent	5	kg

Table B30. Inventory for 1-unit power conditioning system for IFB.

Process	Source	Amount	Unit
Unit Output			
IFB Power Conditioning System		1	p
Materials and Assemblies			
Inverter, 500 kW {GLO}| market	Ecoinvent	0.12	p

B1.3.4 Balance of Plant Accessories

The BOP accessories are other supplemental parts provided by the manufacturers that do not belong to the previous BOP components. The LCI on the accessories for VRFB is provided in **Table B31**, which include the steel and polyvinylfluoride used for shells and skids to support the BMS, pumps and stack cells. **Table B32** includes the LCI on the accessories for ZBFB; metals are reported to be used as the stack support for this battery system. No additional information on BOP accessories used for IFB were provided by the manufacturer.

Table B31. Inventory for 1-unit balance of plant accessories for VRFB.

Process	Source	Amount	Unit
Unit Output			
VRFB Balance of Plant		1	p
Materials and Assemblies			
Steel, unalloyed {RoW}| production	Ecoinvent	553	kg
Polyvinylfluoride {RoW}| production	Ecoinvent	26	kg
Processes			
Welding, arc, steel {RoW}| processing	Ecoinvent	188	m
Drawing of pipe, steel {RoW}| processing	Ecoinvent	274	kg
Powder coat, steel {RoW}| processing	Ecoinvent	25	m^2
Sheet rolling, steel {RoW}| processing	Ecoinvent	279	kg
Calendering, rigid sheet {RoW}| processing	Ecoinvent	26	kg

Table B32. Inventory for 1-unit balance of plant accessories for ZBFB.

Process	Source	Amount	Unit
Unit Output			
ZBFB Balance of Plant		1	p
Materials and Assemblies			
Steel, unalloyed {RoW}| production	Ecoinvent	210	kg
Aluminum, primary, ingot {RoW}| production	Ecoinvent	5	kg
Titanium primary, triple-melt {GLO}| production	Ecoinvent	5	kg
Processes			
Metal working, average for steel product {RoW}| processing	Ecoinvent	210	kg

Appendix B References

[1] Chalamala, B.R.; Soundappan, T.; Fisher, G.R.; Anstey, M.R.; Viswanathan, V.V.; Perry, M.L., 2014. Redox flow batteries: an engineering perspective. Proceedings of the IEEE. 102(6), 976-999.

[2] Wernet, G.; Bauer, C.; Steubing, B.; Reinhard, J.; Moreno-Ruiz, E.; Weidema, B., 2016. The ecoinvent database version 3 (part I): overview and methodology. The International Journal of Life Cycle Assessment [online]. 21(9), 1218–1230. Available at: http://link.springer.com/10.1007/s11367-016-1087-8 (accessed May 9, 2019).

[3] Park, M.; Jung, Y.J.; Ryu, J; Cho, J., 2014. Material selection and optimization for highly stable composite bipolar plates in vanadium redox flow batteries. Journal of Materials Chemistry A. 2(38), 15808-15815.

[4] Cunha, Á. Martins, J.; Rodrigues, N.; Brito, F.P., 2015. Vanadium redox flow batteries: a technology review. International Journal of Energy Research. 2015, 39(7),889-918.

[5] Steiner, R, 2007a. Aluminium milling, average, RoW, allocation, cut-off. Ecoinvent Database Version 3.4. Swiss Centre for Life Cycle Inventories: Dübendorf, Switzerland.

[6] Steiner, R., 2007b. Aluminium drilling, conventional, RoW, allocation, cut-off. Ecoinvent Database Version 3.4. Swiss Centre for Life Cycle Inventories: Dübendorf, Switzerland.

[7] Jungbluth, N, 2007a. Selective coating, stainless steel, black chrome, RoW, allocation, cut-off. Ecoinvent Database Version 3.4. Swiss Centre for Life Cycle Inventories: Dübendorf, Switzerland.

[8] Blaser, S, 2007a. Sheet rolling, aluminium, RoW, allocation, cut-off. Ecoinvent Database Version 3.4. Swiss Centre for Life Cycle Inventories: Dübendorf, Switzerland.

[9] Das, S., 2011. Life cycle assessment of carbon fiber-reinforced polymer composites. The International Journal of Life Cycle Assessment. 16(3), 268-282.

[10] Romaniw, Y. A., 2013.The relationship between light-weighting with carbon fiber reinforced polymers and the life cycle environmental impacts of orbital launch rockets. PhD Dissertation. Georgia Institute of Technology, Atlanta, GA.

[11] Weber, S.; Peters, J.F.; Baumann, M.; Weil, M., 2018. Life cycle assessment of a vanadium redox flow battery. Environmental science & technology. 52(18), 10864-10873.

[12] Autter, J., 2007. Sohio process, RoW, allocation, cut-off. Ecoinvent Database Version 3.4 Swiss Centre for Life Cycle Inventories: Dübendorf, Switzerland.

[13] Dussault, M., 2007.Polyacrylamide production, RoW, allocation, cut-off. Ecoinvent Database

[14] Prifti, H.; Parasuraman, A.; Winardi, S.; Lim, T.M.; Skyllas-Kazacos, M., 2012. Membranes for redox flow battery applications. Membranes. 2(2), 275-306.

[15] Schwenzer, B.; Zhang, J.; Kim, S.; Li, L.; Liu, J.; Yang, Z., 2011. Membrane development for vanadium redox flow batteries. ChemSusChem. 4(10), 1388-1406.

[16] Hischier, R., 2007a. Polyethylene production, high density, granulate, RoW, allocation, cut-off. Ecoinvent Database Version 3.4 Swiss Centre for Life Cycle Inventories: Dübendorf, Switzerland.

[17] Hischier, R., 2007b. Extrusion production, plastic film, RoW, allocation, cut-off. Ecoinvent Database Version 3.4. Swiss Centre for Life Cycle Inventories: Dübendorf, Switzerland.

[18] Wang, W.; Luo, Q.; Li, B.; Wei, X.; Li, L.; Yang, Z.,2013. Recent Progress in Redox Flow Battery Research and Development. Advanced Functional Materials. 23, 970-986

[19] Moskalyk, R.R.; Alfantazi, A.M., 2003. Processing of vanadium: a review. Minerals Engineering. 16(9), 793-805.

[20] Dassisti, M.; Cozzolino, G.; Chimienti, M.; Rizzuti, A.; Mastrorilli, P.; L'Abbate, P, 2016. Sustainability of vanadium redox-flow batteries: Benchmarking electrolyte synthesis procedures. Int. J. Hydrog. Energy. 17477-16488.

[21] Chen, S.; Fu, X.; Chu, M.; Liu, Z.; Tang, J., 2015. Life cycle assessment of the comprehensive utilisation of vanadium titano-magnetite. Journal of Cleaner Production. 101, 122-128.

[22] Hischier, R., 2007c. Blow moulding production, RoW, allocation, cut-off. Ecoinvent Database Version 3.4 Swiss Centre for Life Cycle Inventories: Dübendorf, Switzerland.

[23] Jungbluth, N., 2007b. Pump production, 40W, RoW, allocation, cut-off. Ecoinvent Database Version 3.4. Swiss Centre for Life Cycle Inventories: Dübendorf, Switzerland.

[24] Hischier, R., 2007d. Extrusion production, plastic pipes, RoW, allocation, cut-off. Ecoinvent Database Version 3.4. Swiss Centre for Life Cycle Inventories: Dübendorf, Switzerland.

[25] Treyer. K., 2007. Chromium steel pipe, RoW, allocation, cut-off. Ecoinvent Database Version 3.4. Swiss Centre for Life Cycle Inventories: Dübendorf, Switzerland.

[26] Althaus, H. J., 2007. Brass production, RoW, allocation, cut-off. Ecoinvent Database Version 3.4. Swiss Centre for Life Cycle Inventories: Dübendorf, Switzerland.

[27] Blaser, S, 2007a. Sheet rolling, aluminium, RoW, allocation, cut-off. Ecoinvent Database Version 3.4. Swiss Centre for Life Cycle Inventories: Dübendorf, Switzerland.

[28] Tuchschmid, M., 2007. Inverter production, 500 kW, RoW, allocation, cut-off. Ecoinvent Database Version 3.4. Swiss Centre for Life Cycle Inventories: Dübendorf, Switzerland.

APPENDIX C: Environmental Impact Assuming the Harmonized System Boundary

C1. The LCI and LCIA on Modified System Boundary

Because of the variations in data level provided by the manufacturers for the BOP and the accessories (as noted above in Section B1.3), sensitivity to the assumed system boundary is evaluated in the Section 3.4.2 in Chapter 3. The details are provided here. The modification of the flow battery system boundary includes two steps, the first step is to simply subtract the cell stack and BOP accessories, which are not core functional components for the flow batteries and will vary with changes in design parameters. The second step is to modify the BOP components, specifically the BMS and PCS, to make sure the LCI of the three flow batteries correspond to the same level of detail, which is necessary because the data provided by the three manufacturers take into account different classes of components (see **Table 3.1** in Chapter 3). For BMS, the process control system in ZBFB, for which the data was broken down by material, is changed to a component-based breakdown, as was provided for VRFB and IFB, and was then assessed using the standard electronic parts in Ecoinvent. Also, the thermal management system for all three flow batteries is removed, because the data provided by the three manufactures are not at the same level for comparison. For the PCS, the inner transformer in VRFB is removed as the ZBFB and IFB data did not include this component. Also, the inverter in ZBFB is replaced with the standard process "inverter, 500 kW" [1] from Ecoinvent normalized to the power output for ZBFB. The details on the modification of the LCI with respect to the BOP components for the three flow batteries are provided in **Table C1**.

Table C1. Changes to LCI for the modified balance of plant system for the three flow batteries.

	Before	After
Battery management system (BMS)		
VRFB	• Aluminum, primary, ingot {RoW}| production 133 kg • Printed wiring board, for power supply unit, Pb containing {GLO}| production 30 kg • Titanium primary, triple-melt {GLO}| production 50 kg • Electronics, for control units {RoW}| production 50 kg • Cable, unspecified {GLO}| production 20 kg • Metal working, average for aluminum product {GLO}| processing 133 kg • Metal working, average for metal product {GLO}| processing 50 kg • Sheet rolling, aluminum {RoW}| processing 133 kg	• Printed wiring board, for power supply unit, Pb containing {GLO}| production 30 kg • Electronics, for control units {RoW}| production 50 kg • Cable, unspecified {GLO}| production 20 kg
ZBFB	• Aluminum, primary, ingot {RoW}| production 20 kg • Steel, unalloyed {RoW}| production • Copper {RoW}| production 20 kg • Metal working, average for aluminum product {GLO}| processing 20 kg • Metal working, average for steel product {RoW}| processing 20 kg • Metal working, average for copper product {RoW}| processing 20 kg	• Electronics, for control units {RoW}| production 10 kg • Cable, unspecified {GLO}| production 10 kg • Printed wiring board, for power supply unit, Pb containing {GLO}| production 20 kg
IFB	• Carbon fiber felt | production 100 kg • Printed wiring board, for power supply unit, Pb containing {GLO}| production 0.44 kg • Resistor, auxiliaries and energy use {GLO}| market 20 kg • Integrated circuit, logic type {GLO}| production 0.22 kg • Chromium steel pipe {GLO}| production 18 kg • Brass {RoW}| production 5 kg • Wire drawing, copper {RoW}| processing 5 kg	• Printed wiring board, for power supply unit, Pb containing {GLO}| production 0.44 kg • Resistor, auxiliaries and energy use {GLO}| market 20 kg • Integrated circuit, logic type {GLO}| production 0.22 kg • Chromium steel pipe {GLO}| production 18 kg • Brass {RoW}| production 5 kg • Wire drawing, copper {RoW}| processing 5 kg
Power conditioning system (PCS)		

VRFB	• Transformer, high voltage use {GLO}| production 66 kg • Inverter, 500kW {GLO}| market 1p	• Inverter, 500kW {GLO}| market 1p
ZBFB	• Copper {RoW}| production 5 kg • Wire drawing, copper {RoW}| processing 5 kg • Metal working, average for copper product {RoW}| processing 5 kg	• Inverter, 500kW {GLO}| market 0.05 p
IFB	• Inverter, 500 kW {GLO}| market 0.12p	• Inverter, 500 kW {GLO}| market 0.12p

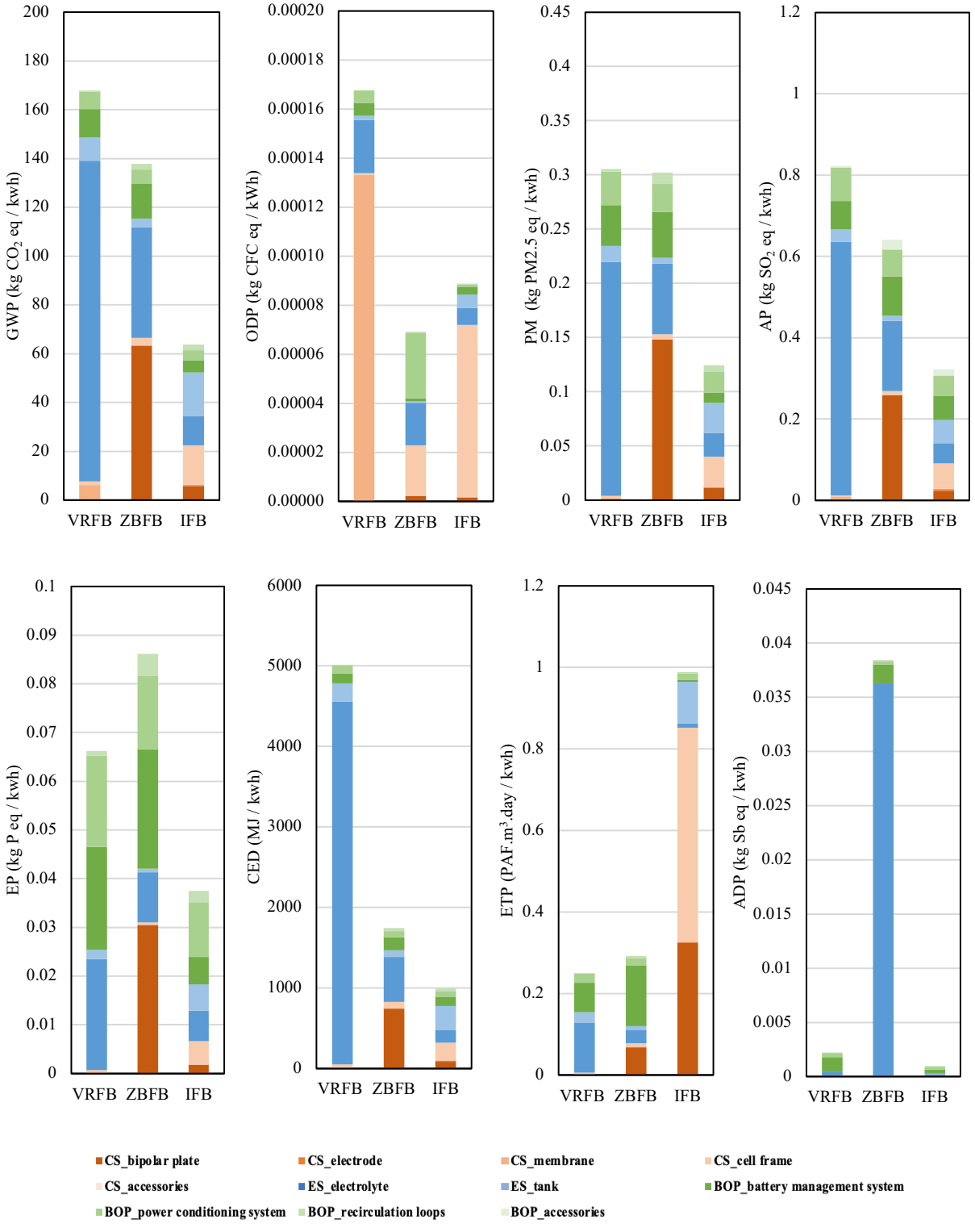
GWP (kg CO_2 eq / kwh)
ODP (kg CFC eq / kWh)
PM (kg PM2.5 eq / kwh)
AP (kg SO_2 eq / kwh)
EP (kg P eq / kwh)
CED (MJ / kwh)
ETP (PAF.m^3.day / kwh)
ADP (kg Sb eq / kwh)
VRFB ZBFB IFB
CS_bipolar plate
CS_electrode
CS_membrane
CS_cell frame
CS_accessories
ES_electrolyte
ES_tank
BOP_battery management system
BOP_power conditioning system
BOP_recirculation loops
BOP_accessories

Figure C1. The environmental impact of flow battery production, assuming the harmonized system boundary. Flow battery types include: VRFB = vanadium redox flow battery; ZBFB = zinc-bromine flow battery; and IFB = all-iron flow battery. Flow battery components include: cell stack (CS), electrolyte storage (ES) and balance of plant (BOP).

Appendix C References

[1] Tuchschmid, M., 2007. Inverter production, 500 kW, RoW, allocation, cut-off. Ecoinvent Database Version 3.4. Swiss Centre for Life Cycle Inventories: Dübendorf, Switzerland.

APPENDIX D: Sensitivity Analysis on Membrane and Carbon Fiber Felt Production

D1. Scenario Analysis for Materials Use

Three different core materials used in the battery systems are selected for the scenario analysis to explore the uncertainties associated with the data available for evaluating materials in the battery systems. Alternative processing routes for the V_2O_5 used in the VRFB electrolyte are explored; another membrane material called Daramic® [1-3] is evaluated as an alternative to Nafion® [2-4, 5]; and three alternative processing routes for carbon fiber felt used as electrodes in VRFB and IFB are evaluated.

D1.1 The Detailed Information for V_2O_5 Scenario Analysis

Five different processing routes for V_2O_5 production are considered for the scenario analysis. Scenario A1 and A2 represent the V_2O_5 produced as a by-product from the steel slag during the steel manufacturing process. The data on Scenario A1 is our baseline scenario derived from real production data taken at a blast furnace steel plant at PAN Steel located in China, Sichuan [6]; details are provided in Section B1.2.1, Tables B14-B15. Scenario A2 refers to the V_2O_5 production in a South Africa mining plant [5] for which the V_2O_5 production from vanadium-bearing slag is simulated using literature data. The data for Scenario A2* add up the allocated impact from the steel production using monetary allocation rule, for which the data are modified step-by-step starting from the mining, electric arc furnace steel production, vanadium-bearing slag production to V_2O_5 production based on Ecoinvent. Though all three of these scenarios are based on V_2O_5 being produced as a by-product of steel production, the processing routes, production conditions such as the ore concentrations, product yield and energy loss due to inefficiency considered for these scenarios vary.

Scenarios A3 and A4 use data on V_2O_5 production assuming it is made from crude oil burning residue; these data are provided from ESU – services, a sustainability consulting company in Germany [7]. Scenario A3 is based on the detailed production data of an oil plant through questionnaire, and Scenario A4 is based on the stoichiometric calculations with estimated electricity use [7]. The allocated impacts from crude oil processing are not considered as no further data on the extraction of crude oil and the burning in power plant are provided. We collected the LCI data for these five scenarios based on an up-to-date literature review. It should be noted that the scenario analysis presented here is different than conventional sensitivity analysis used in LCA studies, which focus on the same manufacturing process but variable production parameters. Rather, the LCI data collected for these scenarios are extracted from different studies, which means each scenario is completely independent of each other. This is also the case for the next scenario analysis on Nafion® and Daramic® membranes and carbon fiber felt production.

D1.2 The Detailed Information for Membrane Materials Scenario Analysis

Based on the literature data [5], we found the raw processing or intermediate materials used to produce the Nafion® membrane are tetrafluoroethylene, trichloromethane, and chlorodifluoromethane, which are or contain ozone depleting materials. Hence, the use of different membranes for the flow battery system with less ozone depleting materials is worthy of exploration. Here we propose Scenarios B1 and B2, which correspond to the LCI information for the production of two different membrane materials: B1 for Nafion® and B2 for Daramic®. The data for Scenario B1 is derived from an up-to-date LCA study on VRFB, which is also used in our baseline LCIA [5] (see also Section B1.1.3). For

Scenario B2, the composition of the Daramic® is assumed to be a combination of polyethylene (45 wt%) and silica (55 wt%) [1]; the related energy consumption and facility utilization values are modified from the Ecoinvent data set "battery separator production" [8].

D1.3 The Detailed Information for Carbon Fiber Felt Scenario Analysis

In this analysis, Scenario C1 is our baseline scenario with detailed data extracted from a modeling approach that assumes polyacrylonitrile (PAN) as the precursor (see Section SB.1.2)). Scenario C2 is also PAN-based but uses estimated data based on the information provided by SGL Carbon SE, one of the main suppliers of felt electrodes [9]. The data source for Scenario C3 is also based on the information provided by SGL Carbon SE [9], but the carbon fiber felt is biogenic rayon-based using cellulose as the precursor. In Scenario C2, the process flow for the carbon fiber felt produced from the PAN includes the 'Sohio' process, polymerization and fiber spinning, dry felting, stabilization, carbonization and graphitization. To make sure the data used are comparable with Scenario C1, the fiber spinning process is ignored due to lack of information, and the required Sohio process is adapted from the "Sohio process" [10] in Ecoinvent, and the polymerization is replaced by the Ecoinvent data set for "polyacrylamide production" [11], which is consistent with the assumptions made in Scenario C1. However, the reported energy use and materials use for the carbon fiber felt production in Scenario C2 are different from Scenario C1, as noted in Table D1. For Scenario C3, the process flow for carbon fiber using cellulose as a precursor is reported to be pulp production, viscose process, fiber spinning, dry felting, stabilization, carbonization and graphitization. The production of cellulose as a raw material, and sulfuric

acid and caustic soda as processing materials are simulated using Ecoinvent, whereas the rest of the processes are simulated based on the data provided in the literature, see Table D2 [9].

Table D1. The detailed inventory information on carbon fiber felt production based on Scenario C2 [9].

Unit: 1 kg Carbon fiber felt production	
Input	**Amount**
Heat, natural gas	342 MJ
Heat, other than natural gas	24 MJ
Electricity	2.9 kWh
Polyacrylonitrile	1.90 kg
Methyl methacrylate	0.1 kg

Table D2. The detailed inventory information on carbon fiber felt production based on Scenario C3 [9].

Unit: 1 kg Carbon fiber felt production	
Input	**Amount**
Heat, natural gas	389 MJ
Heat, other than natural gas	8 MJ
Electricity, from biomass	144 MJ
Cellulose fiber	4 kg
Sulfuric acid	3.2 kg
Sodium hydroxide	2.4 kg
Carbon disulfide	0.036 kg

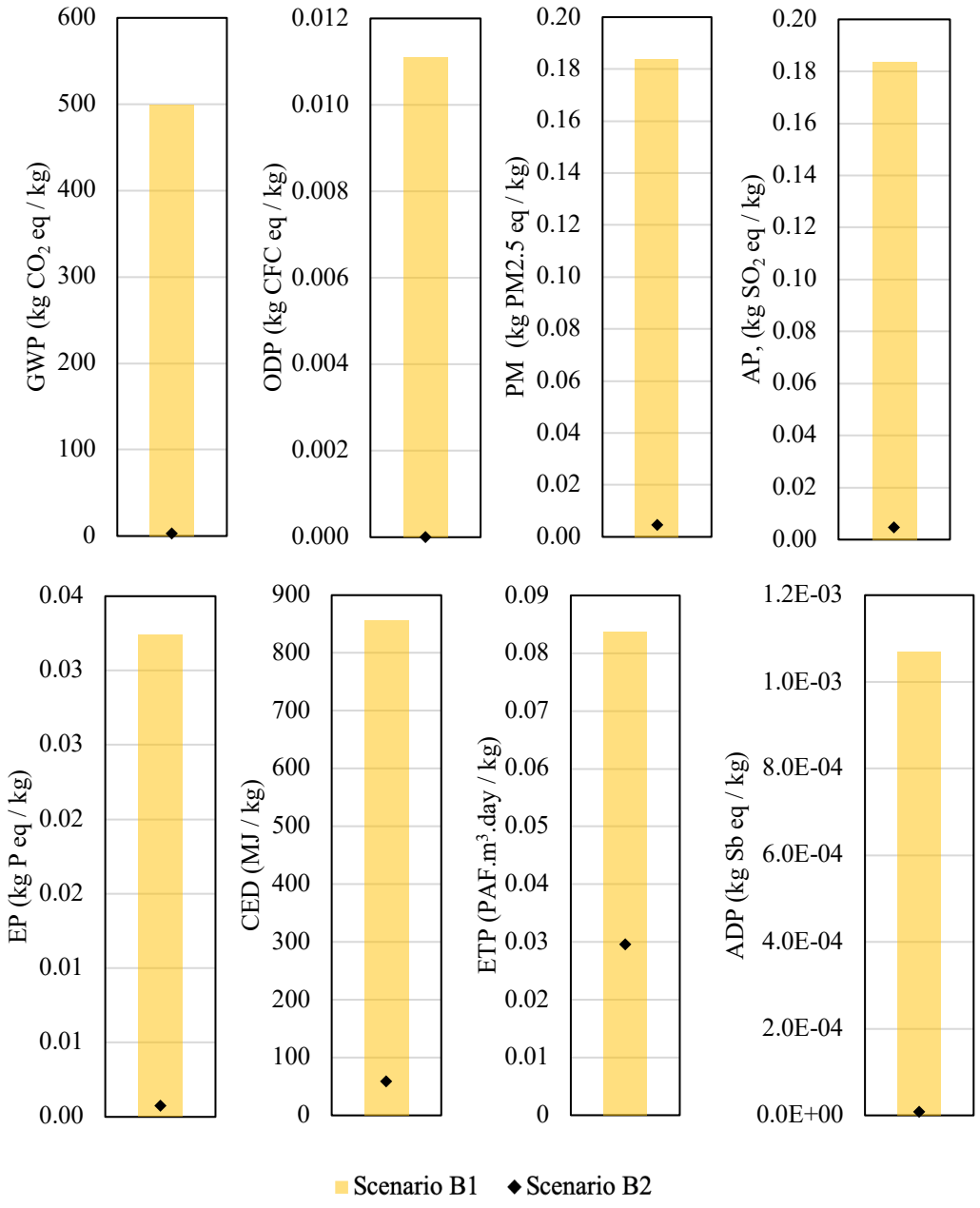

Figure D1. The environmental impact per kg of material, for Nafion® and Daramic® membrane production.

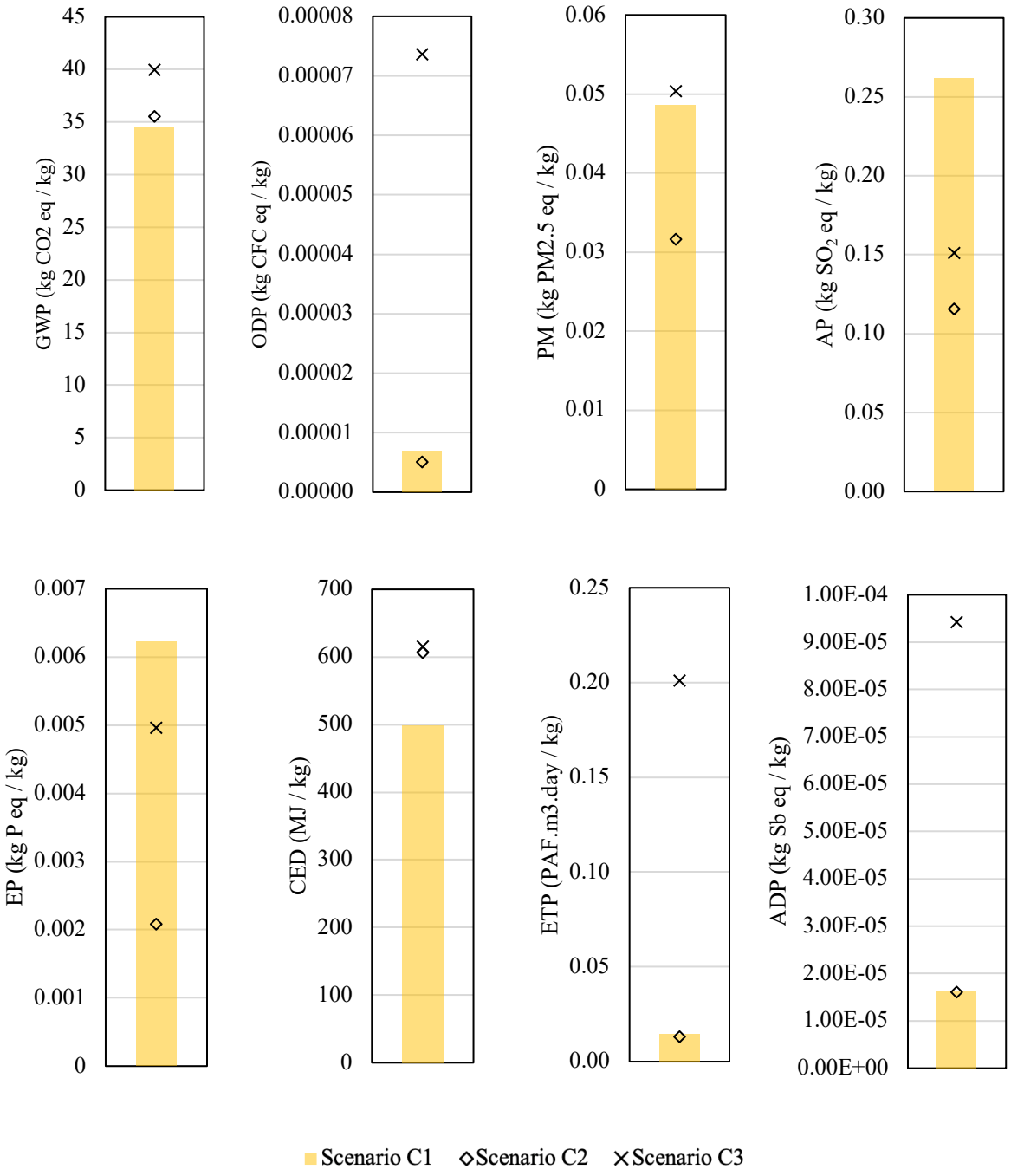

Figure D2. The environmental impact per kg of material, for carbon fiber felt production assuming various production scenarios.

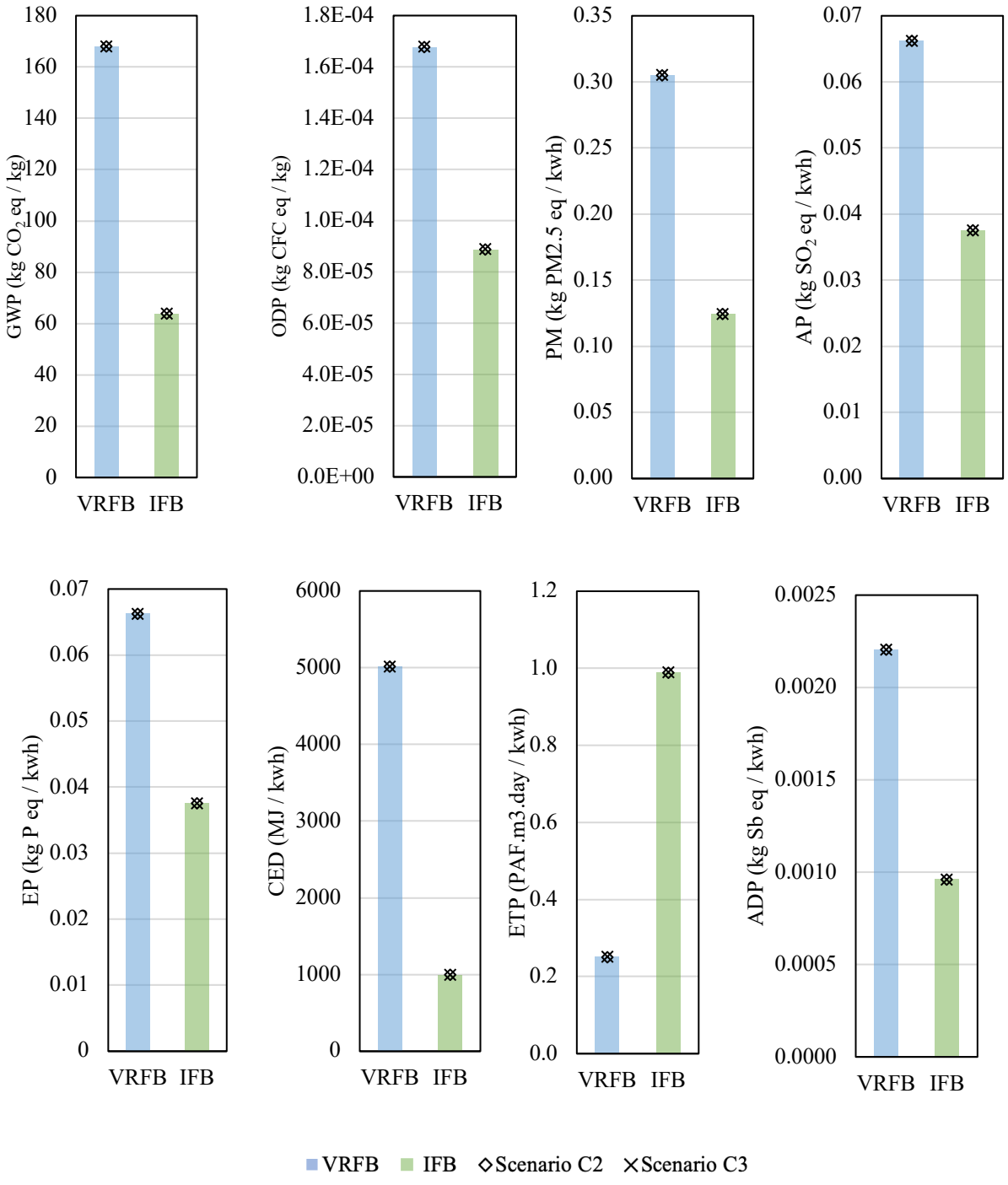

Figure D3. The environmental impact associated with VRFB and IFB production, assuming various scenarios for carbon fiber felt production.

Appendix D References

[1] Mohammadi, T.; Skyllas-Kazacos, M., 1995. Characterization of novel composite membrane for redox flow battery applications. Journal of Membrane Science. 98(1-2), 77-87

[2] Prifti, H., Parasuraman, A.; Winardi, S.; Lim, T.M.; Skyllas-Kazacos, M., 2012. Membranes for redox flow battery applications. Membranes. 2(2), 275-306

[3] Schwenzer, B.; Zhang, J.; Kim, S.; Li, L.; Liu, J.; Yang, Z., 2011. Membrane development for vanadium redox flow batteries. ChemSusChem. 4(10), 1388-1406

[4] Banerjee, S.; Curtin, D.E., 2004. Nafion® perfluorinated membranes in fuel cells. Journal of Fluorine Chemistry. 125(8), 1211-1216

[5] Weber, S.; Peters, J.F.; Baumann, M.; Weil, M., 2018. Life cycle assessment of a vanadium redox flow battery. Environmental science & technology. 52(18), 10864-10873

[6] Chen, S.; Fu, X.; Chu, M.; Liu, Z.; Tang, J., 2015. Life cycle assessment of the comprehensive utilisation of vanadium titano-magnetite. Journal of Cleaner Production. 101, 122-128

[7] Jungbluth, N.; Eggenberger S. Life Cycle Assessment for Vanadium Pentoxide (V_2O_5) from secondary resources. ESU-services Ltd. http://esu-services.ch/data/abstracts-of-lcis/#c154 (accessed November 11, 2018)

[8] Notter, D., 2007. Battery separator production, RoW, allocation, cut-off. Ecoinvent Database

[9] Minke, C.; Kunz, U.; Turek, T., 2017. Carbon felt and carbon fiber – A techno-economic assessment of felt electrodes for redox flow battery applications. Journal of Power Sources. 342, 116-124

[10] Autter, J., 2007. Sohio process, RoW, allocation, cut-off. Ecoinvent Database Version 3.4 Swiss Centre for Life Cycle Inventories: Dübendorf, Switzerland

[11] Dussault, M., 2007.Polyacrylamide production, RoW, allocation, cut-off. Ecoinvent Database Version 3.4 Swiss Centre for Life Cycle Inventories: Dübendorf, Switzerland

APPENDIX E: Processing Chemicals for Flow Batteries and Lithium-ion Batteries

In order to assess polymers and composites with no available information, we expanded the system boundary by including the processing chemicals or compositional chemicals used in the production chain. By doing that, the life cycle thinking is also integrated as the targeted chemicals are not only associated with the assembly and use of flow battery anymore, but the related materials used during the manufacturing stage are also considered. Based on the capability of ecoinvent for providing extensive data on up-stream chemicals and review on pertinent research articles and industry reports, the primary materials could be expanded for further assessment are provided in the following. It should be noted that the boundary of processing chemicals included is cut to not contain chemicals used for basic production activities such as mineral extraction and petroleum refining. Since almost all the industrial materials are produced from those elementary processes, there is no much sense to add those chemicals for comparison in this part of analysis. Also, it is observed that several chemicals are actually by-products from other production activities, thus the processing chemicals are not considered if they are not pertinent to the production of by-products. In addition, we collected extra quantitative information for the production of vital materials correlated with the battery functional performance such as electrolyte chemicals for RFBs and cathode active materials for LIBs. By doing that, we were able to highlight the weight of hazardous processing chemicals used to manufacture those core materials that can't be missed or replaced during the battery production process.

In this study, different electrolyte active chemicals are used as vital materials corresponding to each of the three RFBs technologies. For example, the vanadium pentoxide is the essential active material used in the vanadium redox flow battery (VRFB) system. In

most cases, vanadium pentoxide (V_2O_5) is a typical by-product of the steel manufacturing process as it is produced from the vanadium-bearing slag seen as residue after steel is made from vanadium-abundant iron ores [ref]. We only considered processing chemicals required to produce V_2O_5 from vanadium-bearing slag as chemicals used for iron ores mining and steel making is without scope. According to the paper published by Chen et al. [1], processing chemicals required for the production of 1 kg V_2O_5 include ammonium sulfate ($(NH_4)_2SO_4$, 0.78 kg), sulfuric acid (H_2SO_4, 0.69 kg) and soda ash (Na_2CO_3, 1.49 kg). As the active material used in the zinc-bromine flow battery (ZBFB) system, zinc bromide is produced from zinc oxide (ZnO, 0.36 kg) mixing with bromine (Br_2, 0.71 kg), while the relative weight use is comprised based on the stoichiometric calculation due to no available publicly data. The production of Br_2 is extracted from bromine-containing liquors (brines) in which the chlorine (Cl_2) is used as an oxidant to ease the bromine and the H_2SO_4 is used to maintain the pH value. According to ecoinvent, the production of 1 kg bromine requires the use of 0.6 kg chlorine and 0.0565 kg H_2SO_4 [2]. For IFB, the active chemicals such as ferrous chloride ($FeCl_2$) and potassium chloride (KCl) used in the electrolytes are basic chemicals which are not further expanded to include processing chemicals. However, manganese dioxide (MnO_2), which is mixed with hydrochloric acid (HCl) to balance the pH for the electrolytes, could be further expanded to have processing chemicals include manganese oxide (Mn_2O_3, 1.91 kg) and H_2SO_4 (1.19 kg) according to ecoinvent database [3].

In contrast to RFBs, the vital materials for LIBs are considered to be active chemicals used in the battery cathode. For example, lithium iron phosphate (LFP) is considered to be the active cathode material used in the LFP LIB system. According to the paper published by Majeau-Bettez et al. [4], to manufacture 1 kg of LFP, the associated processing chemicals

include lithium hydroxide (LiOH, 0.46 kg), phosphoric acid (H_3PO_4, 0.65 kg) and iron sulphate ($FeSO_4$, 1 kg), which the calculation is built from a processing model of hydrothermal synthesis assuming a 95% yield. Further, the production of 1 kg LiOH could be expanded to include processing chemicals such as lithium carbonate (Li_2CO_3,1kg) and calcium hydroxide ($Ca(OH)_2$, 0.44 kg) referred from ecoinvent database [5]. The Li_2CO_3 is prepared from the concentrated lithium-rich brine which processing chemicals for the production of 1 kg Li_2CO_3 are reported to be H_2SO_4 (0.04 kg), HCl (0.06 kg), calcium oxide (CaO, 0.18 kg) and sodium carbonate (Na_2SO_4, 3.73 kg) [6]. For lithium nickel cobalt manganese hydroxide (NCM) LIB, the production of NCM is in need of processing chemicals including LiOH (0.25 kg) and nickel cobalt manganese hydroxide ($Ni_{0.4}Co_{0.2}Mn_{0.4}(OH)_2$, 0.95 kg) [7]. In addition, the $Ni_{0.4}Co_{0.2}Mn_{0.4}(OH)_2$ could be produced using nickel sulphate ($NiSO_4$, 0.68 kg), cobalt sulphate ($CoSO_4$, 0.34 kg), manganese sulphate ($MnSO_4$, 0.66 kg) and sodium hydroxide (NaOH, 0.88 kg) [4]. No further expansion on $NiSO_4$ is considered because it is a by-product electrolytic copper refining. Similarly, processing chemicals used for the production of $CoSO_4$ is not included since it is a by-product from the nickel and copper leaching [4]. Lithium manganese oxide (LMO), the core material used in the LMO LIB system, is produced using manganese oxide (Mn_2O_3, 0.92 kg) and Li_2CO_3 (0.22 kg) as processing chemicals with reaction atmosphere transits from inert to oxidizing, thus nitrogen (N_2, 0.79 kg) and oxygen (O_2, 0.72 kg) are both needed during the manufacturing process [7].

In this section, we expanded our assessment to include processing chemicals for those primary materials that are not vital but used in the battery systems as many of them are polymers and composite materials where toxicity data are not available. While those primary materials are not core to the functional performance of the battery systems, the

purpose on assessing their correlated processing chemicals is to identify hazardous chemicals utilized through the battery production chain and seek opportunities on finding for safer alternatives.

- Polyethylene

Polyethylene (PE) is considered to be the simplest and most widely applied polymer in the industry, which is also the case for the six batteries assessed as all of them use PE for multiple purposes such as bipolar plate filler for VRFB, tank and pipe material for VRFB and ZBFB, and separator material for all the three LIBs. The PE is the polymer synthesized using ethylene as the monomer, which is considered as the compositional material for assessment. The reported conversion ratio from ethylene to PE is usually 1.03 for low-density PE and 1.05 for high-density PE [8].

- Polypropylene

As a commonly applied industrial polymer, the polypropylene (PP) is used as cell frame filler for VRFB and separator material for LFP and NCM. PP is the polymer synthesized using propylene as the monomer, which is considered as the compositional material for assessment. The reported conversion ratio from propylene to PP is 1.04 [8].

- Polyvinylchloride

The polyvinylchloride (PVC) is the polymer synthesized using vinyl chloride as the monomer, which is considered as pipe material for the IFB system instead of PE used in the VRFB and ZBFB systems. The reported conversion ratio from vinyl chloride to PVC is 1.03 [8]. Further processing chemicals used to synthesize the vinyl chloride are ethylene and Cl_2,

which for 1 kg of vinyl chloride production, the reported use of ethylene and Cl_2 are 0.49 kg and 0.6 kg [8].

- Glass fiber (E-glass)

The E-glass fiber is used as one of the doping materials for the bulk molding compound (BMC) in the cell frame of VRFB and IFB. According to the data provided by ASM international [9], the typical material compositions and weight ratio of its production are summarized as: silica (SO_2, 52-56%), CaO (21-23%), aluminium oxide (Al_2O_3, 12-15%), boron oxide (B_2O_3, 4-6%) and magnesium oxide (MgO, 0.4 – 4%). Those materials are categorized as the compositional materials for the E-glass fiber and are also assessed using GreenScreen® in this study.

- Carbon felt

The carbon felt itself used as electrode material in the VRFB and IFB systems is classified as a BM 3 chemical with only minor hazard identified. The production of the carbon felt is usually from the high temperature pyrolysis using organic precursors which the polyacrylonitrile (PAN) is among the most commonly applied ones. According to our literature review, for a production of 1 kg of carbon felt, the required use of PAN is estimated to be 2 kg [10]. Next, the polymerization of 1 kg PAN requires the use of acrylonitrile (0.95 kg) and methyl methacrylate (MMA, 0.05 kg), which both of them are complex synthetic organic compounds produced from other simpler organic matters. For example, the associated production of acrylonitrile is referred as the 'Sohio process' in ecoinvent which the production of 1 kg acrylonitrile needs 1.2 kg propylene, 0.507 kg ammonia (NH_3) and 0.0508 kg H_2SO_4 as materials input [11]. The data on the production of MMA is extracted

from the paper published by Andraos et al. [12] and the processing chemicals are hydrogen cyanide (HCN), acetone, H_2SO_4, and methanol. In addition, the processing chemicals used for the production of HCN are methane and NH_3 [12] and the acetone is produced from the oxidation of cumene which another co-product: phenol is also produced [13]. According to the ecoinvent database [14], regarding the production of 1 kg phenol as the unit (1 kg), the production volume of simultaneously formed acetone is 0.617 kg and the required cumene as major reactant is 1.34 kg. Further, the chain process of cumene (1 kg) synthesis demands the input of benzene (0.684 kg) and propylene (0.369 kg) as processing chemicals [15] and the production chain is not further expanded as the benzene and propylene are both products from petroleum refining process which the materials used in the complex but basic processing routes are out of scope.

- Nafion®

Nafion®, a class of sulfonated fluorocarbon polymers, is currently the most widely applied membrane material in fuel cells and RFBs. The production of Nafion® is created by DuPont™ in the late 1960s [16] while very few information is disclosed for its production till now. Based on the most recent LCA study on VRFB published by Weber et al. [17], the production of the Nafion® requires sodium trioxide (SO_3) and tetrafluoroethylene (TFE) to form the intermediate Fluorosulfonyldifluoro-acetyl (FDA). In parallel, one another intermediate texafluoropropylene (HFPO) is synthesized by using hexafluoropropene (HFP), sodium hypochlorite (NaOCl) and NaOH solutions as raw reactants. The FDA and HFPO are treated together with subsequent reactions to form Perfluoro-sulfonylethoxy propylene vinyl ether (PSEPVE) with the aid of sodium Na_2CO_3 and there are no further details could

be extracted for the associated chain reactions. The produced PSEPVE is one backbone chemical and it is used to react again with co-monomer TFE to form the Nafion®, the polymerization yield is assumed to be 90% while the weight ratio of these two monomers is yet to be disclosed. Based on the LCI data provided in this paper, the production of 1 kg Nafion® requires the materials input of 1.3 kg TFE, 0.5 kg SO_3, 3.2 kg HFP, 3.0 kg NaOH, 0.6 kg NaOH and 0.11 kg Na_2CO_3. The production volumes for the intermediates formed during the chain reaction processes are not able to be found.

- Bisphenol-A epoxy-based vinyl ester resin

The data provided by IFB manufacture specifies that the vinyl ester resin is used for the production of bipolar plate. The mostly used vinyl ester resin applied in the industry is the bisphenol-A (BPA) epoxy-based resin and it is viewed as the exact material used in IFB. The data for the production of the BPA epoxy-based vinyl ester resin is extracted from the ecoinvent database [18], the production of 1 kg reference product required multiple materials input such as the BPA (0.07 kg), epoxy resin (0.39 kg), methacrylic acid (MAA) (0.12 kg) and styrene (0.42 kg). Both of those materials can be dated back to up-stream materials production processes. For example, the production of BPA (1 kg) requires the input of phenol (0.838) and acetone (0.261) with the N_2, liquid (0.019 kg) added to assist with the reaction [19] and the related chain processes for the phenol and acetone production is mentioned above. The epoxy resin (1 kg) is produced using BPA (0.612 kg), epichlorohydrin (ECH, 0.273 kg), N_2, liquid (0.019 kg) and NaOH (0.112 kg) as raw materials input [20]. One of the processing chemical, ECH, is produced from allyl chloride and the materials requirement for 1 kg ECH production is documented to be 0.88 kg ally chloride,

0.868 Cl_2, and 0.693 kg CaO [21]. One another processing chemical used for the vinyl ester production is MAA. Based on the data extracted from ecoinvent [22], the production of 1 kg MAA requires the use of 0.787 kg acetone, 0.366 kg of HCN, 0.0258 kg of NaOH and 1.26 kg of H_2SO_4. The last processing chemical, styrene, (1 kg) is produced from benzene (0.774 kg), ethylene (0.278 kg) with the addition of N_2, liquid (0.038 kg) [23].

- Polyester resin

The polyester resin is one important polymer resin used as BMC for the production of the cell frame in the IFB via injection molding. For the production of polyester resin (1 kg), the acetic anhydride (0.1 kg), adipic acid (0.146 kg), ethylene glycol (0.192 kg), phthalic anhydride (0.592 kg) and propylene glycol (0.304 kg) are the processing materials reported to be used [24]. The first mentioned processing chemical, acetic anhydride (1 kg), is produced using acetic acid (1.27 kg) based on the ketene route [25] and the processing materials used to produce acetic acid (1 kg) are carbon monoxide (CO, 0.481 kg), methanol (0.54 kg) and N_2, liquid (0.019 kg) [26]. The second processing chemical, adipic acid (1 kg), is produced by the oxidation of a mixture of cyclohexane (0.73 kg) with nitric acid (HNO_3, 0.36 kg), and the extra processing materials required are NaOH (0.05 kg) and H_2SO_4 (0.08 kg) [27]. The third processing chemical, ethylene glycol (1 kg), is produced from the ethylene oxide (0.853 kg) by the oxidation of ethylene [28]. Similarly, the propylene glycol (1 kg) is produced from the propylene oxide (0.803 kg) by the use of propylene [29]. For the production of 1 kg propylene oxide, the required materials input are propylene (0.763 kg), Cl_2 (1.28 kg) and NaOH (1.38 kg) [30]. Lastly, the processing chemical phthalic anhydride (1

kg) is produced from the xylene (0.95 kg) [31] which is a by-product during the petroleum refining process.

- Isophthalic acid based unsaturated polyester resin

The isophthalic acid based unsaturated polyester resin is reported to be the storage tank material in the IFB system. According to eocinvent [32], the processing cheimcals required for isophthalic acid based unsaturated polyester resin (1 kg) are diethylene glycol (0.07 kg), maleic anhydride (0.16 kg), propylene glycol (0.2 kg), terephthalic acid (0.24 kg), styrene (0.4 kg) and N_2, liquid (0.0363 kg). The production of styrene and propylene glycol are mentioned in previous chemicals processing routes and the diethylene glycol is a by-product from the production of ethylene glycol which is also mentioned above. The maleic anhydride (1 kg) can be produced via several different processing routes and the method we selected here is based on the catalytic oxidation of benzene (1.14 kg) [33]. Lastly, the terephthalic acid (1 kg) is produced using xylene (0.661 kg), acetic acid (0.05 kg), NaOH (0.00145 kg) and N_2, liquid (0.0488 kg) [34].

- N-methtyl-2-pyrrolidone

Serving as the organic solvent used in the cathode and anode for the LFP and NCM LIBs, the N-methtyl-2-pyrrolidone is produced through the reaction of butyrolactone and dimethylamine [4]. The butyrolactone is produced industrially by dehydrogenation of butane-1,4-diol while further processing chemicals used to produce butane-1,4-diol include acetylene, formaldehyde and NaOH [35]. For dimethylamine, methanol and ammonia are processing chemicals required for its production according to ecoinvent [36].

- Lithium hexafluorophosphate

The lithium hexafluorophosphate ($LiPF_6$) is the most successfully commercialized and widely applied electrolyte materials for LIBs. In our case, all the three assessed LIBs use $LiPF_6$ as the electrolyte material which the processing materials required for its production are hydrogen fluoride (HF), lithium fluoride (LiF), phosphorus pentachloride (PCl_5), $Ca(OH)_2$ and N_2, liquid [37]. Further processing chemicals used for the LiF production include Li_2CO_3, HF and NH_3, liquid which the production of Li_2CO_3 was mentioned above. Another required processing chemical, PCl_5, the associated processing chemicals for its production are phosphorous trichloride (PCl_3) and Cl_2, liquid [38]. The production of PCl_3 could be further expanded to include processing chemicals such as phosphorus and Cl_2, liquid [39].

- 1,3-dioxlan-2-one

The 1,3-dioxlan-2-one, which is also called as ethylene carbonate, is widely utilized as the electrolyte solvent for LIBs. The production of 1,3-dioxlan-2-one requires the use of ethylene oxide to react with carbon dioxide, and the production of ethylene oxide uses ethylene to react with oxygen (O_2) [40].

- Polyvinyl fluoride

As the separator material used in the LMO battery system, the polyvinyl fluoride is polymerized using vinyl fluoride as the monomer [41], and further production of vinyl fluoride requires acetylene, zinc (Zn), HF and $Ca(OH)_2$ as processing chemicals [42].

- Hexafluoroethane

One another primary material used in the LMO separator, hexafluoroethane, is reported to be produced through the reaction of tetrafluoroethane with fluorine (F_2) [43]. In addition, the production of tetrafluoroethane could be dated back to the fluorination of trichloroethylene (TCE) with HF, while TCE is further produced through the chlorination of ethylene with Cl_2, gases, and NaOH and N_2, liquid are also needed through the reaction process [44].

Appendix E References

[1] Chen, S.; et al., 2015. Life cycle assessment of the comprehensive utilisation of vanadium titano-magnetite. J. Clean. Prod.101, 122-128.

[2] Sutter, J.; Wernet, G. E., 2007. coinvent 3.4 dataset documentation, bromine production.

[3] Notter, D.; Bauer, C., 2011. Ecoinvent 3.5 dataset documentation, manganese (III) oxide production.

[4] Majeau-Bettez, G.; Hawkins, T.R.; Strømman, A.H., 2011. Life cycle environmental assessment of lithium-ion and nickel metal hydride batteries for plug-in hybrid and battery electric vehicles. Environ. Sci. Technol. 45(10), 4548-4554.

[5] Sutter, J.; Wernet, G., 2011. Ecoinvent 3.5 dataset documentation, lithium hydroxide production.

[6] Notter, D.; Wernet, G., 2011. Ecoinvent 3.5 dataset documentation, lithium carbonate production, from concernitrated brine.

[7] Notter, D.A.; Gauch, M.; Widmer, R.; Wager, P.; Stamp, A.; Zah, R.; Althaus, H.J., 2010. Contribution of Li-ion Batteries to the Environmental Impact of Electric Vehicles. Environ. Sci. Technol. 44, 6550-6556.

[8] Petrochemical industry conversions, S&P Global Platts. Website: https://www.platts.com/IM.Platts.Content/MethodologyReferences/ConversionTables/Images/PTSS1015_Petrochemical_Industry_Conversions_LRG.pdf

[9] Wallenberger, F. T.; Watson, J. C.; Li, H., 2011 Glass fibers. Materials Park, OH: ASM International, 2001, 27-34.

[10] Minke, C.; Kunz, U.; Turek, T., 2017. Carbon felt and carbon fiber-A techno-economic assessment of felt electrodes for redox flow battery applications. J. Power Sources. 342, 116-124.

[11] Sutter, J.; Hischier, R., 2005. Ecoinvent 3.4 dataset documentation, Sohio process.

[12] Andraos, J., 2015. Complete green metrics evaluation of various routes to methyl methacrylate according to material and energy consumptions and environmental and safety impacts: test case from the chemical industry. ACS Sustain. Chem. Eng. 4.1, 312-323.

[13] PERP Program, 2007. Phenol/Acetone/Cumene News Report Alert, Nexant ChemSystems.

[14] Hischier, R.; Moreno-Ruiz, M., 2011 "Ecoinvent 3.4 dataset documentation, Phenol production, from cumene.

[15] Hischier, R.; Classen, E., 2011. Ecoinvent 3.4 dataset documentation, cumene production.

[16] Banerjee, S.; Curtin, D.E., 2004. Nafion® perfluorinated membranes in fuel cells. Journal of Fluorine Chemistry. 125(8), 1211-1216

[17] Weber, S.; Peters, J.F.; Baumann, M.; Weil, M., 2018. Life cycle assessment of a vanadium redox flow battery. Environmental science & technology. 52(18), 10864-10873.

[18] Bureau Veritas, E.; Johnson, E.; Moreno-Ruiz, E., 2013. Ecoinvent 3.4 dataset documentation, bisphenol A epoxy based vinyl ester resin production.

[19] Hischier, R.; Wernet, G., 2011. Ecoinvent 3.4 dataset documentation, bispenol A production, powder.

[20] Valsasina, L.; Moreno-Ruiz, M., 2013. Ecoinvent 3.4 dataset documentation, epoxy resin production.

[21] Chudacoff, M.; Jungbluth, N., 2011. Ecoinvent 3.4 dataset documentation, epichlorohydrin production from allyl chloride.

[22] Sutter, J.; Wernet, G., 2011. Ecoinvent 3.4 dataset documentation, methacrylic acid production.

[23] Valsasina, L.; Moreno-Ruiz, M., 2011. Ecoinvent 3.4 dataset documentation, styrene production.

[24] Hischier, R.; Kunst, H., 2011. Ecoinvent 3.4 dataset documentation, polyester resin production, unsaturated.

[25] Sutter, J.; Hischier, R., 2011.Ecoinvent 3.4 dataset documentation, aceti anhydride production, ketene route.

[26] Athaus, H. J.; Wernet, G., 2011. Ecoinvent 3.4 dataset documentation, acetic acid production, product in 98% solution state.

[27] Athaus, H. J.; Wernet, G., 2011. Ecoinvent 3.4 dataset documentation, adipic acid production.

[28] Chudacoff, M.; Kunst, H.; Wernet, G., 2011. Ecoinvent 3.4 dataset documentation, ethylene glycol production.

[29] Hischier, R.; Kunst, H., 2011.Ecoinvent 3.4 dataset documentation, propylene glycol production, liquid.

[30] Hischier, R.; Wernet, G.; Kunst, H.; 2011. Ecoinvent 3.4 dataset documentation, propylene oxide production, liquid.

[31] Hischier, R.; Kunst, H., 2011. Ecoinvent 3.4 dataset documentation, phthalic anhydride production.

[32] Etienne, B.; Veritas, E. J., E.; Moreno-Ruiz, E., 2011. Ecoinvent 3.4 dataset documentation, isophthalic acid based unsaturated polyester resin production.

[33] Chudacoff, M.; Kunst, H.; Wernet, G., 2011. Ecoinvent 3.4 dataset documentation, maleic anhydride production by catalytic oxidation of benzene.

[34] Hischier, R.; Classen, M., 2011. Ecoinvent 3.4 dataset documentation, purified terephthalic acid production.

[35] Sutter, J.; Hischier, R., 2011. Ecoinvent 3.4 dataset documentation, burane-1,4-diol production.

[36] Levova, T.; Moreno-Ruiz, E., 2011. Ecoinvent 3.4 dataset documentation, dimethylamine production.

[37] Notter, D.; Bauer, C., 2011. Ecoinvent 3.4 dataset documentation, lithium hexafluorophosphate production.

[38] Notter, D.; Bauer, C., 2011. Ecoinvent 3.4 dataset documentation, phophorus pentachloride production.

[39] Hischier, R.; Kunst, H., 2011. Ecoinvent 3.4 dataset documentation, phophorus chloride production.

[40] Chudacoff, M.; Kunst, H., 2011. Ecoinvent 3.4 dataset documentation, ethylene oxide production.

[41] Jungbluth, N.; Dones, R., 2013. Ecoinvent 3.4 dataset documentation, polyvinylfluoride production.

[42] Jungbluth, N.; Weidema, B.; Dones, R., 2011. Ecoinvent 3.4 dataset documentation, vinyl fluoride production.

[43] Parada-Tur, S.; Weidema, B., 2011. Ecoinvent 3.4 dataset documentation, hexafluoroethane production, from fluorination of tetrafluoroethane.

[44] Parada-Tur, S.; Weidema, B, 2011. Ecoinvent 3.4 dataset documentation, tetrafluoroethane production.

APPENDIX F: GreenScreen®-Based Benchmark Results for Primary and Processing Materials Used in The Six Battery Storage Technologies

Table F1. GreenScreen® benchmark results for primary chemicals used in VRFB.

VRFB **CAS No.**	**Chemical Name**	**Benchmark Score**
	Bipolar Plate	
9002-88-4	Polyethylene	BM 2
7782-42-5	Graphite	BM 4
	Cell Frame	
65997-17-3	Glass fiber (E glass)	BM 1
9003-07-0	Polypropylene	BM 2
	Electrode	
7440-44-0	Carbon felt	BM 3
	Membrane	
31175-20-9	Nafion®	BM U
	Current Collector	
7440-50-8	Copper	BM 2
	Electrolyte	
1314-62-1	Vanadium pentoxide	BM 1
7664-93-9	Sulfuric acid	BM 2
7647-01-0	Hydrochloric acid	BM 2
	Tank	
9002-88-4	Polyethylene	BM 2

	Pipe	
9002-88-4	Polyethylene	BM 2

Table F2. GreenScreen® benchmark results for primary chemicals used in ZBFB.

ZBFB		
CAS No.	**Chemical Name**	**Benchmark Score**
	Bipolar Plate	
7440-32-6	Titanium	BM 2
9002-88-4	Polyethylene	BM 2
	Cell Frame	
9002-88-4	Polyethylene	BM 2
	Current Collector	
7440-32-6	Titanium	BM 2
	Electrolyte	
7699-45-8	Zinc bromide	BM 2
7726-95-6	Bromine	BM 2
	Tank	
9002-88-4	Polyethylene	BM 2
	Pipe	
9002-88-4	Polyethylene	BM 2

Table F3. GreenScreen® benchmark results for primary chemicals used in IFB.

IFB		
CAS No.	**Chemical Name**	**Benchmark Score**

	Bipolar Plate	
7782-42-5	Graphite	BM 4
36425-16-8	Bisphenol-A epoxy-based vinyl ester resin	BM U
	Cell Frame	
65997-17-3	Glass Fiber (E glass)	BM 1
113669-95-7	Polyester resin	BM U
	Electrode	
7440-44-0	Carbon felt	BM 3
	Membrane	
9002-88-4	Ultra-high molecular weight polyethylene	BM 2
	Current Collector	
7429-90-5	Aluminum	BM 2
	Electrolyte	
1313-13-9	Manganese dioxide	BM 1
7705-08-0	Iron (II) chloride	BM 2
7647-01-0	Hydrochloric acid	BM 2
7447-40-7	Potassium chloride	BM 2
	Tank	
	Isophthalic polyester	BM U
	Pipe	
9002-86-2	Polyvinylchloride	BM 2

Table F4. GreenScreen® benchmark results for primary chemicals used in LFP.

LFP

CAS No.	Chemical Name	Benchmark Score
	Cathode	
872-50-4	N-methyl-2-pyrrolidone (NMP)	BM 1
1333-86-4	Carbon black	BM 1
9002-84-0	Polytetrafluoroethylene (PTFE)	BM 3
15365-14-7	Lithium iron phosphate	BM U
	Cathode Substrate	
7429-90-5	Aluminum	BM U
	Anode	
872-50-4	N-methyl-2-pyrrolidone (NMP)	BM 1
9002-84-0	Polytetrafluoroethylene (PTFE)	BM 3
7782-42-5	Graphite	BM 4
	Anode Substrate	
7440-50-8	Copper	BM 2
	Electrolyte	
96-49-1	1,3-dioxolan-2-one (Ethylene carbonate)	BM 1
21324-40-3	Lithium hexafluorophosphate (LiPF6)	BM 2
	Separator	
9002-88-4	Polyethylene	BM 2
9003-07-0	Polypropylene	BM 2

Table F5. GreenScreen® benchmark results for primary chemicals used in NCM.

NCM	
CAS No.	**Chemical Name**

	Cathode	
182442-95-1	Lithium nickel cobalt manganese hydroxide	BM 1
872-50-4	N-methyl-2-pyrrolidone (NMP)	BM 1
1333-86-4	Carbon black	BM 1
9002-84-0	Polytetrafluoroethylene (PTFE)	BM 3
	Cathode Substrate	
7429-90-5	Aluminum	BM 2
	Anode	
872-50-4	N-methyl-2-pyrrolidone (NMP)	BM 1
9002-84-0	Polytetrafluoroethylene (PTFE)	BM 3
7782-42-5	Graphite	BM 4
	Anode Substrate	
7429-90-5	Aluminum	BM 2
	Electrolyte	
96-49-1	1,3-dioxolan-2-one (Ethylene carbonate)	BM 1
21324-40-3	Lithium hexafluorophosphate (LiPF6)	BM 2
	Separator	
9002-88-4	Polyethylene	BM 2
9003-07-0	Polypropylene	BM 2

Table F6. GreenScreen® benchmark results for primary chemicals used in LMO.

LMO	
CAS No.	**Chemical Name**
	Cathode

1333-86-4	Carbon black	BM 1
9006-04-6	Latex	BM 2
12057-17-9	Lithium manganese oxide	BM U
	Cathode Substrate	
7429-90-5	Aluminum	BM 2
	Anode	
1333-86-4	Carbon black	BM 1
9006,04,6	Latex	BM 2
7782-42-5	Graphite	BM 4
	Anode Substrate	
7440-50-8	Copper	BM 2
	Electrolyte	
96-49-1	1,3-dioxolan-2-one (Ethylene carbonate)	BM 1
21324-40-3	Lithium hexafluorophosphate (LiPF6)	BM 2
	Separator	
7631-86-9	Silica (SiO2)	BM 1
85-44-9	Phthalic anhydride	BM 1
67-64-1	Acetone	BM 1
9002-88-4	Polyethylene	BM 2
76-16-4	Hexafluoroethane	BM 3
24937-79-9	Polyvinylidene fluoride (PVDF)	BM U

Table F7. GreenScreen® benchmark results on all the processing chemicals used in the six battery storage technologies.

CAS No.	Chemicals Name	Benchmark Score
Polyethylene: VRFB bipolar plate filler, tank and pipe material; ZBFB bipolar plate and cell frame filler, tank and pipe material; IFB membrane; LFP, NCM and LMO separator material		
9002-88-4	Polyethylene	BM 2
74-85-1	Ethylene	BM 2
Polypropylene: VRFB cell frame filler, LFP and NCM separator		
9003-07-0	Polypropylene	BM 2
115-07-1	Propylene	BM 2
Polyvinylchloride: IFB pipe		
9002-86-2	Polyvinylchloride	BM 2
75-01-4	Vinyl chloride	BM 1
74-85-1	Ethylene	BM 2
7782-50-5	Chlorine	BM 2
Glass fiber (E-glass): VRFB and IFB cell frame filler		
65997-17-3	Glass Fiber (E glass)	BM 1
7631-86-9	Silica (SiO_2)	BM 1
1303-86-2	Boron oxide (B_2O_3)	BM 1
1305-78-8	Calcium oxide (CaO)	BM 2
1344-28-1	Aluminum oxide (Al_2O_3)	BM 2
1309-48-4	Magnesium oxide (MgO)	BM 3
Vanadium pentoxide: VRFB electrolyte active material		
1314-62-1	Vanadium pentoxide (V_2O_5)	BM 1

497-19-8	Sodium carbonate (Na_2CO_3)	BM 2
7664-93-9	Sulfuric acid (H_2SO_4)	BM 2
7783-20-2	Ammonium sulphate ($(NH_4)_2SO4$)	BM 2
Zinc bromide: ZBFB electrolyte active material		
7699-45-8	Zinc Bromide ($ZnBr_2$)	BM 2
1314-13-2	Zinc Oxide (ZnO)	BM 2
7726-95-6	Bromine (Br_2)	BM 2
7664-93-9	Sulfuric acid (H_2SO_4)	BM 2
7782-50-5	Chlorine (Cl_2)	BM 2
Carbon felt: VRFB and IFB electrode		
1333-86-4	Carbon felt	BM 3
67-56-1	Methanol	BM 1
67-64-1	Acetone	BM 1
74-90-8	Hydrogen cyanide	BM 1
80-62-6	Methyl methacrylate	BM 1
107-13-1	Acrylonitrile	BM 1
74-82-8	Methane	BM 2
98-82-8	Cumene (Isopropyl benzene)	BM 2
115-07-1	Propylene	BM 2
7664-41-7	Ammonia	BM 2
7664-93-9	Sulfuric acid (H_2SO_4)	BM 2
25014-41-9	Polyacrylonitrile (PAN)	BM U
Nafion®: VRFB membrane		
31175-20-9	Nafion®	BM U

116-14-3	Tetrafluoroethylene (TFE)	BM 1
75-45-6	Chlorodifluoromethane	BM 1
67-66-3	Trichloromethane	BM 1
7664-39-3	Hydrogen fluoride (HF)	BM 2
1310-73-2	sodium hydroxide	BM 2
428-59-1	Hexafluoropropylene oxide (HFPO)	BM 2
497-19-8	Sodium carbonate (Na_2CO_3)	BM 2
7664-93-9	Sulfuric acid (H_2SO_4)	BM 2
7446-11-9	Sulfur trioxide	BM 2
7681-52-9	Sodium hypochlorite	BM 2
7782-50-5	Chlorine	BM 2
7727-37-9	Nitrogen, liquid	BM 4
16090-14-5	Perfluoro-sulfonylethoxy propylene vinyl ether (PSEPVE)	BM U
1717-59-5	Fluorosulfonyl DIfluoroacetic (FDA)	BM U
Bisphenol-A epoxy-based vinyl ester resin: IFB bipolar plate filler		
36425-16-8	Bisphenol-A epoxy-based vinyl ester resin	BM U
67-64-1	Acetone	BM 1
71-43-2	Benzene	BM 1
74-90-8	Hydrogen cyanide	BM 1
80-05-7	Bisphenol-A	BM 1
100-42-5	Styrene	BM 1
106-89-8	Epichlorohydrin	BM 1
108-95-2	Phenol	BM 1
79-41-4	Methacrylic acid	BM 2

98-82-8	Cumene (Isopropylbenzene)	BM 2
115-07-1	Propylene	BM 2
74-82-8	Methane	BM 2
7664-41-7	Ammonia	BM 2
7664-93-9	Sulfuric acid	BM 2
1310-73-2	Sodium hydroxide	BM 2
1305-78-8	Calcium oxide (CaO)	BM 2
107-05-1	Allyl chloride	BM 2
7782-50-5	Chlorine	BM 2
24969-06-0	Epoxy resin	BM 3
7727-37-9	Nitrogen, liquid	BM 4
Polyester resin: IFB cell frame filler		
113669-95-7	Polyester resin	BM U
64-19-7	Acetic acid	BM 1
75-21-8	Ethylene oxide	BM 1
1330-20-7	Xylene	BM 1
75-56-9	Propylene oxide	BM 1
108-24-7	Acetic anhydride	BM 1
85-44-9	Phthalic anhydride	BM 1
630-08-0	Carbon monoxide	BM 1
67-56-1	Methanol	BM 1
75-21-8	Ethylene oxide	BM 1
110-82-7	Cyclohexane	BM 2
7697-37-2	Nitric acid	BM 2

124-04-9	Adipic acid	BM 2
107-21-1	Ethylene glycol	BM 2
57-55-6	Propylene glycol	BM 2
7664-93-9	Sulfuric acid	BM 2
1310-73-2	Sodium hydroxide	BM 2
74-85-1	Ethylene	BM 2
7782-50-5	Chlorine	BM 2
115-07-1	Propylene	BM 2
7727-37-9	Nitrogen, liquid	BM 4
Isophthalic polyester: IFB tank		
/	Isophthalic polyester	BM U
71-43-2	Benzene	BM 1
100-42-5	styrene	BM 1
64-19-7	Acetic acid	BM 1
1330-20-7	xylene	BM 1
75-56-9	propylene oxide	BM 1
630-08-0	Carbon monoxide	BM 1
67-56-1	Methanol	BM 1
75-21-8	Ethylene oxide	BM 1
100-21-0	terephthalic acid	BM 1
108-31-6	maleic anhydride	BM 1
111-46-6	diethylene glycol	BM 2
57-55-6	proplyene glycol	BM 2
1310-73-2	sodium hydroxide	BM 2

74-85-1	ethylene	BM 2
7782-50-5	chlorine	BM 2
115-07-1	propylene	BM 2
7727-37-9	Nitrogen, liquid	Bm 4
Lithium iron phosphate: LFP cathode active material		
15365-14-7	Lithium iron phosphate	BM U
1310-65-2	Lithium hydroxide (LiOH)	BM 1
554-13-2	Lithium carbonate (Li_2CO_3)	BM 1
7664-38-2	Phosphoric acid (H_3PO_4)	BM 2
7720-78-7	Iron Sulfate ($FeSO_4$)	BM 2
1305-62-0	Calcium hydroxide ($Ca(OH)_2$)	BM 2
7647-01-0	Hydrochloric acid (HCl)	BM 2
7664-93-9	Sulfuric acid (H_2SO_4)	BM 2
1305-78-8	calcium oxide (CaO)	BM 2
497-19-8	Sodium carbonate (Na_2CO_3)	BM 2
Polytetrafluoroethylene (PTFE): LFP and NCM cathode and anode binder		
9002-84-0	Polytetrafluoroethylene (PTFE)	BM 3
116-14-3	Tetrafluoroethylene (TFE)	BM 1
75-45-6	Chlorodifluoromethane	BM 1
67-66-3	Trichloromethane	BM1
7664-39-3	Hydrogen fluoride (HF)	BM 2
1310-73-2	Sodium hydroxide	BM 2
7664-93-9	Sulfuric acid	BM 2
7727-37-9	Nitrogen, liquid	BM 4

N-methtyl-2-pyrrolidone: LFP and NCM cathode and anode solvent		
872-50-4	N-methyl-2-pyrrolidone (NMP)	BM 1
96-48-0	Butyrolactone	BM 1
50-00-0	Formaldehyde	BM 1
67-56-1	Methanol	BM 1
124-40-3	Dimethylamine	BM 2
110-63-4	Butane-1,4-diol	BM 2
74-86-2	Acetylene	BM 2
1310-73-2	Sodium hydroxide	BM 2
7664-41-7	Ammonia	BM 2
1333-74-0	Hydrogen	BM 2
7727-37-9	Nitrogen, liquid	BM 4
Lithium hexafluorophosphate ($LiPF_6$): LFP, NCM and LMO electrolyte material		
21324-40-3	Lithium hexafluorophosphate ($LiPF_6$)	BM 2
554-13-2	Lithium carbonate (Li_2CO_3)	BM 1
10026-13-8	Phosphorus pentachloride (PCl_5)	BM 2
7664-39-3	Hydrogen fluoride (HF)	BM 2
1305-62-0	Calcium hydroxide ($Ca(OH)_2$)	BM 2
7782-50-5	Chlorine (Cl_2)	BM 2
7719,12,2	Phosphorus trichloride (PCl_5)	BM 2
7664-41-7	Ammonia (NH_3)	BM 2
7647-01-0	Hydrochloric acid (HCl)	BM 2
7664-93-9	Sulfuric acid (H_2SO_4)	BM 2
1305-78-8	calcium oxide (CaO)	BM 2

497-19-8	Sodium carbonate (Na_2CO_3)	BM 2
7789-24-4	Lithium fluoride (LiF)	BM 3
7723-14-0	Phosphorus	BM 3
124-38-9	Carbon dioxide	BM 3
7727-37-9	Nitrogen, liquid	BM 4
1,3-dioxolan-2-one (Ethylene carbonate): LFP, NCM and LMO electrolyte solvent		
96-49-1	1,3-dioxolan-2-one (Ethylene carbonate)	BM 1
75-21-8	Ethylene oxide	BM 1
74-85-1	Ethylene	BM 2
124-38-9	Carbon dioxide	BM 3
Lithium nickel cobalt manganese hydroxide: NCM cathode active material		
182442-95-1	Lithium nickel cobalt manganese hydroxide	BM 1
1310-65-2	Lithium hydroxide (LiOH)	BM 1
554-13-2	Lithium carbonate (Li_2CO_3)	BM 1
7786-81-4	Nickel sulfate	BM 1
10124-43-3	Cobalt sulfate	BM 1
7785-87-7	Manganese sulfate	BM 1
1305-62-0	Calcium hydroxide ($Ca(OH)_2$)	BM 2
1310-73-2	Sodium hydroxide	BM 2
7647-01-0	Hydrochloric acid (HCl)	BM 2
7664-93-9	Sulfuric acid (H_2SO_4)	BM 2
1305-78-8	calcium oxide (CaO)	BM 2
497-19-8	Sodium carbonate (Na_2CO_3)	BM 2
189139-63-7	Nickel cobalt manganese hydroxide	BM U

Polyvinyl fluoride (PVDF): LMO separator material		
24937-79-9	Polyvinyl fluoride (PVDF)	BM U
75-02-5	Vinyl fluoride	BM 1
75-37-6	1,1-difluoroethane	BM 2
74-86-2	Acetylene	BM 2
1305-62-0	Calcium hydroxide ($Ca(OH)_2$)	BM 2
7664-39-3	Hydrogen fluoride (HF)	BM 2
7440-66-6	Zinc (Zn)	BM 2
Hexafluoroethane: LMO separator material		
76-16-4	Hexafluoroethane	BM 3
79-01-6	Trichloroethylene	BM 1
811-97-2	Tetrafluoroethane	BM 2
74-85-1	Ethylene	BM 2
7782-41-4	Fluorine	BM 2
7664-39-3	Hydrogen fluoride (HF)	BM 2
7782-50-5	Chlorine	BM 2
1310-73-2	Sodium hydroxide	BM 2
7727-37-9	Nitrogen, liquid	BM 4
Lithium manganese oxide: LMO cathode active material		
12057-17-9	Lithium manganese oxide	BM U
554-13-2	Lithium carbonate (Li_2CO_3)	BM 1
1317-34-6	Manganese oxide (Mn_2O_3)	BM 1
7647-01-0	Hydrochloric acid (HCl)	BM 2
7664-93-9	Sulfuric acid (H_2SO_4)	BM 2

1305-78-8	calcium oxide (CaO)	BM 2
497-19-8	Sodium carbonate (Na_2CO_3)	BM 2
7727-37-9	Nitrogen, liquid	BM 4

APPENDIX G: The 13 Low Band Gap Polymers and Their Process Chemicals and 'GreenScreen®-Based' Benchmarks

Polymer	CAS No.	Process Chemicals	Benchmark
PDTP-DFBT	67-66-3	chloroform	1
	76-05-1	trifluoroacetic acid	1
	10332-33-9	sodium perborate monohydrate	1
	75-09-2	dichloromethane	1
	110-54-3	hexane	1
	114499-45-5	3,7-dimethyloctylmagnesium bromide	1
	108-88-3	toluene	1
	1461-22-9	tributyltin chloride	1
	110-86-1	pyridine	1
	7726-95-6	bromine	1
	67-56-1	methanol	1
	67-64-1	acetone	1
	108-90-7	chlorobenzene	1
	109-99-9	dehydrotetrahydrofuran	2
	141-78-6	ethyl acetate	2
	109-72-8	n-butyllithium	2
	121-44-8	triethylamine	2
	7719-09-7	thionyl chloride	2
	7664-93-9	sulfuric acid	2
	6163-58-2	tri(*o*-tolyl)phosphine	2
	20624-25-3	sodium diethyldithiocarbamate	2
	64-19-7	acetic acid	2

	60-29-7	diethyl ether	3
	7789-23-3	potassium fluoride	3
	7757-82-6	sodium sulfate	3
	6192-52-5	sodium p-toluenesulfonic acid monohydrate	3
	108-86-1	bromobenzene	3
	51364-51-3	tris(dibenzylideneacetone)dipalladium(0)	4
	389-58-2	4H-cyclopenta[2,1-b:3,4-b']dithiophene	U
	25170-74-5	3,4-difluoro-1,2-diaminobenzene	U
Polymer	CAS No.	Process Chemicals	Benchmark
PBDTT-DPP	1003-31-2	2-thiophenecarbonitrile	1
	106-65-0	dimethyl succinate	1
	67-56-1	methanol	1
	128-08-5	N-bromosuccinimide	1
	67-66-3	chloroform	1
	108-88-3	toluene	1
	68-12-2	N,N-dimethylformamide	1
	32281-36-0	4,8-dihydrobenzo[1,2-b:4,5-b']dithiophen-4,8-dion	2
	109-99-9	dehydrotetrahydrofuran	2
	109-72-8	n-butyllithium	2
	1066-45-1	trimethyltin chloride	2
	865-47-4	potassium tert-butylate	2
	75-85-4	t-amyl alcohol	2
	64-19-7	acetic acid	2
	60-29-7	diethyl ether	3
	584-08-7	anhydrous potassium carbonate	3
	14221-01-3	palladium-tetrakis(triphenylphosphine)	4

Polymer	CAS No.	Process Chemicals	Benchmark
PBDTT-SeDPP	1189-71-5	chlorosulfonyl isocyanate	1
	68-12-2	N,N-dimethylformamide	1
	75-09-2	dichloromethane	1
	110-54-3	hexane	1
	128-08-5	N-bromosuccinimide	1
	67-66-3	chloroform	1
	108-88-3	toluene	1
	67-56-1	methanol	1
	7440-23-5	sodium	1
	288-05-1	selenophene	2
	75-85-4	t-amyl alcohol	2
	64-19-7	acetic acid	2
	32281-36-0	4,8-dihydrobenzo[1,2-b:4,5-b']dithiophen-4,8-dion	2
	109-99-9	dehydrotetrahydrofuran	2
	109-72-8	n-butyllithium	2
	1066-45-1	trimethyltin chloride	2
	60-29-7	diethyl ether	3
	584-08-7	anhydrous potassium carbonate	3
	924-88-9	diisopropyl succinate	3
	14221-01-3	palladium-tetrakis(triphenylphosphine)	4
	85531-02-8	2-butyloctyl bromide	U
Polymer	CAS No.	Process Chemicals	Benchmark
PCPDTFBT	1333-82-0	chromium oxide	1
	107-31-3	methylformate	1
	26299-14-9	pyridinium chlorochromate	1

	71-43-2	benzene	1
	68-12-2	N,N-dimethylformamide	1
	79-44-7	N,N-dimethylcarbamyl chloride	1
	27607-77-8	trimethylsilylfluoromethane-sulfonate	1
	107-21-1	ethylene glycol	1
	10217-52-4	hydrazine hydrate	1
	110-54-3	hexane	1
	108-88-3	toluene	1
	188595-68-8	tert-butylmethyl ether	1
	64-17-5	ethanol	1
	108-90-7	chlorobenzene	1
	872-31-1	3-bromothiophene	2
	109-72-8	n-butyllithium	2
	7553-56-2	iodine	2
	7440-50-8	copper powder	2
	7647-01-0	hydrochloric acid	2
	1310-58-3	potassium hydroxide	2
	12125-02-9	ammonium chloride solution	2
	109-99-9	dehydrotetrahydrofuran	2
	1066-45-1	trimethyltin chloride	2
	121-44-8	triethylamine	2
	7681-82-5	sodium iodide	2
	18908-66-2	2-ethylhexylbromide	2
	7697-37-2	nitric acid	2
	7664-93-9	sulfuric acid	2
	7772-99-8	tinchloride	2

	7719-09-7	thionyl chloride	2
	6163-58-2	tri(*o*-tolyl)phosphine	2
	60-29-7	diethyl ether	3
	7381-30-8	1,2-bis(trimethylsilyloxy)ethane	3
	7757-82-6	sodium sulfate	3
	67-68-5	dimethylsulfoxide	3
	1435-52-5	2,5-dibromo-3-fluorobenzene	3
	498-62-4	3-thiophenecarboxaldehyde	3
	7487-88-9	magnesium sulfate	4
	51364-51-3	tris(dibenzylideneacetone)dipalladium(0)	4
		bis-(3-thienyl)methanol	U
Polymer	CAS No.	Process Chemicals	Benchmark
PDTSTPD	125143-53-5	3,3',5,5'-tetrabromo-2,2'-bithiophene	1
	110-54-3	hexane	1
	64-17-5	ethanol	1
	67-64-1	acetone	1
	128-08-5	N-bromosuccinimide	1
	76-05-1	trifluoroacetic acid	1
	108-88-3	toluene	1
	68-12-2	N,N-dimethylformamide	1
	75-09-2	dichloromethane	1
	67-66-3	chloroform	1
	67-56-1	methanol	1
	109-99-9	dehydrotetrahydrofuran	2
	109-72-8	n-butyllithium	2
	75-77-4	chlorotrimethylsilane	2

	1066-45-1	trimethyltin choride	2
	7664-93-9	sulfuric acid	2
	142-82-5	heptane	2
	934-56-5	trimethylphenyltin	2
	60-29-7	diethyl ether	3
	108-86-1	bromobenzene	3
	773881-43-9	5-octylthieno[3,4-c]pyrrole-4,6-dione	3
	7487-88-9	magnesium sulfate	4
	14221-01-3	palladium-tetrakis(triphenylphosphine)	4
	1089687-03-5	dichlorodi(2-ethylhexyl)silane	U
Polymer	CAS No.	Process Chemicals	Benchmark
PDPP5T	594-19-4	t-butyllithium	1
	108-88-3	toluene	1
	67-66-3	chloroform	1
	128-08-5	N-bromosuccinimide	1
	75-09-2	dichloromethane	1
	86134-26-1	5,5'-bis(trimethylstannyl)thiophene	1
	67-56-1	methanol	1
	110-54-3	hexane	1
	67-64-1	acetone	1
	7664-41-7	ammonia	1
	110-18-9	N,N,N',N'-tetramethylethylenediamine	2
	109-66-0	pentane	2
	61676-62-8	2-isopropoxy-4,4,5,5-tetramethyl-1,3,2-dioxaborolane	2
	60-29-7	diethyl ether	3

	142-82-5	heptane	2
	109-99-9	dehydrotetrahydrofuran	2
	7778-53-2	potassium phosphate tribasic	2
	104934-52-3	3-dodecylthiophene	3
	584-08-7	potassium carbonate	3
	60-00-4	ethylenediaminetetraacetic acid	3
	7487-88-9	magnesium sulfate	4
	14221-01-3	palladium-tetrakis(triphenylphosphine)	4
	51364-51-3	tris(dibenzylideneacetone)-dipalladium	4
	131274-22-1	tritertbutylphosphoniumtetrafluoroborate	4
	1000623-98-2	3,6-bis(5-bromo-2-thienyl)-2,5-dihydro-2,5-di(2'-hexyldecyl)-pyrrolo[3,4-c]-pyrrolo-1,4-dione	4
Polymer	CAS No.	Process Chemicals	Benchmark
PCDTPT	67-56-1	methanol	1
	98-59-9	p-toluenesulfonyl chloride	1
	110-54-3	hexane	1
	67-64-1	acetone	1
	54663-78-4	tributyl(2-thienyl)stannane	1
	64-17-5	ethanol	1
	67-66-3	chloroform	1
	128-08-5	N-bromosuccinimide	1
	68-12-2	N,N-dimethylformamide	1
	108-88-3	toluene	1
	75-09-2	dichloromethane	1
	141-78-6	ethyl acetate	2
	109-94-4	ethyl formate	2

	109-99-9	dehydrotetrahydrofuran	2
	17049-49-9	octylmagnesium bromide	2
	12125-02-9	ammonium chloride solution	2
	121-44-8	triethylamine	2
	136630-39-2	2,7-dibromo-9H-carbazole	2
	1310-58-3	potassium hydroxide	2
	109-72-8	n-butyllithium	2
	61676-62-8	2-isopropoxy-4,4,5,5-tetramethyl-1,3,2-dioxaborolane	2
	64-19-7	acetic acid	2
	6163-58-2	tri(*o*-tolyl) phosphine	2
	75-59-2	tetramethylammonium hydroxide	2
	98-80-6	phenylboronic acid	2
	60-29-7	diethyl ether	3
	7757-82-6	sodium sulfate	3
	67-68-5	dimethylsulfoxide	3
	108-86-1	bromobenzene	3
	593-81-7	trimethylamine hydrochloride	3
	15155-41-6	4,7-dibromo-2,1,3-benzothiadiazole	3
	7647-14-5	sodium chloride	4
	7487-88-9	magnesium sulfate	4
	13965-03-2	bis(triphenylphosphine)palladium(II) dichloride	4
	51364-51-3	tris(dibenzylideneacetone)-dipalladium	4
Polymer	CAS No.	Process Chemicals	Benchmark
PBTTPD	110-54-3	hexane	1
	7726-95-6	bromine	1

	79-37-8	oxalyl chloride	1
	71-43-2	benzene	1
	68-12-2	N,N-dimethylformamide	1
	108-90-7	chlorobenzene	1
	54663-78-4	2-tributylstannlythiophene	1
	67-66-3	chloroform	1
	67-56-1	methanol	1
	67-64-1	acetone	1
	141-78-6	ethyl acetate	2
	109-72-8	n-butyllithium	2
	7447-39-4	copper chloride	2
	110-18-9	N,N,N',N'-tetramethylethylenediamine	2
	109-99-9	dehydrotetrahydrofuran	2
	1066-45-1	trimethyltin choride	2
	64-19-7	acetic acid	2
	7681-38-1	sodium bisulfate	2
	6163-58-2	Tri(*o*-tolyl) phosphine	2
	1003-09-4	2-bromothiophene	2
	60-29-7	diethyl ether	3
	104-75-6	2-ethylhexylamine	3
	104934-52-3	3-dodecylthiophene	4
	7487-88-9	magnesium sulfate	4
	1344-28-1	aluminum oxide	4
	144-55-8	sodium bicarbonate	4
	51364-51-3	tris(dibenzylideneacetone)-dipalladium	4
	9002-84-0	polytetrafluoroethylene	4

	4282-29-5	thiophene-3,4-dicarboxylicacid	4
Polymer	CAS No.	Process Chemicals	Benchmark
PBnDT-DTffBT	78056-39-0	4,5-difluoro-2-nitroaniline	1
	67-56-1	methanol	1
	67-66-3	chloroform	1
	110-54-3	hexane	1
	75-09-2	dichloromethane	1
	108-88-3	toluene	1
	128-08-5	N-bromosuccinimide	1
	267-65-2	benzo[1,2-b:4,5-b'] dithiophene	1
	64-19-7	acetic acid	2
	141-78-6	ethyl acetate	2
	67-63-0	isopropanol	2
	7664-93-9	sulfuric acid	2
	121-44-8	triethylamine	2
	7719-09-7	thionyl chloride	2
	1310-73-2	sodium hydroxide	2
	109-99-9	dehydrotetrahydrofuran	2
	6163-58-2	Tri(*o*-tolyl) phosphine	2
	95-47-6	o-xylene	2
	497-19-8	sodium carbonate	2
	7757-82-6	sodium sulfate	3
		palladium on carbon	4
	144-55-8	sodium bicarbonate	4
	7487-88-9	magnesium sulfate	4
	14221-01-3	palladium-tetrakis(triphenylphosphine)	4

	51364-51-3	tris(dibenzylideneacetone)-dipalladium	4
		(4-(2-ethylhexyl) thiophen-2-yl)trimethylstannane	U
Polymer	CAS No.	Process Chemicals	Benchmark
PBDTTPD	128-08-5	N-bromosuccinimide	1
	67-56-1	methanol	1
	119-61-9	benzophenone	1
	75-05-8	acetonitrile	1
	108-88-3	toluene	1
	75-09-2	dichloromethane	1
	110-54-3	hexane	1
	76-05-1	trifluoroacetic acid	1
	64-17-5	ethanol	1
	67-66-3	chloroform	1
	67-64-1	acetone	1
	54663-78-4	2-tributylstannlythiophene	1
	429-42-5	tetrabutylammonium tetrafluoroborate	2
	109-99-9	dehydrotetrahydrofuran	2
	108-24-7	acetic anhydride	2
	111-86-4	n-octylamine	2
	7719-09-7	thionyl chloride	2
	7664-93-9	sulfuric acid	2
	7440-66-6	zinc dust	2
	1310-73-2	sodium hydroxide	2
	1066-45-1	trimethyltin choride	2
	109-72-8	n-butyllithium	2
	6163-58-2	tri(*o*-tolyl) phosphine	2

	1003-09-4	2-bromothiophene	2
	7757-82-6	sodium sulfate	3
	773881-43-9	5-octylthieno[3,4-c] pyrrole-4,6-dione	3
	7487-88-9	magnesium sulfate	4
	51364-51-3	tris(dibenzylideneacetone)-dipalladium	4
	4282-29-5	thiophene-3,4-dicarboxylicacid	4
	32281-36-0	benzo[1,2-b:4,5-b] dithiophene-4,8-dione	4
	78016-72-5	2-ethylhexyl p-toluenesulfonate	U
Polymer	CAS No.	Process Chemicals	Benchmark
PTB7	67-64-1	acetone	1
	128-08-5	N-bromosuccinimide	1
	68-12-2	N,N-dimethylformamide	1
	75-09-2	dichloromethane	1
	64-17-5	ethanol	1
	67-66-3	chloroform	1
	110-54-3	hexane	1
	67-56-1	methanol	1
	108-88-3	toluene	1
	124-41-4	sodium methylate	1
	107-30-2	chlorodimethyl ether	1
	7726-95-6	bromine	1
	71-43-2	benzene	1
	141-78-6	ethyl acetate	2
	67-63-0	isopropanol	2
	109-72-8	n-butyllithium	2
	538-75-0	N,N′-dicyclohexylcarbodiimide	2

	1122-58-3	4-(dimethylamino)pyridine	2
	109-99-9	dehydrotetrahydrofuran	2
	937-14-4	3-chloroperbenzoic acid	2
	108-24-7	acetic anhydride	2
	7440-66-6	zinc	2
	1310-73-2	sodium hydroxide	2
	1066-45-1	trimethyltin chloride	2
	1313-82-2	sodium sulfide	2
	7646-85-7	zinc chloride	2
	101316-46-5	petroleum ether	2
	7647-01-0	hydrochloric acid	2
	1310-58-3	potassium hydroxide	2
	7439-95-4	magnesium	2
	110-02-1	thiophene	2
	64-19-7	acetic acid	2
	74-96-4	ethyl bromide	2
	7719-09-7	thionyl chloride	2
	124-40-3	dimethylamine	2
	60-29-7	diethyl ether	3
	104-76-7	2-ethylhexanol	3
	133745-75-2	N-fluorobenzenesulfonimide	3
	7757-82-6	sodium sulfate	3
	14221-01-3	palladium-tetrakis(triphenylphosphine)	4
	7487-88-9	magnesium sulfate	4
	5380-42-7	methyl-2-thiophenecarboxylate	4
	78016-72-5	2-ethylhexyl-p toluenesulfate	U

Polymer	CAS No.	Process Chemicals	Benchmark
PSiF-DBT	68-12-2	N,N-dimethylformamide	1
	71-43-2	benzene	1
	64-17-5	ethanol	1
	67-56-1	methanol	1
	110-54-3	hexane	1
	3460-18-2	2,5-dibromonitrobenzene	1
	18416-07-4	dichlorodioctylsilane	1
	54663-78-4	tributyl(2-thienyl)stannane	1
	128-08-5	N-bromosuccinimide	1
	68-12-2	N,N-dimethylformamide	1
	108-88-3	toluene	1
	67-64-1	acetone	1
	5137-55-3	tricaprylmethylammonium chloride	1
	497-19-8	sodium carbonate	2
	67-63-0	isopropanol	2
	1310-73-2	sodium hydroxide	2
	7647-01-0	hydrochloric acid	2
	109-99-9	dehydrotetrahydrofuran	2
	109-72-8	n-butyllithium	2
	7440-50-8	copper powder	2
	7440-31-5	tin powder	2
	7632-00-0	sodium nitrite	2
	61676-62-8	2-isopropoxy-4,4,5,5-tetramethyl-1,3,2-dioxaborolane	2
	98-80-6	phenylboronic acid	2

	60-29-7	diethyl ether	3
	7757-82-6	sodium sulfate	3
	7681-11-0	potassium iodide	3
	108-86-1	bromobenzene	3
	15155-41-6	4,7-dibromo-2,1,3-benzothiadiazole	3
	7487-88-9	magnesium sulfate	4
	144-55-8	sodium bicarbonate	4
	13965-03-2	bis(triphenylphosphine)palladium(II) dichloride	4
	14221-01-3	palladium-tetrakis(triphenylphosphine)	4
Polymer	CAS No.	Process Chemicals	Benchmark
PDTGTPD	110-54-3	hexane	1
	108-88-3	toluene	1
	125143-53-5	3,3',5,5'-tetrabromo-2,2'-bithiophene	1
	128-08-5	N-bromosuccinimide	1
	67-56-1	methanol	1
	67-64-1	acetone	1
	67-66-3	chloroform	1
	75-09-2	dichloromethane	1
	76-05-1	trifluoroacetic acid	1
	109-99-9	dehydrotetrahydrofuran	2
	109-72-8	n-butyllithium	2
	75-77-4	chlorotrimethylsilane	2
	7647-01-0	hydrochloric acid	2
	1066-45-1	trimethyltin chloride	2
	10038-98-9	germanium (IV) tetrachloride	2
	7664-93-9	sulfuric acid	2

	142-82-5	heptane	2
	6163-58-2	tri(*o*-tolyl)phosphine	2
	1518-58-7	diethylammoniumdiethyldithiocarbamate	2
	90224-21-8	2-ethylhexylmagnesium bromide	2
	60-29-7	diethyl ether	3
	773881-43-9	5-octylthieno[3,4-c]pyrrole-4,6-dione	3
	7487-88-9	magnesium sulfate	4
	144-55-8	sodium bicarbonate	4
	51364-51-3	tris(dibenzylideneacetone)-dipalladium	4
		dichlorobis(2-ethylhexyl)germane	U

APPENDIX H: Characterization Criteria and Results of the 34 Toxicity Data Sources

Table H1 – H5 show the initial characterization results for the 34 secondary data sources on the basis of the five performance attributes.

Table H1. The initial characterization results for reliability.

Data Sources	Reliability								
	1. Experimental valid data based on standardized test	2. Reported data based on case study but no experimental details	3. Estimated data using QSAR methods or analog approach	4. Expert judgment based on mechinistic and structural considerations	1. Well recognized international organization, governmental department	2. Research institute or research groups focus on toxicity testing	3. Third party like non-governmental organization, industry, supplier and manufacture reports.		Final score
GHS-Japan	3	2			1			3.5	0.875
Sigma-Aldrich MSDSs	3						0	3.0	0.750
EPI SUITE			1		1			2.0	0.500
VEGA			1			0.5		1.5	0.375
California Proposition 65	3				1			4.0	1.000
TEDX	3	2				0.5		3.0	0.750
GESTIS	3				1			4.0	1.000
CHE		2					0	2.0	0.500
MAK	3				1			4.0	1.000
NIOSH	3				1			4.0	1.000
PAN	3						0	3.0	0.750
ChemSec Sin	3						0	3.0	0.750
(Q)SAR			1		1			2.0	0.500
CCR	3		1		1			3.0	0.750
CESAR	3		1		1			3.0	0.750
ECHA C&L inventory	3						0	3.0	0.750
ECHA CHEM	3				1		0	3.5	0.875
EnviChem	3				1			4.0	1.000
EPA HHBP	3				1			4.0	1.000
EPA OPPALB	3				1			4.0	1.000
GSBL	3				1		0	3.5	0.875
HPVIS	3				1			4.0	1.000
HSNO CCID	3				1			4.0	1.000
J-CHECK	3		1		1			3.0	0.750
NICAS IMAP	3				1			4.0	1.000
OECD HPV	3				1			4.0	1.000
US EPA IRIS	3				1			4.0	1.000
HSDB	3	2				0.5		3.0	0.750
ChemIDplus	3	2				0.5		3.0	0.750
CTD	3					0.5		3.5	0.875
ITER	3		1			0.5		2.5	0.625
CCRIS	3	2				0.5		3.0	0.750
CPDB	3	2				0.5		3.0	0.750
GENE-TOX	3	2				0.5		3.0	0.750

Table H2. The initial characterization results for transparency.

Data Sources	Final Score	
GHS-Japan	4	1.00
Sigma-Aldrich MSDSs	1	0.25
EPI SUITE	2	0.50
VEGA	1	0.25
California Proposition 65	4	1.00
TEDX	2	0.50
GESTIS	3	0.75
CHE	2	0.50
MAK	1	0.25
NIOSH	1	0.25
PAN	2	0.50
ChemSec Sin	1	0.25
(Q)SAR0.75	1	0.25
CCR	1	0.25
CESAR	4	1.00
ECHA C&L inventory	1	0.25
ECHA CHEM	3	0.75
EnviChem	2	0.50
EPA HHBP	1	0.25
EPA OPPALB	0	0.00
GSBL	3	0.75
HPVIS	2	0.50
HSNO CCID	2	0.50
J-CHECK	1	0.25
NICAS IMAP	4	1.00
OECD HPV	3	0.75
US EPA IRIS	4	1.00
HSDB	3	0.75
ChemIDplus	1	0.25
CTD	3	0.75
ITER	4	1.00
CCRIS	2	0.50
CPDB	2	0.50
GENE-TOX	2	0.50

Table H3. The initial characterization results for adequacy.

data source	Human Health Group I		Human Health Group II		Human Health Group II*		Environmental Toxicity& Fate		Physical Hazards		Total number		Index based on Malloy et al. study
GHS-Japan	5	0	5	0	4	0	2	0	2	0	18	0	0.825
Sigma-Aldrich MSDSs	4	0	4	0	3	0	1	0	2	0	14	0	0.654
EPI SUITE	0	0	0	0	0	0	2	0	0	0	2	0	0.175
VEGA	3	0	0	0	1	0	3	0	0	0	7	0	0.374
California Proposition 65	3	0	0	0	0	0	0	0	0	0	3	0	0.084
TEDX	1	0	0	0	0	0	0	0	0	0	1	0	0.028
GESTIS	4	0	4	0	3	0	2	0	2	0	15	0	0.741
CHE	4	0	0	2	0	2	0	0	0	0	4	4	0.167
MAK	3	0	0	0	2	0	0	0	0	0	5	0	0.139
NIOSH	0	2	0	4	0	2	0	0	0	0	0	9	0.111
PAN	4	0	1	1	0	0	2	0	0	0	7	1	0.328
ChemSec Sin	5	0	4	0	3	0	2	0	2	0	16	0	0.769
(Q)SAR	0	4	1	1	0	1	4	0	0	0	4	6	0.461
CCR	4	0	0	0	0	0	4	0	0	0	8	0	0.461
CESAR	0	4	1	1	0	1	4	0	0	0	5	6	0.461
ECHA C&L inventory	4	0	5	0	4	0	2	0	2	0	17	0	0.797
ECHA CHEM	4	0	5	0	4	0	4	0	2	0	19	0	0.972
EnviChem	0	3	0	0	0	0	4	0	0	0	4	3	0.392
EPA HHBP	0	1	0	1	0	0	0	0	0	0	0	2	0.028
EPA OPPALB	0	0	0	0	0	0	0	2	0	0	0	2	0.088
GSBL	0	4	1	2	1	0	4	0	0	0	6	6	0.489
HPVIS	0	4	1	2	1	2	1	0	0	0	3	8	0.255
HSNO CCID	4	0	5	0	4	0	2	0	2	0	17	0	0.797
J-CHECK	0	4	1	4	1	3	4	0	0	2	6	13	0.689
NICAS IMAP	0	4	1	4	1	3	4	0	0	2	6	13	0.689
OECD HPV	0	4	1	2	1	2	2	0	0	0	4	8	0.342
US EPA IRIS	0	3	0	0	0	0	0	0	0	0		3	0.042
HSDB	0	4	1	2	1	2	4	0	0	0	6	8	0.517
ChemIDplus	0	4	1	4	0	4	0	0	0	0	1	12	0.195
CTD	0	2	0	1	0	1	0	0	0	0	0	4	0.056
ITER	1	0	0	0	0	0	0	0	0	0	1	0	0.028
CCRIS	0	2	0	2	0	1	0	0	0	0	0	5	0.070
CPDB	0	2	0	0	0	0	0	0	0	0	0	2	0.028
GENE-TOX	0	1	0	0	0	0	0	0	0	0	0	1	0.014

Table H4. The initial characterization results for volume.

Data sources	Initial number	Indexing
GHS-Japan	3636	0.60
Sigma-Aldrich MSDSs	More than 300'000	1.00
EPI SUITE	Over 40,000	1.00
VEGA	Base on 3,000,000	1.00
California Proposition 65	963	0.37
TEDX	1392	0.44
GESTIS	9400	0.76
CHE	600	0.29
MAK	1200	0.41
NIOSH	677	0.31
PAN	8254	0.73
ChemSec Sin	912	0.36
(Q)SAR	600,000	1.00
CCR	22421	0.90
CESAR	739	0.33
ECHA C&L inventory	124581	1.00
ECHA CHEM	17420	0.86
EnviChem	2548	0.54
EPA HHBP	364	0.21
EPA OPPALB	562	0.28
GSBL	26650	0.93
HPVIS	1148	0.40
HSNO CCID	5452	0.67
J-CHECK	2022	0.50
NICAS IMAP	3215	0.58
OECD HPV	5038	0.65
US EPA IRIS	430	0.24
HSDB	5800	0.68
ChemIDplus	400000	1.00
CTD	22000	0.90
ITER	680	0.32
CCRIS	8000	0.73
CPDB	1150	0.40
GENE-TOX	3000	0.56

Table H5. The initial characterization results for ease of use.

	Input	Output	User expertise	Total	
GHS-Japan	1	1	0.5	3.5	0.88
Sigma-Aldrich MSDSs	1	1	0.5	3.5	0.88
EPI SUITE	1	0.5	0	2.5	0.63
VEGA	0.5	1	0	2.5	0.63
California Proposition 65	1	1	0.5	3.5	0.88
TEDX	0.5	0.5	1	3.0	0.75
GESTIS	1	1	0.5	3.5	0.88
CHE	1	0.5	1	3.5	0.88
MAK	0.5	0.5	0.5	2.5	0.63
NIOSH	1	1	1	4.0	1.00
PAN	1	1	0.5	3.5	0.88
ChemSec Sin	1	1	0.5	3.5	0.88
(Q)SAR	1	0.5	0	2.5	0.63
CCR	1	0.5	0.5	3.0	0.75
CESAR	1	1	0.5	3.5	0.88
ECHA C&L inventory	1	0.5	0.5	3.0	0.75
ECHA CHEM	1	1	0.5	3.5	0.88
EnviChem	0.5	1	0.5	3.0	0.75
EPA HHBP	0	0.5	0	1.5	0.38
EPA OPPALB	0.5	0.5	0	2.0	0.50
GSBL	1	1	0.5	3.5	0.88
HPVIS	1	0.5	0	2.5	0.63
HSNO CCID	1	0.5	0.5	3.0	0.75
J-CHECK	1	0.5	0	2.5	0.63
JECDB	1	0.5	0	2.5	0.63
NICAS IMAP	0.5	1	0	2.5	0.63
OECD HPV	1	1	0	3.0	0.75
US EPA IRIS	1	0.5	0.5	3.0	0.75
HSDB	1	1	0.5	3.5	0.88
ChemIDplus	1	1	0	3.0	0.75
CTD	1	1	0.5	3.5	0.88
ITER	1	1	0	3.0	0.75
CCRIS	1	1	0.5	3.5	0.88
CPDB	1	0.5	0	2.5	0.63
GENE-TOX	1	1	0.5	3.5	0.88

H1. Quantification of Reliability, Transparency and Ease of Use

Table H6. The 4-point maximum-possible score for the reliability, transparency and ease of use.

Performance Attributes		Points	Characterization Basis
Reliability (Total points = test methods points + organizations points)	Test methods	3	Experimentally valid data based on standardized test
		2	Reported data based on case studies but no experimental details
		1	Estimated data using QSAR methods or analog approach
		0	Expert judgment based on mechanistic and structural considerations
	Organizations	1	Well recognized international organization, governmental department
		0.5	Research institute or research groups focused on toxicity testing
		0	Third party like non-governmental organization, industry, supplier and manufacturer reports
Transparency (Total possible points = 4)		1	Methodology description on the data management included
		1	Peer reviews or comments released
		1	Detailed process description of the test included
		1	Citations included
Ease of Use (Total points = input points + output points + user expertise points +	Input and output for chemical-oriented and hazard-trait-oriented data sources	1	CAS No., chemical name and more information
		0.5	CAS No. and chemical name
		0	Not sufficient information
		1	Basic information for the chemicals and necessary toxicity information
		0.5	Only necessary toxicity information
		0	No sufficient information

accessibility points)	Input and output for predictive data sources	1	SMILEs and structure information
		0.5	Only SMILEs
		0	Not sufficient information
		1	Similar structure information and necessary toxicity information
		0.5	Only necessary toxicity information
		0	Not sufficient information
	User expertise	1	Not required for getting the result and understanding the terms
		0.5	Not required for getting the result, may need science or engineering background to understand the terms
		0	Need science or engineering background to understand the contents and result
	Accessibility	1	Free
		0	Not free

H2. Quantification of Adequacy and Volume

In GreenScreen®, the 20 hazard endpoints are categorized into human health hazard (14), ecotoxicity (4) and physical hazard (2). As the "*adequacy*" is characterized by the number of hazard traits included that can be used for the GreenScreen®, there will be the case that the information on this hazard endpoint is mentioned in the data source, but the data are not enough to assign a level of concern as GreenScreen® didn't provide guidance on how to use this type of data. As a result, we decided the value of the data that can't be directly used in GreenScreen® is half that of the data that can be used directly. Instead of normalizing the value on adequacy to be the hazard endpoints included in this data source divided by 20, here we applied a weighting scheme for different groups of hazard based on the survey in

Malloy's study [1] that Human health hazard is 0.39, ecotoxicity is 0.35 and physical hazard is 0.26. The final adequacy score is presented as:

$$\text{Total score} = 0.39*(H_D+H_{ND}*0.5)/14 + 0.35*(E_D+E_{ND}*0.5)/4 + 0.26*(P_D+P_{ND}*0.5)/2$$

where "H" is the number of human health hazards included in the data source, "E" is the number of environmental toxicity & fate hazards included, and "P" is the number of physical hazards included. For data that can be used directly, the subscript "D" is noted, and "ND" notation applies to the data that can't be used directly. For example, in one data source, if there are a total of 15 hazard endpoints mentioned, 10 of them belong to human health group, and 6 of them can be applied directly into GreenScreen®; 3 of them belong to ecotoxicity and 2 of them can be applied directly into GreenScreen®; and 2 of them belong to physical hazard and all can be applied directly into GreenScreen®, then the score is calculated as:

$$0.39*(6+4*0.5)/14 + 0.35*(2+1*0.5)/4 + 0.26*(2+0*0.5)/2 = 0.70$$

For the *volume* associated with each data source, we are referring to the number of chemicals included. Because there is a wide range in this value, from just hundreds of chemicals to over a million of chemicals, the disparity is too large on a linear scale. Therefore, we used a logarithmic scale to replace the original value and then normalized this value to a 0-1 scale. The score for data sources containing over 40,000 chemicals are assigned the highest score, 1.

Appendix H References

[1] Malloy, T.F.; Sinsheimer, P.G.; Blake, A.; Linkov, I., 2013. Use of multi-criteria decision analysis in regulatory alternative analysis: A case study of lead free solder. Int. Environ. Assess. Manag. 9(4), 652-664.